The *in vitro* biological activities of three *Hypoxis* species and their active compounds

Gerhardt Johannes Boukes

Submitted in partial fulfillment of the requirements for the degree of *Philosophiae Doctor* in the Faculty of Science at the Nelson Mandela Metropolitan University.

January 2010

Promoter: Prof Maryna van de Venter
Co-promoter: Prof Vaughan Oosthuizen

DEPARTMENT OF ACADEMIC ADMINISTRATION
EXAMINATION SECTION
SUMMERSTARND NORTH CAMPUS
PO Box 77000
Nelson Mandela Metropolitan University
Port Elizabeth
6013

Enquiries: Postgraduate Examination Officer

Nelson Mandela Metropolitan University
for tomorrow

DECLARATION BY CANDIDATE

NAME: Gerhardt Johannes Boukes

STUDENT NUMBER: 202318478

QUALIFICATION: *Philosophiae Doctor* in Biochemistry

TITLE OF PROJECT: The biological activities of three *Hypoxis* species and their active compounds

DECLARATION:

In accordance with Rule G4.6.3, I hereby declare that the above-mentioned thesis is my own work and that it has not previously been submitted for assessment to another University or for another qualification.

SIGNATURE: _____

DATE: _____

ACKNOWLEDGEMENTS

The author wants to thank the following people:

- To the Father, the Son (Jesus Christ) and the Holy Spirit, I give You all the glory, honour and praise.
- To my parents, Ludwig and Elna, your prayers have carried me through good and bad times. You taught me the fundamentals of life: to remain humble, to reach for my dreams, but most importantly to give God all the glory.
- To my siblings, Ludwig and Jackie, thank you for your support, love and prayers.
- To Sonja, I know you are smiling down from heaven now.
- To my family, thank you for all your support.
- To my promoter, Prof Maryna van de Venter, thank you for letting me live my dream. Thank you for all the help, advice and support and for believing in me. You are one of a kind!
- To my co-promoter, Prof Vaughan Oosthuizen, thank you for all the advice, support and for believing in me.
- To Brodie Daniels for her patience, advice and help with flow cytometry.
- To the Biochemistry and Microbiology postgraduate and postdoctoral students for all their help and support.
- To dr Carl Albrecht for his kind donation of hypoxoside and rooperol.
- To the NMMU, MRC and NRF for financial support.

CONTENTS

List of Figures

List of Tables

Summary

The African potato is used as an African traditional medicine for its nutritional and medicinal properties. Most research has been carried out on *H. hemerocallidea*, with very little or nothing on other *Hypoxis* spp. The main aim of this project was to provide scientific data on the anticancer, anti-inflammatory and antioxidant properties of *H. hemerocallidea*, *H. stellipilis* and *H. sobolifera* chloroform extracts and their active compounds.

The hypoxoside and phytosterol contents of the three *Hypoxis* spp. were determined using TLC, HPLC and GC. *H. hemerocallidea* and *H. sobolifera* chloroform extracts contained the highest amounts of hypoxoside and β-sitosterol, respectively.

For the anticancer properties, cytotoxicity of the *Hypoxis* extracts and its purified compounds were determined against the HeLa, HT-29 and MCF-7 cancer cell lines (using MTT), and PBMCs (using CellTiter-Blue®). *H. sobolifera* had the best cytotoxicity against the three cancer cell lines, whereas *H. stellipilis* stimulated HeLa and HT-29 cancer cell growth. IC_{50} values of hypoxoside and rooperol were determined. DNA cell cycle arrest (using PI staining) occurred in the late G1/early S (confirmed by increased $p21^{Waf1/Cip1}$ expression) and G2/M phases after 15 and 48 hrs, respectively, when treated with *Hypoxis* extracts and rooperol. *H. sobolifera* and rooperol activated caspase-3 and -7 (using fluorescently labelled antibodies) in HeLa and HT-29 cancer cells, and caspase-7 in MCF-7 cancer cells after 48 hrs. Annexin V binding to phosphatidylserines in rooperol treated U937 cells confirmed early apoptosis after 15 hrs. The TUNEL assay showed DNA fragmentation in the three cancer cell lines when treated with *H. sobolifera* and rooperol for 48 hrs. A shift pass the G2/M phase has led to the investigation of endoreduplication, which was confirmed by cell/nucleus size, and anti-apoptotic proteins (Akt, phospho-Akt, phospho-Bcl-2 and $p21^{Waf1/Cip1}$).

U937 cell differentiation to monocyte-macrophages was optimized using PMA and $1,25(OH)_2D_3$, which was confirmed by morphological and biochemical changes. For the anti-inflammatory properties, *Hypoxis* extracts and rooperol significantly increased NO production in monocyte-macrophages (pre-loaded with DAF-2 DA) and phagocytosis of pHrodo™ *E. coli* BioParticles®. The treatments had no effect on COX-2 expression in monocyte-macrophages. The phytosterols significantly increased IL-1β and IL-6 secretion

(using the FlowCytomix Multiplex human Th1/Th2 10plex Kit I) in the PBMCs of one donor.

For the antioxidant properties, *Hypoxis* extracts and rooperol significantly increased ROS production in undifferentiated and differentiated U937 cells, which were pre-loaded with DCFH-DA. *Hypoxis* extracts and purified compounds had ferric reducing activities, but only rooperol had ferric reducing activities significantly greater than ascorbic acid. β-sitosterol, campesterol and cholesterol significantly increased SOD activity in Chang liver cells, while *H. stellipilis*, *H. sobolifera* and rooperol decreased SOD activity.

Anticancer, anti-inflammatory and antioxidant properties of the *Hypoxis* extracts may be attributed to the β-sitosterol content, because *Hypoxis* chloroform extracts contained very little or no hypoxoside. Unidentified compounds, and synergistic and additive effects of the compounds may have contributed to the biological effects. This study confirms previous reports that rooperol is the active compound. Results provide scientific data on the medicinal properties of one of the most frequently used medicinal plants in South Africa.

Keywords: *Hypoxis* spp.; hypoxoside; phytosterols; anticancer, anti-inflammatory and antioxidant activities

Abbreviations

AA	arachidonic acid
ABC	ATP-binding cassette
ACAT	acyl-coenzyme A cholesterol acyltransferase
AcOEt	ethyl acetate
AIDS	acquired immune deficiency syndrome
AIF	apoptosis inducing factor
ALS	amyotrophic lateral sclerosis
AP	activating protein
Apaf-1	apoptosis proteinase activating factor-1
APC	adenomatous polyposis coli/anaphase-promoting complex
APCs	antigen presenting cells
Asp	aspartate
ATM	ataxia telangiectasia mutated
ATP	adenosine triphosphate
ATR	AMT- and Rad3-related
BH_4	(6R)-tetrahydrobiopterin
BRCA	breast cancer susceptibility gene 1/2
BSA	bovine serum albumin
BSS	β-sitosterol
BSTFA	bis(trimethylsilyl)-trifluoroacetamide
BuOH	butanol
CAD	caspase-activated DNase
cAMP	cyclic adenosine monophosphate
CAMP	campesterol
CARD	caspase-recruitment domain
CAT	catalase
CC	column chromatography
CCD	counter current distribution
CD	2-Hydroxypropyl-β-cyclodextrin
CDK	cyclin dependent kinase
CDKI	CDK inhibitor
cGMP	cyclic guanosine monophosphate

CH_3CN	acetonitrile
CHK	checkpoint-transducer serine/threonine kinase
CHOL	cholesterol
cIAP	cellular inhibitor of apoptosis
cNOS	constitutively expressed NOS
CNS	central nervous system
COX-1/2	cyclooxygenase-1/2
$cPLA_2$	cytosolic phospholipase A_2
CTLs	cytotoxic T lymphocytes
cysLT	cysteinyl leukotrienes
DAD	photodiode array detection
DAF-2	5,6-diaminofluorescein
DAF-2 DA	5,6-diaminofluorescein diacetate
DAPI	4’6-diaminidine-2’-phenylindole dihydrochloride
DCF	dichlorofluorescein
DCFH	2’,7’-dichlorofluorescein
DCFH-DA	2, 7-dichlorofluorescein diacetate
DD	death domain
DED	death effector domain
DESMO	desmosterol
DFF40/45	DNA fragmentation factor, 40/45-kDa subunit
DISC	death-inducing signalling complex
DMEM	Dulbecco’s Modified Eagle’s Medium
DMSO	dimethyl sulfoxide
DNA	deoxyribonucleic acid
DPBS	Dulbecco’s phosphate buffered saline
DPPH	1,1-diphenyl-2-picryl hydrazine
E2F	early gene 2 factor
EGF	epidermal growth factor
ELSD	evaporative light scattering detection
eNOS	endothelial NOS
ER	endoplasmic reticulum/endoreduplication
ERGO	ergosterol
EtOH	ethanol

FAD	flavine adenine dinucleotide
fbs	foetal bovine serum
FDA	Food and Drug Administration
FGF	fibroblast growth factor
FID	flame ionization detection
FITC	fluorescein isothiocyanate
FKHRL	Forkhead family of transcription factors
FLAP	5-lipoxygenase activating protein
FMN	flavin mononucleotide
FRAP	ferric reducing ability of plasma
FS	forward scatter
FUCO	fucosterol
GC	gas chromatography
GPX	glutathione peroxidase
GSH	glutathione, reduced
GSK-3	glycogen synthase kinase-3
GSSG	glutathione disulfide, oxidized
GTP	guanosine triphosphate
HBSS	Hanks' Balanced Salt Solution
HBV	hepatitis B virus
HCl	hydrochloric acid
HCV	hepatitis C virus
HDL	high-density lipoprotein
HIV	human immunodeficiency virus
H_2O_2	hydrogen peroxide
HPLC	high performance liquid chromatography
HPV	human papiloma virus
HSP	heat shock protein
HUVECs	human umbilical vein endothelial cells
IAPs	inhibitor of apoptosis proteins
IC_{50}	half maximal inhibitory concentrations
ICAD	inhibitor of CAD
IDVs	integrated density values
IFNγ	interferon γ

IGF-1	insulin-like growth factor 1
IL	interleukin
iNOS	inducible NOS
IPTG	isopropyl-β-thio-galactosidase
IR	infrared
JNK	c-Jun N-terminal kinase
LDH	lactate dehydrogenase
LDL	low-density lipoprotein
LPS	lipopolysaccaharides
LT	leukotrienes
LTA	lipoteichoic acid
MAPK	mitogen-activated protein kinase
Mdc	mediator of DNA damage checkpoint
MeOH	methanol
MFI	mean fluorescence intensity
MS	mass spectroscopy
MSTFA	N-methyl-N-trimethyl-silyltrifluoroacetamide
MTT	3-(4,5-dimethylthiazol-2-yl)-2,5-diphenyltetrazolium bromide
NADH	nicotinamide adenine dinucleotide
NADPH	nicotinamide adenine dinucleotide phosphate
NAIP	neuronal apoptotic inhibitory protein
NBS	Nijmegen breakage syndrome
NCR	National Cancer Registry
NF-κB	nuclear factor-kappa B
NK	natural killer
NMDA	N-methyl-D-aspartate
NMR	nuclear magnetic resonance
nNOS	neuronal NOS
NO	nitric oxide
NO^+	nitrosonium ion
NO_2	nitrogen dioxide
NO_2^-	nitrites
NO_3^-	nitrates
N_2O_2	nitrogen dioxide

N_2O_3	dinitrogen trioxide
NO_x	nitrogen oxides
NOS	nitric oxide synthase
NP	normal phase
NSAIDs	non-steroidal anti-inflammatory drugs
O_2^-	superoxide
ODS	octadecylsilica
OH^-	hydroxyl anion
$ONOO^-$	peroxynitrite
ORAC	oxygen radical absorbance capacity
PARP	poly(ADP-ribose) polymerase
PBMCs	peripheral blood mononuclear cells
PBS	phosphate buffered saline (containing Mg^{2+} and Ca^{2+})
PBSA	phosphate buffered saline A (no Mg^{2+} and Ca^{2+})
PC5	phycoerythrin cychrome 5
PCNA	proliferating-cell nuclear antigen
PDGF	platelet-derived growth factor
PG	prostaglandin
PI	propidium iodide
PI-3K	phosphatidylinositol 3-kinase
PKA/B/C	protein kinase A/B/C
PMA	phorbyl myristate acetate
PPAR	peroxisome proliferator-activated receptor
PS	phosphatidylserine
PTP	permeability transition pores
QA	quinolinic acid
Rb	retinoblastoma
RNA	ribonucleic acid
ROS	reactive oxygen species
RP	reverse phase
RPMI	Roswell Park Memorial Institute
SANBI	South African National Biodiversity Institute
SAPK	stress-activated protein kinase
Ser	serine

SFE	supercritical fluid extraction
SFF	supercritical fluid fractionation
sGC	soluble guanylate cyclase
sIL-1r	soluble IL-1 receptors
SLE	systemic lupus erythematosus
Smac	second mitochondrial activator of caspases
SOD	superoxide dismutase
SPE	solid phase extraction
SRB	sulphorhodamine B
SS	side scatter
STIG	stigmasterol
STN	stigmastenol
sTNFR	soluble TNF receptor
TBARS	thiobarbituric acid reactive substances
TdT	terminal deoxynucleotidyl transferase
TEAC	Trolox equivalent antioxidant capacity
TGF-β	tumour growth factor-β/transforming growth factor-β
TLC	thin layer chromatography
TMCS	trimethylchlorosilane
TMS	trimethylsilyl
TNF	tumour necrosis factor
TPA	12-*O*-tetradecanoylphorbol-13-acetate
TPTZ	Fe^{3+}-tripyridyltriazine
TUNEL	TdT dUTP nick end labelling
TXA_2/B_2	thromboxane A_2/B_2
UK	United Kingdom
US	United States
UV	ultraviolet
VDR	vitamin D receptor
VEGF	vascular endothelial growth factor
VSMC	vascular smooth muscle cell
WHO	World Health Organization
XTT	2,3-bis(2-methoxy-4-nitro-5-sulphophenyl)-2*H*-tetrazolium-5-carboxanilide sodium salt

CHAPTER 1
LITERATURE REVIEW

1.1. Traditional medicine

African traditional medicine is regarded as the oldest and possibly the most diverse of all the world's traditional medicines, but it is the most poorly recorded (Gurib-Fakim, 2006). Approximately 75-80% of Africa's population relies on traditional medicine. People living in developing countries face shortages of medical facilities, funds and newly developed medicine, which force them to be more reliant on natural resources (Louw *et al*., 2002). Traditional medicines are preferred, due to its affordability, accessibility and cultural and religious beliefs (Steenkamp, 2003a). In North America the use of medicinal plants has risen from 3% in 1991 to 37% of the population in 1998. This may be due to the availability of phytomedicine in retail stores, advertisements and an increase in pharmaceutical companies (Briskin, 2000). An increased interest in herbal or traditional medicine may be due to adverse reactions and side effects often seen with synthetic drugs (Erasto *et al*., 2005).

Natural products are regarded as a more environmentally friendly alternative to commercially produced medicines, resulting in a worldwide interest in medicinal plants. It is estimated that only 15% of the world's plants have been screened for their therapeutic values (Louw *et al*., 2002; McGaw and Eloff, 2008). South Africa has approximately 24 000 flora species, which is about 10% of the world's vascular plant flora (McGaw and Eloff, 2008; van Wyk, 2008).

It is estimated that between 35 000 and 70 000 tonnes of renewable (e.g. leaves, flowers, fruits, stems) and non-renewable (e.g. bark, bulbs, rhizomes) resources are collected and distributed between 50 and 100 million consumers, with a trade value of between US$75-150 million in southern Africa. Between 200 000 and 300 000 people are involved in the trade of medicinal plants, which include collectors, traders, healers and wholesalers. In 1998, an estimated 20 000 tonnes of plant material were traded in South Africa. These

figures are based on the informal herbal market trade in KwaZulu-Natal (Makunga *et al*., 2008). In the Eastern Cape 525 tonnes of medicinal plants are traded annually in a region which include Port Elizabeth/Uitenhage, East London, King Williamstown, Queenstown and Umtata, with a value of approximately R 27 million (US$6 million; at time of study) (Dold and Cocks, 2002). The natural plant product and organic sector is the fastest growing sector in the agribusiness industry, and nutrition products a multi billion dollar business world wide. Even in the United States (US) an increase of US$15 billion in 1999 to US$23 billion in 2002 was seen. World wide, approximately 85 000 plant species are reported as medicinally useful. In South Africa approximately 1 000 plant species are traded with a value of US$50-100 million per annum in the informal sector (Makunga *et al*., 2008).

Traditional medicine in the health care lacks safety, efficacy and quality control (Steenkamp, 2003b). A plant's potency, harvested from the wild or cultivated, is affected by the biochemistry of individual species, external factors (including season, geographic location, climate), ecological and growth conditions, and storage and preparation of extracts (Fennell *et al*., 2004). The following sections give an introduction to *Hypoxis* and its compounds, which are one of the most frequently used medicinal plants in South Africa.

1.2. Overview of *Hypoxis*

1.2.1. Identification, classification and distribution

Hypoxis, the 'miracle' medicinal plant of southern Africa, has become a household name for many South Africans. *Hypoxis hemerocallidea* (previously known as *H. rooperi*) topped the list of the 60 most frequently traded plant species in the Eastern Cape, South Africa, when studies were conducted among street traders, traditional healers, store-owners and clinic patients (Drewes and Khan, 2004). *Hypoxis* is known by a variety of common names including magic muthi, yellow stars, star lily, star flower, star grass, African potato, sterretjie, Afrika patat, sterblom, inkbol, gifbol (Afrikaans); inkon(m)fe,

ilabatheka, inkonfe-enkula, igudu (Zulu); moli, molikharatsa (Sesotho); tshuka (Tswana); lilabatseka, zifozonke (Swazi); and lotsane (Drewes *et al*., 2008; Katerere and Eloff, 2008; Mills *et al*., 2005; Singh, 1999). *Hypoxis* species are tuberous perennials with long, strap-shaped leaves and yellow star-shaped flowers. The brownish-black corms, which are yellow inside when freshly cut, have abundant adventitious roots to survive high-stress conditions like drought and fire (Figure 1.1). The corms are used as medicine (Nicoletti *et al*., 1992; van Wyk *et al*., 1997). *Hypoxis* belongs to the small family, Hypoxidaceae, which consists of 9 genera and about 152 species. About 60% of the species belong to the genus, *Hypoxis*, which is distributed on all the continents except Europe (Singh, 1999). In southern Africa, including South Africa, Namibia, Botswana, Lesotho and Swaziland, 30 species are found, which are mainly confined to the eastern region (Singh, 2007). It is found growing in grasslands, low scrubs, meadows and mountainous areas (Nicoletti *et al*., 1992).

Figure 1.1: Characteristics of *H. hemerocallidea*. Strap-shaped leaves and yellow star-shaped flowers (left) (van Wyk, 2008), and brownish-black corms with adventitious roots (right) (Drewes *et al*., 2008).

1.2.2. Medicinal and other uses of *Hypoxis*

Hypoxis spp. are used by the indigenous population groups of South Africa, including the Zulus, Xhosas and Sothos. Medicinal uses include the treatment of intestinal parasites, urinary infections, infertility, vomiting, nausea, cough, palpitations, heart weakness, impotency, anxiety, insanity, lice, common cold, yuppie flu, flu, wounds, arthritis, cancers, human immunodeficiency virus (HIV)/acquired immune deficiency syndrome

(AIDS)-related diseases, hypertension, diabetes, cancer, psoriasis, gastric and duodenal ulcers, tuberculosis, asthma, some central nervous system (CNS) disorders (including epilepsy and childhood convulsions), depression, laxative, vermifuge, burns, prostatitis, benign prostate hyperplasia, prostate adenoma and many more (Buwa and van Staden, 2006; Drewes *et al*., 2008; Erasto *et al*., 2005; Koduru *et al*., 2007; Mills *et al*., 2005; Ojewole, 2006; Ojewole, 2008; Risa *et al*., 2004; Singh, 1999; Steenkamp, 2003a; Steenkamp, 2003b; van Wyk *et al*., 1997; Van Wyk and Gericke, 2000). Weak infusions and decoctions of *Hypoxis* are used as convalescent and strengthening tonics for wasting diseases (van Wyk *et al*., 1997; van Wyk and Gericke, 2000). Certain *Hypoxis* spp. have antibacterial activities against *Eschericia coli*, which is associated with acute bacterial prostatitis, and *Klebsiella pneumoniae* (Buwa and van Staden, 2006; Potgieter *et al*., 1988; Steenkamp *et al*., 2006). Veterinarian uses include fertility enhancement, general ailments, heartwater, abortion, red water (babesiosis) and gallsickness in cattle (Erasto *et al*., 2005; McGaw and Eloff, 2008).

Certain *Hypoxis* spp. are also used as an emetic against fearful dreams; a charm against thunder, lightning and storms; the leaves are used to make rope; and the corms are used to make black polish to apply to the floors of huts. The corms of some species are boiled or roasted for food in times of famine by Xhosa and Sotho people (Singh, 1999).

1.2.3. Glycosides isolated from *Hypoxis*

Glycosides are the main compounds isolated from *Hypoxis* spp. Table 1.1 summarizes the different glycosides identified in *Hypoxis* spp. (Nicoletti *et al*., 1992). Glycosides isolated from *Hypoxis* spp. have a common pent-1-en-4-yne backbone or a slight modification of it (Figure 1.2).

Table 1.1: Different *Hypoxis* spp. found in Africa and the glycosides they contain.

Species	Origin	Glycosides
Hypoxis obtusa Burch	Mozambique	Hypoxoside Obtusides A and B
Hypoxis obtusa Burch.-Complex	Kenya and Zimbabwe	Hypoxoside Mononyasines A and B Obtusides A and B Nyasoside
Hypoxis nyasica Bak.	Malawi	Hypoxoside Nyasoside Nyasicoside Mononyasines A and B Nyaside
Hypoxis angustifolia Lam.	Zimbabwe	Hypoxoside Nyasoside Mononyasines A and B Nyaside Nyasol
Hypoxis interjecta Nel	South Africa	Hypoxoside Obtusides A and B Interjectin
Hypoxis multiceps Buching. Ex Krauss	South Africa	Hypoxoside Obtusides A and B
Hypoxis rooperi T. Moore	South Africa	Hypoxoside
Hypoxis acuminata Eckl.	South Africa	Hypoxoside
Hypoxis nitida Verdoorn	South Africa	Hypoxoside
Hypoxis rigidula Baker	South Africa	Hypoxoside
Hypoxis latifolia Hook.	South Africa	Hypoxoside

Adapted from Nicoletti *et al.* (1992)

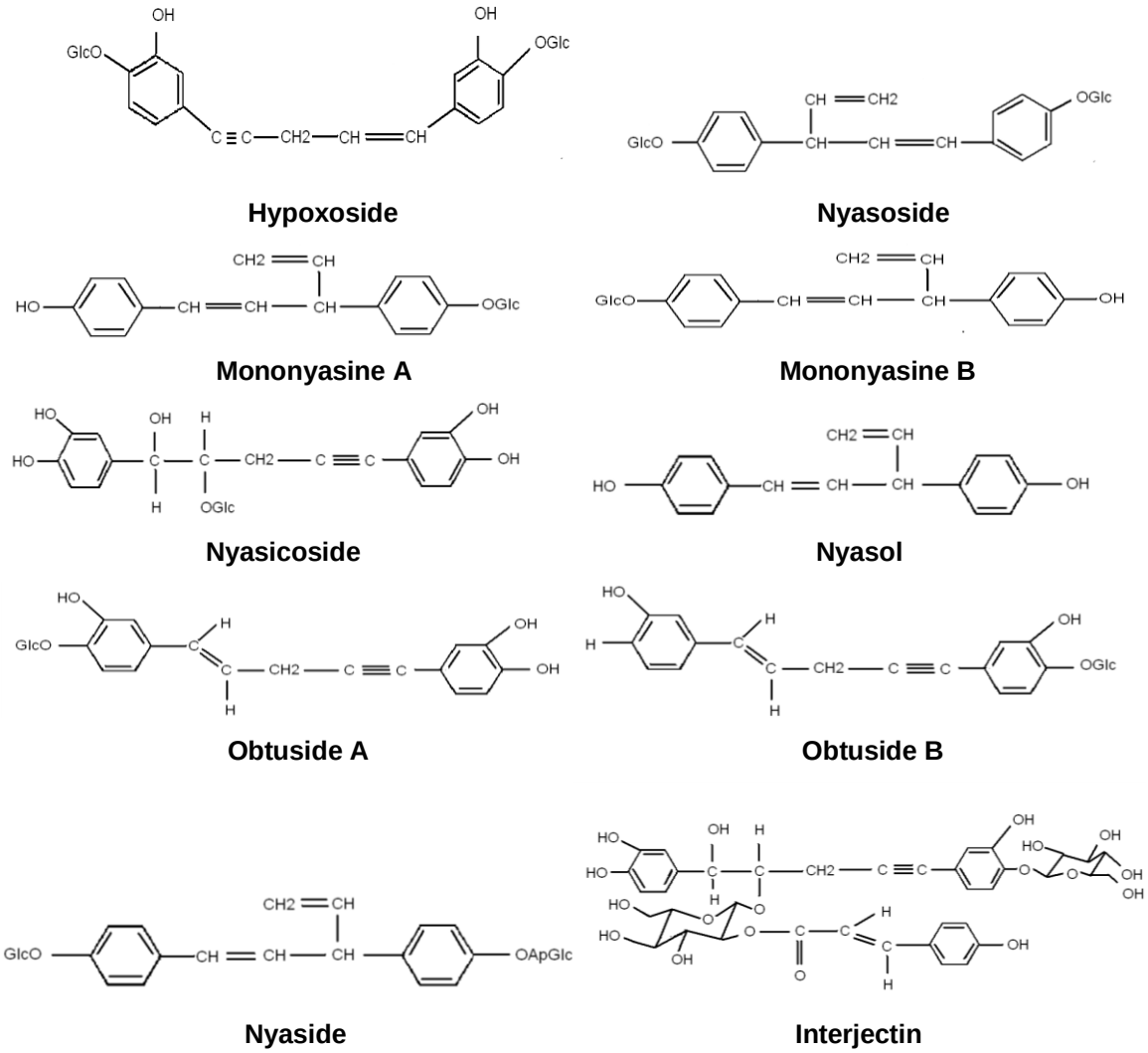

Figure 1.2: Chemical structures of the known glycosides isolated from *Hypoxis* spp. OGl indicates glucose linked to the benzene rings through O-glycosidic bonds (Marini-Bettolo *et al*., 1985; Marini-Bettolo *et al*., 1991; Messana *et al*., 1989; Sibanda *et al*., 1990).

1.2.4. Hypoxoside and rooperol: the compounds of interest

The first pentynene derivative isolated from *Hypoxis* was hypoxoside [(E)-1, 5-bis(4'-β-D-glucopyranosyloxy-3'-hydroxyphenyl) pent-4-en-1-yne] and its aglycone, rooperol (Drewes *et al*., 1984; Drewes *et al*., 1989; Marini-Bettolo *et al*., 1982; Nicoletti *et al*., 1992). Hypoxoside is regarded as a natural product, containing two protective groups in the form of glucose units at the ends of the two benzene rings of the pentynene backbone

(Drewes *et al*., 2008). Rooperol is formed when the glucose units are removed by β-glucosidase or cellulase (Drewes *et al*., 1984; Theron *et al*., 1994). β-glucosidase is mainly found in the gastrointestinal tract and is released by rapidly dividing cancer cells. The synthesis of rooperol has been achieved with limited success due to the sensitivity of the pentynene backbone when basic and acidic conditions were used for deprotonation, resulting in rearrangement of the pentynene backbone (Drewes *et al*., 1989; Mills *et al*., 2005; Potgieter *et al*., 1988).

Several studies – including anticancer (Albrecht *et al*., 1995a), anti-inflammatory (Guzdek *et al*., 1996; Laporta *et al*., 2007a; van der Merwe *et al*., 1993), antioxidant (Laporta *et al*., 2007b; Nair *et al*., 2007b) and antibacterial (Laporta *et al*., 2007a) – have shown that rooperol, and not hypoxoside, is the active compound. Rooperol is an unique compound in having (i) two ortho phenolic groups on the benzene rings, which make it a better anti-oxidant than hypoxoside; (ii) four exposed acidic phenolic groups, which enhances its biological reactivity with cytotoxic action; (iii) a prochiral center at the central -CH_2- group, which can be recognized by enzymes (Drewes *et al*., 2008).

Hypoxoside and rooperol are absent in the circulation after oral ingestion. Only the phase II metabolites of rooperol, glucuronides and sulphates, are present in the blood. The mixed glucuronide-sulphate is the major component, whereas the diglucuronide and disulphate metabolites appear as minor metabolites (20% of major metabolite) due to a shorter half-life (20 hrs) compared to the major metabolite (50 hrs) (Figure 1.3; Albrecht *et al*., 1995b). Like hypoxoside, these metabolites are non-toxic to cells in tissue culture, but are activated when treated with glucuronidase (Smit *et al*., 1995). The metabolizing activity of the gastrointestinal system (particular the colon) and the liver determine the extent of conversion of hypoxoside to rooperol, and rooperol to phase II metabolites (Albrecht *et al*., 1995b).

Kruger *et al*. (1994) have identified hypoxoside and rooperol analogues – containing 2 (bis-dehydroxy)-, 3 (dehydroxy)- and 4 hydroxyl groups – by high performance liquid chromatography (HPLC). Hypoxoside analogues were identified in a *H. hemerocallidea*

methanol (MeOH) extract and rooperol analogues were identified when hypoxoside analogues were treated with β-glucosidase. They found that (i) hypoxoside and rooperol were absent in the blood after oral ingestion of hypoxoside; (ii) hypoxoside was converted to rooperol (found in faeces) due to bacterial glucosidase in the colon; (iii) rooperol phase II metabolites (diglucuronide, disulfate and glucuronide-sulfate conjugates) were present in the blood.

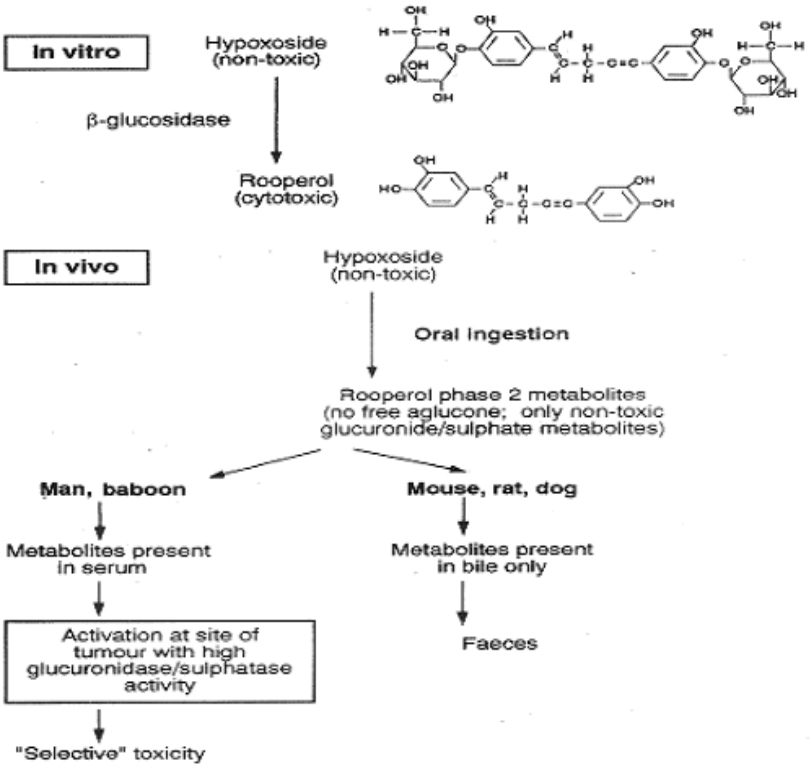

Figure 1.3: Conversion of hypoxoside to rooperol and rooperol to phase II metabolites in *in vitro* and *in vivo* studies, respectively. The presence of rooperol metabolites in the bile of experimental animals (mouse, rat, dog), excluded their use as *in vitro* anticancer models for hypoxoside (Smit *et al*., 1995).

1.2.5. Commercial products of *Hypoxis* and its compounds

Harzol®. The first commercial product of *Hypoxis*, Harzol®, dates back to 1967 when Liebenberg and Pegel became interested in the chemical constituents of *H. hemerocallidea*. Harzol® consisted of β-sitosterol and its sterolin, β-sitosterol glucoside,

which were isolated from *Hypoxis*. In Germany it was used for the treatment of benign prostate hypertrophy [non-cancerous enlargement of the prostate in males (Drewes *et al*., 2008)]. The mechanism of action involved the inhibition of 5α-reductase or preventing binding of dihydrotestosterone within the prostate (Drewes and Khan, 2004; Hostettmann *et al*., 2000; Pegel, 1997; Singh, 1999; van Wyk, 2008).

Moducare®. β-sitosterol and its sterolin (100:1 mass ratio) in Moducare® were first isolated from *Hypoxis*, but these compounds are now isolated from pine oil and soya. It enhances the *in vitro* proliferative response of human T cells, hence its use as an immune system booster (Drewes *et al*. 2008; Drewes and Khan, 2004; Singh, 1999).

Hypo-Plus. Hypo-Plus is used as a food supplement, energy booster and immunity modulator. It contains amino acids, vitamins C, B_6 and B_{12}, anti-oxidant components and phytosterols from *Hypoxis*. It is used for the treatment of diabetes, impotency, gout, arthritis, HIV/AIDS and memory loss (Drewes *et al*., 2008; Drewes and Khan, 2004).

Prostone. Sold as an immune system booster in Europe and contains *Hypoxis* derived phytosterols (Abegaz *et al*., 1999).

Hypoxis extracts are commercially found, on its own or in combination with other plant extracts, in products such as Vuselela, Vikilela, Nutriherb, Down to Earth (Appendix 1), Smart *Hypoxis*, and many more. It is generally found in capsule form, but also in creams, soaps, and more.

Several patents for *Hypoxis* extracts, its compounds and uses have been published between 1970 and 1990. Some of these include:

- Pharmaceutical corm extract of *Hypoxis*, anti-inflammatory and for the treatment of prostate gland hypertrophy by Liebenberg, 1969 (Nicoletti *et al*., 1992).
- Extraction of phytosterol glycosides from *Hypoxis* tubers by Pegel and Liebenberg, 1973 (Nicoletti *et al*., 1992).
- Extraction of sterolins from plant material (Pegel, 1976).
- Active plant extracts of Hypoxidaceae and their use (Pegel, 1979).
- Sterolins and their use (Pegel, 1980).

- Rooperol derivatives by Drewes and Liebenberg, 1982 (Nicoletti *et al*., 1992).
- Extracts of plants of the Hypoxidaceae family for the treatment of cancer by Drewes and Liebenberg, 1983 (Nicoletti *et al*., 1992).
- Rooperol and its derivatives (Drewes and Liebenberg, 1987).
- Process for the preparation of rooperol (Wenteler *et al*., 1991).

1.3. (Phyto)sterols and sterolins

1.3.1. Structural characteristics

Cholesterol ($C_{27}H_{45}OH$) is an important component of animal fat and some vegetable fats (including palm oil, soybean oil, rapeseed oil). It is taken up via nutrition or can be synthesized and stored endogenously in the liver, intestines, adrenal glands and reproductive organs (De Brabander *et al*., 2007). Plant sterols, also known as phytosterols or 4-demethylsterols, are synthesized in plants and must be consumed via the diet by humans and animals (Ling and Jones, 1995). The most commonly found phytosterols are sitosterol (65%), campesterol (30%) and stigmasterol (5%) (Moghadasian, 2000; Pegel, 1997) (Figure 1.4). Phytosterols are structurally and functionally similar to cholesterol. All sterols are derived from hydroxylated polycyclic isopentenoids (Abidi, 2001) and have a characteristic fused 1,2-cyclopentanophenanthrine ring structure, which form the steroid nucleus with a 3β-hydroxyl group and 5,6-double bond. Although the nucleus structures of phytosterols resemble those of cholesterol, they differ regarding the side chain at C-17, double bond at C-22 and substituted methyl or ethyl groups at C-24. β-sitosterol and campesterol have ethyl and methyl groups at C-24, respectively. Stigmasterol is characterized by an ethyl group at C-24 and a double bond at C-22. Sterols, which have undergone 5α-reduction of the double bond (also known as saturation), are known as stanols (e.g. sitostanol, campestanol, cholestanol). Phytosterols are found in free form or as conjugates, where the 3β-hydroxyl group is esterified to fatty acids or glycosides (De Brabander *et al*., 2007; Kritchevsky and Chen, 2005; Lagarda *et al*., 2006; Ostlund, 2002; Quilez *et al*., 2003). In nature, plants contain sterols with their associated sterolins. Sterolins are

glucosides joined to sterols, which are easily destroyed. Sterols lose their immune-enhancing benefits when sterolins are lost (Pegel 1997).

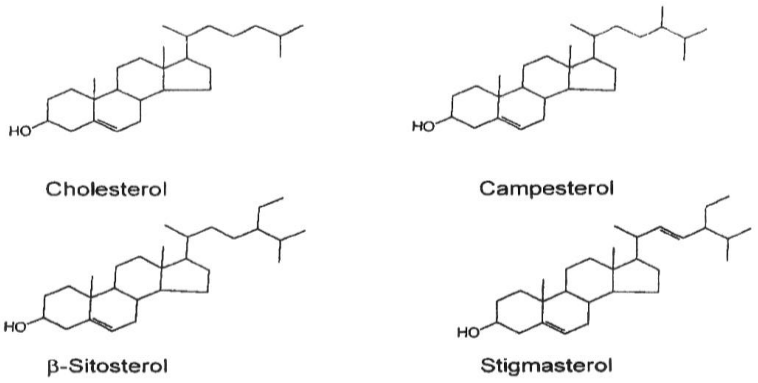

Figure 1.4: Chemical structures of cholesterol and the three most commonly found phytosterols (β-sitosterol, campesterol and stigmasterol) in plants (Awad and Fink, 2000).

1.3.2. Sources, intake and absorption of (phyto)sterols

Phytosterols are found in unrefined vegetable oils (e.g. sunflower, corn, safflower, olive and soybean), nuts (e.g. walnuts, almonds, Brazil nuts, hazelnuts, peanuts and macadamia nuts), vegetables and fruits, bread, cereals (e.g. wheat and corn), margarines, seeds (e.g. sesame seed and wheat germ) and legumes. The estimated daily phytosterol consumption is between 160-400 mg/day, which vary among populations for example Finland: 140-360 mg/day, United Kingdom (UK): 163 mg/day, US: 180 mg/day and Japan: 400 mg/day (de Jong *et al*., 2003; Lagarda *et al*., 2006; Moghadasian, 2000; Ostlund, 2002)

Up to 95% of dietary phytosterols entering the colon will be excreted (Ling and Jones, 1995). The percentage of phytosterols absorbed in the intestine ranges between 0.5-5% and that of phytostanols may be 10% of free phytosterols. These percentages are significantly lower compared to cholesterol (35-70%). Phytostanols may lower free phytosterol absorption and vice versa (de Jong *et al*., 2003; Kritchevsky and Chen, 2005; Ling and Jones, 1995; Ostlund, 2002). Phytosterol absorption increases when esterified to form esters (Moghadasian, 2000; Ostlund 2002). The low absorption of phytosterols and -stanols may be explained by (i) poor esterfication [low affinity of acyl-coenzyme A

cholesterol acyltransferase (ACAT)]; (ii) side chain length and presence of Δ5 double bond (saturation); (iii) mutations and polymorphisms in adenosine triphosphate (ATP)-binding cassette (ABC)G5/ABCG8 transporters, which transport free phytosterols back into the intestinal tract; (iv) micellar solubility; (v) slower transfer rate of sitosterol from the cell surface to intracellular site compared to cholesterol (de Jong *et al*., 2003; Igel *et al*., 2003; Moghadasian, 2000; Ostlund 2002). Increased phytosterol levels are found in the adrenal glands, intestinal epithelia, ovaries and testis, and in trace amounts in the aorta, muscle, skin subcutaneous adipose tissue and liver (de Jong *et al*., 2003).

The presence of low phytosterols in the serum and tissues of healthy humans may be due to (i) binding of sterol(in)s to plant fibers making absorption of digested food in the gut difficult; (ii) modern diet consisting of over-processed food and minimal fruit and vegetables (Moghadasian, 2000). Phystosterol concentrations in the plasma range between 7 and 41 μM (von Holtz *et al*., 1998). Most β-sitosterol research uses 8-16 μM of β-sitosterol, which is within the physiological range.

1.3.3. Cholesterol lowering effects of phytosterols

Coronary heart disease is the leading cause of death in developed countries (Andersson *et al*., 2004). Cholesterol, cholesterol esters and other lipids cause the narrowing and hardening of arteries, which may lead to atherosclerosis and thrombosis. Absorbed plasma sterols circulate the plasma via lipoproteins. Atherosclerosis is characterized by an increase in low-density lipoprotein (LDL) cholesterol and a decrease in high-density lipoprotein (HDL) cholesterol. Blood LDL cholesterol levels are an indicator of heart attack risk (Tapiero *et al*., 2003). Phytosterols and -stanols decrease atherosclerotic lesion size and complexity (de Jong *et al*., 2003).

Phytosterols lower serum's total and LDL cholesterol, without affecting HDL cholesterol and triglycerides. LDL-cholesterol is reduced between 5% and 15% when consuming 1.5-3g of phytosterols daily. LDL-cholesterol lowering by phytosterols depends on the dose of phytosterols consumed, form of phytosterol, vehicle in which phytosterol is

solubilized, diet, genetic factors and starting cholesterol concentration. Lowering of cholesterol by phytosterols is achieved by daily treatment over long periods (> three weeks) of time. Cholesterol lowering activity by phytosterols and -stanols depends on solubilization and incorporation into micelles. Phytosterols increase the pharmaceutical action of the cholesterol lowering agents, statins and fibrates. Phytosterols and statins increase cholesterol elimination and reduce cholesterol biosynthesis, respectively. It is estimated that a 10% decrease in blood cholesterol levels will reduce the risk of cardiovascular diseases by 19-54% depending on a person's age (Andersson *et al*., 2004; De Brabander *et al*., 2007; Ostlund 2002; Quilez *et al*., 2003; Richelle *et al*., 2004). Jakulj *et al*. (2005) have shown that combination treatment of high cholesterol with phytosterols and -stanols, and ezetimbe had a greater total cholesterol and LDL-cholesterol lowering effect than either treatment alone.

The cholesterol-lowering activity of phytosterols and -stanols may be explained by (i) the displacement of cholesterol from mixed micelles by phytosterols and -stanols due to greater hydrophobicity than cholesterol; (ii) a reduced esterfication rate of cholesterol in the enterocytes and cholesterol excretion via chylomicrons; (iii) the upregulation of ABC-transporter expression in intestinal cells by stanols, which may increase cholesterol excretion by enterocytes back into the lumen; (iv) displacing cholesterol from the bile (de Jong *et al*., 2003; Ostlund 2002; Richelle *et al*., 2004; Tapiero *et al*., 2003).

Cholesterol reduction may cause an increase in endogenous cholesterol synthesis; higher LDL-receptor expression and lower circulating LDL-cholesterol concentrations (Ostlund 2002; Tapiero *et al*., 2003).

1.3.4. Benefits/function and roles of sterols

Sterols play an important role in the structure and function of cell membranes. Cholesterol in its free form is an important membrane component and when esterified to fatty acids, plays an important transport and storage role (Pegel, 1997). Phytosterols and -stanols are incorporated into cellular membranes and may influence membrane

properties (de Jong *et al*., 2003). β-sitosterol influences membrane fluidity by altering the lipid composition and influencing signal transduction pathways, which affect cell growth and differentiation (Tapiero *et al*., 2003). Cholesterol is a precursor of sex steroids and corticosteroids in animals, and cardenolides and bufadienolides in plants (De Brabander *et al*., 2007; Pegel, 1997).

β-sitosterol has anti-inflammatory, antioxidant, antipyretic, anti-atherosclerotic, anti-ulcer, anti-neoplastic, anti-complement, antidiabetic, and immune modulating properties (Bouic and Lamprecht, 1999; Lagarda *et al*., 2006; Pegel, 1997). Populations with high soybean-based diets, which are rich in phytosterols, have lower cancer (especially colon and prostate) mortality rates (de Jong *et al*., 2003). Several researchers have shown that β-sitosterol has anticancer activity against several human cancer cell lines, including colon [HT-29 (Awad *et al*., 1996; Awad *et al*., 1998)], prostate [LNCaP (von Holtz *et al*., 1998)] and breast [MDA-MB-231 (Awad *et al*., 2001a; Awad *et al*., 2003a/b) and MCF-7 (Awad *et al*., 2007)] cancer cells. Phytosterols decrease prostatic 5α-reductase and prostatic aromatase activities in rats, which is associated with prostate metabolism and growth (Awad *et al*., 1998; Tapiero *et al*., 2003).

β-sitosterol and its sterolin increase the *in vitro* proliferation of T-cell production, natural killer (NK) cell activity, and secretion of interleukin (IL)-2 and interferon (IFN)γ (Bouic *et al*., 1996; Breytenbach *et al*., 2001). Phytosterols may enhance the activity of Th1 cells and decrease or have no effect on Th2 cells (Bouic and Lamprecht, 1999). Phytosterols decrease IL-4, IL-6 and IL-10 involved in B-lymphocyte differentiation and inflammation, cortisol:DHEA ratio in marathon runners (lower inflammatory response), and overreactive antibody response (Bouic and Lamprecht, 1999; de Jong *et al*., 2003). Increased phytosterol intake may have therapeutic benefits for diseases like tuberculosis, allergies, cancer, chronic viral infections, autoimmune diseases and rheumatoid arthritis (Bouic and Lamprecht, 1999).

Phytosterols are used as emulsifiers, steroidal intermediates and precursors for hormone production, and antipolymerization agents for frying oils in the cosmetic, pharmaceutical and food industry, respectively (Abidi, 2001).

1.3.5. Functional foods

It is estimated that global cardiovascular disease deaths will increase from 14 million (1990) to 23 million (2020), which accounts for one third of all deaths. The serum LDL-cholesterol lowering properties of phytosterols have led to the development of functional foods. Phytosterol esters have been approved as safe in functional foods. The US Food and Drug Administration (FDA) and The Scientific Committee on Food (Europe) have approved the use of phytosterol esters in spreads at 13.3% and 8% by weight, respectively (Lagarda *et al*., 2006). Examples of functional foods are spreadable fats, milk, soy milk, yogurts, yogurt drinks, mayonnaises, bars, meat and soups, vegetable oils, orange juice and green teas (Berger *et al*., 2004; Lagarda *et al*., 2006).

Functional foods are designed and developed to reduce a specific disease risk by enhancing or promoting health. During 2000, Pro-active (a spread or margarine with added phytosterols) was developed in The Netherlands and launched in South Africa. Phytosterols are present in the diet at low levels, but can be increased when added to a suitable food vehicle. Pro-active's manufacturer claimed that the daily intake of 20g of spread (~2g plant sterol) will lower total and LDL cholesterol by 10-15%, and lower ischaemic heart disease by 25% after 2 years. Esterification of sterols with fatty acids increases solubility in lipids and increase incorporation in the lipid phase of food vehicles (Vorster *et al*., 2003). Food vehicles are fat or oil based and include spreads, salad dressings, cream cheese, yogurt, low fat milk products, chocolate, and many more (Berger *et al*., 2004; Vorster *et al*., 2003).

1.3.6. Adverse/side effects of phytosterols

Phytosterols are non-toxic and rarely associated with side effects (Pegel, 1997). Phytosterols may decrease plasma concentrations of carotenoids (α- and β-carotene),

lycopene, calcium, and fat-soluble vitamins A, D, E, and K. Phytosterolaemia/ sitosterolaemia is a rare inherited genetic disorder associated with abnormally high plasma concentrations of phytosterols/sitosterol due to increased absorption rates and decreased elimination rates, which may be due to mutations in the ABC transporters expressed in the intestinal and liver cells. Patients develop Achilles tendon xanthomas, accelerated atherosclerosis (acute myocardial infarction), haemolytic episodes, arthritis and arthralgias (de Jong *et al*., 2003; Moghadasian, 2000; Ostlund, 2002; Richelle *et al*., 2004; Vorster *et al*., 2003). The carotenoid lowering effect of phytosterols can be prevented by a higher intake of fruits or vegetables rich in carotenoids (Berger *et al*., 2004).

Increased phytosterol concentrations in erythrocyte membranes may cause increased fragility and haemolysis. Replacement of cholesterol with phytosterols increases membrane rigidity, which may lead to possible haemorrhagic stroke when serum cholesterol levels are too low. A decrease in intestinal cholesterol and related lipid absorption may influence cellular cholesterol and steroid metabolism and function (Moghadasian 200l; Vorster *et al*., 2003).

CHAPTER 2

AIMS OF THE STUDY AND OVERVIEW OF CHAPTERS

The use of the African potato has been controversial over the last few years. South Africa's previous minister of health, dr. Mantho Tshabalala-Msimang has promoted the use of the African potato not only in South Africa, but also abroad. The following statement has elicited criticism from around the world:

'…and eating garlic, olive oil, beetroot and the African potato boosts the immune system to ensure the body is able to defend itself against the virus (HIV) and live with it…'

In a country with the highest percentage of HIV, statements like these must be proven scientifically.

The main aim of this study was to provide scientific data on the medicinal – including anticancer, anti-inflammatory and antioxidant – properties of three *Hypoxis* spp. and its purified compounds.

The objectives of this study were:

- To identify sterols and sterolins in three *Hypoxis* spp.
- To quantify and compare sterol(in)s and hypoxoside in three *Hypoxis* spp.
- To compare the *in vitro* anticancer activities of three *Hypoxis* spp. and its purified compounds against the HeLa, HT-29 and MCF-7 cancer cell lines.
- To determine the anticancer mechanism(s) of action involved.
- To determine the anti-inflammatory activities of the *Hypoxis* extracts and its purified compounds.
- To determine the antioxidant activities of the *Hypoxis* extracts and its purified compounds.

Chapter 3 focuses on *Hypoxis* spp. selection, extract preparation and the analytical analysis of hypoxoside and (phyto)sterol(in)s in three *Hypoxis* spp. Qualitative and quantitative analysis of (phyto)sterols were performed using TLC and GC, respectively. Quantitative analysis of hypoxoside was performed using HPLC.

Chapter 4 focuses on the anticancer properties of *Hypoxis* spp. and its purified compounds. β-glucosidase and hypoxoside-to-rooperol conversion in HeLa, HT-29 and MCF-7 cancer cells were determined. Cytotoxicity of *Hypoxis* extracts and its purified compounds on HeLa, HT-29 and MCF-7 cancer cells, and PBMCs were performed using MTT and CellTiterBlue® assays, respectively. IC_{50} values of hypoxoside and rooperol were determined for HeLa, HT-29 and MCF-7 cancer cells, and PBMCs. Mechanism(s) of action investigated include DNA cell cycle arrest (confirmed by increased $p21^{Waf1/Cip1}$ expression), caspase-3 and/or -7 activation, phosphatidylserine translocation and DNA fragmentation.

Chapter 5 focuses on endoreduplication, a cell survival strategy, in HeLa, HT-29 and MCF-7 cancer cells induced by *Hypoxis* extracts and its purified compounds. Anti-apoptotic proteins investigated include phospho-Akt, phospho-Bcl-2 and $p21^{Waf1/Cip1}$. In this study, endoreduplication was first seen in the histograms of DNA cell cycle arrest. Phase-contrast light and DAPI fluorescence microscopy confirmed the presence of apoptotic cells and cells undergoing endoreduplication in these three cancer cell lines.

Chapter 6 focuses on the anti-inflammatory properties of *Hypoxis* extracts and its purified compounds. Differentiation of U937 cells to monocyte-macrophages was optimized by using PMA and $1,25(OH)_2D_3$ over different time periods. Monocyte-macrophage differentiation was confirmed by phase-contrast light microscopy, and CD11b and CD14 cell surface marker staining. The effect of *Hypoxis* extracts and its purified compounds on NO production, COX-2 expression and phagocytosis on monocyte-macrophages, and pro- and anti-inflammatory cytokine production in PBMCs were investigated.

Chapter 7 focuses on the antioxidant properties of *Hypoxis* extracts and its purified compounds. The effect of *Hypoxis* extracts and its purified compounds on ROS production in undifferentiated and differentiated U937 cells, antioxidant potential (using the FRAP assay) and SOD activity in Chang liver cells were investigated.

Chapter 8 summarizes the findings of this study.

CHAPTER 3

PLANT SELECTION, EXTRACTION AND ANALYTICAL ANALYSIS OF COMPOUNDS IN *HYPOXIS* SPP

3.1. Plant selection

Corms of *H. hemerocallidea* (voucher number: PEU 14798) and *H. stellipilis* (PEU 14841) were purchased in Port St Johns and Port Elizabeth (Xhosa traditional medicine shop), respectively, in the Eastern Cape, South Africa. Corms of *H. sobolifera* var *sobolifera* (PEU 14840) were collected near Plettenberg Bay in the Southern Cape, South Africa. Corms of the three *Hypoxis* spp. were planted in the same soil type and exposed to equal amounts of sunlight, humidity and water for at least six months before they were harvested and used fresh. The *Hypoxis* spp. were identified by Y. Singh from the South African National Biodiversity Institute (SANBI) and voucher specimens were deposited in the Nelson Mandela Metropolitan University herbarium.

H. hemerocallidea Fisch., C.A. Mey. and Avé-Lall (Figure 3.1) has a broad distribution in the Eastern Cape, KwaZulu-Natal, Gauteng and Limpopo provinces of South Africa, Lesotho, Mozambique, Zimbabwe and further northwards into east Africa. The corms may reach diameters of 100-150 mm (Drewes *et al*., 2008). *H. hemerocallidea* has broad, slightly hairy leaves, which are arranged one above the other and spreading outwards from the center of the plant. The bright yellow, star-shaped flowers are borne on long, green and slender pedicels from October to January (van Wyk *et al*., 1997).

H. stellipilis Ker-Gawl. (Figure 3.1) is mainly found in the grassy areas of the southeastern part (Eastern Cape) of South Africa and is the most commonly sold *Hypoxis* species in the traditional herbal shops of Port Elizabeth, Eastern Cape. *H. stellipilis* grows up to 300 mm. The leaves form a thick, slightly twisted rosette and have dark green upper surfaces with slightly wavy edges and the reverse side is silvery due to the presence of hairs. The bright yellow star-shaped flowers have six orange stamens and are

borne on pinkish, hairy pedicels from March to November. *H. stellipilis* has long adventitious roots (Vanderplank, 1998).

H. sobolifera var *sobolifera* (Jacq.) Nel. (Figure 3.1) is distributed in the Western Cape, Eastern Cape and KwaZulu-Natal, and is mainly found along the coast, where it grows in dune vegetation and open grasslands. The leaves (4-12) are arranged in three ranks and are evenly covered with hairs on both sides. Leaves of plants growing in the shade are 2-3 times longer and broader than those growing in open grassland. Two to six flowers per inflorescence are borne on 40-70 mm long pedicels throughout the season. It grows in clumps via stolon formation and can be easily propagated via rootstock division (Singh *et al*., 2007).

Figure 3.1: Pictures of *H. hemerocallidea* (left), *H. stellipilis* (middle) and *H. sobolifera* var *sobolifera* (right).

3.2. *Hypoxis* extracts

3.2.1. Background

Traditional healers use mainly water and boiling to prepare extracts from medicinal plants, due to limited access to lipophilic solvents (Buwa and van Staden, 2006; Louw *et al*., 2002). Inexpensive and freely available alcohols [including ethanol (EtOH) and MeOH] are also used to prepare extracts, which possess antimicrobial and anti-inflammatory properties (Louw *et al*., 2002). All of the active compounds may not be extracted when using a single extraction solvent, for example non-polar solvents will

extract more non-polar compounds, whereas polar solvents will extract more polar compounds. The dosage depends on the solvent used during extraction, for example higher dosages of water extracts can be administered, while the same dosage of a lipophilic solvent extract may be dangerous (Buwa and van Staden, 2006). The bulbs and tubers of bulbous, tuberaceous and rhizomatous plants can be kept for longer periods and herbalists claim that these storage organs contain the highest concentration of medicinal compounds (Louw *et al*., 2002).

3.2.2. Materials and Methods

H. sobolifera extracts. Corms of *H. sobolifera* were crushed using a mortar and pestle, and homogenizer. Polar solvents used for extraction included water, EtOH, MeOH and acetone, whereas the non-polar solvents used for extraction included chloroform ($CHCl_3$) and dichloromethane. Solvents were added to the plant material in a 10:1 (v/w) ratio, vortexed and extracted for 24, 48 and 72 hrs. The supernatants were removed by evaporation in vacuo (EtOH, MeOH, acetone, $CHCl_3$ and dichloromethane extracts) and freeze-dried (water extract). *H. sobolifera* was chosen to prepare polar extracts to test if more polar solvents would yield any hypoxoside, because hypoxoside was absent in the chloroform extracts (section 3.3.3.2).

Chloroform extracts. Corms of *H. hemerocallidea*, *H. stellipilis* and *H. sobolifera* were washed, peeled, grated and crushed using a mortar and pestle. $CHCl_3$ was added to the plant material in a 1:1 (v/w) ratio, vortexed (five min), extracted (15 min) and centrifuged (3600 x g for five min) at room temperature. The supernatant was removed and the extracting method repeated with the same plant material. The $CHCl_3$ was evaporated *in vacuo* and the mass of extracts determined. After mass determination the extracts were redissolved in $CHCl_3$ until further use.

3.2.3. Results and Discussion

Different solvents were used to extract compounds and to optimize extraction from *H. sobolifera*. The percentage yield for each solvent extract of *H. sobolifera* is summarized in Table 3.1.

Table 3.1: Percentages of yield for *H. sobolifera* extracts, using different polar and non-polar solvents over different time periods.

Solvent	Crushing method	% Plant extract yield* over time		
		24 hrs	**48 hrs**	**72 hrs**
Water	Mortar and pestle	4.0	6.0	6.5
	Homogenizer	4.5	4.5	5.8
EtOH	Mortar and pestle	4.5	5.5	7.5
	Homogenizer	3.5	5.25	4.5
MeOH	Mortar and pestle	4.5	6.5	6.0
	Homogenizer	3.3	6.0	6.3
Acetone	Mortar and pestle	1.0	4.0	5.0
	Homogenizer	7.0	6.0	4.5
CH_3CN	Mortar and pestle	25	32	55
	Homogenizer	15	36	30
Dichloromethane	Mortar and pestle	22	21	43
	Homogenizer	5.3	21	31

* Dry weight of extract as percentage of wet weight of starting material

Most of the previous studies focused on water, MeOH and EtOH extracts of *Hypoxis*, in particular *H. hemerocallidea*. In this study we were interested in phytosterols in addition to the already identified compound, hypoxoside. Phytosterols are non-polar compounds; hence more non-polar solvents (including $CHCl_3$ and dichloromethane) would give the highest percentages of yield (as seen in Table 3.1). The yield of chloroform extracts of *H. hemerocallidea*, *H. stellipilis* and *H. sobolifera* is presented in Table 3.2.

Table 3.2: Percentages of yield for *Hypoxis* extracts, using chloroform. Plant material was extracted twice for 15 min.

***Hypoxis* spp.**	**Initial weight of fresh plant material (g)***	**Final dry weight (g)***	**Percentage yield (w/w)**
H. hemerocallidea	342	1.34	0.39
H. stellipilis	532	3.01	0.57
H. sobolifera	348	0.57	0.16

* average of three extractions

Percentages of yield for chloroform extracts were low, which may be due to the shorter extraction period. *H. stellipilis* and *H. sobolifera* yielded the highest and lowest percentages of extract, respectively. Standard deviations of the three extractions are not shown due to high variability. Variability may be due to the degree of grating, crushing with mortar and pestle, and vortexing.

3.3. Analytical Analysis of Compounds in *Hypoxis* spp.

3.3.1. General Background

Quality, safety and efficacy data on plants, their extracts and active ingredients, and correct identification of species concerned (fresh, dried or powdered form) are urgently needed in a country where traditional medicine is used by the majority of the population. In South Africa, a relatively small number of plant species has been scientifically validated. Recently, pharmaceutical monographs containing identity standards and quality control profiles for 60 indigenous plant species (including *H. hemerocallidea*), used in traditional medicine were drawn up, based on World Health Organization (WHO) guidelines (Springfield *et al*., 2005).

3.3.1.1. (Phyto)sterol(in)s isolation

Phytosterols are qualitatively and quantitatively analyzed in food to evaluate their contribution to the overall diet intake and used in certain control processes (e.g. adulteration in vegetable oils). The cholesterol lowering and beneficial physiological effects (Chapter 1, section 1.3.3) of phytosterols and -stanols have led to their quantification in foods and diets. Phytosterols are found in food as free sterols, steryl esters, steryl glycosides (syn. sterolins) and acylated steryl glycosides. No reference method has been developed for phytosterol and -stanol analysis in sterol-enriched food (Lagarda *et al*., 2006; Piironen *et al*., 2000). Phytosterols are separated with great difficulty from cholesterol and from each other due to the similarity in structures when using physical methods, unless powerful methods [gas chromatography (GC) and HPLC] with thousands of theoretical plates are used (Ostlund, 2002). Sterol analysis involves the extraction of a lipid fraction from homogenized sample material, saponification (alkaline hydrolysis), extraction of non-saponifiables, extract clean up, sterol derivatization and separation with quantification.

(i) *Sterol isolation and extraction.* Most methods used to extract lipids will also extract phytosterols. Phytosterol extraction depends on the matrix (nature of source), physical state (liquid or solid) and form (free, esterified or glycosylated) of phytosterols. Different solvent systems used for phytosterol extraction include acetonitrile (CH_3CN): MeOH (high sterol yield), CH_3CN: MeOH: water, hexane, methylene chloride, and acetone. CH_3CN and MeOH can be replaced by dichloromethane and isopropanol, respectively. Supercritical fluid extraction (SFE) and supercritical fluid fractionation (SFF) give high sterol yields of approximately 95-100% (Abidi, 2001; Lagarda *et al*., 2006; Moreau *et al*., 2002; Piironen *et al*., 2002). Non-polar solvents extract free phytosterols and phytosteryl fatty-acid esters, whereas more polar solvents extract steryl glycosides (many carbohydrate groups) and fatty-acylated steryl glycosides (Moreau *et al*., 2002; Piironen *et al*., 2002).

(ii) Saponification. Saponification or alkaline hydrolysis with ethanolic potassium hydroxide is used to hydrolytically cleave phytosterol conjugates to release free sterols. This process is laborious and cannot be used to hydrolyze the hemiacetyl bond between the sterol and carbohydrate moiety of steryl glycosides. Acid hydrolysis with hydrochloric acid (HCl) is used to liberate sterols from their glycosides, but is not suitable for certain phytosterols (e.g. fucosterol) found in certain plant families due to decomposition and isomerization (Moreau *et al*., 2002; Piironen *et al*., 2000). Enzymatic methods (e.g. β-glucosidase and cholesterol ester hydrolase) have been used to solve the problems associated with alkaline and acid hydrolysis and to cleave steryl glycosides to yield free phytosterols (Moreau *et al*., 2002). Solvent removal with anhydrous sodium phosphate and alumina yields an unsaponifiable residue suitable for chromatographic quantification (Abidi, 2001; Lagarda *et al*., 2006). The unsaponifiable fraction represents approximately 1% of total material in food lipids and contains phytosterols, carotenoids, tocopherols, and other hydrocarbons. These can be further extracted with non-polar solvents (hexane, cyclohexane and hexane/diethyl ether) (Piironen *et al*., 2000).

(iii) Separation/purification of sterols. Thin layer chromatography (TLC) and column chromatography (CC) are accessible and affordable procedures used for sample clean up and purification. TLC is a simpler technique but is only appropriate for small quantities of compounds (<200 mg), while CC is more complex but can be used to separate and purify larger quantities. These techniques can be used for qualitative analysis and sterol estimates but not for quantification due to inadequate analytical precision. These techniques are laborious, time-consuming, lack automation and large volumes of organic solvents are required. Solid phase extraction (SPE) is more often used to isolate sterols, because it is faster, many samples can be separated or purified, and less solvents are required (Abidi, 2001; Lagarda *et al*., 2006; Piironen *et al*., 2000).

(iv) *Forming sterol derivatives.* Sterol and stanol separation is possible without derivatization, but resolution of sterols and their corresponding stanols is not as good as that of their trimethylsilyl (TMS) derivatives. Derivatives yield better peak shape, resolution, sensitivity and higher stability with thermally labile unsaturated sterols

(Lagarda *et al*., 2006; Moreau *et al*., 2002; Piironen *et al*., 2000). Derivatizing agents used include TMS, acetate, N-methyl-N-trimethyl-silyltrifluoroacetamide (MSTFA) in anhydrous pyridine and bis(trimethylsilyl)-trifluoroacetamide (BSTFA) containing 1% of trimethylchlorosilane (TMCS) (Lagarda *et al*., 2006). The former two derivatizing agents are the most commonly used (Abidi, 2001).

(v) *Analysis*. Sterol peaks are represented by retention times relative to a reference standard or internal standard (Abidi, 2001). Examples of internal standards are 5α-cholestane, betulin, cholestane, 5 β-cholestan-3α-ol (epicoprostanol) and 5α-cholestan-3β-ol. The internal standard must be structurally similar to the analyte's structure e.g. epicoprostanol resembles sterol's structure (Lagarda *et al*., 2006). The use of standards is important to eliminate analytical errors like fluctuations in instrument operating conditions and other experimental variables. The two most commonly used methods for sterol analysis are GC and HPLC. GC is the technique of choice due to shorter analysis time (capillary columns), less peak interference, better resolution and sensitivity (detecting individual sterols in the low nanogram range). GC separation depends on the sterols' polarity and volatility. Partitioning between the sterol and stationary liquid phase is influenced by both polarities. Volatility (related to molecular mass, size and volume) can be increased by derivatization. Increasing the polarity of the stationary phase will improve the resolution of a sterol mixture with similar structures. Non-polar stationary phases (100% polysiloxane) are the most commonly used, but better resolution is achieved with slightly more polar stationary phases (e.g. 95% dimethylpolysiloxane: 5% diphenyl). The SAC-5 column (Supelco) has been specially developed for reproducible analysis of sterols. Very few packed GC columns have been used for phytosterol analysis.

HPLC operates under milder column temperatures and non-destructive detection conditions compared to GC. It is more suitable for analyzing thermally unstable sterols (Abidi, 2001), but high lipophilicity of sterols makes sample processing and chromatography difficult (Lagarda *et al*., 2006). Reverse phase (RP) HPLC is more frequently used than normal phase (NP) HPLC. RP-HPLC uses low volatile polar

organic solvents in water, which equilibrate the bonded silica stationary phase; gives reproducible chromatographic peak characteristics, good column selectivity; hydrophobic interaction between the analyte and stationary phase increase with increasing molecular mass and decreasing number of double bonds in sterols. Alkylsilica stationary phases [e.g. octadecylsilica (ODS)] and polar organic solvents (e.g. CH_3CN and MeOH) are most frequently used. An isocratic system is mostly used, while a gradient system is used for the analysis of a wide range of compounds (Abidi, 2001). HPLC is not selective enough to separate sterols and their stanols (Piironen *et al*., 2000). NP-HPLC separates phytosterol lipid classes (free sterols, fatty acyl sterols, steryl glycosides and acylated steryl glycosides), while RP-HPLC separates molecular species (individual compounds) comprising a lipid class. Although methods are available for the simultaneous analysis of non-polar (free sterols and fatty acyl sterols) and polar (steryl glycoside and acylated steryl glycoside) sterol lipid classes, the most accurate way of quantification is to analyze these classes separately (Moreau *et al*., 2002).

Sterols can be detected by ultraviolet (UV; 200-210 nm), photodiode array detection (DAD), mass spectroscopy (MS), nuclear magnetic resonance (NMR), infrared (IR), evaporative light scattering detection (ELSD) and flame ionization detection (FID) (Abidi, 2001; Lagarda *et al*., 2006). It is important to note that sterols are unstable and best stored in non-lyophilized form at -20 ºC. Sterol oxidation can be prevented by removing oxygen via nitrogen. The sensitivity of a technique depends on the sterol structures and detectors coupled to the chromatographic instrument (Lagarda *et al*., 2006).

3.3.1.2. Hypoxoside isolation

Marini-Bettolo *et al*. (1982) isolated and identified the first glycoside, hypoxoside, from *H. obtusa* Bush (found widespread in southeast Africa, especially Mozambique). Hypoxoside has been identified in several *Hypoxis* spp. including *H. acuminata*, *H. angustifolia*, *H. interjecta*, *H. latifolia*, *H. multiceps*, *H. nitida*, *H. nyasica*, *H. rigidula* and *H. hemerocallidea*. Other glycosides identified in the family *Hypoxidaceae* include

obtusides A and B, mononyasines A and B, nyasoside, nyasicoside, nyaside and nyasol (Chapter 1, Table 1.1) (Galeffi *et al*., 1987; Marini-Bettolo *et al*., 1982; Marini-Bettolo *et al*., 1985; Marini-Bettolo *et al*., 1991; Messana *et al*., 1989; Nicoletti *et al*., 1992; Sibanda *et al*., 1990).

Hypoxoside, also known as the diglucoside of (E)-1,5-bis(3',4'-dihydroxyphenyl)pent-4-en-yne, has a characteristic pentynene backbone, two benzene rings and two glucose units (at C-4 position of the benzene rings). The molecular structure is $C_{29}H_{34}O_{14}$ with a molecular mass of 606.59 g/mol and is very soluble in water and MeOH. Hypoxoside is hydrolyzed (removing the glucose moieties) by β-glucosidase or cellulase to form an aglycone, rooperol, with a molecular structure of $C_{17}H_{14}O_4$ (Figure 3.2) (Drewes *et al*., 1984; Marini-Bettolo *et al*., 1982). Drewes *et al*. (1984) described the isolation of hypoxoside from *H. hemerocallidea* and the chemical synthesis of a tetramethoxy derivative of hypoxoside.

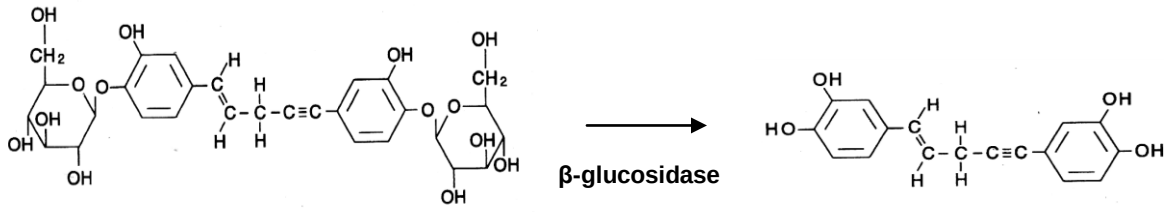

Hypoxoside **Rooperol**

Figure 3.2: Chemical structures of hypoxoside and rooperol, where the former is converted to the latter by β-glucosidase *in vitro* (Albrecht *et al*., 1995a).

Hypoxoside was first extracted from *Hypoxis* using MeOH, partitioned between H_2O and n-butanol (BuOH), and purified through countercurrent distribution (CCD) between H_2O: ethyl acetate (AcOEt): n-BuOH using a Craig Post apparatus. NMR was used to determine the chemical structure of hypoxoside (Marini-Bettolo *et al*. 1982; Nicoletti *et al*., 1992). HPLC is the method of choice for hypoxoside isolation and purification (Drewes *et al*., 1984; Drewes *et al*., 1989; Kruger *et al*., 1994; Nair and Kanfer, 2006).

Hypoxoside is present at high concentrations in *Hypoxis* spp. Marini-Bettolo *et al*. (1982), Drewes *et al*. (1984) and Kruger *et al*. (1994) found hypoxoside yields of 3.7%,

3.5-4.5% and 10%, respectively. Seasonal variation (Drewes *et al*., 1994) and method of *Hypoxis* drying (Nair and Kanfer, 2006) may influence hypoxoside concentrations.

The hypoxoside and (phyto)sterol(in) content of *H. stellipilis* and *H. sobolifera* has not been measured in previous studies. This chapter focuses on the identification and quantification of (phyto)sterols, sterolins and hypoxoside in chloroform extracts of three *Hypoxis* spp.

3.3.2. Materials and Methods

Reagents and chemicals. Sterol standards [β-sitosterol (purity > 90%), campesterol (purity > 65%), cholesterol (purity > 99%), desmosterol (purity ≥ 85%), ergosterol (purity ≥ 95%), fucosterol (purity ~ 95%), stigmasterol (purity ~ 95%) and stigmastenol (purity > 95%)] were purchased from Sigma Chemical Co. (MO, USA). HPLC grade CH_3CN and MeOH were purchased from Romil Ltd. (Cambridge, UK). Water was obtained from a Milli-Q Compact System (Millipore, Bedford, MA). MODUCARE® was purchased from a pharmacy.

3.3.2.1. TLC

Sterol(in)s. A MODUCARE® (Aspen Pharmacare) tablet (containing 20 mg sterols and 0.2 mg sterolins) was used as a standard to identify sterol(in)s in *Hypoxis* extracts, due to the unavailability of commercial sterolin standards. A MODUCARE® tablet was dissolved in chloroform (1 mL), vortexed for five min, extracted for 15 min at room temperature, centrifuged using an Eppendorf 5804R centrifuge at 18 000 x g for five min at room temperature and the supernatant, containing the sterol/sterolins, removed. MODUCARE® (5 µg), β-sitosterol (2 µg) and stigmasterol (2 µg) standards (Supelco, USA), and *Hypoxis* extracts (500 µg) dissolved in chloroform were spotted onto 20 x 20 cm silica coated aluminum plates (Merck, Germany) and air dried. Chromatogram tanks were equilibrated for one hour using toluene: diethyl ether (40:40, v/v) and CH_3CN: ethyl acetate: formic acid (5:4:1, v/v/v) as mobile phases for sterol and sterolin identification,

respectively. TLC plates were developed for ±20 min or until the solvent front was ±1 cm from the top of the plate. Detection of sterols and sterolins was performed as described by Scott and Springfield (2004). In brief, TLC plates were dried at room temperature and developed by firstly dipping into a solution containing 5% sulfuric acid in 96% EtOH for 15 s followed by a solution containing 1% vanillin in 96% EtOH for 15 s and dried at room temperature. Once dried, plates were heated at 80 - 100 ºC for five min. Photos of the developed TLC plates were taken with the AlphaImager™ 3400 (Alpha Innotech.).

3.3.2.2. HPLC

Hypoxoside. HPLC analysis of hypoxoside was performed using a Beckman System Gold high performance liquid chromatograph equipped with Solvent Module 128 and Diode Array Detector Module 169. The column used for HPLC hypoxoside separation was a Nucleosil C18 column (Supelco, 5 µm, 150 x 4.6 mm i.d.). Detection of hypoxoside was performed as described by Nair and Kanfer (2006). In brief, CH_3CN: H_2O (20:80, v/v, degassed) was used as mobile phase in isocratic mode at a flow rate of 1 mL/min and the injection volume was 10 µL. Detection was achieved in the range of 200 - 400 nm and hypoxoside was detected at a wavelength of 260 nm. Stock solutions of hypoxoside (1 mg/mL), *H. hemerocallidea* (5 mg/mL), *H. stellipilis* (10 mg/mL) and *H. sobolifera* (10 mg/mL) were prepared in MeOH and filtered through 0.2 µm syringe filters (Corning Incorporated, New York, USA). Dilutions (10-100 µg/mL) of hypoxoside for the standard curve were also prepared in MeOH.

Sterols. The above mentioned HPLC system was used for sterol analysis. Optimization of sterol separation included the testing of different isocratic, flow and gradient methods using Hypersil 5 C8 300Å (Phenomenex, 5µm, 250 x 4.60mm i.d.) and Nucleosil C18 columns. An isocratic system of CH_3CN: MeOH (90:10; v/v; degassed) at a flow rate of 0.5 mL/min, using the Nucleosil C18 column, was used to separate a sterol mixture consisting of 100 µg/mL each of β-sitosterol, desmosterol, stigmastenol and stigmasterol. *Hypoxis* chloroform extracts (same concentration as for hypoxoside analysis) and sterol

standards were dissolved in MeOH. Detection wavelengths were 210 nm and 290 nm for sterols and internal standard (thymol), respectively. Standards and plant extracts (50-500 μL) were injected and chromatographic separation performed at room temperature.

3.3.2.3. GC

Stock solutions (1 mg/mL) of each sterol standard (β-sitosterol, campesterol, cholesterol, desmosterol, ergosterol, fucosterol, stigmasterol and stigmastenol) were prepared using MeOH. Stock solutions (5 mg/mL) of the *Hypoxis* chloroform extracts (*H. hemerocallidea*, *H. stellipilis* and *H. sobolifera*) were also made using MeOH. Dilutions (2.5-100 μg/mL) were prepared in MeOH for all of the sterol standards. For β-sitosterol an additional 200 μg/mL concentration was prepared. GC analysis of sterols was performed using a Thermo Finnigan Focus gas chromatograph equipped with a FID and an Autoinjector AI3000, with Delta Chromatography 5.0 software. The column used for GC separation was a SAC^{TM}-5 capillary column (Supelco, 30 m x 0.25 mm i.d. x 0.25 μm film thickness). The thermal conditions were: 80 ˚C for 2 min; 10 ˚C/min to 300 ˚C; 300 ˚C for 14 min. The carrier gas was helium (1 mL/min constant flow) and the injection volume was 2 μL (splitless). Sensitivity was set at 1. Standard curves were prepared for each of the eight sterol standards. Sterols were identified by spiking the sterol mixture (containing 100 μg/mL of each sterol standard) with each sterol standard [adding 10, 20, 30, 40, 50, 60, 70 and 80 μL (10 μL = ± 9.9 μg of sterol standard) of the 1 mg/mL stocks of β-sitosterol, campesterol, cholesterol, desmosterol, ergosterol, fucosterol, stigmasterol and stigmastenol, respectively]. An increase in peak area was used as criteria to identify each peak.

3.3.3. Results and Discussion

3.3.3.1. TLC analysis of (phyto)sterol(in)s

Chloroform has been shown to be very effective in dissolving sterols (Toivo *et al*., 2000) due to its non-polar nature. The presence of (phyto)sterols and sterolins in the

chloroform extracts of *H. hemerocallidea*, *H. stellipilis* and *H. sobolifera* was confirmed via TLC. Modification of the mobile phase, toluene: diethyl ether: 1.75 M acetic acid (1:1:1, v/v/v) used by Scott and Springfield (2004), to toluene: diethyl ether (40:40, v/v) resulted in better sterol separation (Figure 3.3).

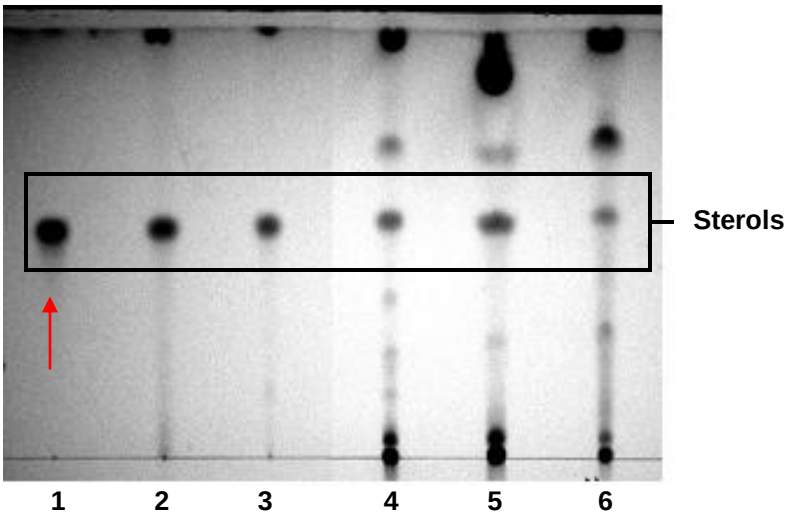

Figure 3.3: TLC plate of the sterols found in *Hypoxis* spp. chloroform extracts. (1) MODUCARE®, (2) β-sitosterol, (3) stigmasterol, (4) *H. hemerocallidea*, (5) *H. sobolifera* and (6) *H. stellipilis*. Red arrow represents most probably β-sitosterol, which is the main sterol found in MODUCARE®.

The spots of the phytosterol standards (stigmasterol and β-sitosterol) had the same Rf value of 0.53. Cholesterol, campesterol, desmosterol, ergosterol, fucosterol and stigmastenol migrated the same distance on the TLC plates, with the spots differing only in colour ranging from pink to blue (data not shown). This made it impossible to identify and quantify individual phytosterols in the *Hypoxis* extracts, using TLC. Phytosterols can be separated by using silver ion chromatography (silver impregnated TLC or HPLC), which will separate phytosterols based on their total number of carbon-carbon double bonds (Moreau *et al*., 2002). Sterol separation can also be improved by two-dimensional TLC, which uses multiple solvents for development. Sterol content (as seen from the intensity of the spots) was the greatest for the *H. sobolifera* extract followed by the *H. hemerocallidea* extract.

The mobile phase used for sterolin identification consisted of CH_3CN: ethyl acetate: formic acid (5:4:1, v/v/v). The sterolins in the *Hypoxis* extracts could not be identified or quantified due to the unavailability of sterolin standards (Figure 3.4). Sterolins present in the chloroform extracts of *Hypoxis* were compared to those found in a MODUCARE® tablet.

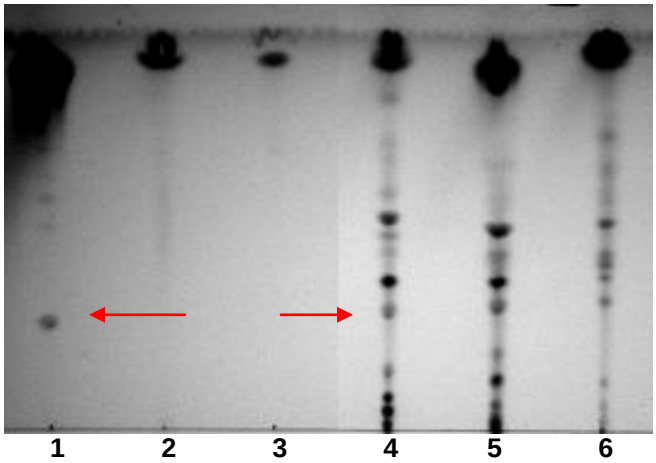

Figure 3.4: TLC plate of the sterolins found in *Hypoxis* spp. chloroform extracts. (1) MODUCARE®, (2) β-sitosterol, (3) stigmasterol, (4) *H. hemerocallidea*, (5) *H. sobolifera* and (6) *H. stellipilis*. Red arrows represent most probably β-sitosterol glycoside, which is the main sterolin found in MODUCARE®.

From the results obtained, different sterolins (based on Rf values) were detected and differences in sterolin composition could clearly be seen between the three *Hypoxis* spp. (Figure 3.4, lanes 4 - 6). Sterolin content (as seen from the intensity of the spots) was the greatest for the *H. sobolifera* extract followed by the *H. hemerocallidea* extract. Extraction of sterols with polar (water, EtOH, MeOH, acetone) and nonpolar (CH_3CN, dichloromethane) solvents yielded more sterolins and sterols, respectively (Appendix 3).

Similar phytosterol structures, differing only in the number and position of the double bond(s), and number of carbons in the side chain, make separation very difficult. Only a few purified phytosterols are commercially available at a very high price (Zhang *et al*., 2005). Unavailability of all phytosterols and their analogues (e.g. sterolins) make identification and quantification almost impossible.

3.3.3.2. HPLC analysis of hypoxoside and (phyto)sterols

HPLC-DAD is becoming the method of choice for screening drugs, vitamins, natural products and identification of active compounds in plants (Springfield *et al*., 2005).

Hypoxoside. The presence of hypoxoside has been identified in several South African *Hypoxis* spp. (Nicoletti *et al*., 1992; Chapter 1, Table 1.1) including *H. hemerocallidea* (Drewes *et al*., 1984; Drewes *et al*., 1989; Kruger *et al*., 1994; Nair and Kanfer, 2006), but not in *H. stellipilis* or *H. sobolifera*. The HPLC method described by Nair and Kanfer (2006) was used to quantify hypoxoside content in the chloroform extracts of three *Hypoxis* spp. (Figure 3.5).

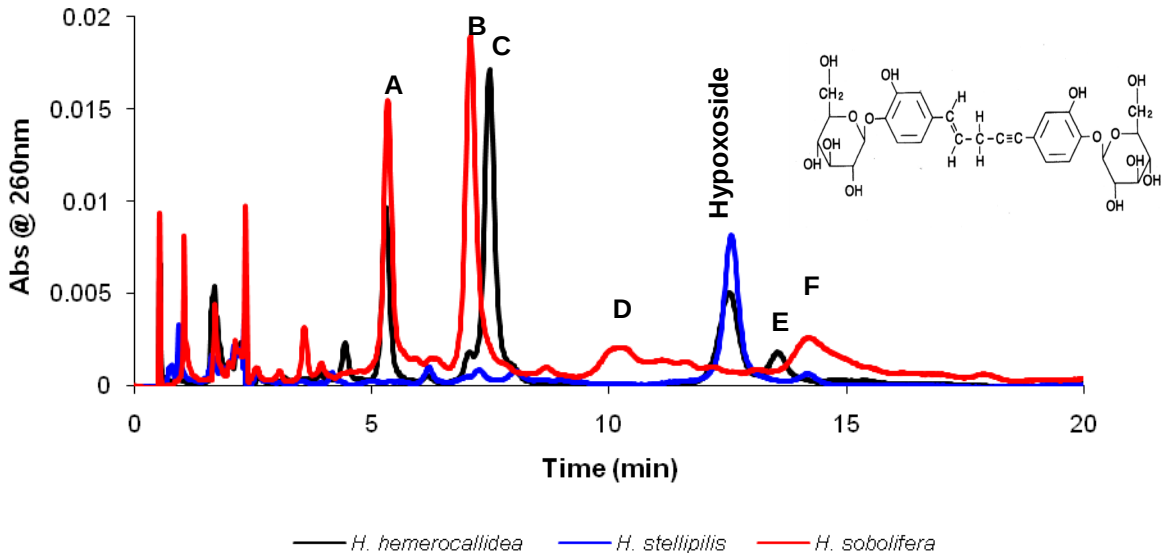

Figure 3.5: HPLC chromatogram overlays of the hypoxoside content of *Hypoxis* chloroform extracts. The Nucleosil C18 column, a mobile phase of CH_3CN: H_2O (20:80; v/v) and a flow rate of 1 mL/min were used for hypoxoside separation. Retention times (min) of unidentified compounds were (A) 5.3; (B) 6.3; (C) 7.5; (D) 10.3; (E) 13.55; (F) 14.1. Hypoxoside standard eluted at R_t of 12.5 min. One representative of three experiments performed. Stock solutions of *H. hemerocallidea*, and *H. stellipilis* and *H. sobolifera* were 5 and 10 mg/mL, respectively.

Hypoxoside was detected after 12.5 min and quantified from a standard curve (Appendix 3) of hypoxoside concentration (ranging between 5 - 100 µg/mL) as a function of peak area (R^2 = 0.9971, R_t = 12.5 min). Hypoxoside content of the three *Hypoxis* spp. is summarized in Table 3.3. Of the three *Hypoxis* species tested for hypoxoside content,

only *H. hemerocallidea* and *H. stellipilis* contained hypoxoside. *H. sobolifera*, which showed the highest anticancer activity (Chapter 4, section 4.3), had undetectable levels of hypoxoside.

HPLC chromatograms were overlaid to allow for more direct analysis of similar and different compounds found in the three *Hypoxis* spp. (Figure 3.5). The compound representing peak A (5.3 min) was found in *H. hemerocallidea* and *H. sobolifera*, whereas compounds representing peaks B (6.3 min) and C (7.5 min) were only found in *H. hemerocallidea* and *H. sobolifera*, respectively. Peaks A, B and C may represent novel or previously identified glycosides. Glycosides differ from species to species (Chapter 1, Table 1.1).

Since chloroform, the solvent used in this study, is not the best solvent for hypoxoside extraction, the presence of this glycoside in *H. sobolifera* was investigated using more polar solvents. A water extract of *H. sobolifera* has shown no hypoxoside content (data not shown), whereas EtOH, MeOH and acetone extracts of *H. sobolifera* yielded 2.05, 2.06 and 2.04 µg/mg of extract respectively (Appendix 3). Previous studies have used EtOH (Drewes *et al*., 1984; Drewes *et al*., 1989; Pegel, 1979) and MeOH (Kruger *et al*., 1994; Nair and Kanfer, 2006) to extract hypoxoside from *H. hemerocallidea*. Traditional healers and herbalists use water and boiling to prepare *Hypoxis* extracts, which may yield more hypoxoside and sterolins (Pegel, 1976). Due to the polar nature of hypoxoside it would be better to use more polar solvents for extractions in future, if more emphasis is placed on the effect of hypoxoside in the *Hypoxis* extracts. Two analogues of hypoxoside have been identified by Kruger *et al*. (1994), namely dehydroxyhypoxoside (one -OH group) and bis-dehydroxyhypoxoside (no -OH groups). Dehydroxyhypoxoside and bis-dehydroxyhypoxoside eluted after hypoxoside (two -OH groups), because a decrease in -OH groups is associated with an increase in retention times (in RP-HPLC). Shifts for rooperol and its analogues were greater when glucose moieties were removed (Kruger *et al*., 1994). Peaks E and F may represent one or both of hypoxoside's analogues.

(Phyto)sterols. TLC was used for the qualitative analysis of sterols but due to its poor resolution properties HPLC and GC were used for sterol quantification. HPLC operates under non-destructive detection conditions and is suitable for the analysis of thermally unstable sterols. A mobile phase of CH_3CN: MeOH (90:10, v/v) at a flow rate of 0.5 mL/min, using the Nucleosil C18 column, separated a sterol mixture (consisting of 100 µg/mL each of β-sitosterol, desmosterol, stigmasterol and stigmastenol) (Figure 3.6).

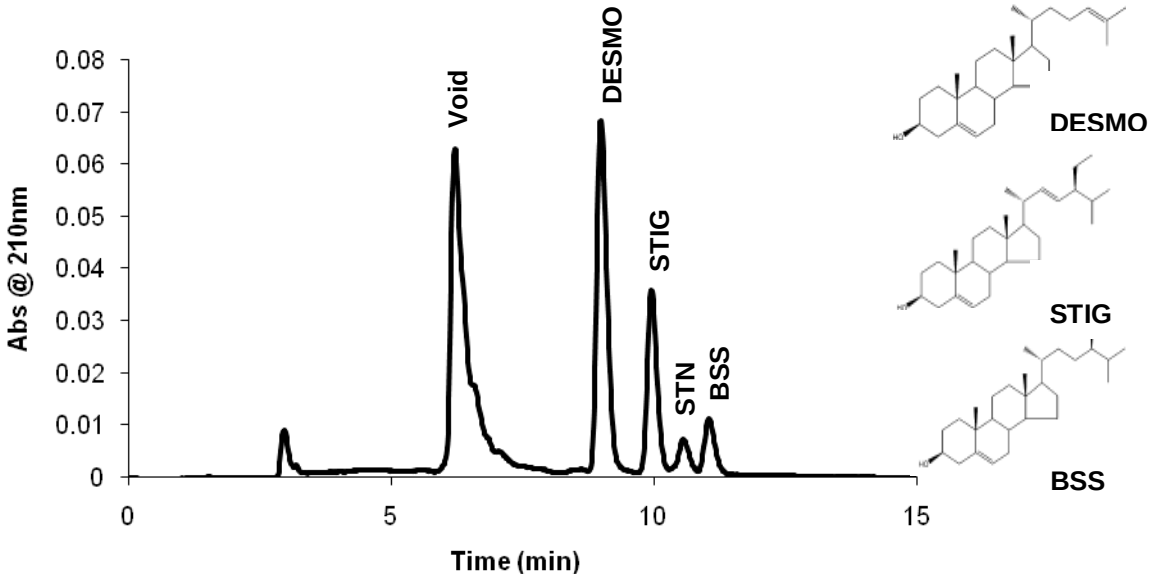

Figure 3.6: HPLC chromatogram of the separation of a sterol mixture. The Nucleosil C18 column, a mobile phase of CH_3CN: MeOH (90:10; v/v) and a flow rate of 0.5 mL/min were used for sterol separation. Retention times (min) of DESMO, STIG, STN and BSS were 9.0, 10.0, 10.6 and 11.1, respectively. Abbreviations: DESMO = desmosterol, STIG = stigmasterol, STN = stigmastenol, BSS = β-sitosterol

(Phyto)sterols in the chloroform extracts of the *Hypoxis* spp., could not be identified and quantified. Overlaid HPLC chromatograms of the sterol mixture and *H. sobolifera* chloroform extract are shown in Figure 3.7. Overlays of *H. hemerocallidea* and *H. stellipilis* are shown in Appendix 3.

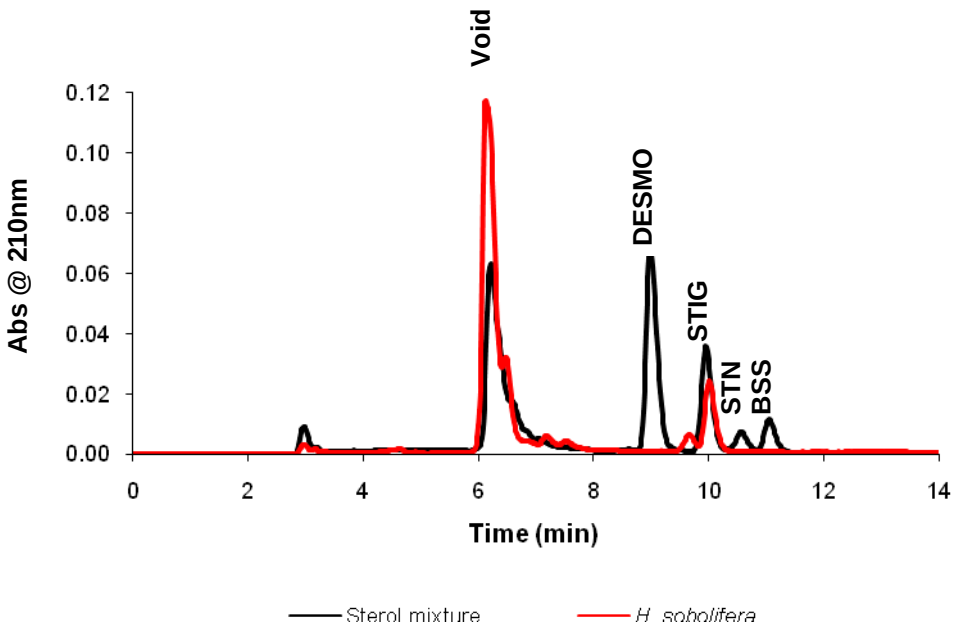

Figure 3.7: HPLC chromatogram overlays of the separation of a sterol mixture and *H. sobolifera*. The Nucleosil C18 column, a mobile phase of CH_3CN: MeOH (90:10; v/v) and a flow rate of 0.5 mL/min were used for sterol separation. Stock solution of *H. sobolifera* was 10 mg/mL. Abbreviations: DESMO = desmosterol, STIG = stigmasterol, STN = stigmastenol, BSS = β-sitosterol

Sterol standards were dissolved in MeOH, hence separation of the standard mixture, whereas *Hypoxis* chloroform extracts were redissolved in MeOH. Poor solubilization of the chloroform extract in MeOH and separation at room temperature may have contributed to poor sterol separation.

3.3.3.3. <u>GC analysis of (phyto)sterols</u>

GC is the technique of choice to analyze the presence of sterols in food (Contarini *et al*., 2002; Cunha *et al*., 2006; Goudjil *et al*., 2003; Lagarda *et al*., 2006; Toivo *et al*., 2000) due to shorter analysis times, less peak interference, improved resolution, greater detection sensitivity (low nanogram range) and thermal stability of the capillary columns (Abidi, 2001). Although the *Hypoxis* chloroform extracts were also redissolved in MeOH (as was the case for HPLC), sterol separation with GC did occur due to separation at very high temperature (300 ºC) compared to separation at room temperature with HPLC. The SAC-5^{TM} capillary column, consisting of 95% dimethylpolysiloxane and 5% phenyl, is specially packed for the analysis of plant and animal sterols. The sterol mixture (100

μg/mL of each sterol), consisting of β-sitosterol (30.6 min), campesterol (29.3 min), cholesterol (27.8 min), desmosterol/ergosterol (28.9 min), fucosterol (28.3 min), stigmasterol (29.7 min) and stigmastenol (30.9 min) was well separated, except for desmosterol and ergosterol, which eluted at the same retention time, with good resolution on the SAC-5™ column within a period of 32 min (Figure 3.8).

From GC analysis, it was clear that β-sitosterol was the main phytosterol found in the chloroform extracts of *H. hemerocallidea*, *H. stellipilis* and *H. sobolifera*. Trace amounts (<2 μg/mg of *Hypoxis* extract) of campesterol and stigmastenol were found in all three *Hypoxis* spp. extracts, whereas trace amounts of desmosterol/ergosterol and stigmasterol were found in certain *Hypoxis* spp. only. A standard curve (Appendix 3) of β-sitosterol concentration (ranging between 10 - 100 μg/mL) as a function of peak height (R^2 = 0.9531, R_t = 30.6 min) was used to quantify β-sitosterol content. *H. sobolifera* contained the most β-sitosterol with ±2.5 and 7.5 times more β-sitosterol compared to *H. hemerocallidea* and *H. stellipilis*, respectively (Table 3.3).

The presence of β-sitosterol and campesterol as the two major phytosterols in *Hypoxis* correspond to published data (Moghadasian, 2000; Pegel, 1976). According to a minireview by Moghadasian (2000), 95% of dietary phytosterols consist of sitosterol and campesterol (approximately 65 and 30%, respectively), whereas the other phytosterols (mainly stigmasterol) and stanols make up the other 5%. This was the first time that GC was used to identify and quantify the presence of sterols in *Hypoxis* extracts. Nair *et al*. (2006) have used HPLC to determine the presence of β-sitosterol, stigmasterol and stigmastenol in commercially available oral dosage forms reported to contain material or extracts of *Hypoxis*. Using the SAC-5™ capillary column in the present study eliminated time-consuming preparation steps, for example extraction of lipid fraction from sample material, saponification (alkaline hydrolysis), extraction of nonsaponifiables and derivatization of the sterol standards and *Hypoxis* extracts (Toivo *et al.*, 2000).

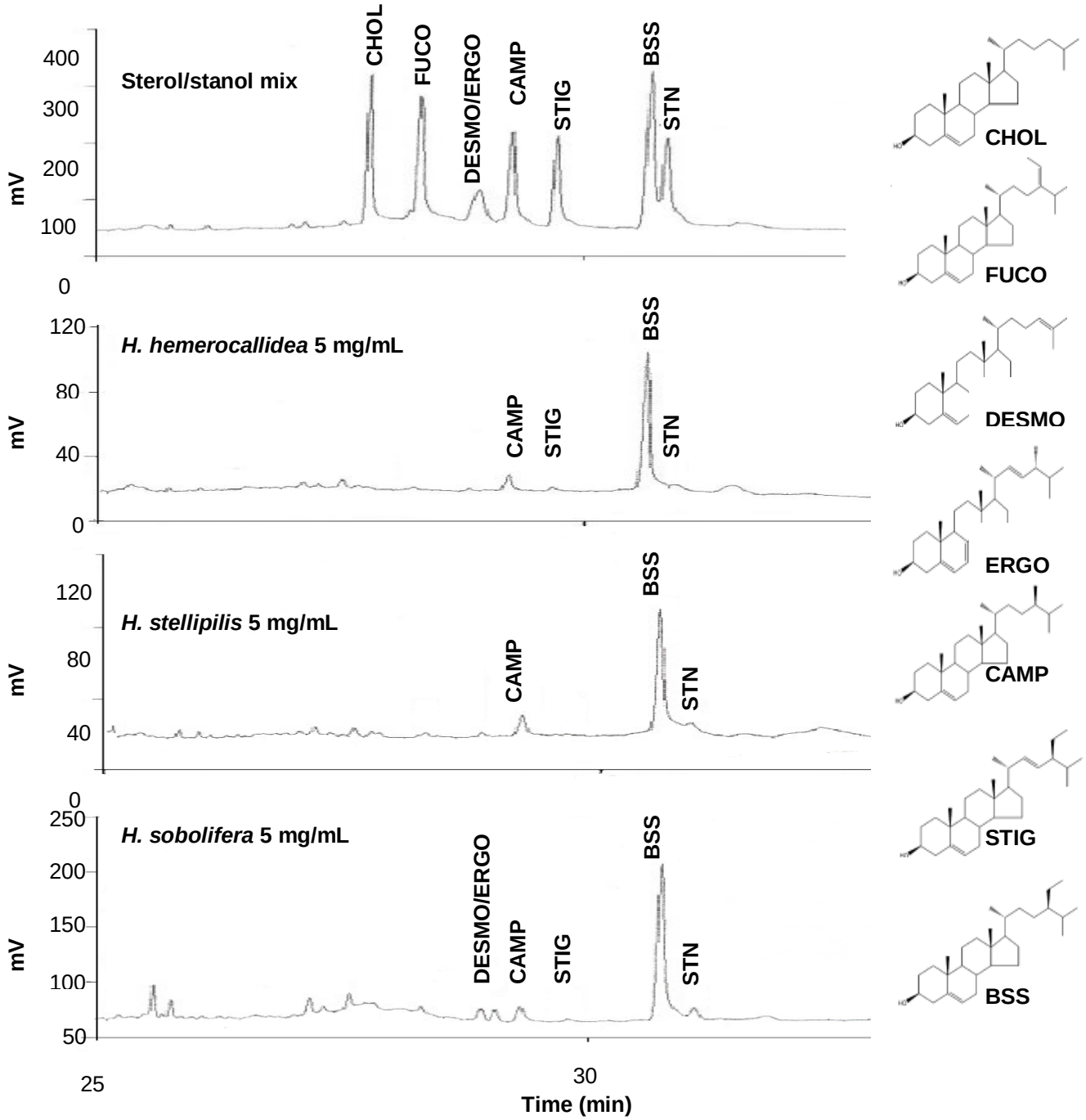

Figure 3.8: GC chromatograms of a sterol standard mixture and *Hypoxis* chloroform extracts. The SAC^{TM}-5 capillary column, temperature gradient and helium at a flow rate of 1 mL/min were used for sterol separation. One representative of three experiments performed. Abbreviations: CHOL = cholesterol, FUCO = fucosterol, DESMO/ERGO = desmosterol/ergosterol, CAMP = campesterol, STIG = stigmasterol, BSS = β-sitosterol, STN = stigmastenol

Retention times of sterols depend on the ring double bond(s), alkyl substituents and side-chain double bond(s). Saturation of phytosterols (i.e. phytostanols) causes an increase in the analyte's retention time (e.g. stigmastenol elutes after stigmasterol). Sterols with a double bond at the C-7 position have longer retention times than those at the C-5 position (e.g. stigmasterol elutes before stigmastenol). Additional methyl or ethyl groups influence the sterol's hydrophobicity, thus increasing the retention time [e.g. campesterol (methyl) elutes before sitosterol (ethyl)]. The structure-retention relationship also depends on molecular mass and polarity. Campesterol is less polar than the highly unsaturated ergosterol and will elute after ergosterol. Cholesterol with one double bond and without a 24-ethyl group will elute after polar ergosterol, but before stigmasterol (24-ethyl group and 22-double bond) (Abidi, 2001).

Table 3.3: Summary of the (phyto)sterol and hypoxoside content of *H. hemerocallidea*, *H. stellipilis* and *H. sobolifera* chloroform extracts.

Compound	**Content (µg/mg)**		
	H. hemerocallidea	***H. stellipilis***	***H. sobolifera***
Hypoxoside	2.45 ± 0.05	1.59 ± 0.04	ND*
β-sitosterol	5.88	2.01	14.94
Campesterol	Trace**	Trace	Trace
Cholesterol	ND	ND	ND
Desmosterol/ Ergosterol	ND	ND	Trace
Fucosterol	ND	ND	ND
Stigmasterol	Trace	ND	Trace
Stigmastenol	Trace	Trace	Trace

* ND = not detected
** Trace amounts (< 2 µg/mL)

3.4. Conclusion

This was the first time that hypoxoside and phytosterol contents were quantified in *H. stellipilis* and *H. sobolifera*. Both the hypoxoside and phytosterol contents were shown

to vary between the three *Hypoxis* spp. The *H. sobolifera* chloroform extract contained the highest content of β-sitosterol, followed by *H. hemerocallidea* and *H. stellipilis*. The *H. hemerocallidea* chloroform extract contained the highest content of hypoxoside followed by *H. stellipilis*, whereas hypoxoside was absent in the *H. sobolifera* chloroform extract. Kruger *et al*. (1994) have also shown a difference in the content of hypoxoside, dehydroxyhypoxoside and bis-dehydroxyhypoxoside found in the MeOH extracts of *H. hemerocallidea* and *H. latifolia*. The presence of unidentified compounds (Figures 3.5 and 3.8) in the *Hypoxis* chloroform extracts needs further investigation. The presence of hypoxoside, β-sitosterol, trace amounts of phytosterol(in)s and unidentified compounds in *Hypoxis* spp. may have synergistic and/or additive effects on biological activities. This may explain the different *in vitro* biological activities seen in the next few chapters.

Hypoxis extraction with more polar solvents will yield greater quantities of hypoxoside. It was the first time that phytosterols were identified and quantified (β-sitosterol) in *Hypoxis* spp. using a GC method. The presence of β-sitosterol as the major phytosterol in *Hypoxis* spp. was confirmed. The other phytosterols identified were present in trace amounts, which did not allow for quantification.

Further investigation is required to determine the implications of these findings in the uses of *Hypoxis* as a traditional remedy. Consumption of the three different *Hypoxis* spp., which have different sterol(in)s and hypoxoside content, may have adverse or favorable effects.

Peer-reviewed journal article published from this chapter

Boukes, G.J., van de Venter, M., Oosthuizen, V. 2008. Quantitative and qualitative analysis of sterols/sterolins and hypoxoside contents of three *Hypoxis* (African potato) spp. Afr. J. Biotechnol. 7 (11): 1624-1629.

CHAPTER 4

IN VITRO ANTICANCER ACTIVITY AND MECHANISM(S) OF ACTION OF THREE *HYPOXIS* SPP.

4.1. General Background

4.1.1. Cancer definition

Cell homeostasis requires a balance between cell proliferation and programmed cell death (Simstein *et al*., 2003). Cancer is characterized by a succession of genetic mutations, each contributing to one or different types of growth advantages (Fadeel and Orrenius, 2005). Genetic changes of the apoptotic machinery cause unregulated proliferation of cells, which preserve genetic mutations and give rise to tumourigenesis (Collins *et al*., 1997; Simstein *et al*., 2003; Srivastava *et al*., 2005).

Two classes of cancer genes are found, namely oncogenes and tumour suppressor genes. Oncogenes are associated with a dominant gain-of-function. Mutant forms of normal cell protooncogenes are involved in signalling pathways in cell proliferation. Suppressor genes are associated with a recessive loss-of-function. In normal cells, tumour suppressor genes encode for proteins that negatively regulate cell cycle progression e.g. pRb and p53. Mutations play a major role in spontaneous and hereditary cancers (Collins *et al*., 1997; Hanahan and Weinberg, 2000).

Cancer cells have the following characteristics:

- Evade apoptosis by altering the components of the apoptotic machinery.
- Self-sufficient in providing growth signals to proliferate.
- Insensitive to anti-growth signals to be able to continuously divide and survive.
- Sustained angiogenesis – growth of blood vessel formation – for constant supply of oxygen and nutrients.
- Immortality by multiplying without limit.

- Tissue invasion and metastasis – cancer cells escape the primary tumour mass and colonize a new area where nutrients and space are abundant. Metastasis is responsible for 90% of human cancer death (Hanahan and Weinberg, 2000).

Carcinogenesis is a multistage process where normal cells are transformed into cancerous cells, involving initiation [reaction between carcinogen and deoxyribonucleic acid (DNA) of cell resulting in DNA damage], promotion (increased cell proliferation) and progression (additional genetic mutations and spread of cancer) (Balunas and Kinghorn, 2005; Reddy *et al*., 2003).

4.1.2. World and South African cancer statistics

Cancer is amongst the three most common causes of death in developed countries, with an increase seen in developing countries (Houghton *et al*., 2007).

The 2000-2001 National Cancer Registry (NCR), containing South African cancer statistics, has shown that males and females have a lifetime risk of 1 in 6 and 1 in 8 chance of getting cancer, respectively. The five leading cancers in males were prostate (1 in 23), lung (1 in 69), oesophageal (1 in 82), colorectal (1 in 97) and bladder (1 in 108). The five leading cancers in females were breast (1 in 29), cervix (1 in 35), uterus (1 in 144), colorectal (1 in 162) and oesophageal (1 in 196). The most common cancer, not necessary resulting in death, in South Africa is skin cancer (basal/squamous cell carcinomas and malignant melanoma) with 20 000 reported new cases and 700 deaths (mainly malignant melanoma) each year (www.cansa.org.za).

It is estimated that over 10 million cancer cases (excluding non-melanoma skin) and 6 million deaths worldwide occurred in 2000. This represents a 22% increase in cancer incidence and mortatility rate since 1990. Cancer is the second leading cause of death after cardiovascular diseases in the US (Balunas and Kinghorn, 2005, Srivastava *et al*., 2005). According to 2005 statistics released by the World Health Organization (WHO), 7.6 million (13.6%) of a total of 58 million deaths worldwide were due to cancer. The

leading cancer types resulting in overall mortality include lung-, stomach-, liver-, colon- and breast cancer. In South Africa, approximately 41 000 deaths were due to cancer in 2005. More than 70% of the deaths occurred in low to middle-income countries, where resources for cancer diagnosis, treatment and prevention are limited or non-existent. It is estimated that the annual cancer death rate will rise to 12 million deaths in 2030. It is estimated that 84 million people will die in the next decade (2006-2016) if action is not taken against cancer. The most frequent cancer deaths in men globally are lung, stomach, liver, colorectal, oesophagus and prostate, and in women are breast, lung, stomach, colorectal and cervical (www.who.int).

Three main factors contribituing to cancer are incorrect diet (section 4.1.4.), genetic predisposition and, physical- (UV or ionizing radiation), chemical- (asbestos, tobacco smoke, aflatoxin and arsenic) and biological [viruses (e.g. hepatitis B virus (HBV), human papiloma virus (HPV) and HIV); bacteria (e.g. *Helicobacter pylori*), parasites (e.g. schistosomiasis)] carcinogens (Reddy *et al*., 2003; WHO). Cancer risk factors in low to middle income countries include tobacco and alcohol use, low fruit and vegatable consumption and chronic infections [HBV, hepatitis C virus (HCV) and HPV]. In high income countries risk factors include tobacco and alcohol use, and obesity. Avoiding these risk factors can prevent more than 40% of cancers (www.who.int).

4.1.3. Treatments available

The type of cancer treatment depends on the cancer type, the site, tumour size, metastasis and how it is affecting normal body functions. Most common treatments available include:

- Surgery – physical removal of cancerous growth or tissue.
- Radiotherapy – stream of high energy particles (neutrons or protons) or radioactive source, which damage or destroy cancer cells.
- Cytotoxic chemotherapy – administration of natural or synthetic compounds, which directly target cancer cells.

- Hormonal manipulation – influencing cell growth by altering the production or activity of cells.
- Biological therapy (syn. immunotherapy, biotherapy or biological response modifier therapy) – boosts body's natural defense or immune system against cancer.
- Combinational therapy (Houhton *et al.*, 2007; www.cansa.org.za; www.who.int).

Advanced treatments may have a 5-year survival rate of 75% or more for certain cancers e.g. breast, testis, melanoma and uterine corpus, whereas survival rates are less than 15% for pancreas-, lung-, liver- and stomach cancer (WHO).

Like any other anticancer agents, plant-based agents lack specificity to kill cancer cells and drug resistance occur with time. Combination therapy is used to combat resistance, but is only temporary (Srivastava *et al.*, 2005).

4.1.4. Cancer and diet

The importance of a healthy diet to combat disease has been recognized for centuries. Hipprocrates (480 BC) described the relationship between a diet and health as follows:

"Positive health requires a knowledge of man's primary constitution (genetics) and the powers of various foods, both those natural to them and those resulting from human skill (diet)."

It is estimated that nutritional factors contribute to 20-60% of cancer worldwide and a third of cancer in Western countries (McCullough and Giovannucci, 2004). Cancer incidence and mortalilty rates vary dramatically across the globe. Cancer rates among populations migrating from low (e.g. Japanese or Chinese) to high (e.g. US) incidence countries change significantly, reaching the same cancer rates within 3 generations. For example the risk of colon cancer, which may be associated with high fat diets, changes within a few decades of migration, and that of breast cancer changes within the second generation. Thus environmental and lifestyle rather than genetic factors, which are unlikely to occur within a few decades, play a role in cancer development and rates

(Persky and van Horn, 1995; Willett, 2001). Factors contributing to cancer development include excessive energy intake (associated with rapid growth in children and obesity in adults), physical inactivity, high alcohol consumption, smoking, food preparation (pickling, salting and smoking of foods; high temperature cooking) and high polyunsaturated and animal or saturated fat intake. Many of these factors are also associated with diabetes and cardiovascular diseases. Changing the diet by consuming more fruit, vegetables, dietary fiber, monounsaturated fats (e.g. olive oil); less red meat and animal fat; moderate alcohol consumption; minimizing consumption of salt-cured, pickled and smoked foods; increasing physical activity; and taking supplements or micronutrients (selenium, folic acid, vitamins C/D/E, β-carotene, calcium) may decrease the high incidence of cancer. Protective effects of fruits and vegetables are controversial and contradictable due to conflicting research studies. Phytochemicals – carotenoids, organosulfur (e.g. allicin in garlic), phenolic/polyphenols (e.g. isoflavones in soybeans, catechins in tea, phenolic esters in coffee, phenolic acid in red wine, quercetin in onions), vitamins C and E, phytoestrogens, lignans, isothiocyanates, terpenes, glucosinolates and fiber – are possible anticancer and chemopreventive constituents (Willett, 2000; Greenwald *et al*. 2001; Riboli and Norat, 2003; Reddy *et al*., 2003; McCullough and Giovannucci, 2004).

A Mediterranean diet – consisting of high monounsaturated: saturated dietary fat ratio; moderate alcohol consumption; high consumption of legumes, fruit, vegetable and cereals; low consumption of meat and meat products; moderate consumption of milk and dairy products – has shown a decrease in cancer incidence rates when compared to diets in Scandinavian countries, the UK and the US (Trichopoulou *et al*., 2000). Cancers related to high fat diets (e.g. breast cancer) is higher in the US than Japan. Low breast, prostate and colon cancer incidence in the Japanese and Chinese population is associated with low fat diets and high soyfood (genistein) intake (Persky and van Horn, 1995).

4.1.5. Cancer and plants (natural products)

Plants have played a pivotal role in the development of effective anticancer agents. More than 60% of the currently used anticancer agents are derived from natural sources, including plants, marine organisms and microorganisms (Cragg and Newman, 2005). Table 4.1 summarizes the plant derived antitumour agents in clinical use and -development stages.

Table 4.1: Summary of the plant-derived antitumour agents in clinical use and -development stages (Balunas and Kinghorn, 2005; Cragg and Newman, 2005; Srivastava *et al*., 2005).

	Plant-derived antitumour agents
Clinical use	Vinca alkaloids i.e. vinblastine and vincristine (vinorelbine, vindesine); camptothecin (topotecan, irinotecan); taxanes i.e. paclitaxel/taxol® (docetaxel); podophyllotoxin (etoposide, teniposide); elepticine (elliptinium); homoharringtonine.
Clinical development	Olomucine (roscovitine), combretastatins (combretastatin A4 phosphate), rohitukine (flavopiridol).
Preclinical development	Bruceantin, pervilleine A, betulin (betulinic acid), naphthaquinones (β-lapachone), triterpenoid acids i.e. oleanolic and ursolic acids (CDDO), thapsigargin, indirubins (3´-monooxime and 5-bromoindirubin derivatives), maytansine.

() = derivatives/analogs

4.1.6. Apoptosis versus necrosis

Apoptosis and cell proliferation play important roles in maintaining homeostasis in various cell populations. During normal physiology, approximately 10 billion cells are made in the human body each day to balance cells that die during apoptosis. These numbers increase significantly during aging or disease when apoptosis increases. Apoptosis is important during various developmental processes, removal of pathogen-invaded cells, embryogenesis, removal of autoreactive T cells and low responsive B cells, immune responses, and wound healing. Insufficient, excessive or unregulated apoptosis leads to diseases such as cancer, AIDS, ischaemia, neurodegenerative diseases

(Parkinson-, Alzheimer-, Huntington's disease), amyotrophic lateral sclerosis (ALS), autoimmune lymphoproliferative syndrome and autoimmune diseases (Elmore, 2007; van Engeland *et al*., 1996).

Necrosis occurs during pathological processes mediated by viruses, bacteria and protozoa. It is associated with the secretion of cytokines (resulting in inflammation and infection), nitric oxide (NO) and reactive oxygen species (ROS) production, and physiological processes (tissue renewal, embryogenesis and immune response). In the presence of excess ROS and NO, apoptosis can be switched to necrosis (Proskuryakov *et al*., 2003).

Apoptosis and necrosis can occur simultaneously, independently and sequentially. Morphological and biochemical features of both apoptosis and necrosis may be present in the same cell. Induction of apoptosis or necrosis may be determined by signal type and degree. Table 4.2 summarizes the morphological features of apoptosis and necrosis. Many biochemical features (caspase activation and oligonucleosomal DNA fragmentation), associated with apoptosis, are usually absent in necrosis (Proskuryakov *et al*., 2003). The focus of this study was on apoptosis and only the biochemical features of apoptosis are summarized in section 4.1.6.1. Apoptosis activation is triggered by various stimuli e.g. growth factor withdrawal, chemotherapeutic drugs, crosslinking of death signal transmitting signals, and others (Murphy *et al*., 2000).

Table 4.2: Comparison of the morphological features occurring during apoptosis and necrosis (Elmore, 2007; Fadeel and Orrenius, 2005; Gorczyca, 1999; Kroemer *et al*., 2009; Proskuryakov *et al*., 2003).

Apoptosis	**Necrosis**
Energy dependent	Energy independent
Controlled process	Uncontrolled and passive process
Effect single cells/small clusters of cells	Effect field of cells
Intact plasma membrane and 'blebbing'	Disrupted plasma membrane/loss in integrity/leaky
Cell shrinkage (round cells, dense cytoplasm, tightly packed organelles,	Cell and organelle (mitochondria) swelling (oncosis)

chromatin condensation)	
Cytoplasm retained in apoptotic bodies	Cytoplasm released
Pyknosis*, karyorrhexis**	Karyolysis***, pyknosis, karyorrhexis
Minor modifications of cytoplasmic organelles	Cytoplasmic vacuolization, nuclear swelling, rupture of plasma and nuclear membranes
Apoptotic body† formation/phagocytosis	Cell contents released into surrounding environment
No inflammation	Inflammation

* nuclear and cytoplasmic volume reduction
** nuclear fragmentation
*** DNA dissolution
† membrane-enclosed particles containing organelles and nuclear fragments

4.1.6.1. Biochemical features of apoptosis

Biochemical features of apoptosis include caspase activation (section 4.2.5), phosphatidylserine (PS) translocation and externalization in membranes (section 4.2.6), oligonucleosomal DNA fragmentation (section 4.2.7), reduction or loss in mitochondrial membrane potential ($\Delta\Psi_m$), activation of pro-apoptotic Bcl-2 family proteins, intracellular acidification, ROS production, selective proteolysis or cleavage of subset of cellular proteins and ssDNA accumulation (Cryns and Yuan, 1999; Kroemer *et al*., 2009).

Apoptosis is divided into the extrinsic (receptor-mediated), intrinsic (mitochondrial), execution and perforin/granzyme pathways. Figure 4.1 summarizes the key events of apoptosis.

Extrinsic (receptor-mediated) pathway. Death receptors are members of the tumour necrosis factor (TNF) receptor gene superfamily and have cysteine-rich extracellular domains and cytoplasmic domains (~80 amino acids) known as death domains (DDs). DDs transmit death signals from the cell's surface to intracellular signalling pathways. Examples of ligands and their corresponding death receptors are FasL/CD95/Apo1-FasR,

TNF-α-TNFR1, Apo3L-DR3, Apo2L-DR4 and Apo2L-DR2. One or more cytoplasmic DD-containing adapter proteins (e.g. FADD/ MORT1 and TRADD for FasL/FasR and TNF-α/TNFR1, respectively) are recruited and bind receptors, via corresponding DDs, upon ligand-receptor binding. FADD associates with procaspase-8 via dimerization of death effector domains (DEDs) and form a death-inducing signalling complex (DISC), which autocatalytically activates procaspase-8. Caspase-8 activates the execution pathway and/or cleaves cytosolic Bid (Figure 4.1). Bid translocates from the cytosol to the mitochondria and incorporates into the mitochondrial membrane, where it plays a role in the intrinsic pathway. Mitochondria can act as an amplifier in CD95-induced apoptosis when the mitochondrial pathway is activated via Bid cleavage by caspase-8 (Cryns and Yuan, 1999; Elmore 2007; Fadeel and Orrenius, 2005; Nagata, 2000; Simstein *et al*., 2003; Sun *et al*., 1999). Viral proteins (containing two DEDs) may inhibit death receptor binding by competing with procaspase-8 or -10 for binding to DED of FADD/MORT1. FLIP (also known as Casper/I-FLICE/FLAME-1/CASH/CLARP/ MRIT) is expressed in mammalians and contains two DEDs resembling viral proteins. FLIP resembles caspase-8 and -10 in structure, but is devoid of protease activity. FLIP binds FADD/MORT1 and caspase-8 or -10 (Cryns and Yuan, 1999).

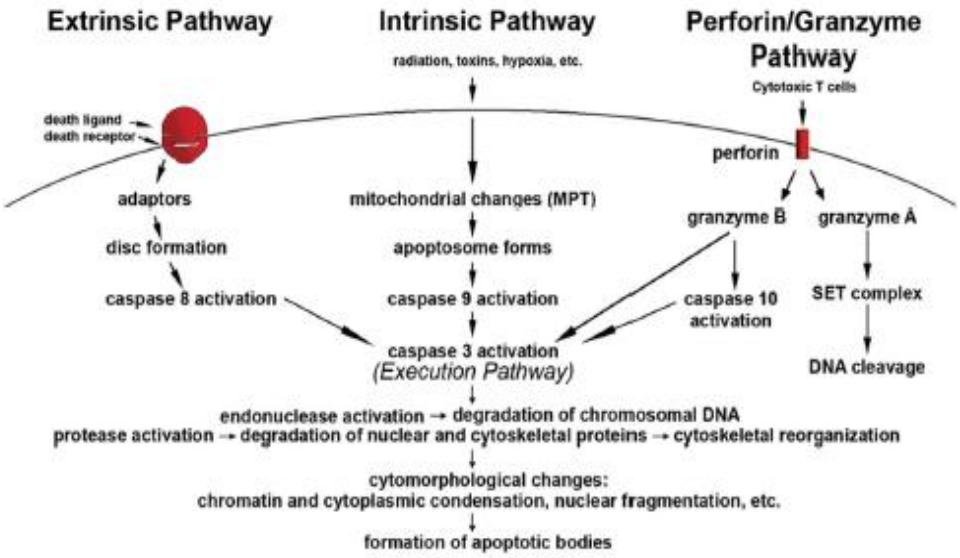

Figure 4.1: Schematic representation of the biochemical events associated with the four pathways involved in apoptosis (Elmore, 2007). See text for more detail.

Intrinsic (mitochondrial) pathway. Negative (absence of certain growth factors, hormones and cytokines) and positive stimuli (e.g. radiation, toxins, hypoxia, hypothermia, viral infections and free radicals) directly act on targets in the cell, causing internal cell damage and initiate mitochondrial events. Stimuli target the inner mitochondrial membrane leading to a loss in mitochondrial transmembrane potential ($\Delta\Psi m$; depolarization), which may be mediated by opening of mitochondrial permeability transition pores (PTP). Mitochondria may also swell resulting in outer membrane rupturing (without loss in mitochondrial membrane potential). Pro-apoptotic proteins (cytochrome c, Smac, Omi and procaspase-9) are released from the mitochondrial intermembrane space into the cytosol prior to depolarization. Cytochrome c binds and activates the adapter molecule, apoptosis proteinase activating factor (Apaf)-1, and in the presence of ATP/dATP binds procaspase-9 to form the apoptosome (Figure 4.1). The apoptosome is regarded as the counterpart of DISC formed in receptor-mediated apoptosis and forms the central part of the mitochondrial pathway. Procaspase-9 undergoes autoactivation to yield active caspase-9, which activates the execution pathway. Activated caspase-9 can be translocated to the nucleus and may participate in nuclear fragmentation. Inhibitor of apoptosis proteins (IAPs) inhibits apoptotis by preventing active caspases binding to their substrates. Smac (second mitochondrial activator of caspases) and Omi inhibit IAP activity, which promotes apoptosis (Blanc *et al*., 2000; Cryns and Yuang, 1999; Del Bello *et al*., 2004; Elmore, 2007; Fadeel and Orrenius, 2005; Mooney *et al*., 2002; Simstein *et al*., 2003; Sun *et al*., 1999; Wolf, 1999).

The Bcl-2 family is regulated by the tumour suppressor protein, pRb, and consists of pro-apoptotic (e.g. Bax, Bak, Bok, Bid, Bad, Bik, Bim, Bcl-X_S, Krk, Mtd, Nip3, Noxa and Bcl-B) and anti-apoptotic (e.g. Bcl-2, Bcl-X_L, Mcl-1, Bfl-1/Al, Bcl-W and Bcl-G) proteins, which regulate mitochondrial events. Anti-apoptotic proteins are integral membrane proteins of the mitochondria, endoplasmic reticulum and nuclear envelope, whereas pro-apoptotic proteins are mainly found in the cytosol and get integrated into the mitochondrial membrane when activated. Bcl-2 family members form homo- and heterodimers, which play an important role in cytochrome c release by influencing mitochondrial membrane permeability during apoptosis. Cytochrome c release is

blocked by Bcl-2/Bcl-X_L or promoted by Bax/Bak. The latter may be involved in formation of membrane pores to release cytochrome c. Bid is more potent in inducing cytochrome c release than Bax (Cryns and Yuang, 1999; Elmore, 2007; Fadeel and Orrenius, 2005; Hanahan and Weinberg, 2000; Mooney *et al*., 2002; Simstein *et al*., 2003; Sun *et al*., 1999). Bcl-2 inhibits Bax ability to form lipid channels. Bcl-X_L binds cytochrome c and secludes it in the mitochondria, thus preventing osmotic swelling of mitochondria and outer membrane disruption induced by stimuli, which may lead to cytochrome c efflux into the cytosol. Depolarization cannot be inhibited by Bcl-2. Apoptotic and necrotic stimuli induce mitochondrial swelling and rupturing of the outer membrane releasing cytochrome c. Overexpression of procaspase-9 blocks Apaf-1 ability to activate caspase-3. Bcl-2 proteins can also act directly on the caspase cascade e.g. Bcl-X_L binds and inactivates Apaf-1, which may interfere with Apaf-1's ability to activate procaspase-9. This may explain Bcl-2/Bcl-X_L inhibition of caspase activation downstream of cytochrome c release. Apaf is selective and does not interact with procaspase-1, -2, -3 or -8 (Cryns and Yuan, 1999; Simstein *et al*., 2003).

Execution pathway. The execution pathway is the converging point of the intrinsic and extrinsic pathways, where execution caspases (caspase-3, -6 and -7) are activated. The execution caspases cleave several substrates, which play an important role in the morphological (Table 4.2) and biochemical features of apoptosis. Caspase-3 is the most important executor caspase, which is activated by all initiator caspases (Elmore 2007). Caspase-3 can activate the mitochondrial pathway by directly cleaving procaspase-9. Procaspase-3 is also recruited to the caspase-9/Apaf-1 complex, where it undergoes proteolysis and gets activated (Blanc *et al*., 2000; Del Bello *et al*., 2004).

Granzyme/perforin pathway. T-cell mediated cytotoxicity is associated with the $CD8^+$ killing of antigen-bearing cells. Cytotoxic T lymphocytes (CTLs) and NK cells target cells via the extrinsic pathway or perforin/granzyme pathway. The latter pathway involves secretion of a transmembrane pore-forming molecule, perforin, and the release of granules through the pore, into the target cell's cytoplasm. Cytoplasmic granules contain granzyme A and B, which are serine proteases. Granzyme A activates a caspase-

independent cell death pathway via ssDNA damage, whereas granzyme B (i) cleaves proteins at Asp residues e.g. procaspase-10 and inhibitor of caspase-activated DNase (ICAD), (ii) uses the mitochondrial pathway to amplify the death signal by cleaving Bid, involved in cytochrome c release, and (iii) directly cleaves and activates procaspase-3 (Figure 4.1) (Elmore, 2007; Fadeel and Orrenius, 2005). This type of pathway occurs upon viral defence and immune surveillance against cancer or homeostasis (Fadeel and Orrenius, 2005).

4.2. Anticancer mechanism(s) of action of *Hypoxis* spp.

Albrecht *et al*. (1995a) investigated the anticancer properties of hypoxoside (converted to rooperol), isolated mainly from *H. hemerocallidea*. No literature could be found on the anticancer mechanism(s) of action of this plant, hence the following sections focus on the anticancer activity and mechanism(s) of action of three *Hypoxis* chloroform extracts and its purified compounds against Hela (cervical), HT-29 (colorectal) and MCF-7 cancer cell lines. Breast and cervical cancer are the two leading cancers in females, whereas colorectal cancer is one of the five leading cancers in both male and female in South Africa. Hence the use of these three cancer cell lines to conduct the studies.

4.2.1. β-glucosidase Activity

4.2.1.1. Background

Chemotherapy lacks selectivity for cancer cells, which may result in adverse side effects (e.g. killing normal cells). Selectivity and efficacy of chemotherapeutic drugs may be enhanced by the conversion of non-toxic prodrugs to active cytotoxic agents via enzymes, expressed at high concentrations and specificity, at the tumour sites. Prodrug activation by endogenous enzymes may be avoided by using enzymes from non-mammalian origin (e.g. caboxypeptidase G2, β-glucosidase, nitroreductase). Factors important when designing prodrugs include: (i) prodrug must be less toxic than the active agent; (ii) it must be chemically stable under physiological conditions; (iii) it must be a

suitable substrate for the enzyme; (iv) the activated agent should be highly diffusible to be easily taken up by tumour cell; and (v) the activated agent must have a short half-life within tumour cells to prevent it from leaking back to normal cells. Increased β-glucuronidase levels (released by monocytes, granulocytes or expressed) are found at the necrotic areas of tumours (bronchial-, pancreatic-, breast-, lung- and gastrointestinal tract carcinomas, and melanomas). β-glucuronidase is normally expressed in the lyzosymes of cells and at high levels in necrotic areas of large tumours. Examples of glucuronide prodrugs are *p*-hydroxy-aniline mustard (aniline mustard), epirubicin, paclitaxel, 9-amino-camptothecin and 5-fluorouracil (de Graaf *et al*., 2002; Smit *et al*., 1995).

Cancer cells, characterized by rapid proliferation, release more enzymes into the surrounding environment than normal cells, which may be a survival strategy. Enzymes associated with the mitochondria, nucleus and cytoplasm are also released when cells are destroyed. Enzymatic changes may be associated with metabolic changes in cancer cells. The rate of enzyme elimination in cancer cells may be delayed, which may explain the high levels of certain enzymes in cancer cells. Cancer cells may also induce the release of enzymes by normal cells. Increased β-glucuronidase and β-glucosidase activities are associated with stomach and colon carcinoma, respectively (Stefanini, 1985).

Natural occurring compounds in plant extracts may not be active themselves, but need to be transformed via metabolic systems in the body to become active substances (Houghton *et al*., 2007). Non-toxic hypoxoside is converted to cytotoxic rooperol via β-glucosidase or cellulase *in vitro*, and non-toxic rooperol phase II metabolites (glucuronide, sulphate or glucuronide-sulphate metabolites), which get activated by glucoronidase and sulphatase, *in vivo* (Albrecht *et al*., 1995a; Drewes *et al*. 1984; Kruger *et al*., 1994; Marini-Bettolo *et al*., 1982; Smit *et al*., 1995).

As mentioned above, β-glucosidase converts non-toxic hypoxoside to cytotoxic rooperol *in vitro*. This section focuses on the β-glucosidase levels in the spent culture medium and lysates of Hela, HT-29 and MCF-7 cancer cells. This was done to determine whether or

not it would be necessary to add β-glucosidase to the culture medium when the effects of the plant extracts and hypoxoside were investigated.

4.2.1.2. Materials and Methods

HeLa, HT-29 and MCF-7 cancer cells were grown to confluency in 10-cm culture dishes in Roswell Park Memorial Institute (RPMI) 1640 cell culture medium containing 25 mM Hepes, 2 mM glutamine (Lonza, Walkersville, MD, USA) and 10% foetal bovine serum (fbs; Gibco, Grand Island, NY, USA) without antibiotics in a humidified 5% CO_2 incubator at 37 ºC. Fbs was not heat-inactivated. The spent medium was removed and kept on ice. The cells were scraped with a Teflon cell scraper, resuspended in 1 mL of sodium acetate buffer (100 mM, pH 5.5) and mechanically lysed using a syringe. The cell lysates were centrifuged using an Eppendorf 5804R centrifuge at 2600 x g for two min at 4 ºC. Twenty µL of sodium acetate buffer (100 mM, pH 5.5) was added to the medium, cell lysate or β-glucosidase standard (20 µL) in a 96 well plate and incubated for five min at room temperature. ρ-nitrophenyl β-D-glycopyranoside (2.5 mM; 160 µL) was added to each well and incubated for 15 min at 37 ºC. The reaction was stopped by adding 60 µL glycine (2 M, pH 10) to each well and the absorbance read at 412 nm using a BioTek® PowerWave XS spectrophotometer (Winooski, VT, USA). A β-glucosidase standard curve (Appendix 4), ranging between 0.1 mU/well (0.00066 µg/µL) and 2 mU/well (0.01325 µg/µL) of β-glucosidase, was performed to determine the concentration of β-glucosidase.

4.2.1.3. Results and Discussion

No published data could be found on the β-glucosidase content of HeLa, HT-29 and MCF-7 cancer cell lysates or media in which these cells are cultured. Considering the importance of β-glucosidase in the metabolism and activation of hypoxoside, this information was essential for further studies on *Hypoxis* extracts and hypoxoside. Table 4.3 summarizes the amount of β-glucosidase in the cancer cell lysates and spent medium.

Table 4.3: β-glucosidase activity and mass in cell lysates and spent medium of confluent monolayers of HeLa, HT-29 and MCF-7 cancer cells.

Cell line		Activity (mU/plate)*	Mass (µg/plate)*
HeLa	Lysate	3.13	0.42
	Medium	41.71	5.51
HT-29	Lysate	3.14	0.42
	Medium	40.64	5.37
MCF-7	Lysate	3.18	0.42
	Medium	40.11	5.29

* where 1 mU = 0.132 µg of β-glucosidase; Plate = 10 cm culture dish containing 10 mL culture medium

β-glucosidase was present at very low concentrations in the medium and lysates of HeLa, HT-29 and MCF-7 cancer cells. This may be because cells are growing *in vitro* rather than *in vivo*, where the environment surrounding the cancer cells is different and more complex. The amount of enzyme also depends on the size of the tumour (de Graaf *et al*., 2002). Previous studies on *Hypoxis* used a β-glucosidase concentration of 100 µg/mL (Albrecht *et al*., 1995a) in *in vitro* anticancer assays. It is important to note that fbs contains β-glucosidase, which can only be inactivated by heating at 56 ºC for at least one hour (Theron *et al*., 1994). Fbs was not heat-inactivated for this assay and it may have contributed to the higher concentration of β-glucosidase in the medium. β-glucosidase concentrations measured in the spent medium and cell lysates were lower than the 100 µg/mL used in previous study by Albrecht *et al*. (1995a). It was therefore decided to add 100 µg/mL β-glucosidase to culture medium for all future investigations of the effects of *Hypoxis* extracts and hypoxoside.

4.2.2. Cytotoxicity of *Hypoxis* extracts and IC_{50} determination of hypoxoside and rooperol

4.2.2.1. Background

Cytotoxicity testing is based on the proliferation of cancer cells in the presence or absence of a test substance after a specific time period. Selectivity of an agent is determined by using different cancer cell lines and normal cell lines. Cytotoxicity can be used to determine if the cytotoxic effect is cytocidal (cells are killed) or cytostatic (cell

growth and division inhibited). The two most common techniques used to assess cell growth are 3-(4,5-dimethylthiazol-2-yl)-2,5-diphenyltetrazolium bromide (MTT) and 2,3-bis(2-methoxy-4-nitro-5-sulphophenyl)-2*H*-tetrazolium-5-carboxanilide sodium salt (XTT). Inhibition of mitochondrial activity by changes in the cellular levels of nicotinamide adenine dinucleotide (NADH), glucose and other factors may cause variations in the results or give negative results associated with dead or nonproliferating cells (Houghton *et al*., 2007). This problem is overcome by using other techniques e.g. sulphorhodamine B (SRB), lactate dehydrogenase (LDH) leakage assay, neutral red and protein (Bradford) assays (indirect determination of cell viability) (Fotakis and Timbrell, 2006; Houghton *et al*., 2007).

The MTT-cell proliferation assay is a quantitative colourimetric assay, sensitive enough to measure cellular proliferation, viability and cytotoxicity (Holst-Hansen and Brünner, 1998). The yellow, water soluble tetrazolium MTT salt is reduced by metabolically active cells to insoluble dark blue-to-purple formazan crystals via the cleavage of the tetrazolium ring by succinate dehydrogenase within the mitochondria (Figure 4.2). The formazan product accumulates in healthy cells due to its impermeability to the cell membranes (Fotakis and Timbrell, 2006; Holst-Hansen and Brünner 1998). The formation of coloured formazan relies on mitochondrial activity (Houghton *et al*., 2007).

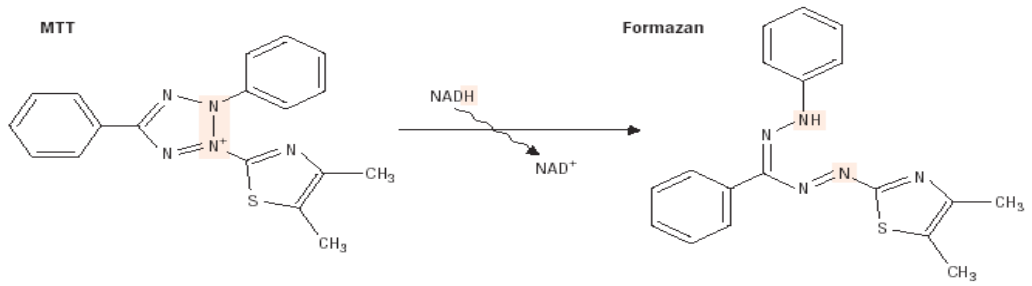

Figure 4.2: Reduction of MTT to formazan by succinate dehydrogenase within the mitochondria (www.biochem.roche.com).

The CellTiter-Blue® cell viability assay is based on the reduction of resazurin (dark blue; little intrinsic fluorescence) into highly fluorescent resorufin (pink) in metabolic active or viable cells (Figure 4.3). Nonviable cells lose their metabolic capacity; hence the indicator dye cannot be reduced.

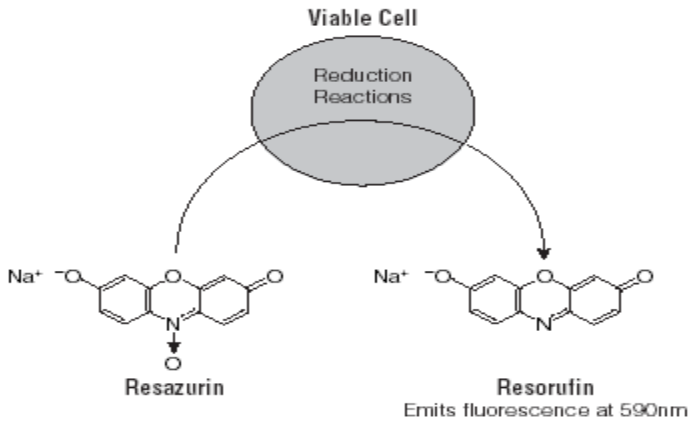

Figure 4.3: Reduction of resazurin to highly fluorescent resorufin in metabolic active cells (www.promega.com).

Most anticancer studies have focused on hypoxoside, which is converted to rooperol. Information on the anticancer properties of crude *Hypoxis* extracts is lacking; hence screening of *H. hemerocallidea*, *H. stellipilis* and *H. sobolifera* against three cancer cell lines was performed. This section focuses on the cytotoxicity of *Hypoxis* extracts and its purified compounds on HeLa, HT-29 and MCF-7 cancer cells, and peripheral blood mononuclear cells (PBMCs).

.4.2.2.2 Materials and Methods

Cell culture conditions. Adherent cancer cell lines (HeLa, HT-29, MCF-7) were routinely maintained in 10-cm culture dishes, without antibiotics in RPMI 1640 cell culture medium containing 25 mM Hepes, 2 mM glutamine (Lonza, Walkersville, MD, USA) and 10% fbs (not heat-inactivated; Gibco, Grand Island, NY, USA) in a humidified 5% CO_2 incubator at 37 ºC.

Treatment. HeLa, HT-29 and MCF-7 cancer cells were seeded at 30 000 cells/mL in 96-well plates and left to attach overnight at 37 ºC in a humidified incubator and 5% CO_2. PBMCs were isolated from venous blood of a healthy donor using heparinised Vacutainer® CPT™ cell preparation tubes (Beckton Dickinson, Plymouth, UK) within 30 min of collection. PBMCs were seeded at 500 000 cells/mL in round bottomed 96-well

plates. *Hypoxis* chloroform extracts were dried in vacuo on the day of the assay using a SpeedVac SC100 (Savant Instruments, NY, USA), resuspended in 0.25% dimethyl sulphoxide (DMSO; v/v), sonicated for 15 min and complete medium (RPMI 1640: 10% fbs), containing 100 µg/mL β-glucosidase, added to reach concentrations of 125-500 µg/mL of *Hypoxis* extract. Hypoxoside and rooperol were resuspended in DMSO (0.25%, v/v), sonicated for 15 min and complete medium containing 100 µg/mL β-glucosidase added to the former and only complete medium added to the latter to reach concentrations of 3.125-200 µg/mL and 1.25-80 µg/mL, respectively. Cisplatin (10 µM and 100 µM) and DMSO (0.25%, v/v) were used as positive- and vehicle controls, respectively. 2-Hydroxypropyl-β-cyclodextrin [CD; Shimoda Biotech (PTY) Ltd.] was dissolved in saline (0.9% NaCl), filter sterilized and cytotoxicity determined at concentrations between 0.5-50 mM. Sterols (β-sitosterol, campesterol, cholesterol and stigmasterol) were dissolved in absolute EtOH (5 mg/mL) by sonication for 15 min and diluted in CD, absolute EtOH and complete medium. Dilutions were made to reach concentrations of 0.8-100 µM, 4 mM and 5% for sterols, CD and EtOH, respectively. Cells were treated for 48 hrs. MTT assay was performed on adherent cells. In brief, treatments were removed via aspiration, 200 µL MTT [0.5 mg/mL (Holst-Hansen and Brünner, 1998)] was added to each well and incubated for three hrs at 37 °C. MTT was removed via aspiration, 200 µL DMSO was added to each well to dissolve the formazan crystals, and the absorbance read at 540 nm using a BioTek® PowerWave XS spectrophotometer. The CellTiter-Blue® cell viability assay was performed on PBMCs, according to the kit's protocol, and the fluorescence read at $560_{Ex}/590_{Em}$ using a Fluoroskan Ascent FL fluorometer (ThermoLabsystems, Finland). The half maximal inhibitory concentrations (IC_{50}) of hypoxoside and rooperol were determined using GraphPad Prism Version 4 (GraphPad Software, San Diego, USA). Statistical significance was determined using the two-tailed Student's t-test.

4.2.2.3. Results and Discussion

After 48 hrs exposure to the *Hypoxis* extracts, hypoxoside and rooperol, the MTT and CellTiter-Blue® cell viability assays were performed on the HeLa, HT-29 and MCF-7

cancer cell lines, and PBMCs, respectively, to determine cytotoxicity (Figure 4.4). Cytotoxicity of the *Hypoxis* extracts, hypoxoside and rooperol was expressed as a percentage of the vehicle control, which was zero. Cisplatin (10 of 100 nM) was used as positive control and cytotoxicity measured at concentrations of 10 and 100 µM. Treatment of HeLa, HT-29 and MCF-7 cancer cells with 10 µM cisplatin killed 85.23±0.77, 45.27±3.69 and 32.67±2.09 percent of the cells, respectively. Treatment of HeLa, HT-29 and MCF-7 cancer cells with 100 µM cisplatin killed 94.34±0.29, 92.26±0.19 and 94.12±0.47 percent of the cells, respectively (data not shown).

Cytotoxicity against the MCF-7 cancer cells was seen with all three *Hypoxis* extracts. *H. hemerocallidea* and *H. sobolifera* extracts at higher concentrations (250 and 500 µg/mL) had cytotoxic effects against the HeLa and HT-29 cancer cells, whereas a *H. stellipilis* extract stimulated growth at higher concentrations in these two cancer cell lines. *H. hemerocallidea* and *H. sobolifera* had the highest cytotoxic effects against HT-29 cancer cells, while *H. sobolifera* had the best overall cytotoxic effect against all three cancer cell lines. Treatment of PBMCs with the three *Hypoxis* spp. extracts showed growth stimulation (Figure 4.4), but the results were not statistically significant. Due to too low cytotoxic effects against the three cancer cell lines, IC_{50} values could not be determined for the *Hypoxis* extracts. The addition of β-glucosidase to the *H. hemerocallidea* extract (500 µg/mL) significantly increased the percentage of HT-29 ($p<0.01$) cancer cells killed. The addition of β-glucosidase to the *H. sobolifera* (125-500 µg/mL) extract significantly increased the percentage of HeLa ($p<0.05$ to $p<0.001$), HT-29 ($p<0.01$ to $p<0.001$) and MCF-7 ($p<0.01$ to $p<0.05$) cancer cells killed.

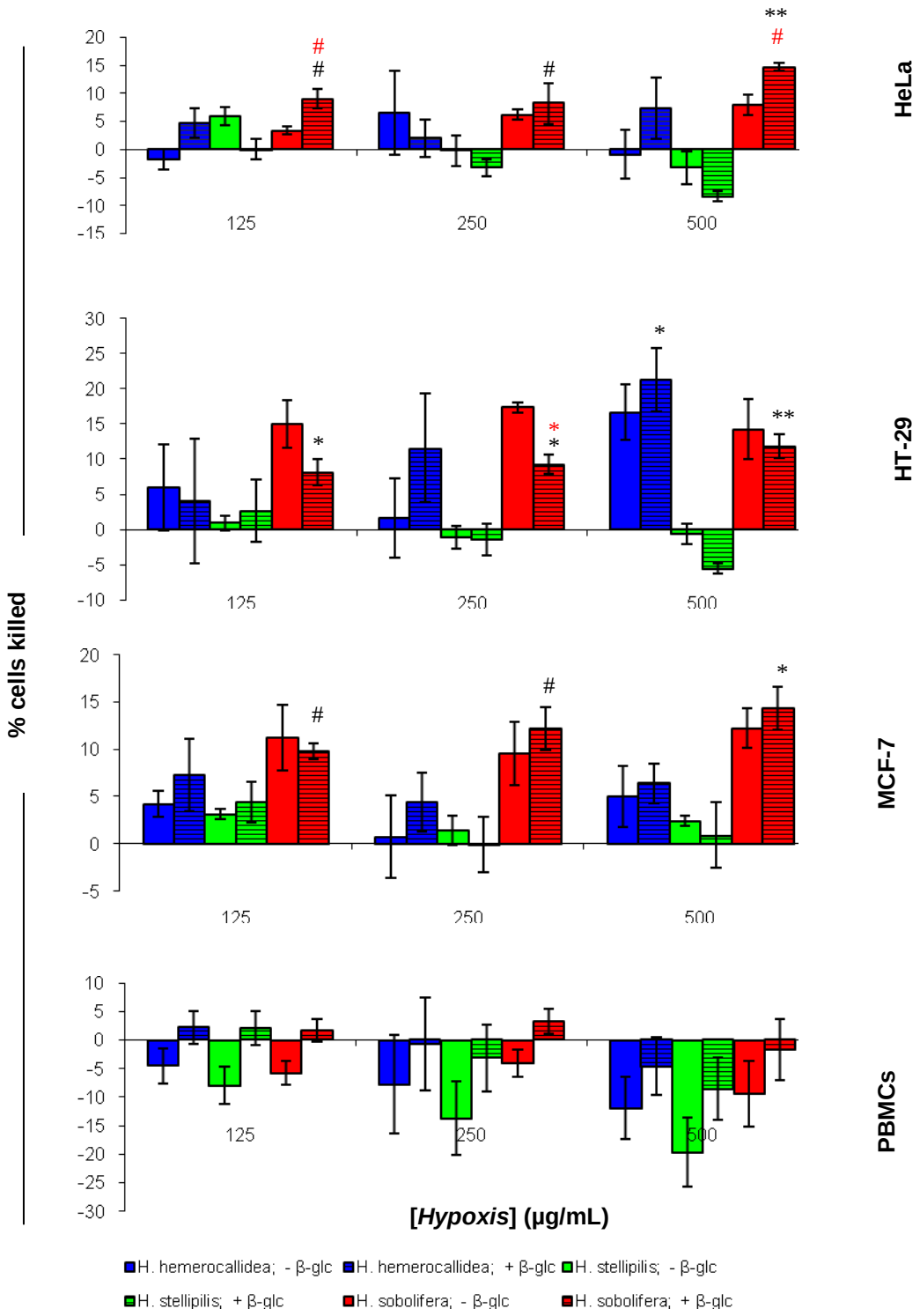

Figure 4.4: Percentage of HeLa, HT-29 and MCF-7 cancer cells, and PBMCs killed when treated with *H. hemerocallidea*, *H. stellipilis* and *H. sobolifera* in the presence and absence of β-glucosidase. Error bars indicate the SEM values of quadruplicate readings. Significance was determined using the two-tailed Student t-test: *p<0.01;

****p<0.001; #p<0.05 (black: control vs tests with β-glucosidase; red: tests with β-glucosidase vs tests without β-glucosidase).**

β-glucosidase added to the *H. hemerocallidea* extract had greater cytotoxic effects compared to *H. stellipilis* and *H. sobolifera*. This may be explained by the higher hypoxoside content present in the *H. hemerocallidea* chloroform extract compared to the other two *Hypoxis* chloroform extracts (Chapter 3, section 3.3). The increase in cytotoxicity seen when β-glucosidase was added to the H. hemerocallidea (against HeLa, HT-29 and MCF-7 cancer cells) and *H. sobolifera* (against HeLa and MCF-7 cancer cells) extracts may be attributed to unidentified compounds that are converted to cytotoxic compounds, because hypoxoside was undetectable in the *H. sobolifera* chloroform extracts (Chapter 3, section 3.3).

Growth stimulation of HeLa and HT-29 cancer cells in the presence of *H. stellipilis* is a concern, because *H. stellipilis* is often sold in herbal shops of the Eastern Cape province, South Africa. Cytotoxicity screening with an aqueous extract of *H. hemerocallidea* has shown growth stimulation of a prostate carcinoma (DU145) and non-malignant breast (MCF-12A) cell line, but inhibited MCF-7 cancer cell growth (Steenkamp and Gouws, 2006). Growth stimulation of PBMCs by the *Hypoxis* extracts shows the absence of toxicity in the extracts.

Cytotoxicity of hypoxoside and rooperol was determined against the HeLa, HT-29 and MCF-7 cancer cell lines, and PBMCs (Figure 4.5A and B). Fifty-percentage inhibition was achieved at very low hypoxoside and rooperol concentrations and IC_{50} values are summarized in Table 4.4.

Hypoxoside, the non-toxic compound isolated from *Hypoxis* spp., is converted to rooperol in the presence of β-glucosidase. Different IC_{50} values for hypoxoside and rooperol may be due to the unknown conversion rate/concentrations of hypoxoside to rooperol, dehydroxyrooperol and bisdehydroxyrooperol (Kruger et al., 1994). The cytotoxicity of the latter two analogues of rooperol has not been investigated. HT-29 cancer cells had the highest IC_{50} value for rooperol, whereas less than 20 μg/mL (<70

μM) was required to kill 50% of HeLa and MCF-7 cancer cells. Low concentrations of hypoxoside and rooperol stimulated growth of PBMCs (Figure 4.5), and their IC_{50} values for these cells from healthy donors were generally lower than for the cancer cell lines (Table 4.4). Hypoxoside IC_{50} values for HeLa, HT-29 and MCF-7 cancer cells were 26.46, 82.80 and 45.62 μg/mL, respectively, which are much higher than the 0.31 and 0.20 μg/mL present in 125 μg/mL of *H. hemerocallidea* and *H. stellipilis* extracts, respectively.

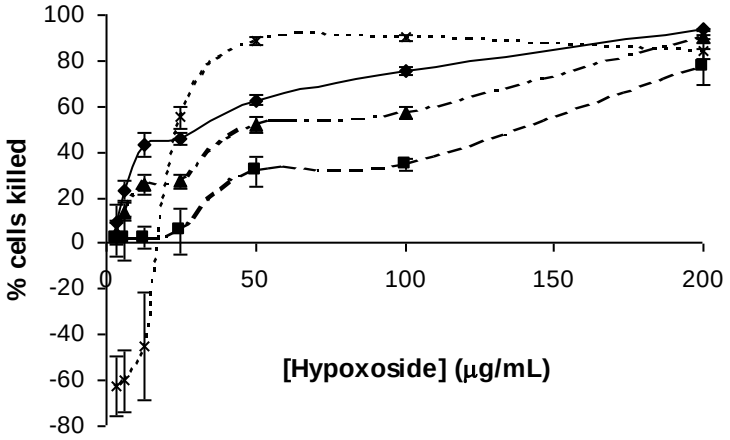

A

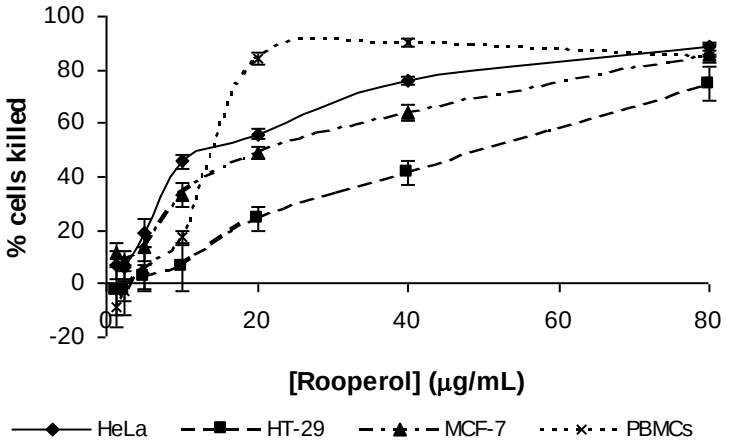

B

Figure 4.5: Cytotoxicity effects of hypoxoside and β-glucosidase (A) and rooperol (B) against the HeLa, HT-29 and MCF-7 cancer cell lines, and PBMCs. Error bars indicate the SD values of eight replicate values.

Table 4.4: IC_{50} values [µg/mL and µM (values in brackets)] of hypoxoside plus β-glucosidase and rooperol treatment of the HeLa, HT-29 and MCF-7 cancer cell lines, and PBMCs after 48 hours.

Treatment	HeLa	HT-29	MCF-7	PBMCs
Hypoxoside	26.46 (43.62)	82.80 (136.50)	45.62 (75.21)	19.31 (31.83)
Rooperol	13.01 (46.09)	29.03 (102.83)	18.66 (66.10)	12.13 (42.97)

In vitro screening of 60 human cancer cell lines by the National Cancer Institute (USA) and five tumour (breast, colon, uterus, melanoma and non-small-cell lung) cell lines by the Huntingdon Research Centre (England) have shown growth inhibition when exposed to purified hypoxoside. Cytotoxicity was due to the conversion of non-toxic hypoxoside to cytotoxic rooperol in the presence of β-glucosidase in foetal calf serum (Albrecht *et al*., 1995a). Albrecht *et al*. (1995a) have shown the absence of cytotoxicity when cancer cells were treated with hypoxoside at concentrations of up to 100 µg/mL. In the presence of β-glucosidase, cytotoxicity was seen at concentrations of 2-10 µg/mL. Theron *et al*. (1994) have shown cytotoxicity when B16-F10-BL6 mouse melanoma cells were treated with rooperol at a concentration of above 11 µM (~ 6.5 µg/mL) and an IC_{50} value of 20 µM (~ 12 µg/mL). In this study, IC_{50} values for HeLa and MCF-7 cancer cells, when treated with rooperol, were between 10-20 µg/mL. Positive *in vitro* results gave rise to a phase I trial in lung cancer patients (Albrecht *et al*., 1995b; Smit *et al*., 1995).

Cytotoxicity of sterols (β-sitosterol, campesterol, cholesterol and stigmasterol) was determined against the HeLa, HT-29 and MCF-7 cancer cell lines and PBMCs (Appendix 4). The best cytotoxicity was obtained against the HT-29 cancer cell line, with very little cytotoxicity against the HeLa and MCF-7 cancer cell lines. High sterol concentrations, ±25-40 µM and ±25-30 µM were needed for cytotoxicity against HeLa and MCF-7 cancer cells, respectively. Sterols had no cytotoxicity against PBMCs, even at concentrations as high as 100 µM.

Researchers have used sterols at concentrations of 8 and 16 µM and incubation periods of 2-16 days with frequent sterol changes (every second day) (Awad *et al*., 1996; Awad *et*

al., 1998; Awad *et al*., 2001a; Awad *et al*., 2003a/b; Awad *et al*., 2005a; Awad *et al*., 2007; von Holtz *et al*., 1998). Awad *et al*. (2005a) exposed Caco2 (a model for human intestinal epithelial cells) cells to cholesterol, campesterol and β-sitosterol (16 μM) for 16 days, changing the medium every second day. Brassinosteroids (steroid plant hormones with similar ring structure to phytosterols) analogues inhibited breast (MCF-7, MDA-MB-468)- and prostate (DU-145, LNCaP) cancer cell growth at micromolar concentrations with minimal effects on normal cells. Non-brassinosteroid plant sterols β-sitosterol, stigmasterol and cholesterol had extremely weak to no detectable activities – even at concentrations of 50 μM. β-sitosterol, stigmasterol and cholesterol showed some cytotoxicity (IC_{50} >30 uM) against the multiple myeloma RPMI 8226 cell line after 72 hrs exposure (Malíková *et al*., 2008).

β-sitosterol was not investigated as active compound in this study because several researchers have already shown mechanisms of action for its anticancer properties. β-sitosterol concentrations in the *Hypoxis* extracts (1.77, 0.61 and 4.50 μM in *H. hemerocallidea*, *H. stellipilis* and *H. sobolifera*, respectively) were lower than the concentrations (8 or 16 μM) used by Awad and co-workers. Awad *et al*. (2003b) have shown that β-sitosterol (16 μM) inhibits MDA-MB-231 human breast cancer cell growth by 70%, while Awad *et al*. (2007) have shown that 8 and 16 μM β-sitosterol decreased MCF-7 breast cancer cell growth by 63 and 81%, respectively, compared to the control. Awad and co-workers have shown that β-sitosterol induces apoptosis by Fas signalling (Awad *et al*., 2007), activates caspases-8 (extrinsic pathway) and -9 (intrinsic pathway) in MCF-7 and MDA-MB-231 human breast cancer cells (Awad *et al*., 2003a; Awad *et al*., 2007) and reduces metastasis in MDA-MB-231 cells (Awad *et al*., 2001a). Choi *et al*. (2003) have shown the induction of Bax in HT116 human colon cancer cells after β-sitosterol treatment. β-sitosterol downregulates cholesterol synthesis from mevalonate and stimulates the MAPK pathway in MDA-MB-231 cells (Awad *et al*., 2003b). Furthermore, β-sitosterol alters membrane lipids (Awad *et al*., 1996) in HT-29 cancer cells and activates the sphingomyelin cycle in LNCaP human prostate (von Holtz *et al*., 1998) and HT-29 colon (Awad *et al*., 1998) cancer cells. Although the β-sitosterol concentrations in the *Hypoxis* chloroform extracts were lower than the concentrations

used in the above mentioned studies, it may have contributed to the cytotoxic effects seen against the HeLa, HT-29 and MCF-7 cancer cells.

Researchers have found conflicting cholesterol lowering effects of phytosterols, which could be ascribed to their bioavailability. Bioavailability may be influenced by slow dissolution rates of sterols from cyclodextrin and low solubility of sterols in aqueous and organic solvents. It may take several days to weeks for highly purified phytosterols to dissolve in bile salt solutions. To increase solubility, phytosterols can be dissolved in oil or egg fat, emulsified in aqueous medium with lecithin, and finely micronized and mixed with fatty foods for *in vivo* studies (Ostlund, 2002). Phytosterol solubility can be increased by esterification to form phytosterol esters. In the present study, poor solubility and release of (phyto)sterols may have contributed to the weak cytotoxicity seen against the HeLa, HT-29 and MCF-7 cancer cells (Appendix 4).

Cyclodextrins are cyclic oligosaccharides consisting of 6 (α), 7 (β) or 8 (γ) glucopyranose subunits, linked by α-(1,4) bonds, with hydrophobic interiors. They are enzymatically produced from starch. Cyclodextrins have hydrophillic exteriors, making them water-soluble, and hydrophobic interiors, which form microenvironments for non-polar molecules (Greenberg-Ofrath *et al*., 1993; Martin Del Valle, 2004). Non-polar drugs, the size of the hydrophobic core, form complexes with the cyclodextrin, thus increasing their solubility in polar aqueous environments. Cyclodextrins are non-toxic (due to lack of absorption from the gastrointestinal tract, *in vivo*), do not denature proteins or interfere with enzymatic reactions, and is rapidly reversible to release the drug. Two factors influence complex formation between cyclodextrin and the drug namely, (i) the size of the drug to fit the cyclodextrin cavity, and (ii) thermodynamic interactions between cyclodextrin, the drug and the solvent. Generally one molecule is included into one cyclodextrin cavity, but sometimes more than one molecule enters a cavity (low molecular weight molecules) or more than one cyclodextrin molecule bind the drug molecule (high molecular weight molecules). Heating increases the solubility of complexes, but may destabilize complexes at too high temperatures (Martin Del Valle, 2004). Greenberg-Ofrath *et al*. (1993) have shown that CDs can be carriers of lipids such

as cholesterol. Concentrations of 5 to 10 mM of hydroxypropyl-β-CD were not toxic to mycoplasma cells. Cyclodextrin carries the drug through the aqueous barrier to the lipophilic surface of biological membranes, where the drug partitions from the complex into the lipophilic membrane. An excess of cyclodextrin may influence the permeability of the membranes (Másson *et al*., 1999).

In this study, cyclodextrin concentration of 4 mM (Appendix 4) was not toxic to the cells investigated and corresponded to the 5 mM cyclodextrin used by Awad and other researchers. The incorrect temperature and amount of sterol molecules entering cyclodextrin may have influenced the uptake of sterols by cyclodextrin. The main reasons for failure of sterols to show cytotoxicity against HeLa, HT-29 and MCF-7 cancer cells may be due to preparation of sterol-cyclodextrin complexes, uptake of sterols by cyclodextrin, too short exposure periods (two days), release of non-polar sterols from cyclodextrin into polar environment and sterol medium that was not replaced daily.

In summary, the cytotoxicity of *Hypoxis* extracts and its purfied compounds were investigated against HeLa, HT-29 and MCF-7 cancer cells, and PBMCs. Cytotoxicity of *Hypoxis* extracts were low, which may be due to very low concentrations (*H. hemerocallidea* and *H. stellipilis*) or no (*H. sobolifera*) hypoxoside in the *Hypoxis* chloroform extracts. Hence very little hypoxoside was converted to rooperol by β-glucosidase, which may have had no effect on cytotoxicity. *Hypoxis* extracts were not toxic to PBMCs. Purified compounds were screened for cytotoxicity to explain its role in the *Hypoxis* extracts. Cytotoxicity of *Hypoxis* extracts may be due to the phytosterol content, especially β-sitosterol, but could not be confirmed. Synergistic and/or additive effects of the purified and unknown compounds in the *Hypoxis* chloroform extracts may have caused the cytotoxicity.

4.2.3. Conversion of hypoxoside to rooperol (time study)

4.2.3.1. Background

Non-toxic hypoxoside is converted to cytotoxic rooperol in the presence of β-glucosidase, *in vitro* (Albrecht *et al*., 1995a).

This section focuses on the conversion rate of hypoxoside to rooperol under the defined culture conditions in the presence of β-glucosidase, and rooperol uptake by HeLa, HT-29 and MCF-7 cancer cells. Albrecht *et al*. (1995a) investigated the morphological effects of hypoxoside after 12 hrs. A time study of hypoxoside conversion to rooperol, and rooperol uptake may explain morphological or biochemical features of apoptosis at earlier time intervals in cancer cells.

4.2.3.2. Materials and Methods

HeLa, HT-29 and MCF-7 cancer cells were seeded at 30 000 cells/mL in 24-well plates and left to attach overnight at 37 ºC in a humidified incubator and 5% CO_2. Cells were treated with hypoxoside (100 µg/mL) and β-glucosidase (100 µg/mL), and 20 µL aliquots removed at 0, 3, 6, 9, 12 and 24 hrs. β-glucosidase activity was inhibited by adding 1 mM nojirimycin bisulfite (2 µL; Sigma) to the aliquots, while keeping on ice. Hypoxoside and rooperol were dissolved in ddH_2O and loaded (5 µL = 5 µg) onto silica coated, aluminium TLC plates and dried. Optimized mobile phase for rooperol separation was chloroform: ethylacetate: formic acid (5:4:1). Samples (10 µL) and standard (rooperol) were spotted onto TLC plates, as described above and developed in chloroform: ethylacetate: formic acid (5:4:1). TLC plates were dried and stained as described in Chapter 3 (section 3.3.2). Densitometry was used to determine the amount of rooperol present in the medium over time. A rooperol standard curve (Appendix 4), ranging between 0.5 µg – 10 µg, was prepared and the integrated density values (IDVs) determined.

4.2.3.3. Results and Discussion

One hundred µg/mL of hypoxoside was used in this study, as Albrecht *et al*. (1995a) found no *in vitro* cytotoxicity against murine and human melanoma cell lines when serum was heat-inactivated. Converted rooperol in the medium was determined from a rooperol concentration as a function of IDV standard curve (R^2 = 0.9905; Appendix 4) and plotted as a kinetic curve (Figure 4.6).

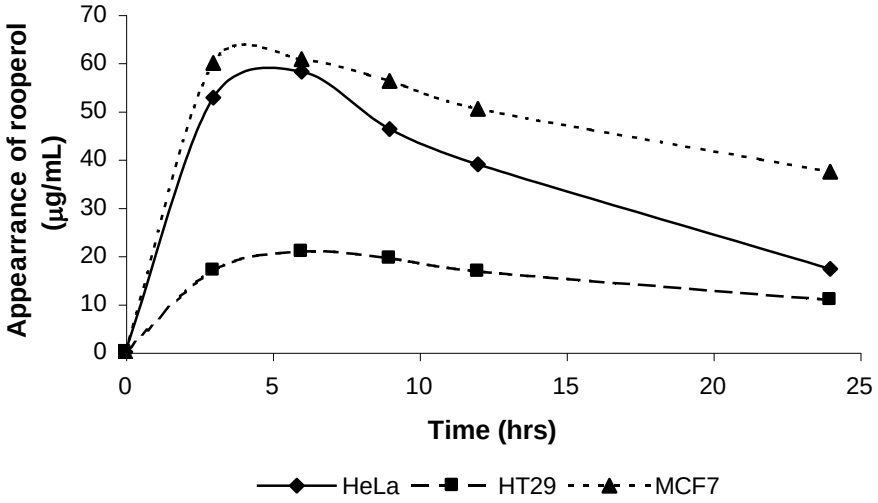

Figure 4.6: Amount of rooperol (µg/mL) present in the culture medium of each cell line (HeLa, HT-29 and MCF-7) after conversion of hypoxoside (100 µg/mL) to rooperol via β-glucosidase (100 µg/mL) over a time period of 24 hrs.

A large percentage of hypoxoside was converted to rooperol in the medium of HeLa, HT-29 and MCF-7 cancer cells after three hrs of exposure. The maximum concentration of rooperol in the culture medium of HeLa and MCF-7 cancer cells was 60 µg/mL, and 20 µg/mL in the culture medium of HT-29 cancer cells. A high percentage (~ 60 %) of hypoxoside was converted to rooperol in the culture medium of HeLa and MCF-7 cancer cells. Morphological changes, associated with apoptosis, may occur as early as 6 hrs when treated with hypoxoside. Albrecht *et al*. (1995a) have shown amorphous chromatin clumps after 12 hrs, cytoplasm vacuolization after 16 hrs and massive vacuoles and disintegrating cells after 24 hrs using phase contrast micrographs in BL-6 mouse melanoma cells exposed to 50 µg/mL hypoxoside and 100 µg/mL β-glucosidase.

Transmission electron micrographs have shown vacuoles in the cytoplasm, amorphous material in vacuoles, disintegrating mitochondria, condensed cytoplasm and fragmented nuclei in BL-6 cells after 24 hrs of treatment. Scanning electron micrographs of UCT-Mel 1 melanoma cells have shown pore formation in the plasma membranes and apoptotic body formation afer 24 hrs.

This study provides data on the rate at which hypoxoside is converted to rooperol by β-glucosidase. Morphological and biochemical apoptotic features in HeLa, HT-29 and MCF-7 cancer cells may be detected before 12 hrs. The conversion rate of hypoxoside to rooperol also forms part of optimizing the exposure time of these compounds to HeLa, HT-29 and MCF-7 cancer cells. Hypoxoside conversion to rooperol and rooperol uptake by cancer cells need further investigation by repeating the experiment or by using more accurate kinetic studies.

4.2.4. DNA cell cycle arrest

4.2.4.1. Background

DNA plays a pivotal role in the development and treatment of cancer. DNA damage is associated with cancer development (mutations) and treatment (radiation therapy and/or chemotherapeutic agents) in normal and cancer cells, respectively. DNA damage, associated with treatment, is also responsible for most side effects in normal cells (Kastan and Bartek, 2004). The normal cell cycle is divided into the G0, G1, S, G2 and M phases (Figure 4.7). G0/G1, G2/M and S phases are characterized by diploid (2N), tetraploid (4N) and intermediate (ranging from 2N to 4N) DNA content, respectively. The DNA histogram represents DNA content distribution for a population of cells through the cell cycle (Hodgetts *et al*., 1988). G0 and G1 phases are associated with growth and reorganization, whereas the S and M phases are associated with DNA synthesis and mitosis, respectively (Pestell *et al*., 1999; Planchais *et al*., 2000).

4.2.4.1.1. DNA cell cycle arrest and progression machinery

Cell cycle progression is controlled by two mechanisms, namely (i) protein phosphorylation for cells to enter the next phase and (ii) cell cycle checkpoints, which monitor the completion of critical events after each phase and are able to prevent cells from entering the next phase (Collins *et al*., 1997a).

CDKs. Cyclin-dependent kinases (CDKs; ser/thr protein kinases) are activated when bound to cyclin subunits to form active cyclin-CDK complexes, each with unique substrate specificity. CDK levels remain constant, whereas cyclin levels vary during the cell cycle due to expression and degradation. Eleven CDKs are found in mammalian cells and the most commonly found cyclin-CDK complexes in early-to-mid G1, late G1-to-S and G2/M phases are cyclin D-CDK4/6, cyclin A/E-CDK2 and cyclin B-CDK1, respectively (Figure 4.7). Cyclin-CDK complexes function in the G1 and G2 phases to initiate S phase and mitosis, respectively (Chibazakura *et al*., 2004; Collins *et al*., 1997a; Nojima, 2004; Pestell *et al.*, 1999).

CDK-cyclin complexes are regulated by phosphorylation, dephosphorylation and CDK inhibitor (CDKI) binding. Two types of CDK inhibitors are found in cells, namely the Ink4 and Cip1/Kip1 families. The Ink4 family consists of $p16^{Ink4a}$, $p15^{Ink4b}$, $p18^{Ink4c}$ and $p19^{Ink4d}$ members and inhibits cyclin D-CDK4 complexes (early G1) by competing with cyclin D for binding to CDK4 and dissociates cyclin D-CDK4 complexes. The Cip1/Kip1 family consists of $p21^{Cip1/Kip1}$, $p27^{Kip1}$ and $p57^{Kip2}$ members and inhibits cyclin A/D/E-CDKs activities by associating with cyclin-CDK complexes (Nojima, 2004; Pestell *et al.*, 1999). Cip/Kip family members are found in the cytoplasm and nucleus of the cell and may function as (i) potential assembly factors (enhancing cyclin D and CDK4 binding in the cytoplasm by acting as a bridge, and promote translocation into the nucleus), (ii) regulators of apoptosis (anti-apoptotic or pro-survival depends on cyclin B-CDK1 inhibition and G2 arrest; p21 is cleaved by caspase-3 and relocates from the nucleus to the cytoplasm, resulting in increased CDK2, (iii) transcriptional cofactors [p21 regulates nuclear factor (NF)-κB, STAT3, Myc, E2F and C/EBP activity, and inhibits

genes encoding for DNA polymerase α, topoisomerase II, CDK-1 and cyclin B, which is involved in progression] (Coqueret, 2003).

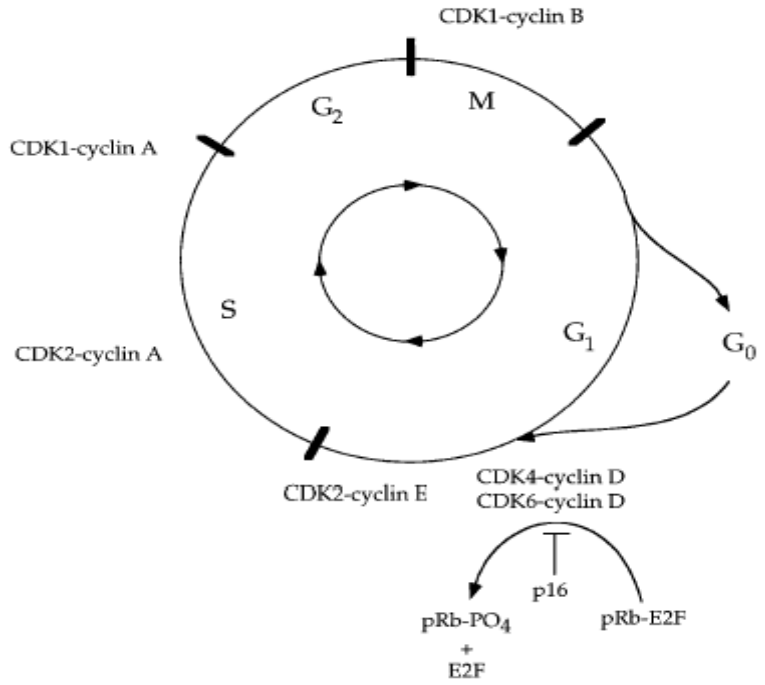

Figure 4.7: DNA cell cycle representing the five phases, CDKs and cyclins involved (Collins *et al*., 1997a).

Checkpoints/restriction points. Progression from one phase to the next depends on passage through the cell cycle checkpoints. Cell cycle checkpoints are mechanisms used by cells to ensure that earlier processes, like DNA replication (underreplicated and repair to damaged DNA) and mitosis (segregated chromosomes), are complete (Collins *et al*., 1997a; Kastan and Bartek, 2004). Activated checkpoints relay signals to the cell cycle progression machinery where cell cycle progression is delayed to prevent mutations. Cell cycle checkpoints are not an essential part of the cell cycle progression machinery and are not activated in every cell, as is the case with kinases. The link between cancer and the cell cycle is proliferation, where the former is characterized by inappropriate cell proliferation and the latter controls the cell cycle machinery (Collins *et al*., 1997a). Cell cycle checkpoints rapidly induce cell cycle arrest when receiving a stress signal by activating damage DNA repair- and replication-stalling mechanisms. Cell cycle arrest is maintained until DNA repair is complete. Uncontrolled checkpoints may result in DNA

damage leading to inceased mutation rates, chromosome instability, and aneuploidy contributing to tumour development (Nojima, 2004).

4.2.4.1.2. Checkpoints and progression

G0/G1 phase, checkpoint and G1-S progression. Two tumour suppressor pathways, p53 and pRb, are involved in the G1 phase of the cell cycle. These pathways are also commonly deregulated in human cancer (Kastan and Bartek, 2004).

p53 tumour gene, the most commonly mutated gene in cancer (50%), encodes for a 53 kDa transcription factor (p53), which induces gene expression associated with cell cycle regulation, DNA damage repair and apoptosis (Nojima, 2004; Fadeel and Orrenius, 2005). The ATM(ATR)/CHK2(CHK1)-p53/MDM2-p21 pathway is the most important checkpoint responding to DNA damage in the G1 phase. ATM (ataxia telangiectasia mutated)/ATR (AMT- and Rad3-related) and checkpoint-transducer serine/threonine kinases (CHK)1/2 phosphorylate the p53 transcription factor, causing MDM2 (an ubiquitin ligase) to dissociate from p53. This leads to stabilization and accumulation of p53 protein, which transcriptionally target several genes including the CDK inhibitor, $p21^{Waf1/Cip1}$ (Kastan and Bartek, 2004; Nojima, 2004). p53 expression levels are low in the absence of cellular stress, but increase due to different stresses (e.g. DNA damage). If DNA damage is too severe, p53 will induce apoptosis. Other possible G1 checkpoints may involve proteosomal degradation of cyclin D resulting in $p21^{Waf1/Cip1}$ release, which binds cyclin E-CDK2 and inactivates its kinase activity. Another mechanism may involve an increase in $p16^{Ink4a}$ and $p21^{Waf1/Cip1}$, which bind and inactivate cyclin D-CDK4/6 and cyclin E-CDK2, respectively (Nojima, 2004).

The tumour suppressor, retinoblastoma (pRb) protein, plays an important role in G1 arrest and G1-S progression. Rb, in its un(hypo)phosphorylated form, binds the early gene 2 factor (E2F) to form a transcriptional repressing complex in early to mid-G1 phase, hence G1 arrest. Cyclin D-CDK4/6 and cyclin E-CDK2 phosphorylate the pRb family of nuclear phosphoproteins in mid-G1 and late G1/early S phase, respectively,

which become hyperphosphorylated (and inactive) and is released from the E2F complex resulting in G1-S progression. E2F regulates the expression of genes required for S phase entry and DNA synthesis (Avni *et al*., 2003; Collins *et al*., 1997a; Nojima, 2004). Phosphorylation of pRB is prevented by the inhibition of cyclin-CDK activity by CDKIs.

In quiescent cells, cyclin D levels are low but increase in the nucleus during the G1 phase. Overexpression of cyclin D promotes cell progression through the G1 phase. When cells enter the S phase, cyclin D moves from the nucleus into the cytoplasm (Pestell *et al*., 1999). CDC25 phosphatase removes inhibitory phosphates from CDKs and promotes cell cycle progression. CDC25A overexpression activates cyclin A/E-CDK2 (Nojima, 2004). Cyclin E and A levels peak late in G1 phase and bind CDK2 with maximum function at G1/S transition. Overexpression of cyclin-E decreases the time it takes for the cell to finish the G1 phase and enter the S phase. Effect of cyclin D and -E is dependent and independent, respectively, on pRb (Pestell *et al*., 1999). During genotoxic stress, CHK 1/2 activity increases and phosphorylates CDC25A, which gets tagged for proteolysis and degradation. Cyclin E/A-CDK2 complex activity gets inhibited (see below), thus inducing the G1/S checkpoint. The CDC25A-degradation pathway is activated faster than the p53 pathway, because it does not need transcription and accumulation of newly synthesized products (Kastan and Bartek, 2004; Nojima, 2004).

$p21^{Waf1/Cip1}$ trancription is induced by the tumour suppressor p53, antimitogenic cytokine transforming growth factor (TGF)-β and phorbol ester tetradecanoyl-phorbol acetate. $p21^{Waf1/Cip1}$ may regulate transcription of genes involved in growth arrest, apoptosis, aging and senescence after DNA damage. $p21^{Waf1/Cip1}$ and $p27^{Kip1}$ inhibitors are associated with the active form of cyclin D-CDK4/6, whereas low Kip/Cip1 concentrations inhibit CDK2 but not CDK4/6. G1-S progression depends on inhibitor free cyclin E-CDK2, but tolerates inhibitor bound cyclin D-CDK4/6. In the nucleus more $p21^{Waf1/Cip1}$ and $p27^{Kip1}$ will bind cyclin D-CDK4/6 complexes, rendering cyclin E-CDK2 free to be active. During cell cycle arrest Kip/Cip protein levels increase – saturating

cyclin D-CDK4/6 – and binding cyclin E-CDK2, which blocks G1-S progression (Coqueret, 2003). $p21^{Waf1/Cip1}$ thus has a cell cycle arrest and progression function.

S phase and checkpoint. The S phase is characterized by DNA replication. Checkpoints activated during the S phase may be in response to DNA replication stress (chemical agents e.g. aphidicolin, methyl methanesulfonate, UV), which may interfere with the DNA machinery (e.g. replication forks, DNA polymerase, DNA replication) or in response to double stranded breaks (intra-S-phase checkpoint). CDC25A degradation is involved in the S-phase checkpoint, by inhibiting the S-phase promoting activity of cyclin E-CDK2 and blocking DNA replication. Other proteins that get phosphorylated and are involved in the S phase checkpoint include the breast cancer (BRCA) susceptibility gene 1/2, Nijmegen breakage syndrome (NBS) gene 1, CHK1 and mediator of DNA damage checkpoint (Mdc) protein 1 (Nojima, 2004). DNA synthesis can be halted by (i) $p21^{Cip1/Waf1}$ binding preventing the cyclin A/E-CDK2 complex from loading CDC45 onto chromatin, which is necessary for recruiting DNA polymerase α into assembled pre-replication complexes (blocks initiation of DNA replication), (ii) preventing pRb phosphorylation (pRb inhibits E2F-dependent transcription of S phase genes for S phase entry) and (iii) ATM-mediated phorphorylation of NBS1 and SMC1 (cohesion protein). Other kinases may be involved in delaying DNA synthesis (Kastan and Bartek, 2004; Nojima, 2004). Hypophosphorylated Rb may reappear before mitosis and play a role in inhibiting S phase progression, but the mechanism is poorly understood. Hypophosphorylated Rb associated with G1 arrest can be prevented by cyclin E overexpression, but cyclin E cannot overcome S phase arrest associated with hypophosphorylayed Rb expression (Avni *et al*., 2003). Avni *et al*. (2003) have shown the accumulation of hypophosphorylated Rb in S phase damaged chromatin and its existence is dependent on the phosphatase, PP2A. Rb may interact with replication initiation sites after S phase damage.

G2/M phase checkpoint and G2-M progression. The M phase is characterized by the segregation of the genome into two daughter cells and splitting into two new cells. The G2/M checkpoint targets cyclin B-CDK1, which is involved in promoting mitosis. The CDK1 activity during mitotic exit is inhibited by cyclin A/B degradation via the

anaphase-promoting complex (APC) by initiating proteosomal cyclin degradation through ubiquitination. Cyclin destruction is initiated at the metaphase and completed at the anaphase. Towards the end of anaphase, CDK1 activity is extinguished to allow mitotic exit, reassembly of preinitiation complexes at replication origins and establishing the G1 state (Chibazakura *et al*., 2004; Kastan and Bartek, 2004; Pestell *et al*., 1999; Sivaprasad *et al*., 2007; Sudo *et al*., 2004). CDKIs ($p21^{Cip1/Waf1}$ and $p27^{Waf1}$) regulate CDK activity during mitosis by binding mitotic cyclin B-CDK1 and persist from the mid-M to G1 phase. Overexpression of cyclins (e.g. cyclin A) in the absence of CDKIs ($p21^{Cip1/Waf1}$, $p27^{Waf1}$, p107) may result in cells exiting mitosis without separation of sister chromatids (Chibazakura *et al*., 2004). The G2/M checkpoint prevents mitosis initiation after detecting DNA damage during the G2 phase or cells entering G2 from G1/S with damaged DNA. Maintenance of the G2 checkpoint may depend on BRCA1 and p53, which upregulate cell cycle inhibitors (Kastan and Bartek, 2004).

DNA cell cycle arrest is an important starting point in investigating the anticancer mechanism of action. This section focuses on DNA cell cycle arrest in HeLa, HT-29 and MCF-7 cancer cells when treated with *Hypoxis* extracts and rooperol.

4.2.4.2 Materials and Methods

DNA cell cycle arrest. HeLa, HT-29 and MCF-7 cancer cells were seeded at 1.2×10^6 cells/10 mL in 10-cm culture dishes and left to attach overnight at 37 ºC in a humidified incubator and 5% CO_2. DMSO (0.25%, v/v), *Hypoxis* chloroform extracts (125 µg/mL) and rooperol [IC_{50} values (Table 4.4)] were added as described above. *Hypoxis* extract concentrations above 125 µg/mL are too high for *in vitro* studies, whereas concentrations below 125 µg/mL would have shown no effects, hence 125 µg/mL was chosen. After 15 and 48 hrs of treatment, cells were trypsinized for 10 min, resuspended in 100 µL sheath fluid (Beckman Coulter) and transferred to polypropylene tubes. The Coulter® DNA Prep™ reagents kit (Beckman Coulter) was used for DNA cell cycle analysis. Lysis reagent (100 µL; containing <0.1% NaN_3, nonionic detergents, saline and stabilizers) was added to each tube, vortexed and incubated for five min at room temperature. Five

hundred µL of propidium iodide (50 µg/mL) was added and incubated in the dark for 15 min at 37 ºC. Samples were immediately analyzed using a Beckman Coulter Cytomics FC500 (Miami, FL, USA). Biological standards (including human lymphocytes or granulocytes, trout red blood cells and others) are used to correct for the preparation and staining procedures. Trout red blood cells are used more frequently, because it differs from human diploid cells with regard to DNA content (Jakobsen, 1983). Trout red blood cells (Beckman Coulter, 100 µL) were treated as described above and used as internal reference standard.

$p21^{Waf1/Cip1}$ expression. HeLa, HT-29 and MCF-7 cancer cells were seeded at densities of 40 000 cells/mL in 24-well plates and left to attach overnight at 37 ºC in a humidified incubator and 5% CO_2. Cells were treated with DMSO (0.25%, v/v), *H. sobolifera* chloroform extract (125 µg/mL) and rooperol [IC_{50} values (Table 4.4)] for 15 hrs. After exposure, cells were washed with PBSA, trypsinized for 10 min at 37 ºC and resuspended in 1 mL PBS. Cells were centrifuged at 500 x g for five min at room temperature and the supernatant discarded. Cells were washed as described above to remove any traces of trypsin. Cells were fixed and permeabilized using the IntraPrep™ permeabilizing reagent (Beckman Coulter) as described in the kit protocol. In brief, 50 µL of IntraPrep Reagent 1 (5.5% formaldehyde) was added to the cells, vortexed vigorously and fixed for 15 min at room temperature. Fixative was removed by centrifuging cells at 300 x g for five min at room temperature, supernatant discarded and cells washed with 1 mL PBS by centrifugation. Cells were resuspended by vortexing and permeabilized by adding 50 µL of IntraPrep Reagent 2 (PBS-buffered saponin-based permeabilizing and lysing medium), mixed without vortexing and incubated for five min at room temperature. After permeabilization, the permeabilizing reagent was removed, cells washed using cold incubation buffer [0.5% bovine serum albumin (BSA) in PBS], supernatant discarded and cells blocked for 10 min in incubation buffer at room temperature. $p21^{Waf1/Cip1}$ (12D1) rabbit mAbs (Cell Signaling Technology) were added at recommended working dilutions to the cells and incubated for one hour at room temperature. Cells were washed twice as described above. After washing, fluorescein isothiocyanate (FITC) conjugated goat anti-rabbit IgG (H+L chain specific) (Beckman Coulter) was added at recommended working

dilutions. FITC conjugated rabbit IgG, was added to untreated HeLa, HT-29 and MCF-7 cancer cells and used as an isotype control. Cells were incubated for 30 min at room temperature in the dark and washed as described above. Cells were resuspended in 500 μL PBS and read on a Beckman Coulter Cytomics FC500.

4.2.4.3 Results and Discussion

DNA Cell Cycle Arrest. Cell cycle arrest is characterized by a high proportion of cells found in the same cell cycle event at the same time after treatment with an anticancer compound or agent (Planchais *et al*., 2000). Distribution of DNA content in human tumours plays an important role in identifying mechanisms or pathways involved in cancer and treatment (Jakobsen, 1983). DNA cell cycle analysis was performed on HeLa, HT-29 and MCF-7 cancer cells after 15 hrs (Figure 4.8) and 48 hrs (Figure 4.9) of exposure to *H. hemerocallidea*, *H. stellipilis* and *H. sobolifera* extracts, and rooperol.

DNA cell cycle arrest occurred in the late G1 and/or early S-phase of HeLa, HT-29 and MCF-7 cancer cells when treated with *Hypoxis* chloroform extracts and rooperol. The G0/G1 peaks were much smaller than that of the control in all the *Hypoxis* treated cells (Figures 4.8-9). The three *Hypoxis* extracts had similar effects on the three cancer cell lines after 15 hrs of exposure. These effects include S-phase arrest and endoreduplication (ER). After 48 hrs *H. stellipilis* and *H. sobolifera* had greater effects on the three cancer cell lines compared to *H. hemerocallidea*. Rooperol has shown greater S phase arrest in the HT-29 and MCF-7 cancer cells, but less endoreduplication. The opposite was seen for rooperol against the HeLa cancer cell line. After 48 hrs, S phase arrest increased in HeLa cancer cells, while endoreduplication decreased. Endoreduplication increases in rooperol treated MCF-7 cancer cells after 48 hrs. DNA cell cycle arrest occurred in the S and G2/M phases when HT-29 cancer cells were treated with rooperol for 48 hrs. In general, *Hypoxis* extracts and rooperol caused an increase in G2/M phase arrest in the three cancer cells after 48 hrs. From the results obtained, it was not clear if cell cycle arrest occurred in the late Gl and/or early S phase in HeLa, HT-29 and MCF-7 cancer cells. DNA cell cycle arrest in the late G1 and/or early S phase of the cell cycle in HeLa,

HT-29 and MCF-7 cancer cells was further investigated using the CDKI, p21$^{Waf1/Cip1}$ (see below).

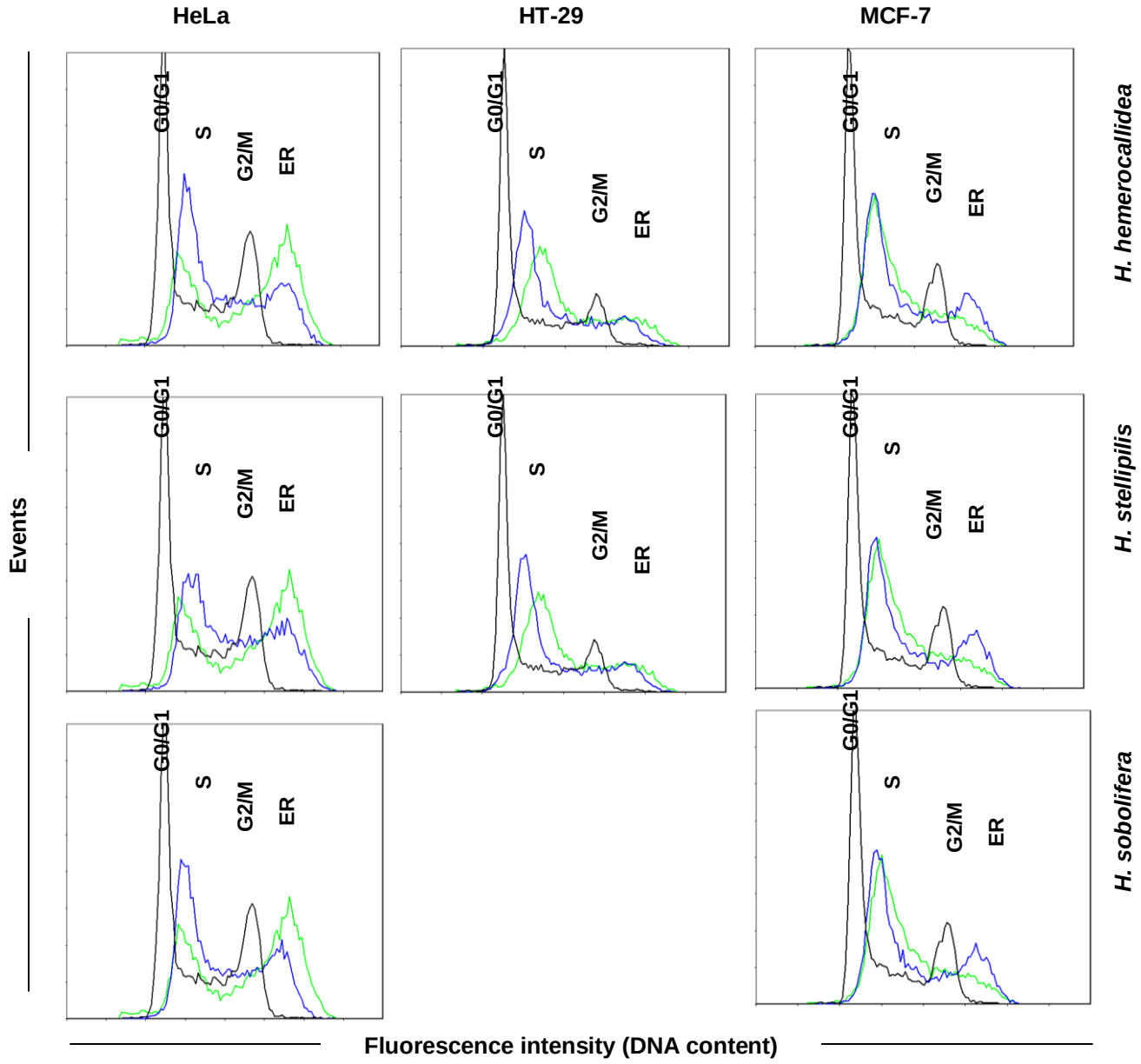

Figure 4.8: Overlay of histograms representing DNA cell cycle arrest in HeLa, HT-29 and MCF-7 cancer cell lines after 15 hrs treatment with DMSO (0.25%; black), *Hypoxis* chloroform extract (125 µg/mL; blue) and rooperol (IC_{50} values; green). Trout red blood cells were used as DNA reference calibrator (Appendix 4). 10 000 events were recorded. The experiment was repeated twice with similar results. Abbreviation: ER = endoreduplication. No results shown for HT29 cells treated with *H. sobolifera* extract at 15 hours due to contamination. See Figure 4.9 for 48 hrs results.

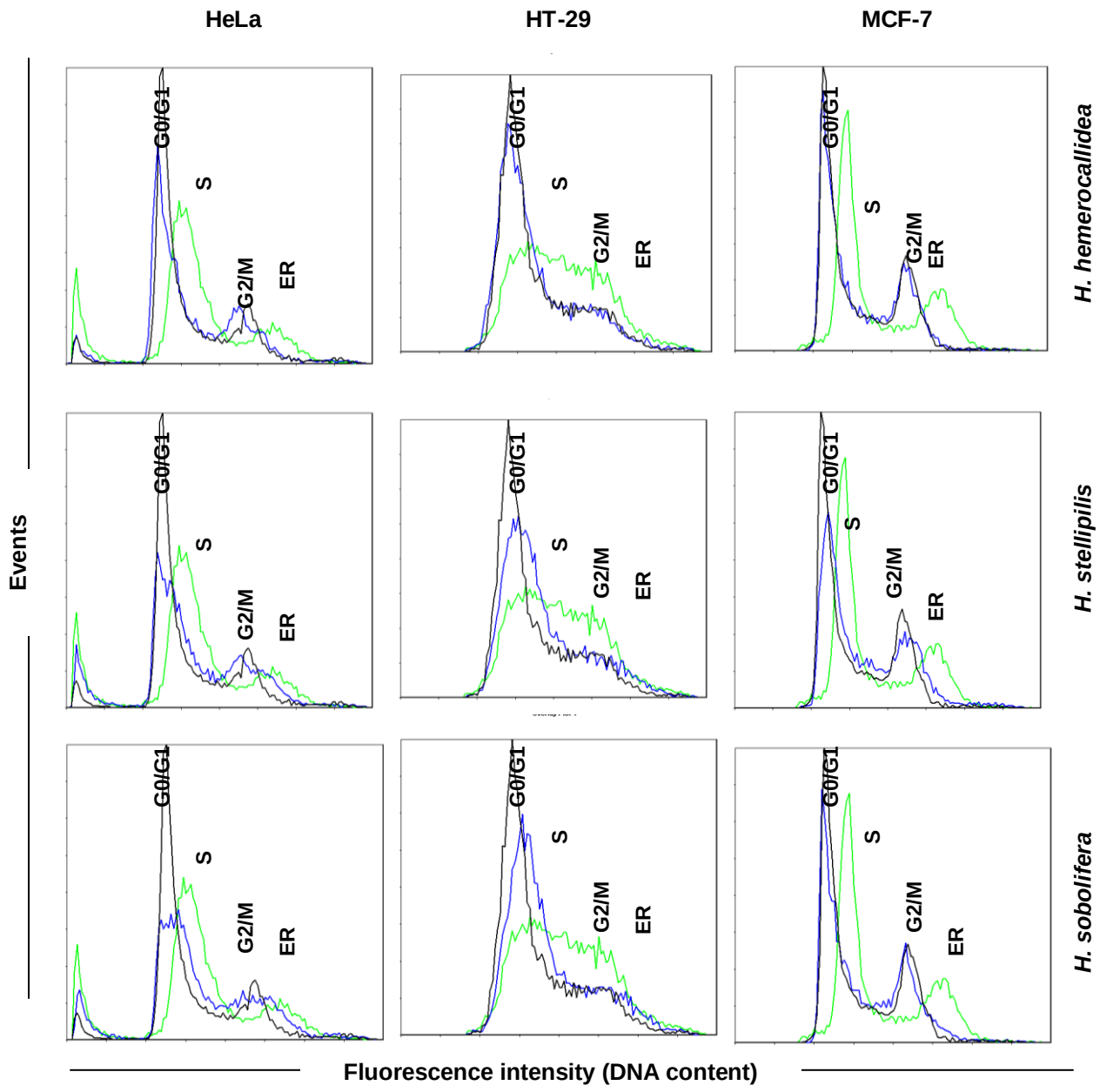

Figure 4.9: Overlay of histograms representing DNA cell cycle arrest in HeLa, HT-29 and MCF-7 cancer cell lines after 48 hrs treatment with DMSO (0.25%; black), *Hypoxis* chloroform extract (125 µg/mL; blue) and rooperol (IC_{50} values; green). Trout red blood cells were used as DNA reference calibrator (Appendix 4). 10 000 events were recorded. The experiment was repeated twice with similar results. Abbreviation: ER = endoreduplication

Rooperol played an important role in late G1 and/or early S phase arrest in all three cancer cell lines. Hypoxoside present in the *H. hemerocallidea* and *H. stellipilis* chloroform extracts (Chapter 3, section 3.3) may have contributed to the cell cycle arrest. Although hypoxoside was absent in the *H. sobolifera* chloroform extract (Chapter 3,

section 3.3), unidentified/unknown compounds may have been responsible for DNA cell cycle arrest. Cancer cell lines were treated with *Hypoxis* extracts in the presence of β-glucosidase. Awad *et al*. (2001a) and Moon *et al*. (2008a) have shown G2/M phase arrest in MDA-MB-231 human breast cancer cells, and U937 and HL60 leukemia cells, respectively, when treated with β-sitosterol. Malíková *et al*. (2008) described G1 phase arrest in MCF-7, MDA-MB-468 and LNCaP cancer cells, and G2/M phase arrest in DU-145 cancer cells when treated with brassinosteroids.

A possible cell survival strategy, endoreduplication, was seen by the shift of histograms past the G2/M peak. The occurrence of endoreduplication is described in Chapter 5.

p21$^{Waf1/Cip1}$ inhibitor activation. p21$^{Waf1/Cip1}$, belonging to the Kip1/Cip1 family of cyclin kinase inhibitors, plays an important role in all phases of the cell cycle. p21$^{Waf1/Cip1}$ levels (Figure 4.10) were determined in HeLa, HT-29 and MCF-7 cancer cells after *H. sobolifera* and rooperol treatment for 15 hrs. *H. sobolifera* was the *Hypoxis* spp. with the best cytotoxicity against all three cancer cell lines investigated (section 4.2.2). Due to limited amounts of antibodies available, *H. sobolifera* and rooperol (cytotoxic compound) were chosen to further investigate cell cycle arrest.

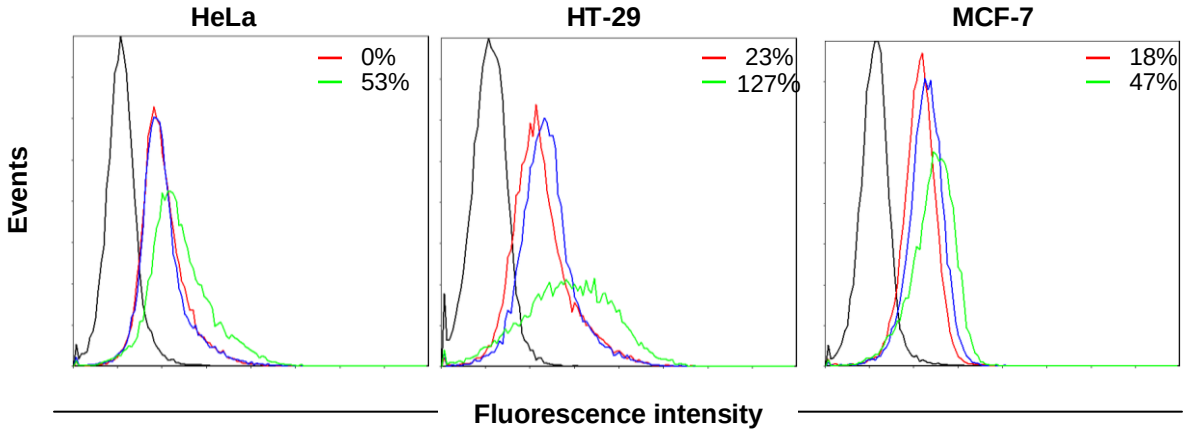

Figure 4.10: Overlay of histograms representing p21$^{Waf1/Cip1}$ expression in HeLa, HT-29 and MCF-7 cancer cell lines after 15 hrs treatment with DMSO (0.25%; red), *H. sobolifera* (125 µg/mL; blue) and rooperol (IC_{50} values; green). Percentages on histograms represent the increase in mean fluorescence intensity of cells staining positive for p21$^{Waf1/Cip1}$ when treated samples were compared to the control. Rabbit IgG was used as isotype control (black). 10 000 events were recorded. One representative of three experiments performed.

$p21^{Waf1/Cip1}$ expression increased when HeLa, HT-29 and MCF-7 cancer cells were exposed to rooperol, and HT-29 and MCF-7 cancer cells exposed to *H. sobolifera*. $p21^{Waf1/Cip1}$ was expressed at greater levels in HT-29 and MCF-7 cancer cells compared to HeLa cancer cells when treated with *H. sobolifera*. Hypoxoside is absent in the *H. sobolifera* chloroform extract (Chapter 3, section 3.3), hence the increase seen in $p21^{Waf1/Cip1}$ levels could not be due to hypoxoside conversion to rooperol and may be due to unidentified compounds present in the extract. Another explanation may be the presence of β-sitosterol (4.5 μM) in the *H. sobolifera* chloroform extract. Moon *et al*. (2008a) have shown an increase in p21 and CDK2 expression in human leukemia U937 and HL60 cells following β-sitosterol (20 μM) treatment. $p21^{Waf1/Cip1}$ levels in this study could not be compared to those reported by Moon *et al*. (2008a) due to flow cytometry and Western blotting detection, respectively.

As mentioned previously, $p21^{Waf1/Cip1}$ levels increase during cell cycle arrest to inhibit cyclin D-CDK4/6 and cyclin A/E-CDK2 activities involved in G1-S progression. It prevents complexes from loading CDC45 onto chromatin, which is necessary for DNA polymerase α recruitment into assembled pre-replication complexes, thus blocking the initiation of DNA replication. It also prevents pRb phosphorylation, thus pRb inhibits E2F-dependent transcription of S phase genes for S phase entry (Coqueret, 2003; Kastan and Bartek, 2004; Nojima, 2004). Considering the increased levels of $p21^{Waf1/Cip1}$ observed in this study, it is likely that this mechanism was activated by rooperol and *H. sobolifera* extract. To confirm this, future studies can focus on cell cycle control mechanisms by measuring the activity of CDK2/4/6; cyclin A/D/E levels and phosphorylated and unphosphorylated pRB in cancer cells after treatment.

4.2.5. Caspase-3 and/or -7 activation

4.2.5.1. Background

Caspases play a central role in the morphological and biochemical features of apoptosis. The caspase family consists of at least 14 members and has the following unifying characteristics:

- Caspases are cysteine proteases containing a conserved QACXG pentapeptide sequence surrounding the active site cysteine residues.
- Caspases are constitutively and ubiquitously expressed as inactive proenzymes, each consisting of a large- and small subunit, and a prodomain. The latter is removed by proteolytic processing at a specific aspartate (Asp) residue and leads to caspase activation when the large and small subunits form a heterodimer.
- Caspases cleave substrates and other procaspases at the carboxy-terminal of an Asp residue.
- Caspases are arranged in a proteolytic cascade, which transmit and amplify the death signal (Cryns and Yuan, 1999; Elmore, 2007; Fadeel and Orrenius, 2004; Kagawa *et al*., 2001; Mc Gee *et al*., 2002).

Individual caspases have the following differences:

- Caspases have different substrate specificities e.g. WEXD (caspase-1, -4 and -5), DEXD (caspase-2, -3, and -7) and (L/V)EXD (caspase-6, -8 and -9).
- Caspases are found at different locations in the cell. Most caspases are localized in the cytoplasm; caspase-2 in the nucleus and Golgi aparatus; caspase-12 on the outer ER membrane; and caspase-2, -3 and -9 may be present in small quantities in the mitochondria.
- The length and sequence of amino terminal prodomains namely long (caspase-1, -2, -4, -5, -8, -9 and -10) and short (caspase-3, -6, -7 and -11) domains differ between caspases. Two distinct protein-protein interaction modules are identified

in long domains namely (i) death effector domains of caspase-8 and -10 bind ligand-activated death receptors via adapter proteins, (ii) prodomains of caspase-1, -2, -4 and -9 contain a caspase-recruitment domain (CARD) and mediates interaction between Apaf-1 and procaspase-9. Prodomains provide a link between the death stimulus and caspase activation (Bratton and Cohen, 2001; Cryns and Yuan, 1999; Mooney *et al*., 2002).

Caspases are divided into initiator/upstream (caspases-2, -8, -9 and -10), executor/effector/downstream (caspases-3, -6 and -7) and inflammatory (caspases-1, -4 and -5) caspases. Initiator caspases can be activated by the extrinsic and/or intrinsic pathways, which convert to the executors in the execution pathway as described in section 4.1.6.1. Interaction between the two pathways amplifies the apoptotic signal. Caspase-8 induces apoptosis directly by cleaving executor procaspases or indirectly by cleaving Bid, which is associated with cytochrome c release from the mitochondria and procaspase-9 activation (Cryns ad Yuang, 1999; Elmore, 2007; Mc Gee *et al*., 2002; Sun *et al*., 1999). Bid can be cleaved by low concentrations of caspase-8 and high concentrations of caspase-3 (Sun *et al*. 1999).

Executor caspases cleave substrates responsible for morphological and biochemical features of apoptosis e.g. cytoskeletal rearrangement, cell membrane blebbing, nuclear condensation and DNA fragmentation (Mc Gee *et al*., 2002). More than 100 proteins are cleaved by caspases e.g. regulatory proteins [poly-ADP-ribose polymerase (PARP)], cytoskeletal or structural proteins (e.g. α-fodrin, gelsolin, cytokeratins, actin), DNA fragmentation (ICAD), proteins involved in DNA replication, transcription and translation, kinases and phosphatases. Many of the substrates' functions are poorly understood or unknown (Cryns and Yuang, 1999; Fadeel and Orrenius, 2005; Janicke *et al*., 1998; Kagawa *et al*., 2001; Mooney *et al*., 2002). Caspase-6 cleaves lamins A and B, which are components of the inner nuclear membranes, and structurally related keratin 18, but degradation may not account for morphological changes (Cryns and Yuang, 1999; Kagawa *et al*., 2001). Cleavage of proteins can lead either to a gain-in-function (Bcl-2/Bcl-X_L converts from anti- to pro-apoptotic proteins; activation of PLCδ) or a loss-in-

function [structural proteins (e.g. cytokeratins, actin and lamins)] (Bratton and Cohen, 2001).

Mammalian IAPs [e.g. neuronal apoptotic inhibitory protein (NAIP), ML-IAP, XIAP/hILP, cellular inhibitor of apoptosis (e.g. cIAP-1/hIAP-2, cIAP-2/hIAP-1), and survivin] act by interacting with receptor complexes. Anti-apoptotic mechanisms of some of these proteins are unclear. IAPs (e.g. XIAP, ML-IAP, cIAP-1/2) mainly inhibit caspases directly. XIAP inhibits caspase-3, -7 and -9, but not caspase-8. NO and its reactive species (eNOS, iNOS, nNOS) are also inhibitors of caspases (Bratton and Cohen, 2001; Cryns and Yuan, 1999).

Caspases play a central role in the morphological and biochemical features of apoptosis. This section focuses on caspase-3 and/or -7 activation in HeLa, HT-29 and MCF-7 cancer cells when treated with *Hypoxis* extracts and its purified compounds, hypoxoside and rooperol.

4.2.5.2. Materials and Methods

Whole cell caspase-3/7 kit. HeLa, HT-29 and MCF-7 cancer cells were seeded at densities of 37 500 cells/mL in 96-well plates at 200 µl/well and left to attach overnight at 37 ºC in a humidified incubator and 5% CO_2. Cells were treated with DMSO (0.25%, v/v; negative control), *Hypoxis* extracts (125 µg/mL), hypoxoside [IC_{50} values (Table 4.4)], rooperol [IC_{50} values (Table 4.4)] and cisplatin (10 µM; positive control) for 15 hrs as recommended in the kit's manual. β-glucosidase (100 µg/mL) was added to *Hypoxis* and hypoxoside treated cells. Caspase-3/7 activity was determined using the CellProbe™ HT Caspase-3/7 whole cell assay kit (Beckman Coulter, CA, USA) as described in the kit protocol. In brief, after the incubation period, substrate [bis-N-CBZ-L-aspartyl-L-glutamyl-L-valyl-L-aspartic acid amide derivative of rhodamine 110 (Z-DEVD-R110)] was diluted using the CellProbe HT buffer and 25 µL added to each well without mixing. Cells were incubated for a further one to three hrs at 37 °C. Fluorescence was measured

at $485_{Ex}/518_{Em}$ using a Fluoroskan Ascent FL fluorometer. Statistical significance was determined using the two-tailed Student's t-test.

Cleaved caspase-3 (Asp175) and caspase-7 (Asp198) antibodies. HeLa, HT-29 and MCF-7 cancer cells were seeded at densities of 40 000 cells/mL in 24-well plates and left to attach overnight at 37 ºC in a humidified incubator and 5% CO_2. Due to limited amounts of hypoxoside, rooperol and *Hypoxis* chloroform extracts, only rooperol (cytotoxic compound) and *H. sobolifera* (best cytotoxicity against HeLa, HT-29 and MCF-7 cancer cell lines) were chosen to perform caspase-3 and/or -7 experiments. Cells were treated with DMSO (0.25%, v/v), rooperol [IC_{50} values (Table 4.4)] and *H. sobolifera* (125 µg/mL) for 48 hrs. After exposure, cells were washed with PBSA, trypsinized for 10 min at 37 ºC and resuspended in PBS. Cells were centrifuged at 500 x g for five min at room temperature and the supernatant discarded. Cells were washed as described above to remove any traces of trypsin. Cells were fixed and permeabilized using the IntraPrep™ permeabilizing reagent as described in the kit protocol (see section 4.2.4.). After permeabilization, cells were washed using 1 mL cold incubation buffer (0.5% BSA in PBS), supernatant discarded and cells blocked for 10 min in 100 µL incubation buffer at room temperature. Cleaved caspase-3 (Asp175) or -7 (Asp198) antibodies were added at recommended working dilutions to the cells and incubated at room temperature for one hour. Cells were washed twice as described above. After washing, FITC conjugated goat anti-rabbit IgG (H+L chain specific) was added at recommended working dilutions. FITC conjugated rabbit IgG was added to untreated HeLa, HT-29 and MCF-7 cancer cells and used as an isotype control. Cells were incubated for 30 min at room temperature in the dark and washed as described above. Cells were resuspended in 500 µL PBS and read on a Beckman Coulter Cytomics FC500.

4.2.5.3. Results and Discussion

Caspase-3 plays a central role in the apoptosis pathway for DNA fragmentation to occur. Due to the absence of activated caspase-3 in MCF-7 cancer cells, caspase-7 was

investigated as a possible role player for DNA fragmentation in the three cancer cell lines.

Whole cell caspase 3/7 kit. The nonfluorescent bisamide substrate (Z-DEVD-R110) enters the cell where it is enzymatically cleaved by caspase-3/7 to fluorescent monoamide and then to highly fluorescent rhodamine 110 free dye molecules. Figure 4.11 summarizes the caspase-3/7 activation results obtained.

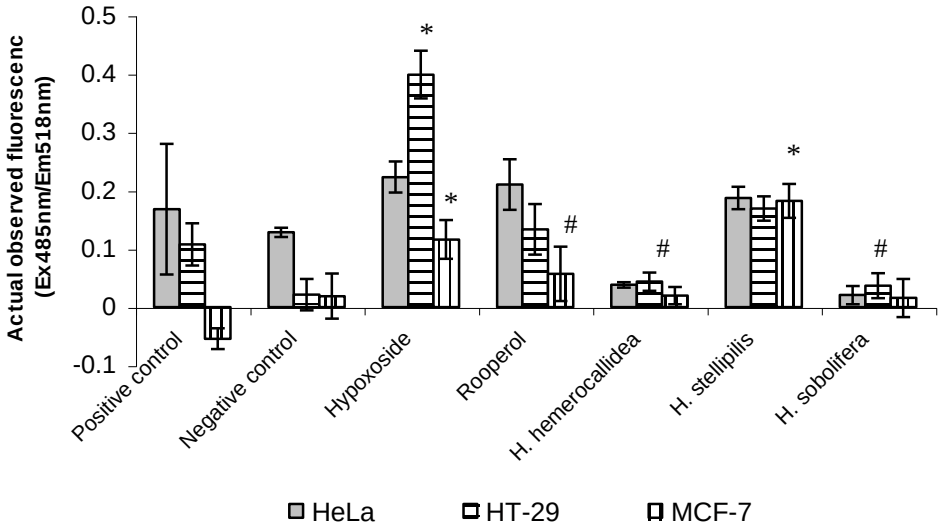

Figure 4.11: Detection of caspase 3/7 activities with the CellProbe HT Caspase 3/7 Whole Cell Assay in HeLa, HT-29 and MCF-7 cancer cell lines after 15 hrs treatment with *Hypoxis* extracts (125 µg/mL), hypoxoside (IC_{50} values) and rooperol (IC_{50} values). Positive control = 10 µM cisplatin; negative control = 0.25% DMSO. Error bars represent SEM values of quadruplicates. One representative of two experiments performed. Significance was determined using the two-tailed Student t-test: *p<0.005; #p<0.05

Caspase-3/7 activity in HT-29 cancer cells was significantly increased by hypoxoside ($p<0.005$), *H. hemerocallidea* ($p<0.05$) and *H. sobolifera* ($p<0.05$), while caspase-3/7 activity in MCF-7 cancer cells was significantly increased by hypoxoside ($p<0.005$), rooperol ($p<0.05$) and *H. stellipilis* ($p<0.05$). Non-significant increases in caspase-3/7 activity were seen when HeLa cancer cells were treated with hypoxoside, rooperol and *H. stellipilis*, and when HT-29 cancer cells were treated with rooperol and *H. stellipilis*. The positive control, cisplatin, did not activate any caspase-3/7 activity in MCF-7 cancer cells. Studies with cisplatin have shown caspase-3 activation in Hela (Horký *et al*., 2000) and *CASP3* cDNA transfected MCF-7 (Blanc *et al*., 2000) cancer cells. Increase of

caspase-3/7 by cisplatin treatments in HeLa and HT-29 cancer cells was not significant (Figure 4.11), and may have been activated before 15 hrs. The cisplatin concentration used (10 µM) may have been too low to see any caspase-3/7 activation after 15 hrs. MCF-7 cancer cells lack the CASP3 gene (Janicke, 1998), hence no caspase-3 could be activated and the increased caspase-3/7 activity was probably due to caspase-7 activity.

Cleaved caspase-3 (Asp175) and caspase-7 (Asp198) antibodies. Histogram overlays (Figures 4.12) show the activation of caspase-3 and/or -7 in HeLa and HT-29 cancer cells, and caspase-7 in MCF-7 cancer cells after 48 hrs exposure to *H. sobolifera* and rooperol.

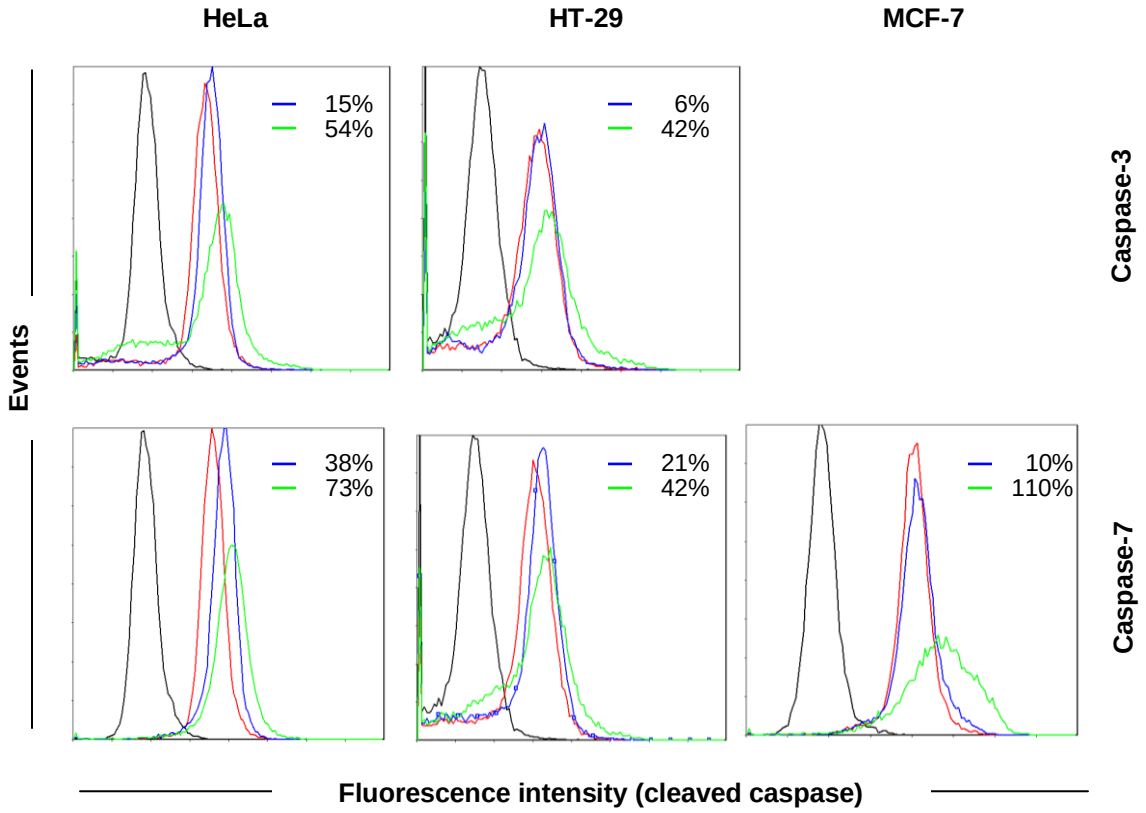

Figure 4.12: Histogram overlays of activated caspase-3 and/or -7 in HeLa, HT-29 and MCF-7 cancer cells when treated with DMSO (025%; red), *H. sobolifera* (125 µg/mL; blue) and rooperol (IC_{50} values; green) for 48 hrs. Percentages on histograms represent the increase in median fluorescence intensity of cells staining positive for active caspase-3 or -7 when treated samples were compared to the control. Rabbit IgG was used as isotype control (black). 10 000 events were recorded. One representative of three experiments performed.

From the above histograms a shift to the right for treated samples compared to the DMSO control represented activation of caspase-3 and/or -7. Caspase-3 and -7 were activated in HeLa cancer cells when treated with *H. sobolifera* and rooperol. In HT-29 cancer cells, caspase-7 was mainly activated by *H. sobolifera* and rooperol, while rooperol activated more caspase-3 than *H. sobolifera*. Rooperol mainly activated caspase-7 in MCF-7 cancer cells. From the results obtained, *H. sobolifera* and rooperol treatment activated more caspase-7 in HeLa and HT-29 cancer cells compared to caspase-3. Janicke *et al*. (1998) have shown a deletion of 47 bp in exon 3 of the CASP3 gene in MCF-7 cancer cells.

Increase in caspase activity (Figure 4.12) in HeLa and HT-29 cancer cells obtained with *H. sobolifera* treatment may be due to β-sitosterol content, because no hypoxoside was detected in the chloroform extract of *H. sobolifera* (Chapter 3, section 3.3). Awad *et al*. (2003a) have shown that β-sitosterol (16 μM) activates caspase-3, -8 (extrinsic pathway) and -9 (intrinsic pathway) in MDA-MB-231 human breast cancer cells after 3 days of treatment. A higher percentage of caspase-9 activated compared to caspase-8, suggests the preferential activation of the intrinsic pathway. The effect of sterols on apoptosis may be indirect, following incorporation of β-sitosterol into the cell membranes. β-sitosterol had no effect on the concentration of caspases, but rather on their activity. Awad *et al*. (2008) have shown caspase-8 activation via Fas signalling (extrinsic pathway) in MDA-MB-231 and MCF-7 human breast cancer cells with β-sitosterol (8-16 μM) treatment after three days. Moon *et al*. (2008a) have shown an increase in caspase-3 levels in human leukemia U937 and HL60 cells after β-sitosterol (>20 μM) treatment for 96 hrs. Longer exposure periods of cancer cells to *Hypoxis* extracts may have yielded higher caspase-3 and/or -7 activities.

In summary, *H. sobolifera* and rooperol activated caspase-3 and/or -7 in HeLa, HT-29 and MCF-7 cancer cells (Figure 4.12). Caspase-3 and/or -7 activation plays a central role in apoptosis. The effect of *H. sobolifera* and rooperol on apoptosis was confirmed by phosphatidylserine translocation and DNA fragmentation.

4.2.6. Phosphatidylserine translocation: annexinV binding

4.2.6.1 Background

Viable cells maintain lipid asymmetry distribution of phospholipids in the cell's plasma membrane. The outer- and inner membrane leaflets consist of choline-containing phospholipids (e.g. phosphatidylcholine, sphingomyelin) and aminophospholipids (e.g. PS, phosphatidylethanolamine), respectively (van Engeland *et al*., 1998).

Lipid asymmetry is maintained by an active Mg^{2+} and ATP-dependent process, facilitated by translocases or flippases (Martin *et al*., 1995; van Engeland *et al*., 1998). Aminophospholipids are translocated from the outer to the inner leaflet and maintained in the inner leaflet of the plasma membrane by aminophospholipid translocase in normal healthy lymphocytes, platelets and erythrocytes. Downregulation and inhibition of translocase during apoptosis cause scramblase (non-specific lipid flipsite) activation, which abolishes lipid asymmetry, by translocating phospholipids from the inner to the outer leaflet of the plasma membrane (Krahling *et al*., 1999; Verhoven *et al*., 1995). Translocase inhibition and scramblase activation have been seen at elevated cytoplasmic Ca^{2+} concentrations (in platelets and erythrocytes), suggesting a role for Ca^{2+} as secondary messenger for PS presentation (Verhoven *et al*., 1995). Disruption of plasma membrane-associated phospholipid-binding cytoskeletal proteins (e.g. spectrin, fodrin), which maintain lipid asymmetry, may also be involved in phospholipid translocation (Martin *et al*., 1995; van Engeland *et al*., 1998). Phospholipids are rapidly distributed to both leaflets by flowing around rupture points during necrosis or plasma membrane rupture (Martin *et al*., 1995).

PS appearance on the outer membrane leaflets lasts from the early execution phase until the final stages (i.e. apoptotic body formation) of apoptosis (van Engeland *et al*., 1998). PS externalization to the outer membrane leaflet occurs after disruption of the mitochondrial transmembrane potential and initiation of the caspase proteolytic cascade, but before morphological changes like cell shrinkage, chromatin condensation,

degradation of cytoskeletal (e.g. cytokeratin)- and nuclear proteins (e.g. nuclear lamins), DNA strand breaks, loss of plasma membrane integrity and membrane blebbing.

PS translocation is not unique to apoptosis, but also occurs in cells undergoing necrosis (Martin *et al*., 1995; Pepper *et al*., 1998; van Engeland *et al*., 1996; van Engeland *et al*., 1998). Annexin V is a 35 kDa Ca^{2+} dependent (mM concentration), phospholipid-binding protein binding reversibly and with high affinity to negatively charged PS (Figure 4.13) (Aubry *et al*., 1999; van Engeland *et al*., 1996; van Engeland *et al*., 1998; Vermes *et al*., 1995). Martin *et al*. (1995) have shown that Annexin V binds only to PS and no binding occurred with phosphatidylcholine, phosphatidylinositol, phosphatidic acid, sphingomyelin and phosphatidylethanolamine.

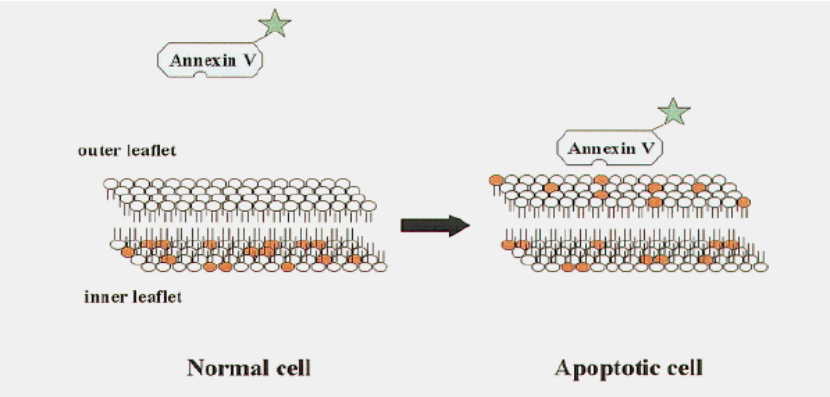

Figure 4.13: Translocation of PS from the inner plasma membrane leaflet to the outer plasma membrane leaflet. Annexin V binds with high affinity to PS (van Engeland *et al*., 1998).

A membrane impermeable dye [e.g. propidium iodide (PI)] is used to discriminate between early apoptotic and necrotic or dead cells. PI measures the integrity of the cell membranes by entering necrotic cells with permeable membranes, but is excluded from apoptotic cells (Aubry *et al*., 1999; Koopman *et al*., 1994; Vermes *et al*., 1995). Studies with Annexin V (labelled with the fluorochrome conjugate, FITC) and PI have revealed four populations of cells namely unstained or viable cells (Annexin ^{neg}, PI ^{neg}), early apoptotic cells (Annexin ^{pos}, PI ^{neg}), late apoptotic cells (Annexin ^{pos}, PI ^{pos}) and unviable, necrotic or permeabilized cells (Annexin ^{neg}, PI ^{pos}) (Aubry *et al*., 1999).

Increased membrane permeability is associated with late apoptosis (Annexin ^{pos}, PI ^{pos}), which is also known as secondary necrosis. Late apoptotic cells normally exclude PI, as loss of membrane integrity does not occur until apoptotic cells are engulfed by macrophages *in vivo*. Phagocytes are absent when cells are cultured *in vitro*, thus membrane permeability in late apoptosis occurs when dying cells detach from the culture dish surface and disintegrate into apoptotic bodies (Martin *et al*., 1995; Pepper *et al*., 1998; van Engeland *et al*., 1996). PS exposure is regulated by changes in energy metabolism (ATP dependent), bivalent cation (Mg^{2+}, Ca^{2+}) concentrations, cytoskeletal organization (Koopman *et al*., 1994) and can be inhibited by caspase inhibitors (Fadeel *et al*., 1999; van Engeland *et al*., 1998).

No inflammation is associated with apoptosis because (i) apoptotic cells do not release their cellular constituents into the surrounding tissue, (ii) apoptotic cells are quickly phagocytosed by surrounding cells preventing secondary necrosis, (iii) engulfing cells do not produce anti-inflammatory cytokines (Elmore, 2007; Verhoven *et al*., 1995).

PS externalization is a cell type-specific event occurring only in certain cell types (e.g. CEM, Jurkat, U937 but not in HL-60, P39, Raji) as shown by Fadeel *et al*. (1999); hence PS cannot be used as the only marker for apoptosis. Translocase or scramblase PS externalization is not a compulsory component of apoptosis, which may explain the absence of PS translocation in certain cells. Caspase activation and other proteolytic enzymes such as calpain may play a role in PS translocation. It is proposed that fodrin, a component of the plasma membrane-associated cytoskeleton, is involved in the rearrangement of plasma membrane PS, but no correlation has been shown by Fadeel *et al*. (1999).

PS translocation plays an important role in the elimination of apoptotic cells, via recognition by phagocytes. The effects of *Hypoxis* extracts and rooperol on PS translocation were investigated in premonocytic human leukemia U937 cells in order to confirm apoptosis induction observed in the previous section.

4.2.6.2. Materials and Methods

Premonocytic human leukemia U937 cells were seeded at 100 000 cells/mL in 24-well plates, treated with DMSO (0.25%, v/v), *Hypoxis* extracts (125 µg/mL), rooperol (20 µg/mL) and cisplatin (50 µM), and incubated for 15 and 48 hrs at 37 ºC in a humidified incubator and 5% CO_2. After the incubation periods, cells were transferred to polypropylene tubes and cells collected by centrifuging at 500 x g for five min at room temperature. Cells were washed in ice-cold Dulbecco's Modified Eagle's Medium (DMEM), treated and stained according to the protocol of the Annexin V-FITC Apoptosis Detection kit (Beckman-Coulter). In brief, cells were washed with cold DMEM and centrifuged at 500 x g for five min at 4 °C. Supernatant was discarded and cell pellets resuspended in ice-cold 1X binding buffer. Annexin V-FITC (1 µL; 25 µg/mL) and PI (5 µL; 250 µg/mL) were added to each tube. Compensation control tubes contained cells with Annexin V-FITC only, PI only and combination of Annexin V-FITC and PI. Tubes were gently mixed and incubated on ice for 15 min in the dark. Samples were read within 30 min on a Beckman Coulter Cytomics FC500.

4.2.6.3. Results and Discussion

The suspension culture, U937 cells, was used for the investigation of membrane integrity to avoid false positive results caused by the dissociation of adherent cells (van Engeland *et al*., 1998). Dot plots (Figures 4.14-15) represent annexin V binding and PI staining of U937 cells after treatment with H. sobolifera and rooperol.

Treatment of U937 cells with rooperol (Figure 4.14ii) and cisplatin (Figure 4.14iii) stained Annexin-V positive and PI negative after 15 hrs of exposure. After 48 hrs most of the cells stained positive for PI and negative for Annexin-V (Figure 4.15). No changes were observed in Annexin-V or PI staining after 15 and 48 hrs treatment with *Hypoxis* extracts (Appendix 4).

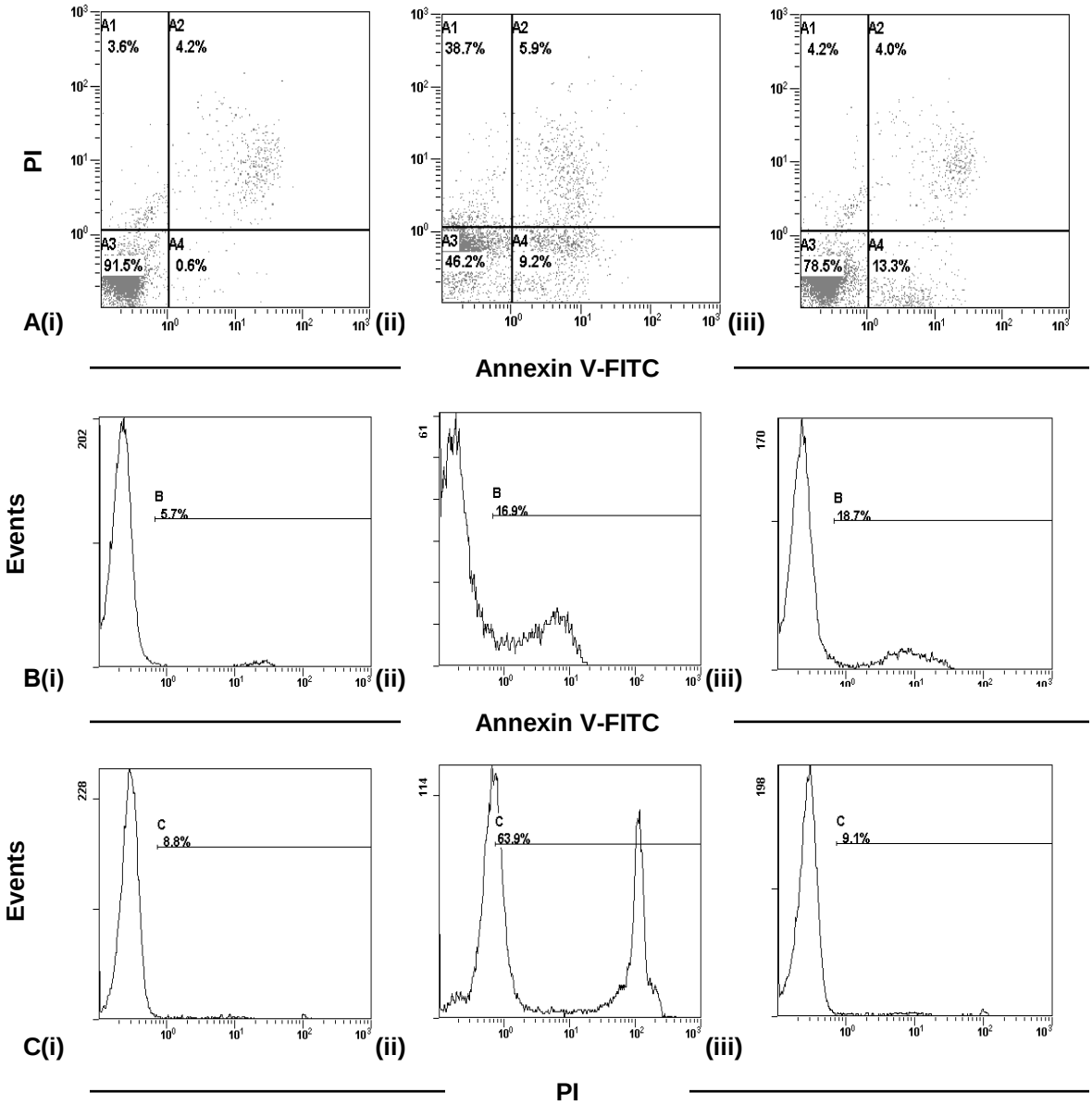

Figure 4.14: Dot plots (A) and histograms (B and C) of Annexin V-FITC and PI stained U937 cells after 15 hrs exposure to DMSO (0.25%; i), rooperol (20 µg/mL; ii) and cisplatin (50 µM; iii). Four quadrants represent unstained/viable cells (A3: Annexin V ^{neg}, PI ^{neg}), early apoptotic cells (A4: Annexin V ^{pos}, PI ^{neg}), late apoptotic cells (A2: Annexin V ^{pos}, PI ^{pos}) and necrotic cells (A1: Annexin V ^{neg}, PI ^{pos}). 20 000 events were recorded. One representative of three experiments performed.

Rooperol altered the plasma membranes of U937 cells, as was evident from the translocation of PS from the inner to the outer leaflet of the plasma membranes. Binding of Annexin V to PS after 15 hrs of rooperol and cisplatin treatment is an indication of early apoptosis (Figure 4.14ii-iii).

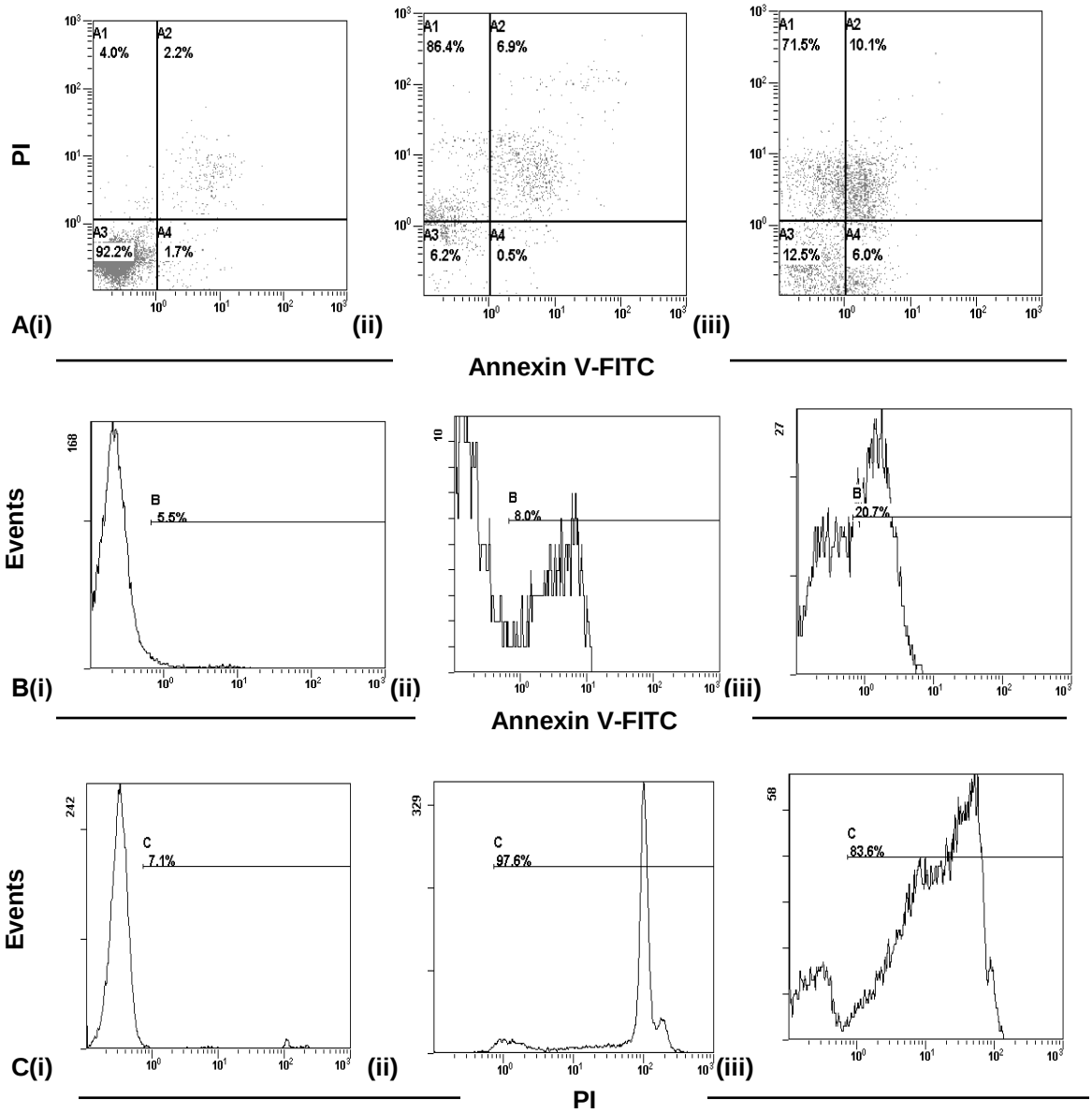

Figure 4.15: Dot plots (A) and histograms (B and C) of Annexin V-FITC and PI stained U937 cells after 48 hrs exposure to DMSO (0.25%; i), rooperol (20 µg/mL; ii) and cisplatin (50 µM; iii). Four quadrants represent unstained/viable cells (A3: Annexin V ^{neg}, PI ^{neg}), early apoptotic cells (A4: Annexin V ^{pos}, PI ^{neg}), late apoptotic cells (A2: Annexin V ^{pos}, PI ^{pos}) and necrotic cells (A1: Annexin V ^{neg}, PI ^{pos}). 20 000 events were recorded. One representative of three experiments performed.

After 48 hrs exposure to rooperol and cisplatin, late apoptosis and necrosis were seen with more cells stained by PI. Annexin V is used to measure early apoptosis (Aubry *et al.*, 1999); hence the best staining of PS by Annexin occurred after 15 hrs of treatment. It is important to use PI (or similar dye) with Annexin V to show that the integrity of the

cell membrane is still maintained. During early apoptosis the plasma membrane is still intact, but becomes leaky with the onset of late apoptosis *in vitro*. This is referred to as secondary necrosis. Exposed PS is recognized by macrophages *in vivo* for phagocytosis of the dying cell (Aubry *et al*., 1999; van Engeland *et al*., 1998). This data is supported by Albrecht *et al*. (1995a) who have shown the formation of pores in the outer membranes of UCT-Mel 1 melanoma cells after hypoxoside treatment, hence destabilizing the outer membranes, while phase contrast and scanning electron micrographs have shown the formation of vacuoles and cells undergoing blebbing, respectively. *H. hemerocallidea*, *H. stellipilis* and *H. sobolifera* showed no early or late apoptosis with Annexin V. This was expected as these *Hypoxis* chloroform extracts contained very little or no hypoxoside (Chapter 3, section 3.3). The major suspected active compound in the *Hypoxis* chloroform extracts used in this study is β-sitosterol (Chapter 3, section 3.3), which will rather be incorporated in the cell membranes over time where it may influence signalling pathways.

4.2.7. DNA fragmentation

4.2.7.1. Background

Caspases-3 and -7 are the only caspases that activate the DNA fragmentation factor, 40-kDa subunit (DFF40 in humans)/caspase-activated DNase (CAD in mice) by cleaving the DNA fragmentation factor, 45-kDa subunit (DFF45)/inhibitor of CAD (ICAD). ICAD has a bifunctional role in the cytoplasm by inhibiting CAD's endonuclease activity and ensuring correct folding of CAD – a chaperone-like function (Fadeel and Orrenius, 2005; Janicke *et al*., 1998; Nagata, 2000; Wolf *et al*., 1999; Yuste *et al*., 2001). CAD, synthesized on ribosomes during protein synthesis, requires Mg^{2+} for DNase activity and functions at neutral pH (Nagata, 2000). ICAD is cleaved at two Asp residues (Asp 117 and Asp 224) to release active CAD, which will degrade DNA at internucleosomal regions. This can be detected as a DNA ladder on an agarose gel (Yuste *et al*., 2001).

DNA fragmentation is a two-step process where DNA is firstly cleaved (randomly; but prefer AT-rich sequences) into 50-300 kbp fragments (high molecular weight DNA degradation) and secondly degraded into smaller inter(oligo)nucleosomal fragments (DNA ladder) of 180-200 bp (Marini *et al*., 1996; Nagata, 2000; Oberhammer *et al*., 1993; Yuste *et al*., 2001). Initial DNA degradation, due to DNA cleavage at nuclear scaffolds, may unfold the chromatin structure to expose spacer regions of nucleosomes (Nagata, 2000). Three hundred kbp and 50 kbp fragments may arise due to the release of rosettes or loops of chromatin, respectively, as they detach from attachment points on the nuclear scaffolding proteins (Oberhammer *et al*., 1993). In contrast to CAD, mitochondrial or pro-apoptotic proteins [e.g. apoptosis inducing factor (AIF) and endonuclease G] enter the nucleus and induce high molecular weight DNA fragmentation without activating the caspase pathway (Elmore, 2007; Fadeel and Orrenius, 2005; Mc Gee *et al*., 2002; Wolf *et al*., 1999). DNA laddering is not found in all cell lines, hence internucleosomal cleavage is not a prerequisite for apoptotic morphology because specific cell types do not exhibit the endonucleolytic pathway. DNA laddering appears to be cell type and agent-specific (Marini *et al*., 1996). Only high molecular weight DNA degradation may be essential for cell death, because several cell types (e.g. breast carcinoma-derived cell line MCF-7, human androgen-independent prostatic cancer cell DU-125, human neuronal-like cell NT2, human neuroblastomas IMR-5 and -32, and human neuroblastoma IMT-5) never produce DNA laddering with treatments that induce typical cytoplasmic and nuclear changes of apoptosis (Oberhammer *et al*., 1993; Yuste *et al*., 2001).

DNA fragmentation may play an important role in cleaving chromosomal DNA before phagocytosis to avoid transformation by activated oncogenes or viral genes, reduce autoimmune diseases, transfer oncogenes from the apoptotic cells to phagocytes and healthy cells, and accelarate apoptosis (Nagata, 2000; Yuste *et al*., 2001). Apoptosis assessment only by biochemical features must be interpreted with caution, because DNA fragmentation is not essential for apoptosis and must be defined with morphological features (Cohen *et al*., 1992).

DNA fragmentation is an important biochemical feature of late apoptosis. This section focuses on DNA fragmentation in HeLa, HT-29 and MCF-7 cancer cells when treated with *H. sobolifera* and rooperol to provide further evidence of apoptosis induction.

4.2.7.2. Materials and Methods

HeLa, HT-29 and MCF-7 cancer cells were seeded in 24-well plates at densities of 40 000 cells/mL and left to attach overnight at 37 ºC in a humidified incubator and 5% CO_2. Cells were treated with DMSO (0.25%, v/v), *H. sobolifera* (125 µg/mL) rooperol [IC_{50} values (Table 4.4)] and cisplatin (50 µM) for 48 hrs. Cells were washed with PBSA, trypsinized for 10 min and resuspended in PBS. Cells were washed with PBS by centrifugation at 500 x g for five min at room temperature to remove trypsin, fixed and permeabilized using the IntraPrep™ Permeabilizing kit according to the kit protocol. DNA fragmentation was investigated using the MEBSTAIN Apoptosis Kit Direct (Immunotech, Marseille, France) and the protocol followed as described in the product insert. In brief, terminal deoxynucleotidyl transferase (TdT) reaction reagent (30 uL), consisting of TdT buffer, FITC-dUTP and TdT in 18:1:1 (v/v/v) ratio, was added to each cell pellet and incubated in the dark for one hour at 37 °C. The negative control contained untreated cells with TdT buffer and FITC-dUTP [19:1 (v/v) ratio] only. Cells were washed as described above and the pellet resuspended in 500 uL of PBS. Samples were analyzed on a Beckman Coulter Cytomics FC500. Mean fluorescence intensity (MFI) of treated cells was expressed as a percentage of the MFI of control cells. Statistical significance was determined using the two-tailed Student's t-test.

4.2.7.3. Results and Discussion

DNA strand breaks in apoptotic cells are detected by 3' OH termini labelling with fluorochrome-conjugated nucleotides in a reaction using exogenous TdT known as the TdT dUTP nick end labelling (TUNEL), TdT assay or *in situ* end-labelling (Gorczyca, 1999). DNA fragmentation is characteristic of late apoptosis and was investigated in HeLa, HT-29 and MCF-7 cancer cells. Only the density plots of treated HT-29 cancer

cells are shown in Figure 4.16A. Density plots for HeLa and MCF-7 cells are shown in Appendix 4. Figure 4.16B summarizes all the DNA fragmentation of treated and untreated HeLa, HT-29 and MCF-7 cancer cells.

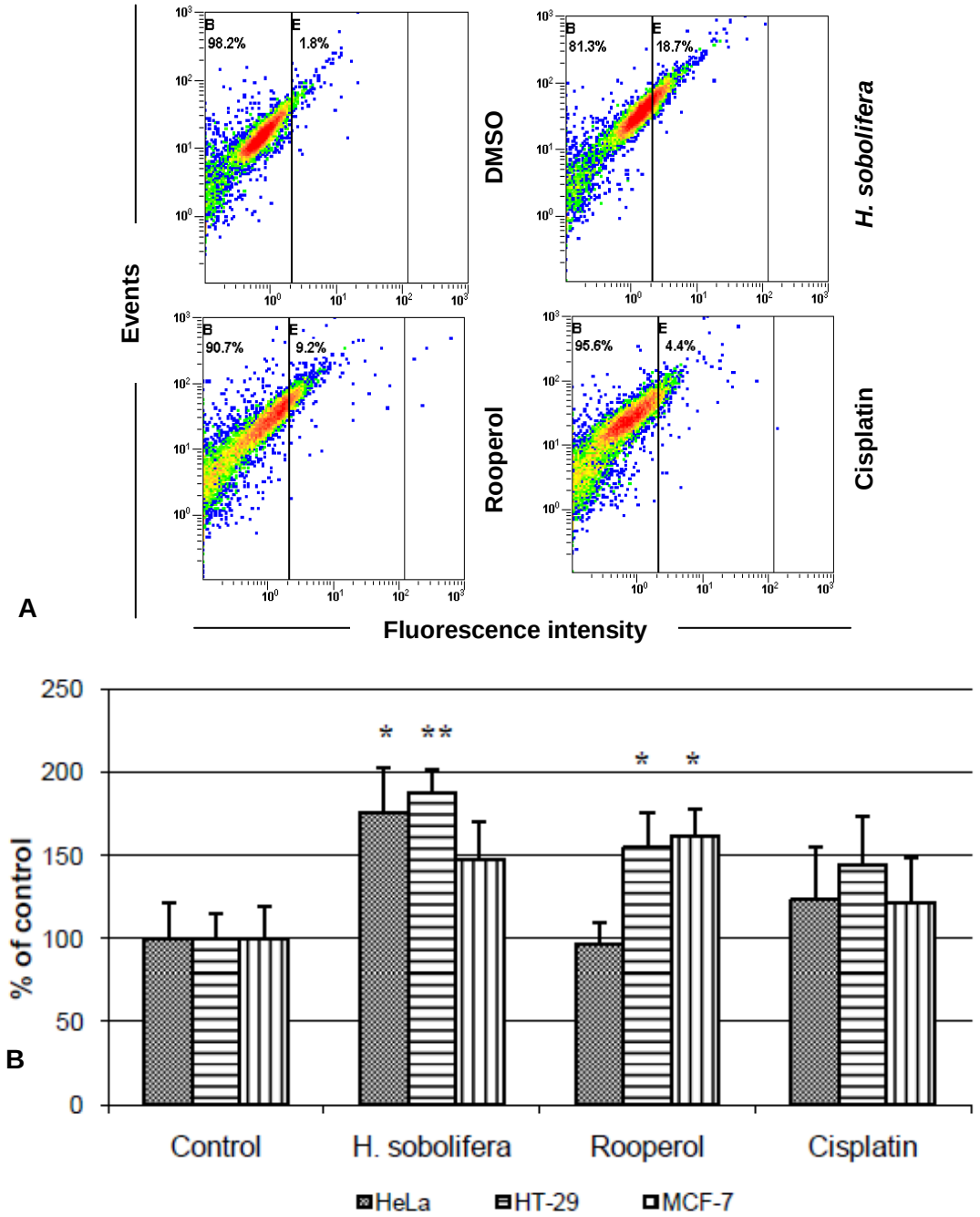

Figure 4.16: DNA fragmentation after 48 hrs exposure to treatments. Density plots (A) of DMSO (0.25%, v/v), *H. sobolifera* (125 µg/mL), rooperol (IC_{50} values) and cisplatin (50 µM) treated HT-29 cancer cells. Bar graph (B) of untreated and treated HeLa, HT-29 and MCF-7 cancer cells. Bar graph percentages represent the increase in mean fluorescence intensity of cells staining positive for DNA fragmentation when treated samples were compared to control. 10 000 events were recorded. Bar graph represents the average of

three individual experiments. Significance was determined using the two-tailed Student t-test: *p<0.05, **p<0.005 compared to control.

More DNA fragmentation [and significant results (Figure 4.16B)] occurred when HeLa and HT-29 cancer cells were treated with *H. sobolifera*, and HT-29 and MCF-7 cancer cells treated with rooperol. DNA fragmentation is clearly shown by a shift from region B to E in the density plots (Figure 4.16A). *H. sobolifera* significantly increased DNA fragmentation in HeLa ($p<0.05$) and HT-29 ($p<0.005$) cancer cells, whereas rooperol significantly increased DNA fragmentation in HT-29 ($p<0.05$) and MCF-7 ($p<0.05$) cancer cells. *H. sobolifera* and rooperol did not significantly increased DNA fragmentation in MCF-7, while rooperol had no effect on HeLa cancer cells. From Figure 4.16 it is clear that MCF-7 cancer cells underwent DNA fragmentation after treatment with *H. sobolifera* (not significantly) and rooperol (significantly).

Caspase-7 was activated in MCF-7 cancer cells after treatment with *H. sobolifera* and rooperol (section 4.2.5.). McGee *et al*. (2002) and Semenov *et al*. (2004) have also shown DNA fragmentation of MCF-7 cancer cells after caspase-7 activation. It is suggested that caspase-3 and -7 are primary and secondary initiators of DNA fragmentation, respectively (Wolf *et al*., 1999). *H. sobolifera* treatment of HeLa, HT-29 and MCF-7 cancer cells caused DNA fragmentation, but apoptosis was absent in the Annexin V study after *H. sobolifera* treatment. For the Annexin V study U937 cells were used, which may explain the absence of apoptosis after *H. sobolifera* treatment. Presence of β-sitosterol (4.5 μM) in the *H. sobolifera* extract may have played a role in DNA fragmentation. Moon *et al*. (2008a) have shown extensive DNA fragmentation in human leukemia U937 and HL60 cells after β-sitosterol (>20 μM) treatment for 96 hrs.

DNA fragmentation is a late apoptosis event (Collins *et al*., 1997b) and was only measured after 48 hrs of treatment with *H. sobolifera* and rooperol in the cancer cell lines. Wolf *et al*. (1999) showed that only caspase-3 and -7 promote DFF45/ICAD inactivation, DFF40/CAD release and DNA fragmentation *in vitro*. They also showed that caspase-3 cleaves the inhibitor more rapidly than caspase-7; hence it may take caspase-7 longer to initiate DNA fragmentation. Longer treatments may be required in

cells lacking functional caspase-3 e.g. MCF-7 cells. Apoptotically activated caspase-7 is almost exclusively associated with mitochondria and microsomes (Semenov *et al*., 2004), which may take longer (via intrinsic pathway) to exert its DNA fragmentation function, than caspase-3 directly cleaved by the extrinsic pathway.

Caspase-3 may be important for oligonucleosomal DNA fragmentation, but other non-caspase proteases like calpains (cleave cytoskeletal protein fodrin and cause membrane blebbing), cathepsin D (lysosomal protease), endonuclease G and AIF may be involved in cell death. Mitochondrial endonuclease G has shown DNA fragmentation (Kagawa *et al*. 2001; Mc Gee *et al*., 2002).

The *H. sobolifera* extract caused DNA fragmentation in the three cancer cell lines investigated, while rooperol caused DNA fragmentation in HT-29 and MCF-7 cancer cells. Caspase-3 and/or -7 activation in *H. sobolifera* treated HeLa, HT-29 and MCF-7 cancer cells may explain DNA fragmentation. DNA fragmentation in rooperol treated HeLa cancer cells may have occurred before 48 hrs; hence the absence of DNA fragmentation.

4.3. Conclusion

Cytotoxicity studies of the three *Hypoxis* spp. have revealed differences in their anticancer properties. *Hypoxis* spp. differed in their cytotoxic effects, which may be attributed to the differences in hypoxoside and phytosterol contents (Chapter 3, section 3.3). Certain *Hypoxis* spp. may promote cancer cell growth, as was the case with *H. stellipilis*. *H. stellipilis* is also the most commonly sold *Hypoxis* spp. in herbal shops in the Port Elizabeth area of the Eastern Cape. The observation of growth stimulation by *H. stellipilis* and the widely reported use of African potato to treat various cancers raise some concern and merits further investigation.

No previous publications could be found on rooperol's mechanism of action in HeLa, HT-29 and MCF-7 cancer cells, or any other cancer cell line. Biochemical analysis of apoptosis in the present study has revealed:

- DNA cell cycle arrest in the late G1 and/or early S phase after 15 hrs of treatment, which was confirmed by increase $p21^{Waf1/Cip1}$ expression. G2/M phase arrest occurred after 48 hrs of treatment.
- Activation of caspase-3 and -7 in HeLa and HT-29 cancer cells, and caspase-7 in MCF-7 cancer cells.
- Phosphatidylserine translocation in U937 cells confirmed early- and late apoptosis.
- DNA fragmentation in HeLa, HT-29 and MCF-7 cancer cells.

H. sobolifera, the *Hypoxis* spp. with the best cytotoxicity and no detectable levels of hypoxoside (thus no rooperol formed), revealed similar trends to rooperol in HeLa, HT-29 and MCF-7 cancer cells as listed above, except for the absence of phosphatidylserine translocation in U937 cells. Cytotoxicity and mechanism of action of sterols may be time dependent. Previous studies have shown effects over a minimum of 3 days, which may explain the weak responses obtained with *Hypoxis* spp. containing relatively high β-sitosterol contents in this study, where a maximum incubation period of 48 hours was used.

This study mainly focused on *Hypoxis* and rooperol's mechanisms of action from the start of the execution pathway to phagocytosis. The intrinsic and extrinsic pathways may have been activated in the cancer cells, and may provide important information regarding the mechanisms of action for *Hypoxis* spp. and rooperol. Caspase-8 and -9 activation in the extrinsic and intrinsic pathways, respectively, can be investigated using fluorescently labelled primary antibodies. Signal transduction pathways [anti (Bcl-X_L)- and pro-apoptotic (Bim, Bax, cytochrome c) proteins] involved in the intrinsic pathway can also be investigated using fluorescently labelled primary antibodies and flow cytometry. A

loss in mitochondrial membrane potential and calcium flux play an important role in apoptosis and can be investigated using appro

CHAPTER 5
CELL SURVIVAL: ENDOREDUPLICATION

5.1. General Background

5.1.1. Definition

Endoreduplication is characterized by two or more successive rounds of DNA replication, in the absence of mitosis. This results in the formation of diplochromosomes, consisting of four chromatids instead of the normal two (Cortés *et al*., 2004; Erenpreisa and Cragg, 2001; Sugimoto-Shirasu and Roberts, 2003; Sutou and Tokuyama, 1974). Three types of endoreduplication are found, namely (i) multiple initiations within a given S phase, (ii) reoccurring S phase and (iii) repeated S and gap phases. Endoreduplication represents an incomplete cell cycle, which is orderly regulated. The occurrence of endoreduplication in high metabolic tissues, for example the endosperm of developing maize kernels and the silk glands of dipterans, is more common (Grafi, 1998).

5.1.2. Inducers

Endoreduplication can occur spontaneously or can be induced by physical treatments (e.g. cold temperatures, X-rays), chemical compounds or mutagens (e.g. α- and β-mercaptoethanol, β-mercaptopyruvate, 8-azaguanine, nitrogen mustard, colchicine, 6-mercaptopurine, piperazine derivative, 4-nitroquinoline, 1-oxide, acridine dyes, captan, Cytoxan), protein kinase inhibitors, lectins, and metabolic and mitotic inhibitors (Bottura and Ferrari, 1963; Grafi, 1998; Sutou and Tokuyama, 1974).

Spontaneous endoreduplication is commonly found in plants, especially in the meristem regions of roots, stems and leaves, large specialized cells accumulating sharp inorganic inclusions, nodule cells, endosperm and xylem cells (Figure 5.1; Hase *et al*., 2005; John and Qi, 2008; Sugimoto-Shirasu and Roberts, 2003). Endoreduplication is rarely found in animals and occur in dipteran salivary glands, tonsils, trophoblasts, giant cells of the

placenta, mammalian liver, human lymphocytes, Chinese hamster cells and tumour cells (Cortés and Pastor, 2003; Cortés *et al*., 2004; Huang *et al.*, 1985).

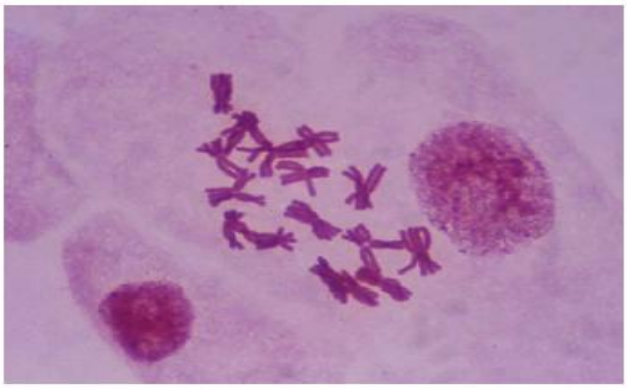

Figure 5.1: Diplochromosome formation during metaphase in the root meristem cells of *Allium cepa*, following acetaldehyde treatment (Cortes *et al*., 2004).

5.1.3. Mechanism of action

The induction mechanisms of endoreduplication are still largely unclear due to a variety of agents inducing endoreduplication and the different cell types where it occurs. Chemical and physical agents inducing endoreduplication by disrupting cytoskeleton assembly include colcemid, colchicines, concanavalin A, nocodazole, taxol and vincristine, and those that damage DNA include X-rays, α-radiation, hydrazine, sodium arsenite/fluoride, mitomycin C, aphidicolin, halogenated nucleosides, zorubicin and 33258 Hoechst (Cortés *et al*., 2004).

Cytoskeleton assembly. The mitotic spindle checkpoint monitors the spindle microtubule structure, chromosome alignment and the attachment of spindle microtubules to kinetochores on the sister chromatids during mitosis. Chromosome segregation during anaphase is delayed until defects in the mitotic spindle are corrected (Moon *et al*., 2008a; Stewart *et al*., 1999). Improper attachment of spindle microtubules to kinetochores may cause longer cell cycle arrest and apoptosis, whereas failed sister chromatid segregation can lead to cell cycle arrest with tetraploid (4N) DNA content and endoreduplication. The latter has been investigated with the microtubule interfering agent, taxol. Microtubules are important for cell replication, division, maintenance of cell shape, and

cellular movement. They undergo a dynamic process of polymerization and depolymerization (Moon *et al*., 2008a). Mitotic abnormalities may be due to mutation or inhibition of mitotic proteins controlling chromosome alignment and segregation (Cortés *et al*., 2004).

Cyclin and CDK. Cyclin degradation or expression, and active or inactive CDKs play an important role in mitosis and endoreduplication. MacAuley *et al*. (1998) investigated cyclin and CDK expression during the transition from DNA replication to endoreduplication in the rat choriocarcinoma derived cell line, Rcho-1 (Figure 5.2). S phase initiation during mitotic- and endocycles involves cycles of cyclin A and E synthesis. Cyclin E is expressed in the cytoplasm, enters the nucleus and initiates DNA synthesis and cyclin A expression. Cyclin A is required for S phase completion. Cyclins E and A are rapidly degraded at the end of DNA synthesis, which may be a requirement to reinitiate another endocycle by activating the origins of activation (Grafi, 1998; MacAuley *et al*. 1998). Failed assembly of cyclin B and CDK1, phosphorylation of CDK1 by CHK1, and an inactive cyclin B-CDK1 complex may be responsible for G2/M phase arrest (Erenpreisa and Cragg, 2001; John and Qi, 2008; MacAuley *et al*., 1998; Sugimoto-Shirasu and Roberts, 2003). Cyclin A/E-CDK2 activities are re-activated and DNA synthesis reinitiated during the first endocycle. At the end of the first endocycle S phase, cyclins A, B and E are degraded. Initiation of a second endocycle occurs in a gap phase when cyclin A/E-CDK2 activities are absent, which may be necessary to reset the cycle for the next DNA replication. DNA synthesis is reinitiated when cyclin A/E-CDK2 is reactivated (McAuley *et al*., 1999).

Cyclin B is expressed in abundance during the first endocycle, but not at all during the following endocycles. This may be due to the start of the first endocycle in the G2 phase of the mitotic cell cycle. The presence of cyclin B in the first endocycle may be due to failed activation of rapid cyclin B degradation associated with mitosis. In the mitotic cell cycle, cyclin B is expressed towards the end of the G2 phase. Cyclin B induction may depend on G1-S cyclin-CDK activity and termination of cyclin A/E-CDK2 activity at the end of the endocycle's S phase (McAuley *et al*., 1998).

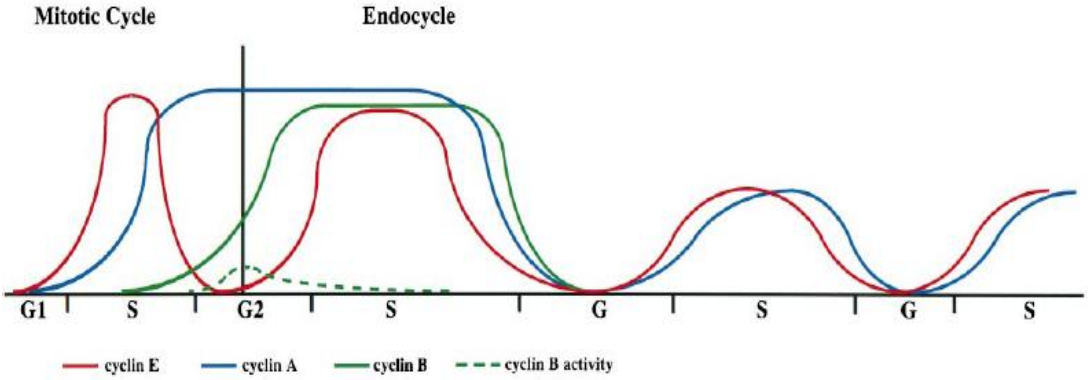

Figure 5.2: The role of cyclins in the mitotic- and endocycles in the rat choriocarcinoma cell line, Rho1 (McAuley *et al*. 1998). See text for more detail.

DNA topoisomerase II. DNA topoisomerase II plays an important role in condensation and anaphase segregation of replicated daughter chromosomes. DNA topoisomerase II levels peak in the G2 phase and early mitosis. Inhibitors of topoisomerase II activity prevent sister chromatid separation after chromosome condensation, resulting in cell cycle arrest in the metaphase (Figure 5.3). Anticancer drugs, interfering with DNA topoisomerase II, are divided into classical 'poisons' for example anthracyclines, epipodophyllotoxins, anthracenediones and aminoacridines, and true catalytic inhibitors for example merbarone, fostriecin, aclarubicin, suramin, novobiocin, chloroquine, and bisdioxopiperazines. Classical 'poisons' cause DNA strand breaks by forming a stable, cleavable complex between the covalently bound topoisomerase II and DNA. True catalytic inhibitors do not form a cleavable complex and target DNA topoisomerase II directly within the cells and interfere with genetic processes for example replication, transcription and chromosome dynamics. 'Poisons' and catalytic inhibitors can both cause endoreduplication (Cortés and Pastor, 2003; Cortés *et al*., 2004).

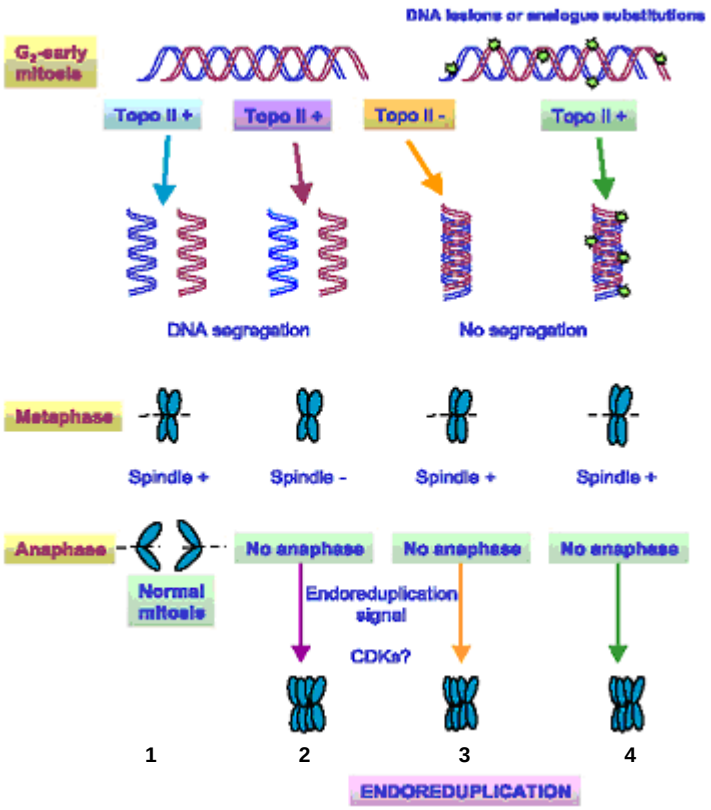

Figure 5.3: Comprehensive model of endoreduplication proposed by Cortes *et al*. (2004). 1) Normal chromosome segregation during mitosis (proper function of topoisomerase II and the spindle apparatus); 2) endoreduplication due to interference with cytoskeletal assembly (proper function of topoisomerase II, but not the spindle apparatus); 3) endoreduplication due to the absence of topoisomerase II activity (poisoning or inhibiting agents); 4) endoreduplication due to modification of DNA, thus hindering topoisomerase II binding (physical or chemical damage; incorporation of base analogues).

Neukam *et al*. (2008) have shown inhibition of topoisomerase II activity and endoreduplication in AA8 Chinese hamster ovary cells when treated with the tea flavanols, epigallocatechin-3-gallate and epigallocatechin at micromolar concentrations, and catechin and epicatechin at millimolar concentrations. The flavonoids, quercitin and luteolin, also cause topoisomerase II inhibition and endoreduplication (Neukam *et al*., 2008).

5.2. Anti-apoptotic Proteins – Cell Survival

5.2.1. Background

Akt and phospho-Akt. Survival factors, including serum, cytokines and growth factors [e.g. insulin-like growth factor 1 (IGF-1), neurotrophins, insulin, platelet-derived growth factor (PDGF)], play important roles in providing anti-apoptotic signals, which is involved in homeostasis (Brunet *et al*., 1999; Frank *et al*., 1995; Kennedy *et al*., 1997). Survival factors activate phosphatidylinositol 3-kinase (PI-3K), which phosphorylates phosphatidylinositol-4-phosphate to phosphatidylinositol-3,4-bisphosphate. The serine/threonine kinase, Akt/PKB, binds phosphatidylinositol-3,4-bisphosphate at the cell membrane, dimerizes and is stabilized in a partially active form. Membrane location and/or dimerization enhance the ability of Akt/PKB to be phosphorylated by PDK1/2 (Frank *et al*., 1997). Akt's ability to deliver the survival signal depends on its kinase activity and activity of its upstream activator, PI-3K (Kennedy *et al*., 1997).

Akt promotes cell survival by phosphorylating and suppressing caspase-9 activity and Bad functions, which are important pro-apoptotic proteins involved in the apoptotic intrinsic pathway (Brunet *et al*., 1999). Brunet *et al*. (1999) have shown Akt phosphorylation of the human Forkhead family of transcription factors (FKHRL1) in the presence of survival factors, which interacts with the scaffolding protein 14-3-3. Phosphorylated FKHRL1 is retained in the cytoplasm and FKHRL1 related transcription inhibited. Upon survival factor withdrawal, FKHRL1 gets dephosphorylated, enters the nucleus and regulates the activity of transcription factors that control cell death genes, for example the Fas ligand. Cell survival, associated with increased Akt levels, is seen in granule and cerebellar neurons, PC12, Rat-1 and COS-7 cells (Frank *et al*., 1997). Ras and Src may activate PI-3K (Franke *et al*., 1997; Kennedy *et al*., 1997).

The PI-3K/Akt signalling pathway may also act through modulating Bcl-2 expression, but Kennedy *et al*. (1997) have shown no significant changes in Bcl-2 and Bcl-X_L levels. They did find inhibition of Ced3/ICE-like proteases that specifically cleave PARP in

fibroblasts upon growth factor withdrawal. Inhibition of apoptosis by activated Akt may be the same or greater than the anti-apoptotic effect exerted by insulin, IGF-1 and PDGF, but these effects are lower than the anti-apoptotic effect exerted by serum. Downstream effectors of growth factor receptors, namely Raf, Ras and Src molecules, were not effective in promoting cell survival once the growth factors, especially serum, were removed. Akt/PKB activation, associated with cell survival, depends on the signal and/or cell type used.

Akt is involved in increased NO synthesis, cell survival, glycogen synthesis, cell growth and proliferation. Akt targets and inhibits glycogen synthase kinase (GSK)-3, via phosphorylation, which may block apoptosis. The mechanism is still unknown, but it is possible that GSK-3 may activate the adenomatous polyposis coli (APC) protein, which may accelerate apoptosis by degrading β-catenin and inhibiting adhesion (Frank *et al*., 1997; Kennedy *et al*., 1997).

Phospho-Bcl-2. The Bcl-2 family members are multifunctional proteins, which homodimerize with themselves (e.g. Bax, Bim, Bad) or heterodimerize with each other (e.g. Bcl-2, Bcl-X_L with Bax, Bak), and bind non-homologous proteins (Bcl-2 and Bcl-X_L interact with Apaf-1, protein kinase Raf-1, Ca^{2+}-activated phosphatase calcineurin, p53 binding protein) (Reed, 1998). The Bcl-2 family consists of pro- and anti-apoptotic proteins involved in apoptosis and cell survival, respectively. The ratio of Bcl-2 family members influences cell survival or apoptosis. The most highly expressed Bcl-2 family members are Bcl-2 and Bax (Frommel and Zarling 1999; Gross *et al*., 1999).

Bcl-2 proteins contain C-terminal hydrophobic domains and are integral proteins localized to cellular membranes of the ER, outer mitochondrial membrane and nuclear envelope. Bax, a pro-apoptotic protein mainly found in the cytosol, is translocated to the mitochondria when receiving a death signal. Upon dimerization, Bax inserts into the mitochondrial membrane and cytochrome c is released. Cytochrome c is released due to (i) pore formation in the mitochondrial membrane resulting in a loss in membrane potential, or (ii) a change in the inner membrane potential resulting in osmotic swelling

of the mitochondria and rupturing of the outer mitochondrial membrane. Cleavage of the C-terminal hydrophobic domain of Bax prevents its insertion into the mitochondrial membrane (Gross *et al*., 1999; Murphy *et al*., 2000; Reed, 1998).

Bcl-2 prevents cytochrome c release by preventing a loss in mitochondrial membrane potential across the inner membrane. A loss in mitochondrial membrane potential is associated with the opening of large conductance inner membrane channels, by Bax, which may be regulated by Bcl-2. Bcl-2 could also protect mitochondria by preventing Bax-induced pores in the outer mitochondrial membrane (Gross *et al*., 1999; Murphy *et al*., 2000; Reed, 1998). Murphy *et al*. (2000) have shown that Bcl-2 prevents Bax translocation from the cytosol to the mitochondria. They also suggested that Bcl-2 occupies the insertion site of Bax or control upstream events necessary for Bax insertion, due to localization in the ER and nuclear envelope. Furthermore, is it unlikely that the mechanism of Bcl-2/Bax heterodimer formation occurs, due to their localization to separate subcellular compartments.

$p21^{Waf1/Cip1}$. p53 prevents structural chromosome abnormalities and control diploid chromosome numbers possibly by maintaining the G1-S cell cycle and spindle checkpoints. p53 deficiency is associated with karyotopic instability, which include chromosome breaks or instability, endoreduplication and polyploidy (Agapova *et al*., 1996 and 1999; Illidge *et al*., 2000). $p21^{Waf1/Cip1/Sdi1}$ expression is upregulated by p53-dependent and -independent mechanisms. p53-independent factors include the transforming growth factor (TGF)-β and mimosine, an agent affecting DNA replication (Bates *et al*., 1998; Chang *et al*., 2000; Datto *et al*., 1995; Roninson, 2002). $p21^{Waf1/Cip1}$ interactions and functions include (i) inhibition of cyclin A/E-CDK2 and cyclin B-CDK1, or stimulation of cyclin D-CDK4/6 complexes; (ii) bind the replication or repair protein, proliferating-cell nuclear antigen (PCNA), which is a cofactor for DNA polymerase δ and ε during replication and enhances the polymerase activity; (iii) binds regulatory proteins, which may inhibit or stimulate transcription (Bates *et al*., 1998; Flores-Rozas *et al*., 1994; Roninson, 2002; Stewart *et al*., 1999). Overproduction of $p21^{Waf1/Cip1}$ leads to cell growth arrest in the G1 and G2 phases, due to $p21^{Waf1/Cip1}$ ability to inhibit cyclin-CDK

complexes (Bates *et al*., 1998; Chang *et al*., 2000; Niculescu *et al*., 1998). $p21^{Waf1/Cip1}$ is a tumour suppressor which prevents or slows down tumour development, but mutations are associated with human cancers and affects its role as CDK inhibitor (Roninson, 2002). See Chapter 4 (section 4.2.4) for more information.

The observation from the previous chapter that rooperol and *Hypoxis* extracts induce endoreduplication prompted an investigation into the possible cell survival strategy of HeLa, HT-29 and MCF-7 cancer cells when treated with *H. sobolifera* and rooperol. The expression of the anti-apoptotic proteins, phospho-Akt, phospho Bcl-2 and $p21^{Waf1/Cip1}$, were measured and the cell morphology investigated.

5.2.2. Materials and Methods

Anti-apoptotic proteins. HeLa, HT-29 and MCF-7 cancer cells were seeded at densities of 40 000 cells/mL in 24-well plates and left to attach overnight at 37 ºC in a humidified incubator and 5% CO_2. Cells were treated with DMSO (0.25%, v/v), *H. sobolifera* (125 µg/mL) and rooperol [IC_{50} values (Table 4.4)] for 15 hrs. After exposure, cells were washed with PBSA, trypsinized for 10 min at 37 ºC and resuspended in PBS. Cells were centrifuged at 500 x g for five min at room temperature and the supernatant discarded. Cells were washed as described above to remove any traces of trypsin. Cells were fixed and permeabilized using the IntraPrep™ permeabilizing reagent as described in the kit protocol. After permeabilization, cells were washed using cold incubation buffer (0.5% BSA in PBS), centrifuged as describe above, supernatant discarded and cells blocked for 10 min in incubation buffer at room temperature. Akt, phospho-Akt (Ser473) and phospho-Bcl-2 (Ser70)(5H2) rabbit mAbs (Cell Signaling Technology Inc.) were added at recommended working dilutions to the cells and incubated for one hour at room temperature. Cells were washed twice as described above. After washing, FITC conjugated goat anti-rabbit IgG (H+L chain specific) (Beckman Coulter) was added at recommended working dilutions. FITC conjugated rabbit IgG, was added to untreated HeLa, HT-29 and MCF-7 cancer cells and used as an isotype control. Cells were

incubated for 30 min at room temperature in the dark and washed as described above. Cells were resuspended in PBS and read on a Beckman Coulter Cytomics FC500.

Phase contrast light microscopy. HeLa, HT-29 and MCF-7 cancer cells were seeded at densities of 40 000 cells/mL in 24-well plates and left to attach overnight at 37 ºC in a humidified incubator and 5% CO_2. Cells were treated with DMSO (0.25%, v/v), *H. sobolifera* (125 µg/mL) or rooperol [IC_{50} values (Table 4.4)] for 48 hrs. After treatment, cells were washed with PBSA, trypsinized for 10 min at 37 °C, resuspended in PBS and viewed under an Axiovert 40C inverted microscope (Carl Zeiss MicroImaging, Göttingen, Germany) with a Ph2-0.4 filter and 40x objective. Photos were taken with a PowerShot A640 digital camera (Canon, China).

4'6-diaminidine-2'-phenylindole dihydrochloride (DAPI) fluorescence staining. HeLa, HT-29 and MCF-7 cancer cells were seeded at densities of 40 000 cells/mL onto 13 mm round glass coverslips (acid washed with 1 M HCl, 70% EtOH and autoclaved), placed into 24-well plates, and left to attach overnight at 37 ºC in a humidified incubator and 5% CO_2. Cells were treated with DMSO (0.25%, v/v) and rooperol [IC_{50} values (Table 4.4)] for 48 hrs. After treatment, medium was aspirated, cells washed with DPBS (containing Ca^{2+} and Mg^{2+}) and fixed with Carnoy's fixative (MeOH: acetic acid, 3:1, v/v) for 10 min. Cells were stained with DAPI (1µg/mL dissolved in 100% MeOH, Sigma) for 10 min at room temperature in the dark, washed with DPBS and coverslips mounted cell side down in glycerol: PBSA (90:10, v/v). Images were taken using an OLYMPUS BX60 fluorescence microscope, XC50 camera and AnalySIS® FIVE software (LifeScience Series).

Forward- and side scatter. Dot plots of forward scatter versus side scatter were obtained during DNA cell cycle analysis performed in Chapter 4 (section 4.2.4) to observe changes in cell size.

5.2.3. Results and Discussion

Anti-apoptotic proteins. Three survival signalling proteins were investigated namely phospho-Akt, phospho-Bcl-2 (Figure 5.4) and p21$^{Waf1/Cip1}$ (Chapter 4; Figure 4.10).

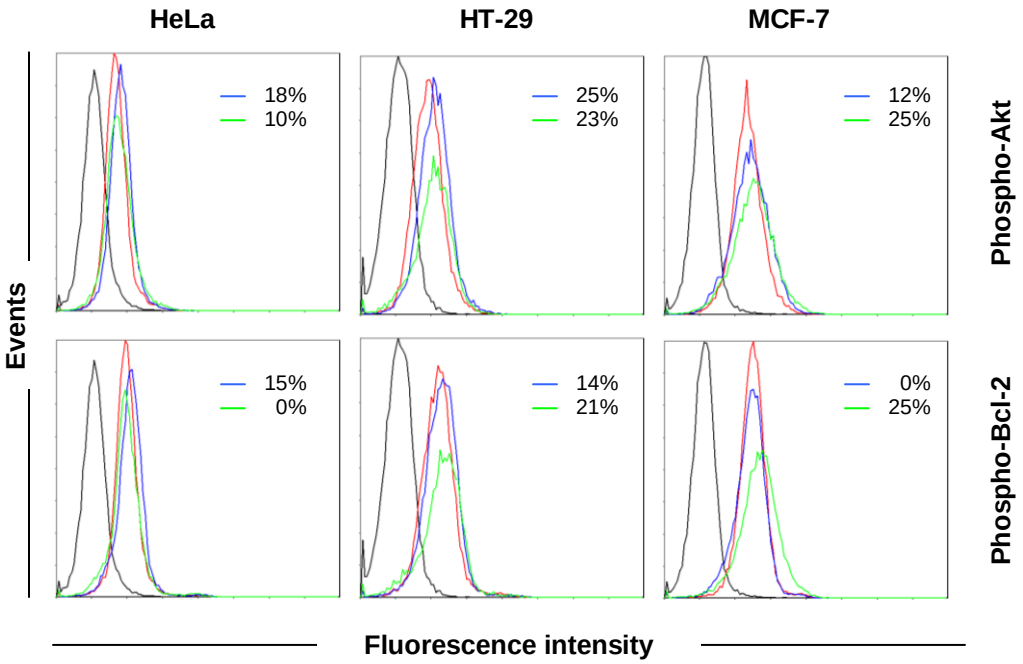

Figure 5.4: Overlay of histograms representing phospho-Akt and phospho-Bcl-2 levels in HeLa, HT-29 and MCF-7 cancer cell lines after 15 hrs of treatment with DMSO (0.25%; red), *H. sobolifera* (125 µg/mL; blue) and rooperol (IC_{50} values; green). Percentages on histograms represent the increase in median fluorescence intensity of cells staining positive for phospho-Akt and phospho-Bcl-2 when treated samples were compared to the control. Rabbit IgG was used as isotype control (black). 10 000 events were recorded. One representative of three experiments performed.

This study has shown an increase in phospho-Akt levels in *H. sobolifera* and rooperol treated HeLa, HT-29 and MCF-7 cancer cells, whereas the unphosphorylated Akt levels remained the same (data not shown). *H. sobolifera* increased phospho-Bcl-2 levels in HeLa and HT-29 cancer cells, whereas rooperol increased phospho-Bcl-2 levels in HT-29 and MCF-7 cancer cells. Increases in p21$^{Waf1/Cip1}$ levels were seen when all three cancer cell lines were treated with rooperol, whereas *H. sobolifera* induced smaller increases in p21$^{Waf1/Cip1}$ expression in HT-29 and MCF-7 cancer cells and no increase in HeLa cancer cells (data shown in Figure 4.10; Chapter 4). Increased phospho-Akt, phospho-Bcl-2 and p21$^{Waf1/Cip1}$ levels in *H. sobolifera* treated HeLa, HT-29 and MCF-7 cancer cells could

not be attributed to rooperol, because hypoxoside was absent in the *H. sobolifera* chloroform extract, and trace amounts of hypoxoside which may have been present could not be converted to rooperol due to the absence of β-glucosidase. Increased phosphorylation of Akt, Bcl-2 and $p21^{Waf1/Cip1}$ was probably due to the presence of β-sitosterol (4.5 μM), trace amounts of other phytosterols (Chapter 3, section 3.3) and/or unidentified compounds. The possibility of synergistic and additive effects between different compounds cannot be ruled out.

Moon *et al*. (2008a) investigated the effect of β-sitosterol on endoreduplication via the Bcl-2 and PI-3K/Akt signalling pathways in human leukemia U937, HL60 and K562 cells. These studies used higher concentrations (10-30 μM) of β-sitosterol and longer treatment periods (24-96 hrs), compared to the low β-sitosterol concentrations present in the *Hypoxis* chloroform extract (4.5 μM) and shorter treatment time (15 hrs) used. To have a better idea on the expression levels of anti-apoptotic proteins, mRNA levels should be measured.

Increased phospho-Akt may have promoted cell survival in HeLa, HT-29 and MCF-7 cancer cells, following *H. sobolifera* and rooperol treatment, by (i) phosphorylating and suppressing caspase-9 and Bad functions and/or (ii) phosphorylating the human Forkhead transcription factor, FKHRL1; hence preventing transcription of genes associated with cell death (Brunet *et al*., 1999). Moon *et al*. (2008a) have shown an increase in PI-3K and Akt phosphorylation, while total PI-3K and Akt levels remained constant over 96 hrs, when U937 cells were treated with β-sitosterol (20 μM). The inhibitor of PI-3K, LY29004, blocked β-sitosterol induced endoreduplication, resulting in an increase in cell numbers with sub-G1 DNA content (apoptotic cells) (Moon *et al*., 2008a). Cell survival, via the PI-3K/Akt-NF-κB pathway, was also seen in chemotherapeutic resistant MCF-7 cancer cells (Simstein *et al*., 2003).

Increased (phospho)-Bcl-2 levels may have promoted cell survival in HeLa, HT-29 and MCF-7 cancer cells, following *H. sobolifera* and/or rooperol treatment, by preventing Bax translocation from the cytosol to the mitochondria and subsequent Bax-mediated

release of mitochondrial cytochrome c. Inhibition of Bax translocation has been seen in HeLa cancer cells, treated with staurosporine and etoposide, which overexpress Bcl-2 (Murphy *et al*., 2000). Follicular lymphoma, a B-cell malignancy, is generally incurable and is characterized by overexpression of the Bcl-2 oncogene, which inhibits apoptosis. Follicular lymphoma differs from benign follicular lymphoma by increased Bcl-2 and phospho-Akt (Ser473) expression, and higher ratios of Bcl-2/Bax and Bcl-2/Bak (Gulmann *et al*., 2005). Treatment of U937 cells with β-sitosterol (>20 μM; 24 hrs) resulted in increased Bcl-2 phosphorylation and endoreduplication. The Bcl-2 inhibitor, HA14-1, blocked β-sitosterol induced endoreduplication, resulting in an increase in cell numbers with sub-G1 DNA content (hence apoptotic cells) (Moon *et al*., 2008a). Moon *et al*. (2008b) have shown that Bcl-2 overexpression prevents SP660125 [c-Jun N-terminal kinase (JNK) inhibitor]-induced apoptosis in U937 leukemia cells by inhibiting caspase-3, -8 or -9 cleavage, inducing G2/M phase arrest and promoting endoreduplication. Overexpression of Bcl-2 counteracts SP660125-induced death by preventing Bcl-2 and Bcl-X_L repression and maintaining AIP levels. JNK, a member of the mitogen-activated protein kinases (MAPK), has apoptotic, cell survival and proliferation properties. JNK substrates include Bcl-2, Bcl-X_L, $p21^{Waf1/Cip1}$ and p53. JNK phosphorylates p53 changing it to a more stable conformation, which leads to increased $p21^{Waf1/Cip1}$ expression, cyclin B-CDK1 inhibition and G2/M arrest. Treatment of MCF-7 and MDA MB-231 breast cancer cells with the JNK inhibitor, SP660125, resulted in G2/M cell arrest and endoreduplication. G2/M arrest is associated with increased $p21^{Waf1/Cip1}$ expression, which inhibits cyclin B-CDK1 activity. JNK inhibition may prevent JNK dissociation from $p21^{Waf1/Cip1}$ and inhibition of cyclin B-CDK1 activity (Mingo-Sion *et al*., 2004).

Increased $p21^{Waf1/Cip1}$ expression (Chapter 4, section 4.2.4) may have promoted cell survival in HeLa, HT-29 and MCF-7 cancer cells, following *H. sobolifera* and/or rooperol treatment, by affecting the cell cycle. $p21^{Waf1/Cip1}$ plays an important role in cell growth arrest associated with DNA damage and often triggering endoreduplication and abnormal chromosome segregation (Roninson, 2002). It may inhibit topoisomerase II activity involved in segregation of replicated daughter chromatids before anaphase.

Topoisomerase II mRNA levels peak towards the end of S phase and start of the G2/M phase (Cortés and Pastor, 2003). β-sitosterol treatment increased $p21^{Waf1/Cip1}$ and CDK2 expression, which is important for entry into the S phase, in U937 and HL60 cells (Moon *et al*., 2008a). $p21^{Waf1/Cip1}$ could promote endoreduplication by partial inhibition of CDKs. Incomplete inhibition of cyclin E/A-CDK2 by $p21^{Waf1/Cip1}$ may allow sufficient activity for initiation of replication, but not enough to proceed to mitosis (Bates *et al*., 1998; Niculescu *et al*., 1998). Anti-apoptotic functions of $p21^{Waf1/Cip1}$ are attributed to procaspase-3 binding, which prevent its conversion to active caspase-3, interactions with caspase-8 and -10, inhibition of apoptosis-regulating kinases and apoptosis-stimulating transcription factors (Roninson, 2002).

$p21^{Waf1/Cip1/Sdi1}$ may induce growth arrest associated with the depletion of mitotic- and replication-associated proteins, which leads to abnormal mitosis and endoreduplication (Cortés *et al*., 2004; Mingo-Sion *et al*., 2004). Chang *et al*. (2000) have shown a decrease in the RNA levels of genes controlling different stages of mitosis, when HT1080 human fibrosarcoma cells were treated with isopropyl-β-thio-galactosidase (IPTG), which induces $p21^{Waf1/Cip1}$ expression. These include CDK1 and cyclin B involved in the mitosis initiating complex; polo-like kinases involved in mitosis onset, mitotic checkpoint control and cytokinesis; CDK1 interacting protein (CKsHs1) involved in the mitotic checkpoint control; centrosome associated kinesin (MCAK); centrosome-associated kinase (AIK1) involved in spindle formation; proteins involved in spindle checkpoint (e.g. CENP-A/P, MAD2, BUBR1); and proteins involved in cytokinesis (e.g. Prc1, Aim1, citron kinase). Maintaining high $p21^{Waf1/Cip1}$ levels long enough will deplete the cellular pool of mitosis control proteins. Mitosis-initiating proteins need to be regenerated after $p21^{Waf1/Cip1}$ shutoff before cells can enter mitosis. If these proteins are not re-synthesized to sufficient levels, abnormal mitosis will occur (Chang *et al*., 2000).

Cell cycle arrest, associated with endoreduplication, occurs mainly in the G2/M phase. G2/M phase arrest occurred when U937 and HL60 leukemia cells (Moon *et al.*, 2008a) and MDA-MB-231 breast cancer cells (Awad *et al*., 2001a) were treated with β-sitosterol. In this study, G2/M phase arrest occurred in HeLa, HT-29 and MCF-7 cancer

cells when treated with *Hypoxis* extracts and rooperol for 48 hrs (Chapter 4; section 4.2.4). β-sitosterol present in the *Hypoxis* extracts may have caused G2/M phase arrest. G2/M arrest may be explained by the inability of cells to activate cyclin B. Activation of cyclin B-CDK1 may depend on prior activation of CDK2 activity. $p21^{Waf1/Cip1}$ mediated arrest could block cell cycle progression in late S or early G2/M phase prior to cyclin B-CDK1 activation, hence the importance of cyclin A-CDK2 in S-phase exit. Cells blocked in the G2/M phase by $p21^{Waf1/Cip1}$ are impaired in their ability to sense their position in the cell cycle following release, hence entering another S phase and endoreduplication occurs (Bates *et al*., 1998). Sutou and Tokuyama (1974) investigated endoreduplication in a Chinese hamster cell line when treated with 4-nitroquinoline. Endoreduplicated cells were found in the late S phase and mainly in the G2/M phase. After the gap phase, the cells entered a long S phase, which is equivalent to two ordinary S phases. The long S-phase may be explained by a shortage in precursors to produce double the amount of DNA needed for diplochromosomes (Sutou and Tokuyama, 1974).

β-sitosterol may further promote endoreduplication and apoptosis by altering microtubule dynamics and thus interfering with spindle formation during mitosis. It also induces ERK phosphorylation, which is involved in cell survival, but had no effect on JNK and p38 MAPK phosphorylation, which are involved in apoptosis (Moon *et al*., 2008a).

Phase-contrast light and DAPI fluorescence microscopy. Morphological studies on HeLa, HT-29 and MCF-7 cancer cells revealed the presence of enlarged ('giant') cells (Figure 5.5) and nuclei (Figure 5.5 and 5.6), associated with endoreduplication, when treated with rooperol.

Phase-contrast microscopy (Figure 5.5) has shown the presence of 'giant' cells with enlarged nuclei, and intact plasma and nuclear membranes after rooperol treatment. Apoptotic cells were also seen among the 'giant' cells. Chromatin condensation, cell membrane blebbing and apoptotic body formation were seen in HT-29 (data not shown), HeLa and MCF-7 cancer cells, which are characteristic morphological features of apoptosis. This may suggest that apoptosis follows endoreduplication in certain cells.

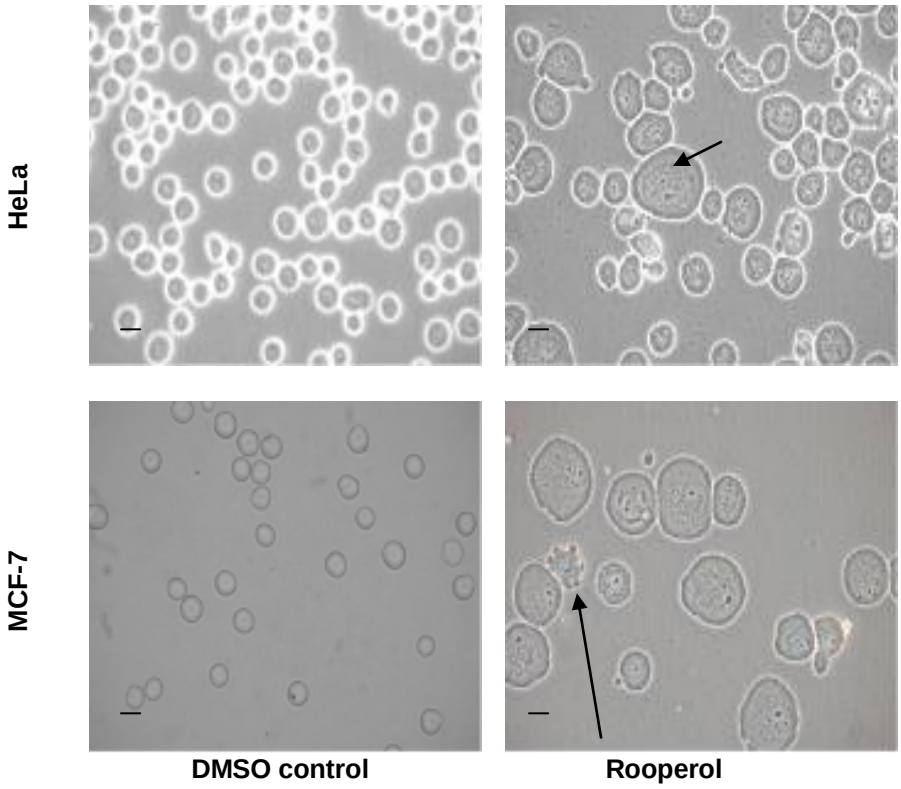

Figure 5.5: Phase-contrast photographs of HeLa and MCF-7 cancer cells when treated with rooperol (IC_{50} values) compared to the DMSO control (0.25%, v/v). Enlarged cells represent 'giant cells', which have undergone endoreduplication. Long arrow represents an apoptotic cell with membrane blebbing and apoptotic body formation. Short arrow represents an enlarged nucleus with condensed chromatin. Bar = ±25 µm.

DAPI microscopy (Figure 5.6) has shown the presence of enlarged nuclei with intact nuclear membranes in the 'giant' cells. Chromatin condensation and ruptured nuclei, associated with apoptosis, were also seen among the 'giant' cells.

The nuclear-to-cytoplasm ratio ensures that the amount of cytoplasm that a cell can make and sustain is proportional to the amount of DNA in the nucleus. Thus the endoreduplicated nucleus can sustain greater cell growth. Increase in cells size and polyploidy may be due to enhanced gene expression and protein synthesis by ribosomes (Sugimoto-Shirasu and Roberts; 2003). An increase in nucleus size was also reported when cells were treated with β-sitosterol (Moon *et al*., 2008a).

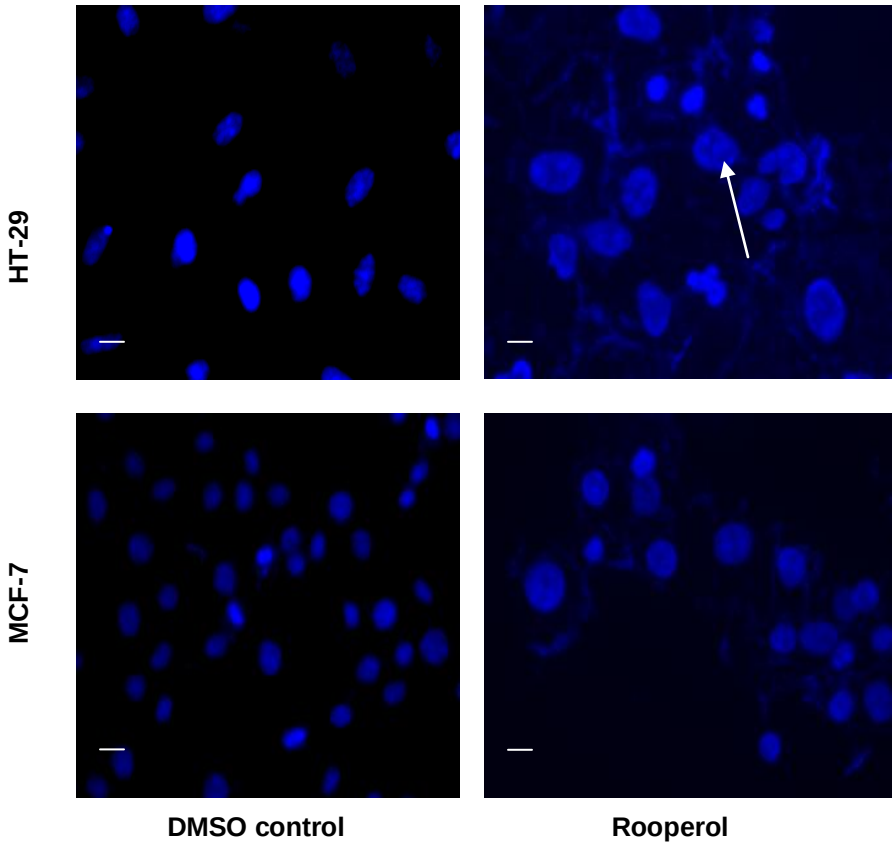

Figure 5.6: Fluorescence images of DAPI stained HT-29 and MCF-7 cancer cells when treated with rooperol (IC_{50} values) compared to the DMSO control (0.25%, v/v). Enlarged nuclei represent 'giant cells', which have undergone endoreduplication. Arrow represents condensed chromatin. Bar = ±5 µm.

An increase in forward- and side scatter represents an increase in cell size and granularity or complexity, respectively, which further confirms endoreduplication. Dot plots of *H. sobolifera* and rooperol treated HeLa, HT-29 and MCF-7 cancer cells have shown an increase in side- and/or forward scatter (Figure 5.7). These dot plots correspond with the phase contrast- and fluorescence (DAPI) photos taken. An increase in forward- and side scatter were seen when U937 and HL60 cells were treated with β-sitosterol (Moon *et al*., 2008a).

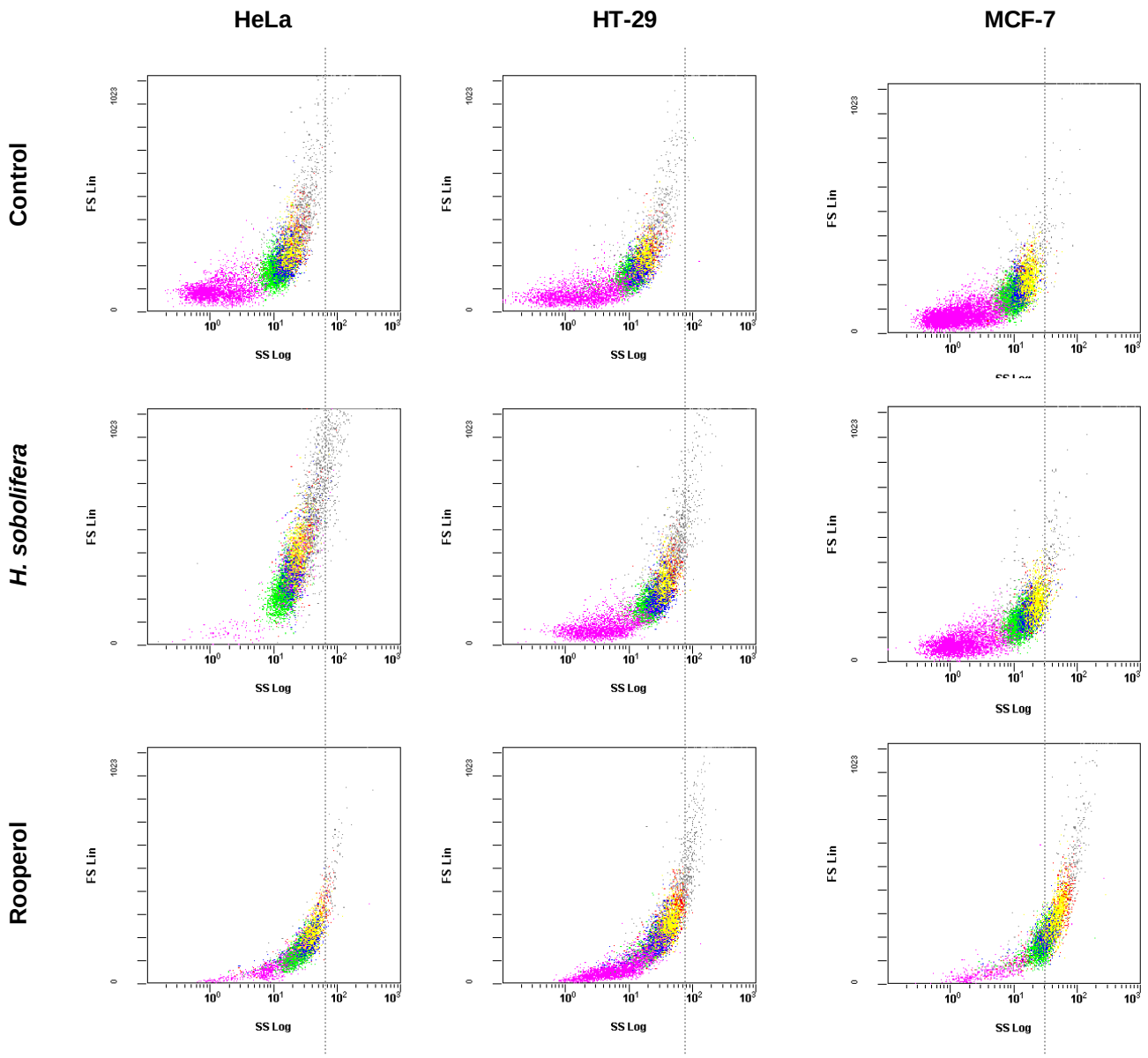

Figure 5.7: Dot plots of forward scatter (FS) vs side scatter (SS) of HeLa, HT-29 and MCF-7 cancer cells when treated with *H. sobolifera* (125 µg/mL) and rooperol (IC_{50} values) for 48 hrs.

Sensitive tumours respond to treatment and undergo apoptosis rapidly, whereas drug resistant tumours respond partially to treatment with delayed death or surviving the death signal (Erenpreisa and Cragg, 2001; Illedge *et al*., 2000). Tumours may become resistant when treated continuously; hence cytotoxic agents are administered every 3-4 weeks with short exposure periods (Puig *et al*., 2008). Endoreduplication may be part of the cell survival strategy, which may be followed by apoptosis. The majority of cells undergoing

endoreduplication die, whereas only a few will survive. During endoreduplication, resistant cells have the ability to repair DNA damage resulting in polyploidy, whereas rapid apoptosis will stop any possibility of DNA repair. Polyploid giant cells have been regarded as reproductively dead, but giant polyploid cells are actively undergoing DNA replication with an exchange between the endocyclic and mitotic populations (Illedge *et al*., 2000).

In vivo treatment of tumours with cisplatin results in tumour shrinkage and formation of giant tumour cells that do not proliferate but undergo DNA synthesis. After several weeks of latency, the tumour resumes progression and consists of small, diploid, rapidly proliferating cells. *In vitro* treatment of tumour cells has shown an initial stop of mitotic activity, but DNA duplication continued (Puig *et al*., 2008). Giant polyploid cells can die through mitotic catastrophe, but many polyploid cells survive for weeks as non-proliferative mono- or multi-nucleated giant cells acquiring a 'senescence phenotype'. A limited number of extensive colonies, consisting of small diploid cells differing from parental cells by abnormal chromosomal and increased resistance to cytotoxic drugs, form from the giant cells. DNA endoreduplication, polyploidy, depolyploidization and the generation of escape cells are characteristics of tumour relapse after chemotherapy (Puig *et al*., 2008).

Endoreduplication and genetic destabilization of tumour cells may be a consequence of radiation therapy and chemotherapy. Such genetic destabilization may lead to certain cells to bypass normal cell cycle arrest and apoptotic mechanisms, resulting in increased malignancy or treatment resistant tumour cells (Chang *et al*., 2000; Niculescu *et al*., 1998). Giant cell formation may be an important repair response after cancer treatment and provide the tumour with an additional mechanism of resistance and survival of death signals (Illedge *et al*., 2000).

5.3. Conclusion

Endoreduplication seen in the DNA histograms (Chapter 4, section 4.2.4) has led to the investigation of endoreduplication in HeLa, HT-29 and MCF-7 cancer cells treated with *H. sobolifera* (*Hypoxis* spp. with the best cytotoxicity) and rooperol (cytotoxic compound). Morphological and biochemical analysis revealed:

- 'Giant' cell formation with enlarged nuclei (phase-contrast and DAPI) is associated with endoreduplication.
- An increase in size and granularity/complexity are associated with endoreduplication.
- Activation of the anti-apoptotic proteins: phospho-Akt, phospho-Bcl-2 and $p21^{Waf1/Cip1}$.
- Increased levels of $p21^{Waf1/Cip1}$ confirms late G1/early S phase cell cycle arrest after 15 hrs. G2/M phase arrest occurring after 48 hrs may explain endoreduplication (Chapter 4, section 4.2.4).

Endoreduplication is a possible cell survival strategy, which may be followed by apoptosis. Apoptotic cells (morphological characteristics: chromatin condensation, cell blebbing and apoptotic body formation) were seen among the endoreduplication cells. Endoreduplication seen in this study may suggest cancer cells becoming resistant to *Hypoxis* extracts and its purified compounds, which may be of importance and interest for further studies.

This is the first time that endoreduplication was investigated in cancer cells following *Hypoxis* and rooperol treatment.

<u>Peer-reviewed journal articles accepted/submitted from chapters 4 and 5</u>

Boukes, G.J., Daniels, B.B., Albrecht, C.F., van de Venter, M. 2010. Cell survival or apoptosis: rooperol's role as anticancer agent. Oncol. Res. In press.

Boukes, G.J., van de Venter, M. Anticancer properties of three *Hypoxis* spp. (African potato) against HeLa, HT-29 and MCF-7 cancer cell lines. Submitted to a peer-reviewed journal.

CHAPTER 6
ANTI-INFLAMMATORY ACTIVITY

6.1. General Background

Inflammation is a response to tissue injury triggered by physical or chemical stimuli and microbiological toxins to inactivate or destroy invading organisms, remove irritants and initiate tissue repair. It is involved in different pathologies including arthritis, asthma, multiple sclerosis, colitis, inflammatory bowel disease and atherosclerosis. The initial response in inflammation involves the release of lipid-derived autacoids (e.g. eicosanoids), large peptides (e.g. cytokines), small peptides (e.g. bradykinin) and amines (e.g. histamine) from injured and migrating cells. These give rise to the clinical and pathological signs and symptoms of inflammation, which include vascular permeability, vasoconstriction, vasodilation, pain, fever, chemotaxis and leukocyte adhesion, tissue and endothelial damage (Guzik *et al*., 2003).

Eicosanoids are divided into prostaglandins, thromboxanes and leukotrienes, which are biologically active metabolites derived from the 20-carbon polyunsaturated fatty acid, arachidonic acid (AA) (Nelson and Cox, 2000; Shale *et al*., 1999). Eicosanoids mediate and modulate the action of a variety of biological processes; are produced on demand; target parent or neighbouring cells (paracrine effect) and have a short biological life (Rocca and FitzGerald, 2002).

AA is released from the membrane phospholipid bilayer via cytosolic phospholipase A_2 ($cPLA_2$) activity in response to physical, chemical, hormonal and cytokine stimuli. AA is converted to prostaglandin H_2 (PGH_2) via PGH-synthase [syn. cycloxygenase (COX)-1/2; see section 6.4] activity in a two step reaction, involving (i) cyclization of AA to form the endoperoxidase intermediate, PGG_2 (cyclooxygenase activity), and (ii) reduction of the 15-hydroperoxy group to form PGH_2 (peroxidase activity). PGH_2 is converted to biologically active prostaglandins (PGE_2, $PGE_{2\alpha}$, PGD_2 and PGI_2) and thromboxanes

(TxA_2 and TxB_2) by cell-specific prostaglandin synthases (Awad *et al*., 2005b; Clancy *et al*., 2000; Gasparini *et al*., 2003; Rocca and FitzGerald, 2002).

Thromboxanes are produced in platelets and are involved in blood vessel constriction and blood coagulation. PGs are found in almost all living animal cells, tissues and glands, where they are associated with erythema (redness) and edema (swelling) leading to heat and pain (Shale *et al*., 1999). PGs regulate physiological and pathological processes including platelet aggregation, inflammation, pain, uterine contraction during ovulation, labour and abortion, mucin secretion to protect gastric mucosa from acid and proteolytic enzymes in the stomach, blood flow to organs, wake-sleep cycle, bone metabolism, body temperature, embryo implantation, nerve growth and development, wound healing, glomerular filtration and water balance, blood vessel tone and immune responses (Dubois *et al*., 1998; Nelson and Cox, 2000; Sheng *et al*., 2001).

Leukotriene (LT) synthesis is triggered by bacteria, viruses, fungi, protozoa, IgG, and C3. It involves the oxidation of AA by 5-lipoxygenase in the presence of the AA-binding protein, 5-lipoxygenase activating protein (FLAP), to form the epoxide intermediate LTA_4 (Peters-Golden *et al*., 2004; Rocca and FitzGerald, 2002). LTA_4 is (i) hydrolysed by LTA_4 hydrolase to LTB_4, which is a leukocyte chemoattractant and activator; or (ii) is conjugated to reduced glutathione by LTC_4 synthase to form LTC_4, which is involved in the pathogenesis of asthma and is the parent compound of the cysteinyl LTs (cysLTs) LTD_4 and LTE_4. LTB_4, cysLT or both are synthesized primarily by neutrophils and dendritic cells, mast cells and eosinophils, and macrophages, respectively.

Other functions of LTs include leukocyte accumulation to the inflammation site, enhanced phagocytosis and amplified microbicidal mechanisms (increasing NO and ROS release), generation of inflammatory mediators including cytokines (e.g. TNFα, IL-8) and chemokines (e.g. MCP-1, MIP-1β), bronchoconstrictors and vasoactive mediators released by mast cells (contributing to asthmatic responses), and contraction of the muscle lining of the airways to the lungs. LT synthesis is regulated by genetic, endogenous (e.g. hormones, cytokines, small molecules, reactive species) or exogenous

(e.g. toxins, dietary factors, pharmacologic agents) factors. Defects in LT synthesis have been seen in HIV infection, malnutrition, diabetes mellitus, cirrhosis, vitamin D deficiency, postsepsis and asthmatic attacks (Nelson and Cox, 2000; Peters-Golden *et al*., 2004).

H. hemerocallidea and rooperol have anti-inflammatory and anti-diabetic properties (Nair *et al*., 2007a; Ojewole, 2006; Steenkamp *et al*., 2006; van der Merwe *et al*., 1993). *Hypoxis* extracts and its purified compounds may influence NO production, COX-2 expression and phagocytosis in monocyte-macrophages, and pro- and anti-inflammatory cytokine production in PBMCs; hence these were investigated in the following sections.

6.2. Monocyte-to-Macrophage Differentiation

6.2.1. Background

A range of chemical, natural, biological and pharmacological agents can be used as inducers of cell differentiation. Specific agents differentiate leukemic cells into specific progeny including granulocytes, monocytes, monocyte-macrophages and megakaryocytes. For example, human promyelocytic leukemia HL-60 cells are differentiated to (i) granulocytes by retinoids, DMSO, hypoxanthine, camptothecin, antifolates, anthracyclins and bis-hydroxamic acids; (ii) megakaryocytes by aphidicolin; (iii) monocytes by bryostatin 1, butyric acid and tunicamycin; and (iv) monocyte-macrophages by phorbol esters [e.g. phorbol myristate acetate (PMA)] and 1α,25-dihydroxyvitamin D_3 [$1,25(OH)_2D_3$]. The complete mechanism of leukemic differentiation is still unclear and differentiation may be via:

- Membrane mediated events and signal transduction pathways.
- Receptor-mediated processes.
- Remodeling of superfine chromatin structure.
- Alterations in transmethylation of DNA or ribonucleic acid (RNA).
- Transcriptional factors acting as regulators.

- Protooncogenes (Tsiftsoglou *et al*., 2003).

Differentiation inducers of human promonocytic U937 leukemia cells to monocyte-macrophages include cytokines [e.g. IL-6 and TGF-1β (Tsiftsoglou *et al*., 2003)], phorbol esters [e.g. PMA (Kulseth *et al*., 1998; Shayo *et al*., 1997) and 12-*O*-tetradecanoylphorbol-13-acetate (TPA; Lu and Pitha, 2001)], retinoic acid (Kulseth *et al*., 1998) and $1,25(OH)_2D_3$ (Kulseth *et al*., 1998; Rots *et al*., 1999; Tsiftsoglou *et al*., 2003). The functional abilities of tissue macrophages vary depending on the tissue of residence. U937 cells exposed to $1,25(OH)_2D_3$, PMA and retinoic acid differentiate into macrophage-like cells involved in phagocytosis, secretion and antibody-dependent cellular cytotoxicity, respectively (Kulseth *et al*., 1998).

$1,25(OH)_2D_3$ inhibits proliferation and induces differentiation of normal and leukemic myeloid cells to monocyte-macrophages via the intracellular vitamin D receptor (VDR) (Fleet, 2004; Rots *et al*., 1999; Tsiftsoglou *et al*., 2003). VDR interacts with VDR elements, which are specific DNA sequences, to transcriptionally activate target genes in the presence of vitamin D_3 (Tsiftsoglou *et al*., 2003). $1,25(OH)_2D_3$ is an activator of various signal transduction pathways leading to the stimulation of protein kinase (PK)A/C, MAPK, and other protein kinases (Fleet, 2004). PMA-induced differentiation occurs via activation of the PKC signal transduction pathway component (García *et al*., 1999; Tsiftsoglou *et al*., 2003), which modulates the activity of the transcription factors like NF-κB, activating protein (AP)1-3 and Ets (García *et al*., 1999; Kim *et al*., 1998).

For proliferating cells to differentiate, DNA replication needs to be controlled. Cells entering DNA replication from a synthesis phase require cyclins, which assemble with CDKs (Martinez *et al*., 2006; Rots *et al*., 1999). CKIs inhibit cyclin-CDK activities in the different cell cycle phases, resulting in cell cycle arrest. $1,25(OH)_2D_3$ induces $p21^{Waf1/Cip1}$ and $p27^{Kip1}$ expression in U937 cells, which may cause cell cycle arrest during U937 cell differentiation to monocyte-macrophages. CDK levels stay constant throughout differentiation, but cyclins A, D, and E levels increase during the proliferation burst (short period of proliferation prior to differentiation), while $p21^{Waf1/Cip1}$ and $p27^{Kip1}$

levels increase during the proliferation burst and cell growth inhibition. An initial increase in proliferation followed by proliferation inhibition precedes differentiation and involves cyclin and CDK induction (Rots *et al*., 1999). Cell cycle arrest occurs in the G0/G1 phase prior to differentiation (Kim *et al*., 1998; Rots *et al*., 1999). PMA may cause differentiation in U937 cells by decreasing or inhibiting topoisomerase I and II activity. Topoisomerase activity may be regulated by phosphorylation via protein kinases (e.g. PKC) and AP-1-dependent genes (Pérez *et al*., 1994; Shayo *et al*., 1997).

This section focuses on the optimization of the concentration of PMA and $1,25(OH)_2D_3$, and exposure time required to differentiate U937 cells to monocyte-macrophages.

6.2.2. Materials and Methods

Human promonocytic leukemia U937 cells were seeded at 200 000 cells/well in 24-well plates in RPMI1640: 10% fbs. Cells were treated with PMA (Sigma) and $1,25(OH)_2D_3$ (Alexis Biochemicals, Lausen, Switzerland) at concentrations of 10, 50 and 100 nM and incubated in a humidified incubator at 37 °C and 5% CO_2 for 24, 48 and 72 hrs.

Phase contrast microscopy. After PMA and $1,25(OH)_2D_3$ treatment, cells were viewed under an Axiovert 40C inverted microscope with a Ph2-0.4 filter and 40x objective. Photos were taken with a PowerShot A640 digital camera.

Cell viability. After differentiation, cells were resuspended and transferred to polypropylene tubes. Accutase (300 µL; Sigma) was added to the wells treated with PMA and incubated for 15 min at 37 ºC. Cells were resuspended in PBS (500 µL) and transferred to the appropriate polypropylene tubes. Tubes were centrifuged at 300 x g for five min at room temperature and the supernatant discarded. Cells were washed with 1 mL PBS by centrifugation, as described above, to remove differentiation agents and Accutase. Cells were resuspended in 500 µL propidium iodide (PI; 50 µg/mL; Beckman Coulter) and incubated for 15 min at 37 ºC. Samples were analyzed using a Beckman

Coulter Cytomics FC500. Cells with intact plasma membranes will not take up the dye, whereas non-viable cells will stain positive with PI.

Cell surface marker staining. The procedure as for cell viability, prior to PI staining, was followed. Cells were resuspended and blocked in 500 µL blocking buffer (1% BSA and 1% foetal bovine serum in PBS) for 15 minutes at room temperature and centrifuged as described above. Cells were stained in the dark with 10 µL CD11b-FITC and 10 µL CD14- phycoerythrin cychrome 5 (PC5) for 30 min at room temperature, washed with PBS as described above and resuspended in PBS (500 µL). Samples were analyzed using a Beckman Coulter Cytomics FC500.

6.2.3. Results and Discussion

Phase contrast microscopy. U937 cells treated with PMA attached to the surface of the plate; hence treatment with Accutase was necessary to remove the attached cells. Monocyte-macrophages differentiated with PMA attached to the bottom of the wells, grew flat on the surface of the plate, formed clumps and had protruding pseudopodia (Figure 6.1). Monocyte-macrophages differentiated with $1,25(OH)_2D_3$ formed clumps with protruding pseudopodia (Figure 6.1).

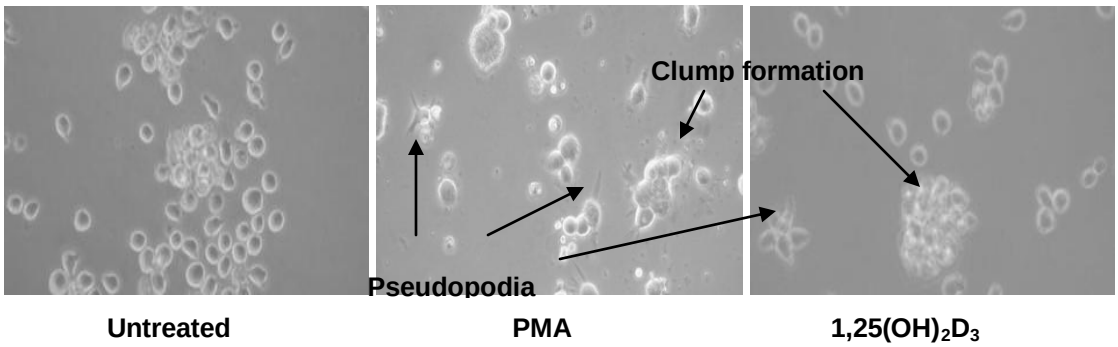

Figure 6.1: Phase contrast photographs of U937 cells differentiated to monocyte-macrophages. Photographs represent differentiated monocyte-macrophages that had been treated with 10 nM PMA or 10 nM $1,25(OH)_2D_3$ for 24 hrs.

The above results confirm the morphological characteristics (adherent cells, protruding pseudopodia and clump formation) associated with PMA differentiated U937 cells to

monocyte-macrophages seen by Barbieri *et al*. (2003). Kulseth *et al*. (1998) have also shown adherent and nonadherent monocyte-macrophages when U937 cells were differentiated with PMA, and $1,25(OH)_2D_3$ and retinoic acid, respectively. Macrophages, differentiated from monocytes, may become 'giant' like and multinucleated. Gradual spreading and flattening, membrane ruffling and extension as the nucleus to cytoplasm ratio increases are signs of differentiating monocyte-macrophages. Biochemical changes during monocyte-to-macrophage differentiation include an increase in acid phosphatase, β-glucosaminidase, and macrophage tissue transglutaminase activities, and expression of FcγR-, transferrin-, type I macrophage scavenger-, and mannose receptors (Huh *et al*., 1996). The spreading ability of macrophages is important for phagocytosis and the migratory process to the inflammatory site. Expression of inducible nitric oxide synthase (iNOS) and NO production require differentiation and activation of macrophages. Activated macrophages simultaneously release NO, superoxide (O_2^-) and its dismutation product, hydrogen peroxide (H_2O_2) (Cruz *et al*., 2007).

Cell viability following U937 differentiation with PMA or $1,25(OH)_2D_3$. Cell viability of PMA- and $1,25(OH)_2D_3$-differentiated U937 cells were determined using PI (Table 6.1).

Table 6.1: Percentage of viable U937 cells over time after differentiation to monocyte-macrophages with PMA and $1,25(OH)_2D_3$.

Time (hrs)	Percentage of viable U937 cells after differentiation							
	PMA				$1,25(OH)_2D_3$			
	control	10 nM	50 nM	100 nM	control	10 nM	50 nM	100 nM
24	75.6	51.6	46.1	47.5	75.6	78	80	80.1
48	76.8	40.9	42.4	42.6	76.8	81.2	81.6	82.4
72	NA*	NA	NA	NA	81.8	73	72	66.8

* NA = not analyzed

In general, PMA caused a reduction in cell viability with an increase in time and concentration. After 72 hrs, cell viability could not be determined for PMA differentiated U937 cells, due to shortage of viable cells to complete 10 000 events. Cell viability increased when U937 cells were differentiated with $1,25(OH)_2D_3$, which may be

explained by an increase in proliferation. This may be explained by a 'burst of rapid proliferation' before differentiation, which was concentration dependent and seen after 24 and 48 hrs of treatment. Brown *et al*. (2003) have also described a 'burst of rapid proliferation' preceding differentiation. Cell differentiation does not require cell division or DNA synthesis, and is initiated in the G1 phase, G1-S progression and S phase (Brown *et al*., 2003). Rots *et al*. (1999) have shown a burst of proliferation followed by growth inhibition and differentiation, when U937 cells were treated with $1,25(OH)_2D_3$. Cultures containing differentiated cells consist of a percentage of apoptotic cells. Several inducers cause apoptosis together with differentiation but the proportion of differentiated cells, in most cases, is much higher than apoptotic cells (Tsiftsoglou *et al*., 2003). Kulseth *et al*. (1998) have shown a decrease in viable U937 cells when exposed to PMA and retinoic acid (~30%) for three days, compared to $1,25(OH)_2D_3$ (~70%). Cell viability percentages obtained by Kulseth *et al*. (1998) correspond to the results obtained in this study.

Monocyte-macrophage cell surface marker expression after differentiation. Differentiated monocyte-macrophages were stained with anti-CD11b and CD14 labelled with FITC and PC5, respectively. Figures 6.2 and 6.3 represent overlaid histograms of expressed CD11b and CD14, when U937 cells were treated with PMA and $1,25(OH)_2D_3$, respectively. Monocyte to monocyte-macrophage differentiation is associated with increased surface expression of CD11b and CD14 (Brown *et al*., 2003).

U937 cells exposed to PMA for 24 hrs did not express significant amounts of CD11b and CD14. After 48 hrs >70% of U937 cells expressed CD11b and 35-40% of U937 cells expressed CD14. In general, higher PMA concentrations were associated with less CD11b expression, which may be due to PMA's toxicity to U937 cells (Table 6.1). After 72 hrs most of the U937 cells were killed.

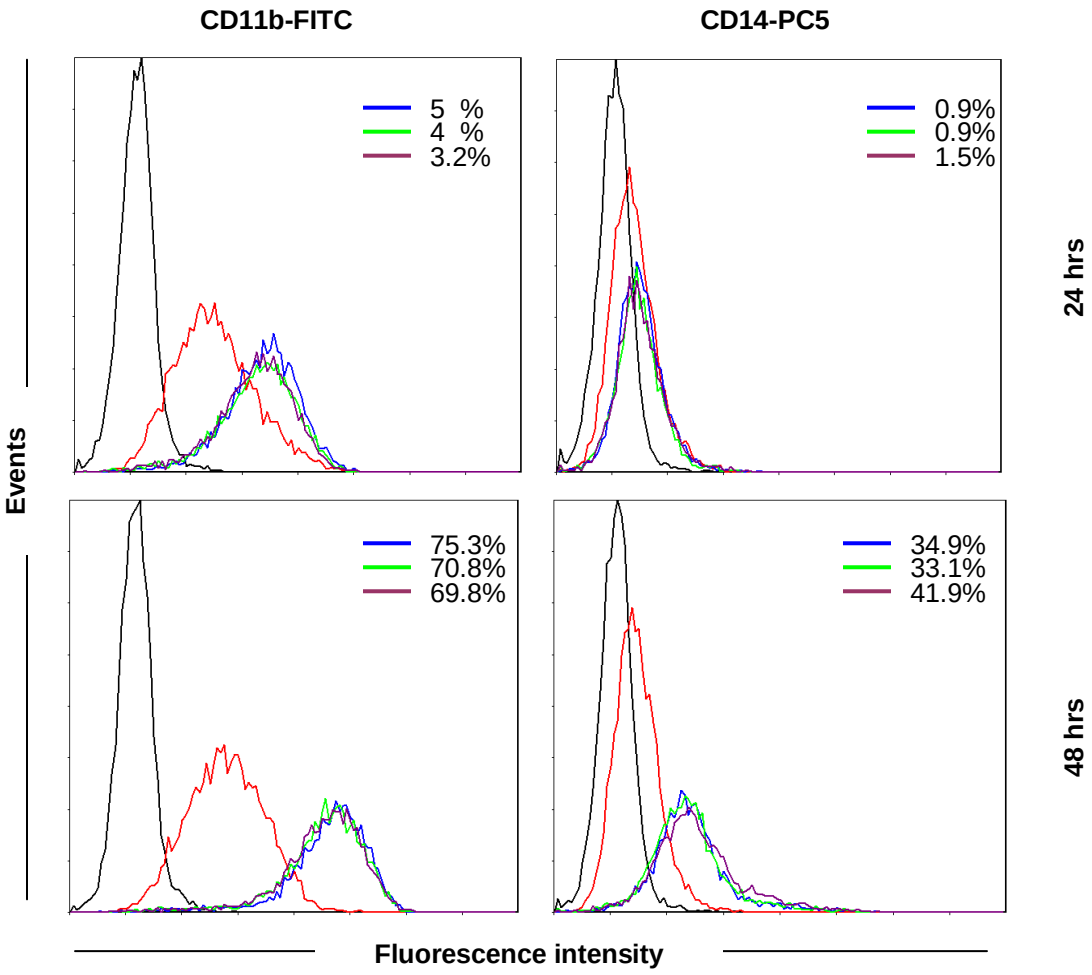

Figure 6.2: PMA differentiation of U937 cells to monocyte-macrophages. CD11b-FITC and CD14-PC5 were used as cell surface markers for differentiated monocyte-macrophages. Percentages represent the shift in PMA treated samples compared to the control, when a region was set from the end of the control peak. Black = unstained; red = DMSO control; blue = 10 nM PMA; green = 50 nM PMA; purple = 100 nM PMA. Representative of two experiments performed. 10 000 events were recorded.

Barbieri *et al*. (2003) have shown an increase in CD14 expression when U937 cells were differentiated with PMA. García *et al*. (1999) described an increase in the expression of the β2-integrin family (CD11a-c/CD18) in U937 cells during differentiation. They have shown that PMA differentiation of U937 cells was influenced by the nuclear transcription factors NF-κB, AP-1 and PU.1.

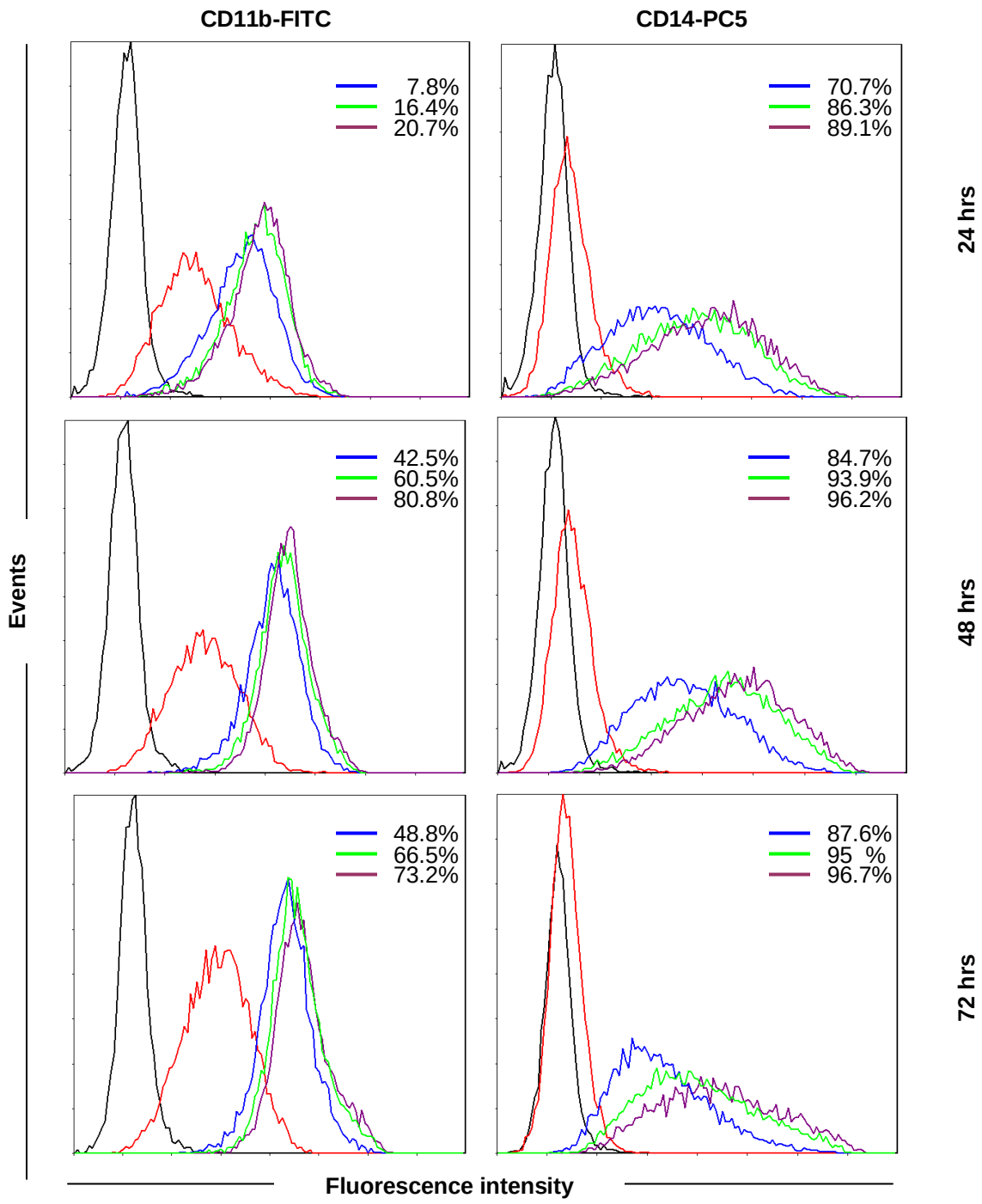

Figure 6.3: 1,25(OH)$_2$D$_3$ differentiation of U937 cells to monocyte-macrophages. CD11b-FITC and CD14-PC5 were used as cell surface markers for differentiated monocytes-macrophages. Percentages represent the shift in 1,25(OH)$_2$D$_3$ treated samples compared to the control, when a region was set from the end of the control peak. Black = unstained; red = DMSO control; blue = 10 nM 1,25(OH)$_2$D$_3$; green = 50 nM 1,25(OH)$_2$D$_3$; purple = 100 nM 1,25(OH)$_2$D$_3$. 10 000 events were recorded.

CD11b and CD14 cell surface marker expression during U937 cell differentiation with $1,25(OH)_2D_3$ was concentration- and time dependent. CD11b expression on monocyte-macrophages increased between 24 and 48 hrs [5.4, 3.7 and 3.9 times more with 10, 50 and 100 nM of $1,23(OH)_2D_3$, respectively, compared to the control] of treatment, but was similar between 48 and 72 hrs. CD14 expression on monocyte-macrophages increased after 24 hrs. Treatment with 10 nM and, 50 and 100 nM $1,25(OH)_2D_3$ expressed 70% and 85%, respectively, more CD14 compared to the control. After 48 and 72 hrs 10 nM and, 50 and 100 nM $1,25(OH)_2D_3$ expressed >80% and >90%, respectively, more CD14 compared to the control.

A previous study has shown that expression of CD14 mRNA, measured after 24 hrs, was only seen when exposed to $1,25(OH)_2D_3$, and not to PMA or retinoic acid. This was the case even after 72 hrs (Kulseth *et al*., 1998). Overproduction of $p21^{Waf1/Cip1}$ and $p27^{Kip1}$ induces CD11b and CD14 expression in U937 cells (Rots *et al*., 1999).

Differentiation of U937 cells to monocyte-macrophages following $1,25(OH)_2D_3$ treatment was confirmed with initial proliferation, increased CD11b and CD14 expression, clump and pseudopodia formation. $1,25(OH)_2D_3$ was the agent of choice for differentiation due to higher viability compared to PMA treatment. The time and $1,25(OH)_2D_3$ concentration chosen to differentiate U937 cells were 24 hrs and 100 nM, respectively. The main reason for choosing the shorter differentiation time period was based on higher cell viability.

6.3. Nitric Oxide Production

6.3.1. Background

Production of NO. NO is a diffusible, intercellular messenger molecule with the following characteristics:

- Colourless gas.

- Free radical due to odd number of electrons.
- Relatively unstable in the presence of oxygen.
- Very short half life (<15 s).
- Rapidly decomposes to form nitrogen oxides (collectively known as NO_x), which include nitrogen dioxide (NO_2), nitrites (NO_2^-), nitrates (NO_3^-) and dinitrogen trioxide (N_2O_3) (Bertholet *et al*., 1999; Clancy *et al*., 1998; Miller and Grisham, 1995; Tiscornia *et al*., 2009).

NO is produced when the amino acid L-arginine is catalytically oxidized to L-citrulline by nitric oxide synthase (NOS). At least three isoforms of NOS are found, namely constitutively expressed NOS in endothelial (eNOS) and neuronal (nNOS) cells, and inducible iNOS (Table 6.2) (Beck *et al*., 1999; Guzik *et al*., 2003; Tiscornia *et al*., 2009). These three NOS isoforms have similar molecular structures (~60 % homology), belong to the cytochrome P450 reductase-like family and require multiple co-substrates, which include nicotinamide adenine dinucleotide phosphate (NADPH), O_2, and co-factors [e.g. calmodulin, (6R)-tetrahydrobiopterin (BH_4), flavine adenine dinucleotide (FAD), flavin mononucleotide (FMN) and iron protoporphyrin (heme)] (Bertholet *et al*., 1999; Clancy *et al*., 1998; Guzik *et al*., 2003; Korhonen *et al*., 2005). Active NOS is a tetramer consisting of two NOS proteins and two molecules of the Ca^{2+} regulatory protein, calmodulin. nNOS and eNOS binding to calmodulin is stabilized with an increase in free intracellular Ca^{2+} levels, leading to NOS activation and NO production. Decrease in Ca^{2+} concentration is associated with a decrease in NO production. iNOS is regulated at transcriptional level (e.g. by NF-κB) and is independent of Ca^{2+} levels. Calmodulin binding to iNOS is tight, even at low Ca^{2+} concentrations (Guzik *et al*., 2003; Kim *et al*., 1998; Korhonen *et al*., 2005; Miller and Grisham, 1995). The main factors influencing NO production are cell type, calcium concentration, inducer, NOS source, time and NO's mechanism of action (Miller and Grisham, 1995; Tiscornia *et al*., 2009).

Table 6.2: Summary of the characteristics of the three NOS isoforms (Beck *et al*., 1999; Bertholet *et al*., 1999; Clancy *et al*., 1998; Guzik *et al*., 2003; Korhonen *et al*., 2005; Miller and Grisham, 1995; Nussler and Billiar, 1993).

Feature	eNOS	nNOS	iNOS
Calcium dependent/ independent	Dependent	Dependent	Independent
Mediators of NO production	Acetylcholine, thrombin, bradykinin, glutamate, shear force, ADP, VEGF***	Acetylcholine, thrombin, bradykinin, glutamate, insulin, NMDA****	Bacterial endotoxins (LPS, LTA**), peptidoglycan, dsDNA, RNA); pro-inflammatory cytokines (IFNα/β/γ, TNFα, IL-1β), hypoxia
Cell types/ tissue expression	Endothelial cells, cardiac myocytes, platelets, neurons	Neurons in the central/peripheral/ autonomous nervous system. Skeletal muscle, neutrophils, VSMC*, platelets, epithelial cells, pancreatic β cells	Most resting cells, Cardiac myocytes, glial cells, VSMC, endothelium, neurons, hepatocytes, VSMC, bone marrow cells, monocytes/macrophages, keratinocytes, β-cells, chondrocytes, synoviocytes, neutrophils
Synonyms	NOS III	NOS I	NOS II
Originally cloned from	Endothelial cells	Neuronal cells	Macrophages
Subcellular location	Golgi apparatus, plasmalemma, caveolae Mainly membrane bound	Cytosol, ER, sarcolemma, postsynaptic densities caveolae	Phagosomes
Availability	Constitutive	Constitutive	Induced

* VSMC = vascular smooth muscle cell
**LTA = lipoteichoic acid
***VEGF = vascular endothelial growth factor
****NMDA = N-methyl-D-aspartate

Induced iNOS expression is characterized by the production of large quantities (nano- to micromolar concentrations) of NO after a lag period of a few hours (6-8 hrs), which may be due to the synthesis of the enzyme and cofactors. NO production is sustained over a long period of time (few hours/days), depending on the enzyme's activity and may become cytotoxic to healthy cells, causing tissue damage. Constitutively expressed nNOS and eNOS are characterized by the production of small quantities (pico- to

nanomolar concentrations) of NO within a few seconds, which are short-lived with direct activities that maintain normal cellular functions (Figure 6.4). iNOS produces a 1000-fold more NO than eNOS/nNOS (Beck *et al*., 1999; Clancy *et al*., 1998; Guzik *et al*., 2003; Miller and Grisham, 1995; Nussler and Billiar, 1993; Tiscornia *et al*., 2009).

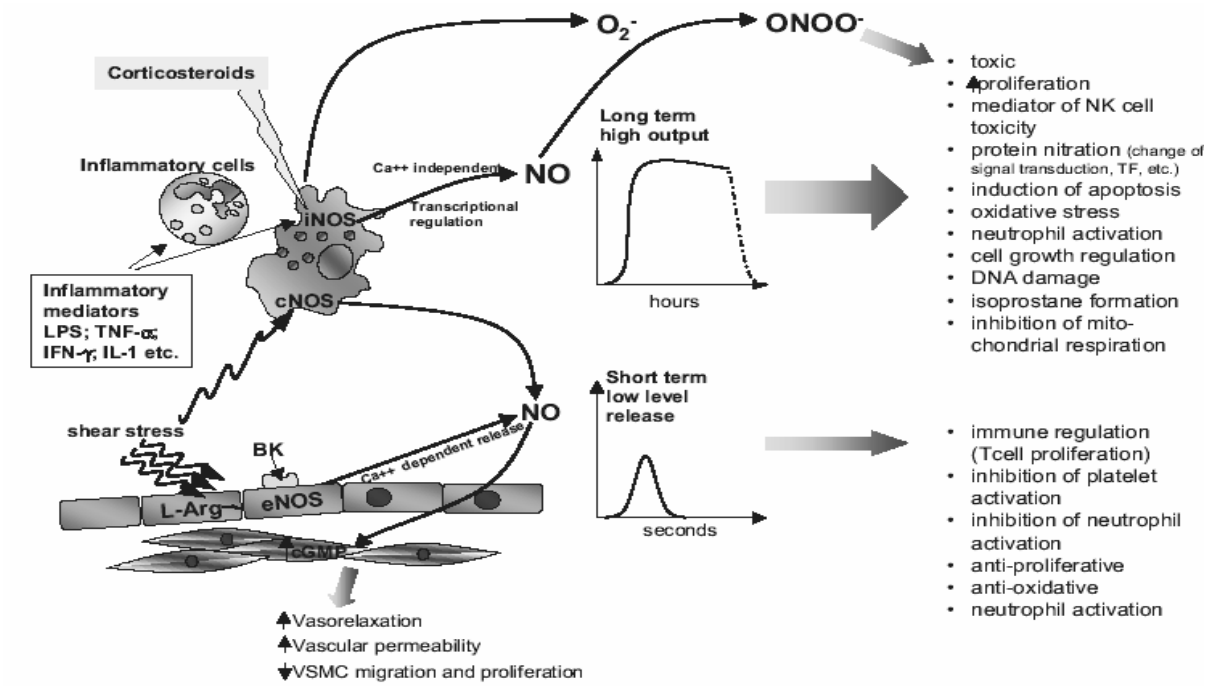

Figure 6.4: Diagram summarizing the characteristics and functions of NOS (Guzik *et al*., 2003).

Physiological or pathophysiological role of NO. NO plays an important role in host defense, immunity and inflammatory responses. Low levels of NO, produced by eNOS and nNOS, are involved in several physiological or pathophysiological roles including regulation of vascular endothelial homeostasis (e.g. vasorelaxation of the smooth muscle, vascular permeability and protection against the adhesion of leukocytes or platelets to blood vessel walls), normal cell signalling pathways, activating inflammatory transcription factors (e.g. AP-1 and NF-κB), bronchodilation, neurotransmission or neural activity in central or peripheral nervous system, nonspecific host defenses, circulation and blood pressure, immune regulation of T helper cell proliferation, cytokine production and macrophage-dependent killing of intracellular parasites (Clancy *et al*., 1998; Korhonen *et al*., 2005; Moilanen *et al*., 1997; Nussler and Billiar, 1993; Tiscornia *et al*.,

2009). The molecular mechanism involved in the physiological or pathophysiological functions of NO are directly associated with NO formed by eNOS and nNOS. NO regulates enzyme activity by reacting with transition metals (e.g. iron, copper, zinc) present in enzymes and other proteins. NO targets the ferrous iron group of soluble guanylate cyclase (sGC), which converts guanosine triphosphate (GTP) to the intracellular signalling molecule cyclic guanosine monophosphate (cGMP), which in turn targets cGMP dependent protein kinases involved in the above-mentioned functions (Beck *et al*., 1999; Guzik *et al*., 2003; Korhonen *et al*., 2005; Nussler and Billiar, 1993).

NO and inflammation. During inflammation, a large amount of NO is produced by iNOS, surpassing the physiological amounts produced by nNOS and eNOS (Guzik *et al*., 2003). NO is a poor reactive free radical and is rapidly oxidized to more active radicals including peroxinitrite ($ONOO^-$), nitrogen dioxide (N_2O_2) and others (Miller and Grisham, 1995; Tiscornia *et al*., 2009). In general, the absence or presence of iNOS induced NO production is associated with anti- or pro-inflammatory activities, respectively. This viewpoint is controversial and is not the case during infection where NO produced by iNOS is important to kill invading microorganisms. Inhibition of NO formation may promote growth and spread of infection resulting in increased tissue damage (Miller and Grisham, 1995). Two indirect mechanisms of action are associated with iNOS expressed NO production. Firstly, the formation of *S*-nitrosothiols (*S*-nitrosylation), which modify the activity of several proteins including transcription factors, kinases involved in signalling pathways, caspases, ion channels and metabolic proteins. NO reacts with molecular oxygen (O_2) in aqueous solutions to form N_2O_3, which rapidly decomposes to nitrite and the nitrosonium ion (NO^+). The latter is responsible for nitrosylation (Beck *et al*., 1999; Korhonen *et al*., 2005; Miller and Grisham, 1995). Secondly, NO together with O_2^- form $ONOO^-$, which targets proteins, lipids and nucleic acids important for cell survival and cell signalling. It mediates cytotoxic effects including DNA damage, LDL oxidation, isoprostane formation, tyrosine nitration, inhibition of enzymes involved in the citric acid cycle and mitochondrial electron transport chain, and apoptosis (Clancy *et al*., 1998; Guzik *et al*., 2003; Korhonen *et al*., 2005; Miller and Grisham, 1995). The role of NO as an anti- or pro-inflammatory,

however, depends on time, constitutive or induced NOS involved in NO production, cellular source of NO production, amount of NO produced, NO targets and generation of other reactive nitrogen species from NO (Clancy *et al*., 1998; Miller and Grisham, 1995).

Diseases associated with overproduction (toxic levels) of NO. Many inflammatory diseases are associated with the overproduction of NO, including rheumatic diseases [e.g. systemic lupus erythematosus (SLE), osteoarthritis, vasculitis, Sjögren syndrome, rheumatoid arthritis], ischaemic heart disease, heart failure, circulatory shock, stroke, neurodegenerative disorders and endothelial dysfunction. It is proposed that NO may be involved in the pathogenesis of autoimmune diseases (Clancy *et al*., 1998; Tiscornia *et al*., 2009). NO overproduction by activated macrophages can injure hepatocytes, pancreatic islet cells and lymphocytes via intracellular iron release, inhibition of mitochondrial function [aconitase (citric acid cycle), NADPH/succinate-ubiquinone oxidoreductase (mitochondrial respiratory chain)] and inhibition of DNA synthesis (ribonucleotide reductase) (Miller and Grisham, 1995; Nussler and Billiar, 1993).

Inhibition of iNOS. Drugs targeting NOS and NO bioavailability can be used to treat inflammatory diseases. NO is scavenged by haemoglobin, methylene blue, pyocyanin (*Pseudomonas coereleus*), glucocorticoids, arginine analogues (including L-NMMA, L-NAME), flavonoids, NO gas inhalation, leptin, statin therapy, NO donors, peroxisome proliferator-activated receptor (PPAR)γ activators, antioxidants, and non-steroidal anti-inflammatory drug (NSAIDs; e.g. aspirin) (Guzik *et al*., 2003). Many physiological or synthetic agents inhibit cytokine-induced iNOS at transcriptional level. iNOS expression can be prevented by binding and activation of NF-κB by cyclosporin A, dexamethasone and dithiocarbamates (Beck *et al*., 1999). iNOS induction can be inhibited by glucocorticosteroids, and cytokines [e.g. transforming growth factor (TGF)-β, IL-4, IL-8 and IL-10] (Clancy *et al*., 1998; Guzik *et al*., 2003; Nussler and Billiar, 1993). Constitutively expressed NOS (cNOS) and iNOS are inhibited by substrate analogs, flavoprotein and heme binders, whereas calmodulin inhibitors inhibit cNOS (Nussler and Billiar, 1993).

NO and cancer. NO has anti- and pro-apoptotic functions in cells. Large quantities of NO present over a long period of time have pro-apoptotic effects by (i) directly targeting the mitochondria causing loss in mitochondrial membrane potential and increased cytochrome c release. NO binds cytochrome c oxidase in the mitochondrial electron transport chain, leading to increased O_2^- production, which interacts with NO to form $ONOO^-$. The latter induces mitochondrial dysfunction and cytochrome c release; (ii) inducing p53 expression and accumulation, resulting in cell cycle arrest due to $p21^{Waf1/Cip1}$ upregulation or apoptosis due to increased Bax expression and cytochrome c release; (iii) activating JNK/stress-activated protein kinase (SAPK) group of MAPK and caspase-3 activation; (iv) increasing ceramide production due to increased sphingomyelinase activity. Ceramide activates cytochrome c release, JNK/SAPK activation, suppression of Bcl-2 expression and PKB/Akt inhibition (Brüne *et al*., 1998; Choi *et al*., 2001; Chung *et al*., 2001).

Low or physiological NO production protects cells against pro-apoptotic stimuli, including TNFα, oxidative stress and serum or glucose deprivation, and have anti-apoptotic effects by (i) increasing cGMP production, which suppress cytochrome c release and ceramide production, and increase Bcl-2 expression and PKB/Akt activation; (ii) inhibiting caspase *S*-nitrosylation; (iii) regulating anti-apoptotic related gene expression e.g. heat shock protein (HSP)70/32 and anti-apoptotic Bcl-2 family members (Brüne *et al*., 1998; Choi *et al*., 2001; Chung *et al*., 2001).

NO has physiological and pathophysiological activities, which play an important role in health and disease states. Since NO plays a key role in inflammation and previous studies have shown anti-inflammatory activity of *Hypoxis*, the NO production of monocyte-macrophages when treated with *Hypoxis* extracts and its purified compounds was investigated in this section.

6.3.2. Materials and Methods

Human promonocytic leukemia U937 cells were counted, resuspended in RPMI1640: 10% fbs (complete medium), and differentiated with 100 nM $1,25(OH)_2D_3$ for 24 hrs in a humidified incubator at 37 °C and 5% CO_2. Cells were investigated for clump- and pseudopodia formation, which are morphological characteristics of monocyte-macrophages. Differentiating agent was removed by centrifugation at 250 x g for five min at room temperature, medium discarded, cells washed with 1 mL complete medium as described in section 6.2.2 and resuspended in complete medium at cell densities of $1x10^6$ cells/mL. Cells were uniformly stained by adding 5,6-diaminofluorescein diacetate (DAF-2 DA; 1 μg/mL). Cells were mixed, covered with foil and incubated for 30 min at 37 ºC. Excess DAF-2-DA was removed and cells washed twice as described above. Fifty thousand cells were added to polypropylene tubes and treated with DMSO (0.25%, v/v) as vehicle control, *H. hemerocallidea* (125 μg/mL), *H. stellipilis* (125 μg/mL), *H. sobolifera* (125 μg/mL), hypoxoside (50 μg/mL), rooperol (20 μg/mL), CD (4mM)/EtOH (5%, v/v), β-sitosterol (30 μM), campesterol (30 μM), cholesterol (30 μM), stigmasterol (30 μM) or PMA (10 or 20 nM) for six hours at 37 °C. After treatment, cells were pelleted and washed with PBS as described above. Cells were resuspended in PBS (500 μL) and samples read on a Beckman Coulter FC500 flow cytometer. Mean fluorescence intensity (MFI) of treated cells was expressed as a percentage of the MFI of control cells. Statistical significance was determined using the two-tailed Student's t-test.

6.3.3. Results and Discussion

Intracellular NO was measured by loading the cells with the membrane permeable derivative 5,6-diaminofluorescein diacetate (DAF-2 DA), which is transformed to 5,6-diaminofluorescein (DAF-2) by non-specific cytosolic esterases. Inside the cells, DAF-2 reacts directly with N_2O_3, which is produced by a second order reaction of NOS with oxygen under aerobic conditions, to form the highly green-fluorescent derivative triazolofluorescein (DAF-2 T) (Tiscornia *et al.*, 2009). NO production was measured after six hours of treatment of differentiated monocyte-macrophages (Figure 6.5).

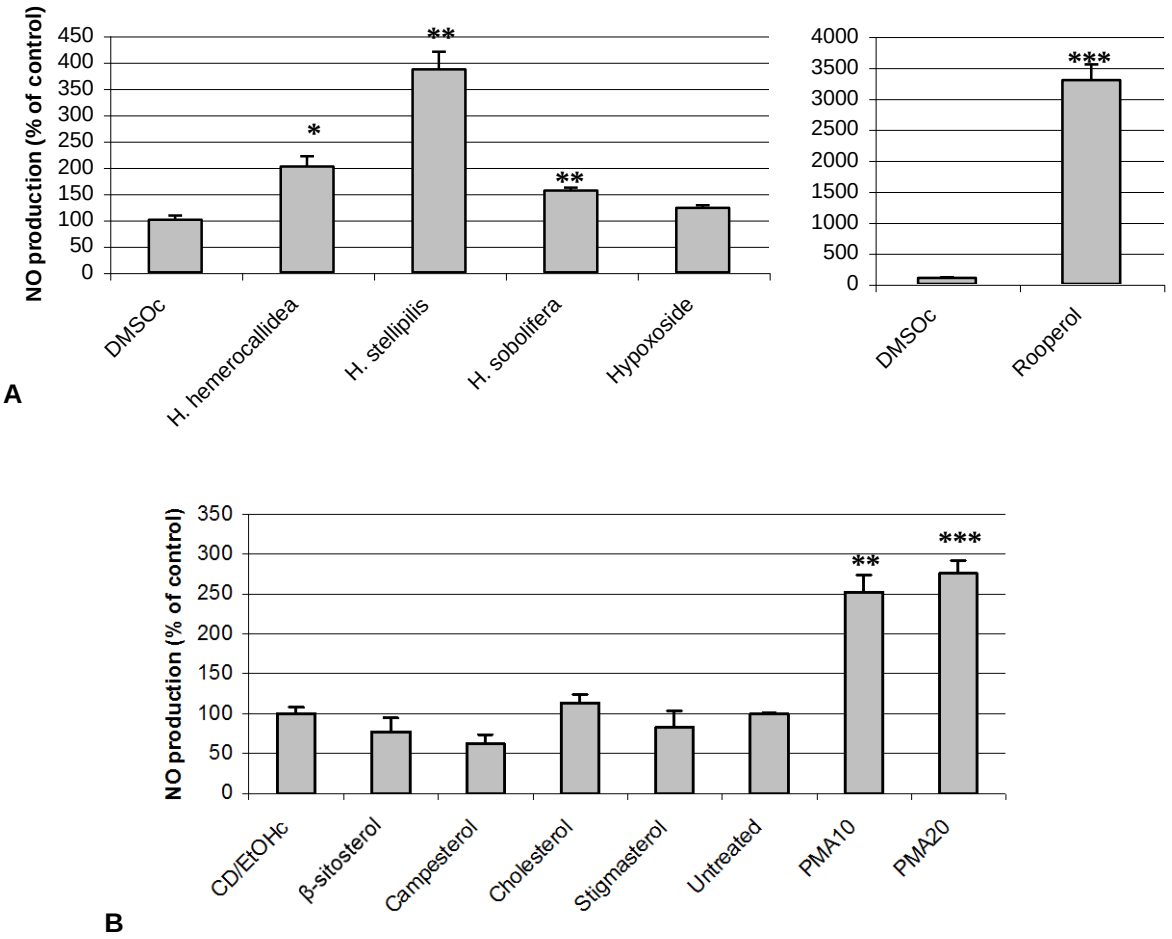

Figure 6.5: NO production by monocyte-macrophages in response to DMSO, *Hypoxis* chloroform extracts, hypoxoside and rooperol (A), CD/EtOH, (phyto)sterols and PMA (B) treatment. The y-axis of NO production in response to rooperol is ten times greater than NO production in response to Hypoxis chloroform extracts and hypoxoside treatment. Bar graph percentages represent the increase in mean fluorescence intensity of cells staining positive for NO production when treated samples were compared to control. Error bars represent the SD of triplicate values. One representative of three experiments performed. Significance was determined using the two-tailed Student t-test: *p<0.01; **p<0.001; ***p<0.0001 compared to control.

Significant amounts of NO were produced when monocyte-macrophages were treated with the three *Hypoxis* extracts, rooperol and PMA. When compared to the controls, *H. hemerocallidea*, *H. stellipilis*, *H. sobolifera*, rooperol and PMA (10 nM) produced 2.0, 3.9, 1.6, 32.9 and 2.5 times more NO, respectively. NO production by hypoxoside and cholesterol was not significantly different from the control, with only a 1.2 and 1.1 fold increase, respectively. β-sitosterol, campesterol and stigmasterol had no effect on NO production. Overlaid histograms of the treatments increasing NO production

significantly are summarized in Appendix 6. Wallerath *et al*. (2002) have shown that β-sitosterol and stigmasterol, found in red wine, do not contribute significantly to eNOS upregulation.

This is the first time that the effect of *Hypoxis* extracts and its purified compounds were tested for NO production on monocyte-macrophages. NO production within 6 hrs suggests the expression of iNOS in human monocyte-macrophages. Kim *et al*. (1998) have found that very little NO was produced when U937 cells were differentiated with 32 nM PMA, which confirm the choice of $1,25(OH)_2D_3$ as differentiating agent.

6.4. Cyclooxygenase-2

6.4.1. Background

Two isoforms of COX are found, namely constitutively expressed COX-1 and inducible COX-2 (Barbieri *et al*., 2003). COX-1 and -2 have similar structures (60% homology) and catalyze the conversion of AA to PGH_2, but are encoded by two genes located on different chromosomes. COX-1 is involved in housekeeping functions and produce PGs, which mediate physiological functions. These include gastric mucosa and nephron maintenance and cytoprotection, renal blood flow regulation and platelet aggregation (DuBois *et al*., 1998; Gasparini *et al*., 2003; Morita, 2002; Rocca and FitzGerald, 2002). COX-1 mRNA and protein levels are relatively stable in many cells and tissues. COX-1 induction has, however, been seen in THP-1 and megakaryocytes treated with phorbol esters; endothelial cells treated with shear stress/VEGF; lung fibroblasts treated with TGFβ; and synovial cells treated with IL-1α (Morita, 2002; Rocca and FitzGerald, 2002).

COX-2 is expressed in inflamed (macrophages, synoviocytes, fibroblasts, osteoblasts, tumour cells and endothelial cells) and neoplastic (hyperproliferation, transformation, tumour growth, invasion and metastasis) tissues (Gasparini *et al*., 2003). COX-2 is almost undetectable under resting conditions, but is induced by pro-inflammatory cytokines (e.g. IL-1α/β, IL-6, IL-8, IL-11, TNF-α, IFNγ), growth factors [e.g. serum,

fibroblast growth factor (FGF) a and b, insulin, IGF, VEGF, epidermal growth factor (EGF), PDGF, TGFβ], phorbol esters, lipopolysaccharide (LPS), NO, PGE_2, hypoxia and hormones (DuBois *et al*., 1998; Gasparini *et al*., 2003; Morita, 2002; Rocca and FitzGerald, 2002). COX-2 produces PGs, which are involved in pain, inflammation and fever (Nelson and Cox, 2000). COX-1 mRNA, protein and activity are unchanged during inflammation, but COX-2 expression increases significantly resulting in increased PG production (Morita, 2002).

COX-1 and -2 catalyze the production of different PGs, for example COX-1 and -2 expression in rat peritoneal macrophages (induced by LPS) and human umbilical vein endothelial cells (HUVECs; induced by IL-1β) favour TXA_2 and PGE_2/PGI_2 production, respectively. PGI_2 and TXB_2 maintain vascular homeostasis. The former is a vasodilator and platelet aggregation inhibitor synthesized by the vascular endothelium, while the latter is a vasoconstrictor and platelet aggregation promoter synthesized by platelets. An imbalance between PGI_2 and TXB_2 is associated with thrombotic and cardiovascular disorders. The ratio of PGI_2/TXB_2 produced is not fixed and differs according to the COX isoform activated. Induction of COX-2 has been associated with the production of harmful prostanoids due to COX-2 involvement in inflammatory disorders like rheumatoid arthritis and osteoarthritis (Caughey *et al*., 2001; Morita, 2002).

COX-2 and cancer. COX-2 is overexpressed in breast, colorectal, gastric, lung, pancreatic, head and neck, oesophageal, urinary bladder, ovarian, cervical and prostate cancer. Overexpressed COX-2 may promote carcinogenesis by increasing proliferation, transformation, invasion, metastasis, angiogenesis, differentiation, metaplasia, hyperplasia, dysplasia, immunosuppression, cellular motility and apoptosis resistance (Chun and Surh, 2004; Gasparini *et al*., 2003; Sheng *et al*., 2001; Shigemasa *et al*., 2003; Spizzo *et al*., 2003). Apoptosis resistance includes reduced levels of pro-apoptotic proteins (e.g. Bax), and increased levels of anti-apoptotic proteins (e.g. Bcl-2) in mammary tumours (Half *et al*., 2002). Higher COX-2 levels may be due to expression by carcinoma cells themselves or infiltrating macrophages within the tumours (Zha *et al*., 2004). Many human malignancies produce more PGs than normal tissues from which

they arise. COX-2 is overexpressed due to increased transcription and enhanced mRNA stability (Chun and Surh, 2004; Kojima *et al*., 2001). Increased COX-2 levels are associated with increased PG synthesis, especially PGE_2, which suppresses immunosurveillance by downregulating B- and T lymphocyte proliferation, NK cell cytotoxic activity, and TNFα and IL-10 secretion (Gasparini *et al*., 2003; Kojima *et al*., 2001). PGE_2 released by macrophages inhibits the production of Th1 type cytokines (e.g. IL-2, IFNγ) and increase the production of Th2 type cytokines (e.g. IL-4, IL-5) in human lymphocytes. Cytokines stimulating COX-2 expression include IL-1α/β, TNF-α and TGF-β, whereas IL-4, IL-10 and IFNγ downregulate COX-2 expression and PG production (Barrios-Rodiles and Chadee, 1998). Sheng *et al*. (2001) have shown that PGE_2 increases proliferation, motility and morphogenesis in LS-174 human colorectal carcinoma cells, by activating the PI-3K/PKB pathway, involved in cell survival (Chapter 5, section 5.2).

COX-2 expression is suppressed by anti-inflammatory cytokines (e.g. IL-4, IL-10, IL-13), glucocorticoids, aspirin, coxibs (e.g. celecoxib, rofecoxib, etorixoxib) and NSAIDs (e.g. sulindac sulfide, indomethacin, piroxicam); hence inhibiting PG production (Barnes, 1998; DuBois *et al*., 1998; Morita, 2002; Rocca and FitzGerald, 2002). These inhibitors of COX induce apoptosis by increasing AA concentration, leading to the stimulation of sphingomyelinase activity, which converts sphingomyelin to pro-apoptotic ceramide. Ceramide also inhibits the survival characteristics of carcinomas overexpressing COX-2 as described above. Coxibs together with chemotherapy treatment are more effective and increase apoptosis. Possible synergistic and additive effects between coxibs and conventional anticancer treatments exist and minimize chemotherapeutic agents' side effects like mucositis, diarrhoea, chronic pain, fever and other inflammatory toxic effects (Chan *et al*., 1998; Gasparini *et al*., 2003).

A 30-50% decrease in adenomatous polyps, disease incidence and mortality from colorectal cancer were seen with the regular and prolonged use of aspirin and NSAIDs. Sulindac and celecoxib suppress adenomatous polyps and regression of existing familial adenomatous polyposis (DuBois *et al*., 1998; Gasparini *et al*., 2003; Half *et al*., 2002;

Kojima *et al*., 2001; Sheng *et al*., 2001; Tsujii *et al*., 1997). Side effects of NSAIDs include duodenal erosion, gastrointestinal ulcers or -bleeding, platelet dysfunction and normal renal function disruption, which may be due to suppression of COX-1 derived PG production. Inhibition of COX-2 dependent PG synthesis by COX-2 inhibitors may prevent the side effects associated with NSAIDs (Chun and Surh, 2004; DuBois *et al*., 1998; Nelson and Cox, 2000).

Cross-talk between COX and NOS. Similarities existing between NOS and COX include: (i) COX and NOS are involved in the biosynthesis of PGs, thromboxanes and prostacyclin, and NO, respectively; (ii) constitutive (COX-1, nNOS and eNOS) and inducible (COX-2 and iNOS) isoforms exist; (iii) COX-2 and iNOS are induced by similar agents, including LPS and IL-1β; (iv) anti-inflammatory steroids (e.g. dexamethasone) inhibit the induction of iNOS and COX-2, but had no effect on constitutive expressed isoforms (Clancy *et al*., 2000; Salvemini *et al*., 1993).

NOS and COX cross-talk may be via (i) direct oxidation of the iron-heme center at the active site of COX by NO (Gasparini *et al*., 2003; Salvemini *et al*., 1993). Most of NO effects are mediated via interaction with iron or iron containing enzymes. NO binds the heme-iron prosthetic group of sGC leading to its stimulation and increased cGMP production, which is involved in platelet aggregation inhibition and vascular smooth muscle relaxation. NO effects on iron-containing enzyme activity may be stimulatory (e.g. sGC) or inhibitory (e.g. aconitase) (Salvemini *et al*., 1993); (ii) indirectly through $ONOO^-$ formation leading to increased lipid peroxidation (Gasparini *et al*., 2003). COX activity can produce O_2^- anion, which will react with NO to form $ONOO^-$. $ONOO^-$ may modulate eicosanoid synthesis by COX-2 activation and prostacyclin synthase inactivation (Baker *et al*., 1999).

Controversy exists whether NO activates or inhibits PG synthesis. Clancy *et al*. (2000) have shown that NO activates COX-1, but inhibits COX-2 derived PG production. Inhibition of PG production by NO is associated with a decrease in COX-2 expression and enzyme nitration. Nitration involves the conversion of tyrosine to nitrotyrosine by

NO, which will inhibit the catalytic activity of the enzyme. NO also inhibits COX-2 translocation to a cytosolic compartment, which favours enzyme activity. COX-2 is more sensitive to nitration than COX-1 (Clancy *et al*., 2000). Salvenini *et al*. (1993) have shown that endogenous and exogenous NO plays a role in PGE_2 release by directly activating COX in the mouse macrophage cell line RAW264.7. Where NO and COX pathways are co-expressed in pathological conditions (e.g. rheumatoid arthritis, sepsis, nephrosis), regulation of COX activity by NO may be an important mechanism to amplify or suppress the initial inflammatory response, which may be of therapeutic importance. NO, PGI_2 and PGE_2 release increase cGMP and cyclic adenosine monophosphate (cAMP) levels in effector cells, which may have synergistic roles in amplifying the physiological and pathological response (Salvemini *et al*., 1993).

COX-1, eNOS and their products are protective against atherosclerosis due to platelet aggregation inhibition and smooth muscle proliferation, while COX-2, iNOS and their products are involved in the pathogenesis of inflammatory disorders. The amount and rapidity of NO and PG production determine the damage caused. Large amounts of NO cause further inflammation, cellular damage and apoptosis (Baker *et al*., 1999).

COX-2 plays an important role in the production of prostaglandins, which are involved in inflammation. This section focuses on the COX-2 expression in monocyte-macrophages when treated with *Hypoxis* extracts and its purified compounds.

6.4.2. Materials and Methods

Human promonocytic leukemia U937 cells were differentiated with 100 nM $1,25(OH)_2D_3$ as described in section 6.3.2. Cells were investigated for clump- and pseudopodia formation, as before. Differentiating agent was removed by centrifugation at 250 x g for five min at room temperature, medium discarded, cells washed with 1 mL RPMI1640: 10% fbs (complete medium) by centrifugation as described above and resuspended in complete medium. Fifty thousand cells were added to polypropylene tubes and treated with DMSO (0.25%, v/v), *H. hemerocallidea* (125 µg/mL), *H. stellipilis* (125 µg/mL), *H.*

sobolifera (125 μg/mL), hypoxoside (50 μg/mL), rooperol (20 μg/mL), CD (4mM)/EtOH (5%, v/v), β-sitosterol (30 μM), campesterol (30 μM), cholesterol (30 μM) or stigmasterol (30 μM) in the presence of 250 ng/mL LPS for six hrs at 37 °C in the dark. After treatment, cells were collected by centrifugation as described above, supernatant discarded and fixed with 500 μL of 4% (v/v) formaldehyde (diluted in PBS) for 10 min at 37 °C. After fixation, cells were chilled on ice for one minute, centrifuged and washed as above to remove the fixative. Cells were resuspended in ice-cold 90% (v/v) MeOH (500 μL) and permeabilized for 30 min on ice. MeOH was removed by centrifuging and washed twice in incubation buffer (0.5% BSA in PBS) as described above. Cells were resuspended in 100 μL incubation buffer and blocked for 10 min at room temperature. COX-2 primary antibody (Cell Signaling Technology Inc.) was added at recommended working dilutions to the cells and incubated for one hour at room temperature. Cells were washed twice as described above. After washing, FITC conjugated goat anti-rabbit IgG (H+L chain specific) was added at recommended working dilutions. Cells were incubated in the dark for a further 30 min at room temperature and washed as described above. Cells were resuspended in PBS (500 μL) and read on a Beckman Coulter Cytomics FC500.

6.4.3. Results and Discussion

Monocyte-macrophages were simultaneously stimulated for COX-2 production with LPS when treated with *Hypoxis* extracts and its purified compounds. From the histograms in Figure 6.6, a shift of the main peak to the left or to the right represents decreased or increased COX-2 expression, respectively.

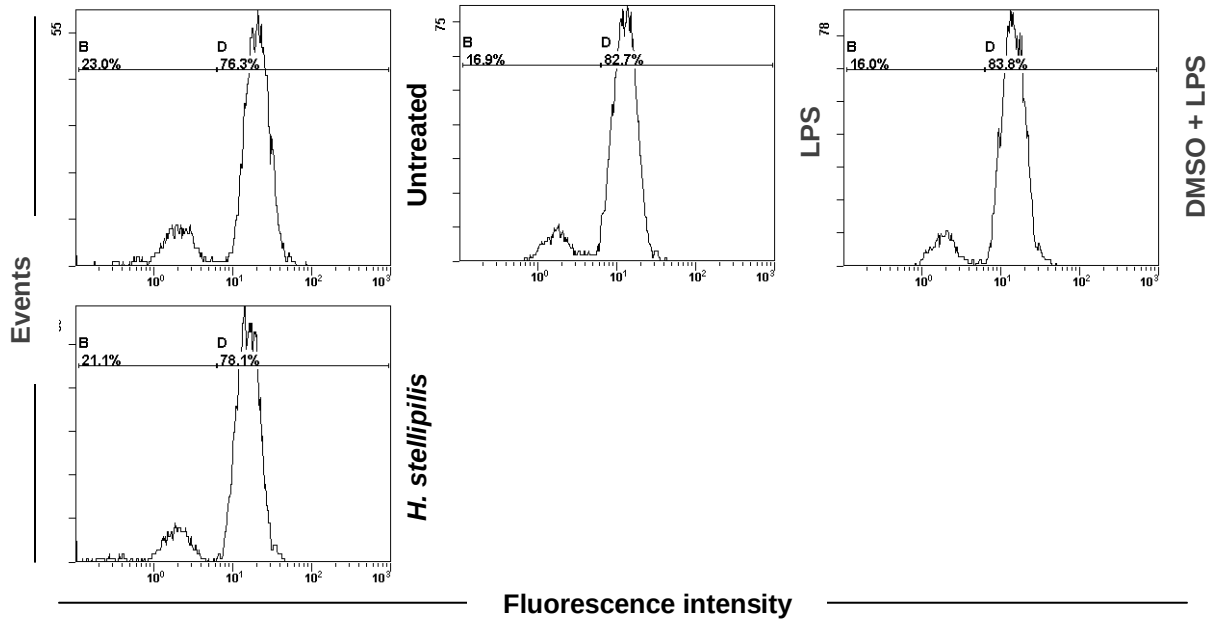

Figure 6.6: Histograms of COX-2 expression in monocyte-macrophages after six hrs of treatment with *Hypoxis* extracts and its purified compounds in the presence of LPS (250 ng/mL). Percentages in region D on histograms represent the change in COX-2 levels. 10 000 events were recorded.

From the above (and Appendix 6) results, no increase or decrease in COX-2 levels were seen, when treated with *Hypoxis* extracts and its purified compounds. The two peaks may represent two populations of COX-2, with peak B representing cells expressing low levels of COX-2 and peak D representing cells expressing high levels of COX-2. A small increase in COX-2 expression (peak D) was seen when monocyte-macrophages were treated with LPS compared to untreated control. A small decrease in COX-2 expression (peak D) was seen when monocyte-macrophages were treated with *H. stellipilis* when compared to the DMSO control. Due to the small peak shift the experiment was not repeated, hence statistical analysis was not performed. *Hypoxis* extracts and its purified compounds may not affect COX-2 expression, but rather its activity. Laporta *et al*. (2007a) have shown that rooperol was more effective in inhibiting the activity of COX-2 than COX-1. *Hypoxis* and its purified compounds may affect different parts of the inflammation pathway. Van der Merwe *et al*. (1993) have shown that rooperol was more effective in inhibiting LT synthesis in polymorphonuclear leukocytes, than prostaglandins synthesis (TXB_2, PGD_2, $PGF_{2\alpha}$) in platelet microsomes.

COX-2 is absent in undifferentiated U937 cells (Barbieri *et al*., 2003); hence the importance of differentiation to investigate COX-2 levels. Several factors may have contributed to the unsuccessful increase or decrease of COX-2 expression. These include the agent, stimulant, time period and cell type used during differentiation. As mentioned earlier, specific agents differentiate leukemic cells into specific progeny (section 6.2.1). U937 cells were differentiated to monocyte-macrophages by $1,25(OH)_2D_3$, which may have given rise to the wrong progeny of cells to investigate COX-2. Kulseth *et al*. (1998) described the differentiation of U937 cells into macrophage-like cells involved in secretion and phagocytosis when treated with PMA and $1,25(OH)_2D_3$, respectively. Monocyte-macrophages were only stimulated for six hours, which may be too short to see an increase in COX-2 production. Grkovich *et al*. (2006) have shown that COX-2 production was upregulated when U937 cells were differentiated to monocyte-macrophages with 100 nM PMA for 48 hrs, and stimulated with 1 μg/mL LPS for 2-20 hrs. Monocyte differentiation to monocyte-macrophages with PMA (100 nM) caused a high percentage of cell death (Table 6.1); hence PMA was not used as differentiating agent. Lower LPS concentration (250 ng/mL) was used to prevent toxicity. Schuette and LaPointe (2000) have shown that COX-2 production increases with time (max at 20 hrs). Pro-inflammatory cytokines (e.g. IL-1β, IL-2 and TNF-α) and growth factors (e.g. EGF, PDGF) stimulate COX-2 expression in macrophages (Huang *et al*., 2000; Zha *et al*., 2004). To eliminate the uncertainty of which differentiating agent to use, another cell line that does not need to be differentiated e.g. murine $P388D_1$ (Grkovich *et al*., 2006) or RAW 264.7 cells can be used in the future.

The solvent used to prepare *Hypoxis* extracts may play an important role in active compound isolation. EtOH and water extracts of *H. hemerocallidea* had a greater effect on the inhibition of PG production (Jäger *et al*., 1996). Steenkamp *et al*. (2006) have also shown that EtOH extracts of *H. hemerocallidea* had higher inhibitory effects on the activity of COX-1 and COX-2, compared to water extracts.

Awad *et al*. (2005b) have shown that β-sitosterol (16 μM) increases PGE_2 and PGI_2 levels, and $cPLA_2$ and COX-2 expression in PC-3 human prostate cancer cells. Awad *et al*. (2001b) have also shown that β-sitosterol and campesterol (16 μM) increase PGI_2 release in VSMCs. In contradiction, Awad *et al*. (2004) have shown that β-sitosterol and campesterol decrease PGE_2 and PGI_2 secretion in LPS-stimulated $P388D_1$/MAB macrophages, with no significant effect on $cPLA_2$ and COX-2 expression. The mechanism of increased or decreased PG production by phytosterols is unclear, but phytosterols may influence the membrane fluidity when incorporated into membranes, which may influence membrane bound enzyme activities involved in AA release and PG production (Awad *et al*., 2001b; Awad *et al*., 2004). The opposing effects on PG release seen in PC-3 cells and VSMCs compared to $P388D_1$/MAB macrophages may have been influenced by the nature of the PG pathway stimuli and cell type (Awad *et al*., 2005b). β-sitosterol was the main phytosterol present in the *Hypoxis* chloroform extracts used in this study, but concentrations were lower (1.77, 0.61 and 4.50 μM in *H. hemerocallidea*, *H. stellipilis* and *H. sobolifera*, respectively) than the 16 μM used by Awad and co-workers.

6.5. Phagocytosis

6.5.1. Background

The human immune system is divided into innate (natural) and adaptive (acquired) immunity (Dale *et al*., 2008; Rocca and FitzGerald, 2002). The innate immune system detects pathogens and apoptotic cells via specific receptors and responds by activating immune competent (phagocytic) cells, synthesizing cytokines and chemokines, and releasing inflammatory mediators. The major phagocytic cells include monocytes, macrophages, NK cells, polymorphonuclear cells, and mast cells (Nair *et al*., 2004). The innate immune response is the first line of antimicrobial host defense and impacts the adaptive immune response.

Monocytes are derived from $CD34^+$ myeloid progenitor cells in the bone marrow and differentiate into monoblast, promonocyte and monocyte stages, before circulating the bloodstream (Kim *et al*., 1998; Martinez *et al*., 2006). After 1-3 days of recirculation they migrate into tissues and become tissue macrophages. In tissues, final stages in macrophage differentiation take place and Kupffer cells, microglial cells, osteoclasts, peritoneal macrophages, and others are formed (Kulseth *et al*., 1998). These tissues are characterized by low oxygen consumption and protein synthesis rates, and modest cytokine production (Martinez *et al*., 2006). Macrophages are found in all organs of the body, body cavities and their linings, and the skin (Kulseth *et al*., 1998).

Mononuclear phagocytes play a role in (i) antigen presentation for T lymphocytes; (ii) phagocytosis; (iii) immunomodulation and (iv) as secretory cells (Dale *et al*., 2008; Jiménez *et al*., 1999; Kulseth *et al*., 1998). Antigen presenting cells (APCs) display antigens in association with major histocompatibility complex class II molecules to lymphocytes, provide costimulatory signals and generate an immune response to eliminate pathogens (Rocca and FitzGerald, 2002). Mononuclear phagocytes ingest material to eliminate waste and debris (e.g. ineffective and aged erythrocytes, and apoptotic cells) (Dale *et al*., 2008), to kill invading pathogens (Dale *et al*., 2008; Guzdek *et al*., 1997; Kulseth *et al*., 1998; Martinez *et al*., 2006), and to trigger the adaptive immune response (Martinez *et al*., 2006). Phagocytes are involved in the secretion of pro- and anti-inflammatory cytokines, chemokines (involved in immune modulation) and inflammatory mediators (e.g. eicosanoids), which modulate the functional capabilities of monocytes and tissue macrophages during inflammation (Dale *et al*., 2008; Jiménez *et al*., 1999; Kulseth *et al*., 1998; Martinez *et al*., 2006).

Phagocytes undergo increased metabolic activity (respiratory burst) during phagocytosis, which is associated with the generation of O_2^- when oxygen is reduced by NADPH oxidase (found in the cell membranes of phagocytes). O_2^- undergoes several reactions to form reactive oxygen intermediates including H_2O_2, hydroxyl radical, and hypoclorous acid, which are microbicidal agents. Respiratory burst can be induced by intact bacteria, opsonized particles, endotoxins, cytokines (e.g. TNFα and IFNγ), N-formylated

chemoattractant peptides and activators of PKC (e.g. phorbol esters). Reactive nitrogen intermediates have bactericidal activity (Guzdek *et al*., 1997). Macrophages activate NOS, leading to NO production. NO has cytostatic or cytotoxic activity against viruses, bacteria, fungi, helminthes, protozoa and tumour cells (Jiménez *et al*., 1999; Dale *et al*., 2008), and participates in the production of free radicals (Jiménez *et al*., 1999). Interaction between reactive oxygen and nitrogen intermediates forms $ONOO^-$, which increases cytotoxicity and inflammation (Guzdek *et al*., 1997). NO may regulate phagocytosis as was shown by hydroxyapatite-induced phagocytosis in the murine macrophage cell line, RAW264.7 (Gopinath *et al*., 2006).

Apoptotic cells are recognized via the vitronectin and/or PS receptors. Inflammation is generally not associated with apoptosis, because apoptotic cells are phagocytosed to prevent leakage. Apoptotic cells are removed before the integrity of cell membranes is lost. Phagocytosis of apoptotic cells is important to clear nonfunctional dying cells. Kurosaka *et al*. (1998) have shown that phagocytosis of apoptotic CTLL-2 cells by PMA treated THP-1 cells is associated with the production of pro-inflammatory cytokines (e.g. IL-1β and IL-8).

Phagocytes play an important role in the elimination of pathogens and apoptotic cells. Phagocytes activate NOS, which produce NO involved in pathogen elimination. This section focuses on the phagocytic behaviour of monocyte-macrophages when treated with *Hypoxis* extracts and its purified compounds.

6.5.2. Materials and Methods

Human promonocytic leukemia U937 cells were differentiated with 100 nM $1,25(OH)_2D_3$ as described in section 6.3.2. Differentiating agent was removed by centrifugation at 250 x g for five min at room temperature, supernatant discarded, cells washed with RPMI1640: 10% fbs (complete medium) and resuspended in complete medium. One hundred thousand cells were added to polypropylene tubes and treated with DMSO (0.25%, v/v), *H. hemerocallidea* (125 µg/mL), *H. stellipilis* (125 µg/mL), *H. sobolifera*

(125 μg/mL), hypoxoside (50 μg/mL), rooperol (20 μg/mL), CD (4 mM)/EtOH (5%, v/v), β-sitosterol (30 μM), campesterol (30 μM), cholesterol (30 μM), stigmasterol (30 μM) or PMA (10 or 20 nM) for three hrs, which has been optimized as the pretreatment period for best phagocytosis (data not shown). After treatment, compounds were removed by centrifugation as described above. Uptake buffer [Hanks' Balanced Salt Solution (HBSS) with additional 20 mM HEPES] was added to a vial of pHrodo™ *E. coli* BioParticles® Conjugate, sonicated for five min, added (50 μL = 50 μg/mL of pHrodo™ *E. coli* Bioparticles® conjugate) to each tube and incubated in the dark for three hours in a humidified incubator at 37 °C in the absence of CO_2. Cells were washed as described above, resuspended in PBS (500 μL) and read on a Beckman Coulter Cytomics FC500. Mean fluorescence intensity (MFI) of treated cells was expressed as a percentage of the MFI of control cells. Statistical significance was determined using the two-tailed Student's t-test.

Phagocytosis only with treatments. Monocyte-macrophages were treated with the *Hypoxis* extracts and its purified compounds for three hrs and pHrodo™ *E. coli* Bioparticle® Conjugate added as described above.

Phagocytosis with treatments together with PMA. Monocyte-macrophages were treated with the *Hypoxis* extracts and its purified compounds, in the presence of 20 nM PMA, for three hrs and pHrodo™ *E. coli* Bioparticle® Conjugate added as described above.

6.5.3. Results and Discussion

The measured phagocytic activity of monocyte-macrophages is based on the acidification of *E. coli* bioparticles, conjugated to the fluorogenic pHrodo™ dye, as they are ingested (Figure 6.7). Fluorescence increases as the phagosome, inside the monocyte-macrophages, becomes more acidic.

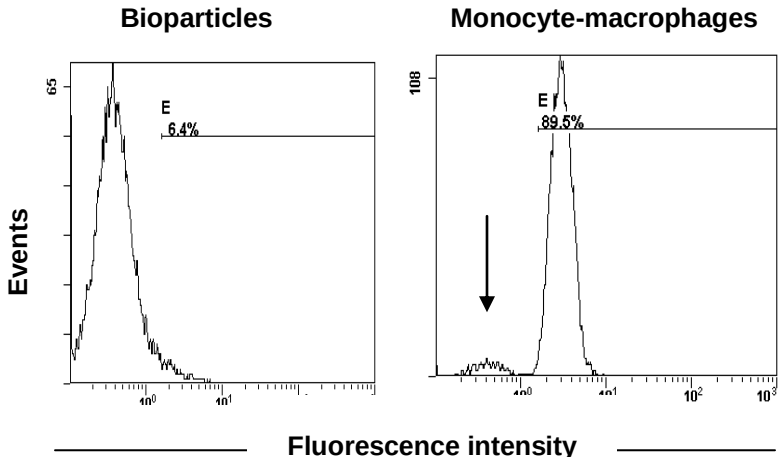

Figure 6.7: Histograms of pHrodo™ *E. coli* bioparticles® and monocyte-macrophages. Arrow represents the position of pHrodo™ *E. coli* bioparticles® after phagocytosis by monocyte-macrophages.

Kurosaka *et al*. (1998) have shown that phagocytosis of PMA treated THP-1 cells phagocytosing apoptotic CTLL-2 cells occurred quickly and were completed within three hrs. They also showed that phagocytosis may be temperature dependent, with better phagocytosis at 37 °C than 20 °C. Hence the incubation of treated monocyte-macrophages with pHrodo™ *E. coli* Bioparticles® for three hours at 37 °C.

Phagocytosis in absence of PMA. Differentiated monocyte-macrophages were treated for three hours, in the absence of PMA (Figure 6.8).

Small, but significant increases (10-20%) in phagocytosis were seen when monocyte-macrophages were treated with the three *Hypoxis* spp., rooperol and β-sitosterol. PMA was used as the positive control. *H. sobolifera* ($p<0.001$) had a significantly greater effect on phagocytosis compared to *H. hemerocallidea* and *H. stellipilis* ($p<0.01$). This may be explained by *H. sobolifera*'s higher β-sitosterol content (Chapter 3, section 3.3), since β-sitosterol in this study also increased phagocytosis significantly ($p<0.01$). Increase in phagocytosis seen with *H. hemerocallidea* and *H. stellipilis* are unlikely to be due to rooperol, because β-glucosidase was not added to the *Hypoxis* extracts. The hypoxoside present in these two *Hypoxis* spp. could not have played a role and

phagocytosis was probably due to its β-sitosterol content. The crude *Hypoxis* extracts contain additional compounds (Chapter 3, section 3.3), which may have been responsible for phagocytosis. Hypoxoside, campesterol, cholesterol and stigmasterol had no significant effect on phagocytosis.

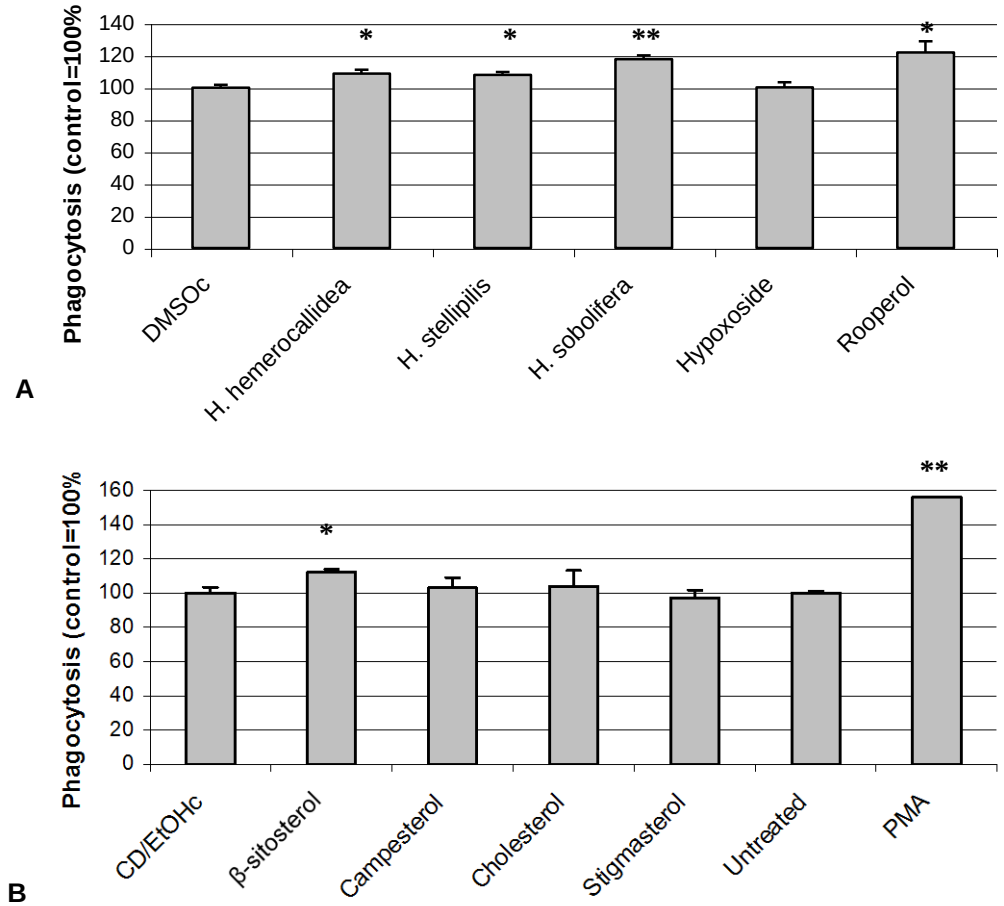

Figure 6.8: Phagocytosis of pHrodo™ *E. coli* bioparticles® by monocyte-macrophages, pretreated with DMSOc, *Hypoxis* chloroform extracts, hypoxoside and rooperol (A), and CD/EtOHc, (phyto)sterols and PMA (B) in the absence of PMA. Bar graph percentages represent the increase in mean fluorescence intensity of cells staining positive for phagocytosis when treated samples were compared to control. Error bars represent the SD of triplicate values. Significance was determined using the two-tailed Student T-test: *p<0.01; **p<0.001; ***p<0.0001 compared to control.

Phagocytosis with simultaneous PMA treatment. Monocyte-macrophages were treated for three hours in the presence of 20 nM PMA (Figure 6.9).

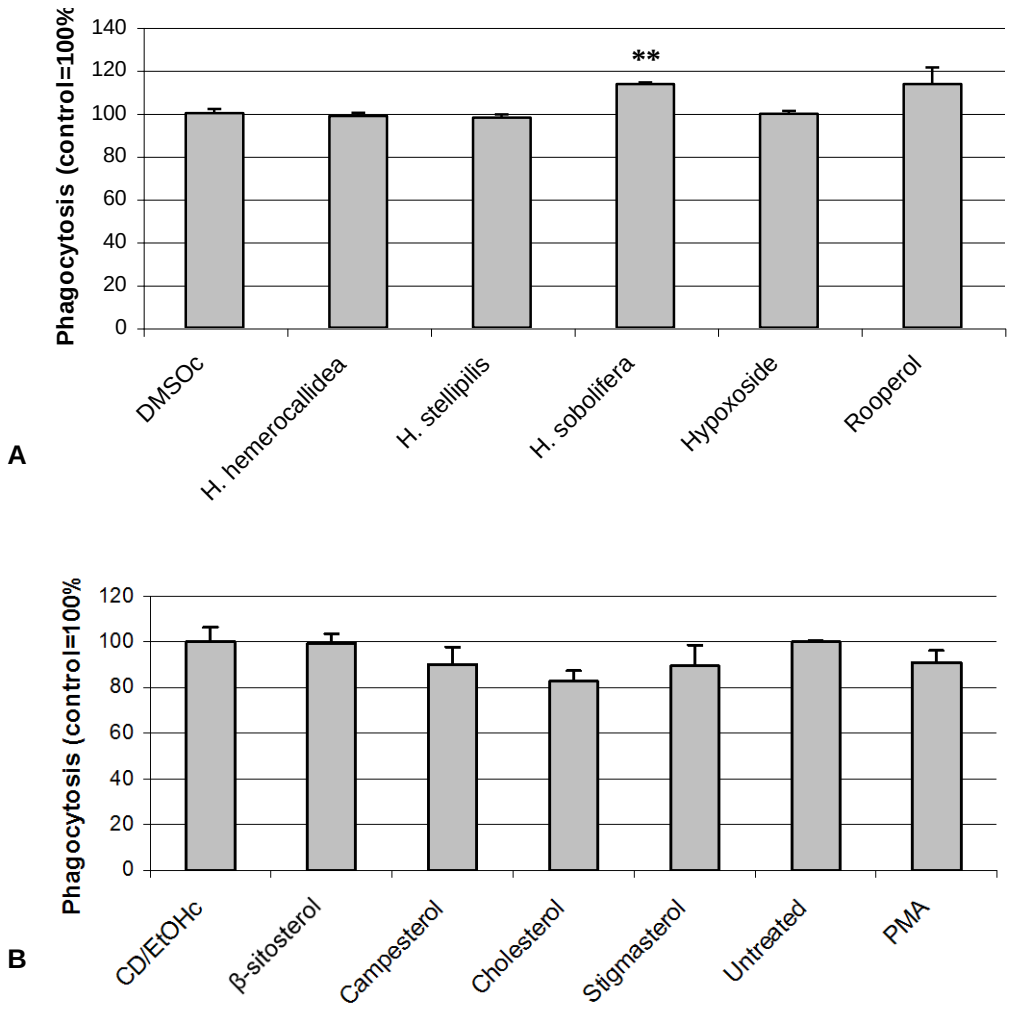

Figure 6.9: Phagocytosis of pHrodo™ *E. coli* bioparticles® by monocyte-macrophages, pretreated with DMSOc, *Hypoxis* chloroform extracts, hypoxoside and rooperol (A), and CD/EtOHc, (phyto)sterols and PMA (B) in the presence of PMA (20 nM). Bar graph percentages represent the increase in mean fluorescence intensity of cells staining positive for phagocytosis when treated samples were compared to control. Error bars represent the SD of triplicate values. Significance was determined using the two-tailed Student t-test: *p<0.01; **p<0.001; ***p<0.0001 compared to control.

Simultaneous treatment of monocyte-macrophages with *Hypoxis* and its purified compounds, and PMA has shown a decrease in phagocytosis. Only *H. sobolifera* and rooperol slightly increased phagocytosis, with the former being significantly different from the control.

Density plots (Figure 6.10) clearly show the increase in phagocytosis when treated with *H. sobolifera* and rooperol, in the presence of PMA. Phagocytosis density plots of *H. hemerocallidea*, *H. stellipilis*, hypoxoside, β-sitosterol, campesterol, cholesterol, stigmasterol and PMA treated monocyte-macrophages are shown in Appendix 6.

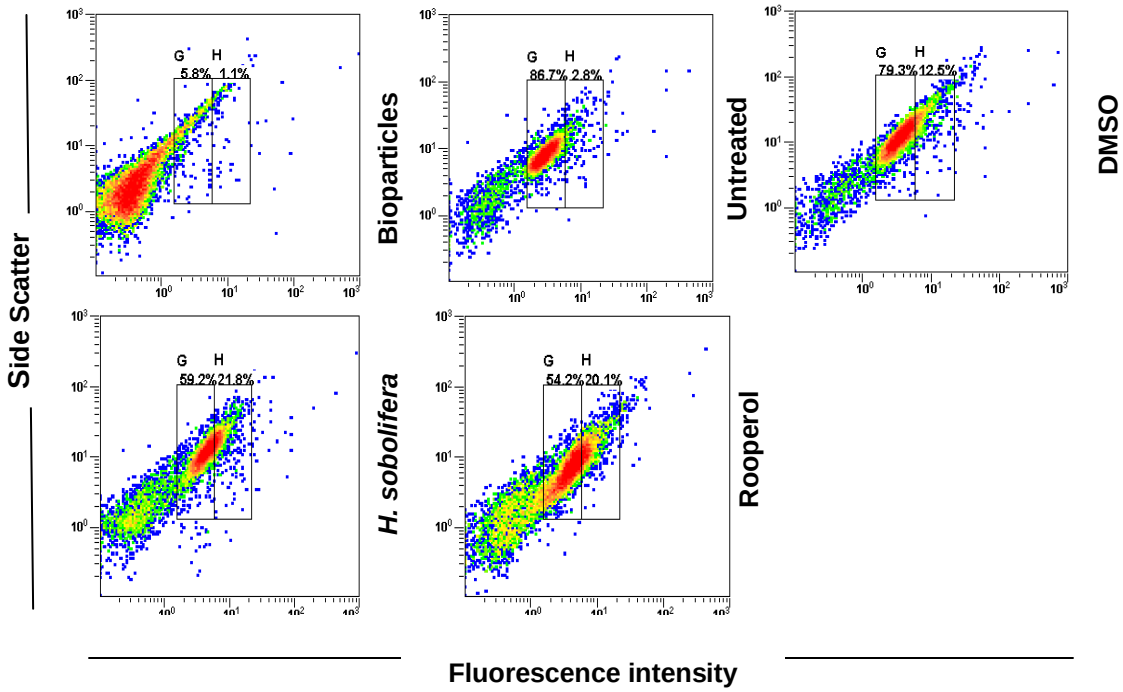

Figure 6.10: Density plots of phagocytosis of pHrodo™ *E. coli* bioparticles® by monocyte-macrophages, pretreated with DMSOc, *H. sobolifera* chloroform extract and in the presence of PMA (20 nM).

This was the first time that the effects of *Hypoxis* and its purified compounds on phagocytosis were investigated. Although the increases in phagocytosis were small (10-20%), the results were significantly different. *Hypoxis* extracts, β-sitosterol and rooperol treatment of monocyte-macrophages significantly increased phagocytosis in the absence of PMA. This may play an important role in increasing phagocytosis of pathogenic microorganisms and apoptotic cells.

6.6. Pro- and Anti-inflammatory Cytokines

6.6.1. Background

Cytokines are small (molecular weights of between 8 and 40 000 Da), nonstructural, endogenous inflammatory and immunomodulating proteins (Dinarello, 2000; Gogos *et al*., 2000). Most nucleated cells synthesize and respond to cytokines, which are involved in the host response to disease or infection. Cytokine genes are not expressed unless specifically stimulated in response to stress (Dinarello, 2000). The effect of any cytokine depends on the (i) time of release, (ii) local milieu in which it acts, (iii) presence of competing or synergistic elements, (iv) cytokine receptor density, (v) and tissue responsiveness to each cytokine (Opal and DePalo, 2000).

Pro-inflammatory cytokines include IL-1α/β, possibly IL-6, IL-12, TNFα, and IFNγ. These promote inflammation by upregulating genes encoding enzymes PLA_2, COX-2, and iNOS that increase the synthesis of platelet-activating factor, leukotrienes, prostanoids and NO (Dinarello, 2000; Gogos *et al*., 2000). An excess of pro-inflammatory cytokines is associated with multiple organ-system dysfunctions and mortality (Gogos *et al*., 2000). Anti-inflammatory cytokines include IL-4, possibly IL-6, IL-10, IL-11, IL-13, TGFβ and cytokine inhibitors [including soluble tumour necrosis factor receptor (sTNFR)-I and II, and soluble IL-1 receptors (sIL-1r)]. These cytokines control and downregulate the inflammatory response caused by pro-inflammatory cytokines leading to immune system depression in patients (Dinarello, 2000; Gogos *et al*., 2000; Opal and DePalo, 2000). The human immune response to severe infections is mediated mainly by the primary pro-inflammatory cytokines IL-1 and TNFα and secondary pro-inflammatory cytokines IL-6 and -8. Anti-inflammatory IL-10 and soluble cytokine inhibitors prevent excessive pro-inflammatory cytokine production and may induce a state of immunosuppression in patients (Gogos *et al*., 2000). Certain anti-inflammatory cytokines must be present at greater concentrations than pro-inflammatory cytokines to inhibit their functions (Opal and DePalo, 2000). The balance between pro- and anti-inflammatory cytokines determines the outcome of disease (Dinarello, 2000).

Pro-inflammatory cytokines, including TNF-α, IL-1β and IL-6, may affect apoptosis in human peripheral blood cells. These cytokines reduce spontaneous apoptosis in neutrophils, but have little effect on the lymphocyte population (McNamee *et al*., 2005).

T lymphocytes are divided into $CD4^+$ and $CD8^+$ cells. The former are cytokine secreting helper cells, whereas the latter are cytotoxic killer cells eliminating virally infected cells. $CD4^+$ T helper lymphocytes are classified into Th1 and Th2 cells on the basis of their cytokine production. Th1 cells secrete IL-2, IL-12, IFNγ and TNFα/β, which activate macrophages and promote cell-mediated immune responses against invasive intracellular pathogens. Th2 cells secrete IL-4, IL-5, IL-6, IL-10 and IL-13, which promote humoral immune responses against extracellular pathogens (Breytenbach *et al*., 2001; Opal and DePalo, 2000; Rocca and FitzGerald, 2002).

Pro- and anti-inflammatory cytokines play an important role in the onset and prevention of inflammation, respectively. This section focuses on the effect of *Hypoxis* extracts and its purified compounds on pro- and anti-inflammatory cytokine production in unstimulated PBMCs.

6.6.2. Materials and Methods

PBMCs were isolated from venous blood of two healthy donors (male and female) using heparinised Vacutainer® CPT™ cell preparation tubes (Beckton Dickinson, Plymouth, UK) within 30 minutes of collection. PBMCs were seeded at 500 000 cells/mL in round bottomed 96-well plates and treated with filter sterilized DMSO (0.25%, v/v), *H. hemerocallidea* (125 μg/mL), *H. stellipilis* (125 μg/mL), *H. sobolifera* (125 μg/mL), hypoxoside (50 μg/mL), rooperol (20 μg/mL), CD (4mM)/EtOH (5%, v/v), β-sitosterol (30 μM), campesterol (30 μM), cholesterol (30 μM) or stigmasterol (30 μM) for 48 hrs at 37 ºC in a humidified incubator and 5% CO_2. After treatment, aliquots of the culture media were removed and used immediately or frozen at -20 °C. The FlowCytomix Multiplex human Th1/Th2 10plex Kit I (Bender Medsystems; Vienna, Austria), containing antibodies for IFNγ, IL-1β, IL-2, IL-4, IL-5, IL-6, IL-8, IL-10, IL-12p70 and

TNFα was used as described in the product protocol. Samples were analyzed using the Beckman Coulter FC500 and data analyzed using Bender Medsystems™ FlowCytomixPro 1.0 Software BMSFFS/1.0. Endotoxin levels in the 125 µg/mL *Hypoxis* chloroform extracts were determined using the Limulus Amebocyte Lysate Endochrome™ kit (Charles River Endosafe, SC, USA) as described in the protocol. Mean fluorescence intensity (MFI) of treated cells was expressed as a percentage of the MFI of control cells. Statistical significance was determined using the two-tailed Student's t-test.

6.6.3. Results and Discussion

The FlowCytomix Multiplex human Th1/Th2 10plex cytokine assay is based on the fluorescence bead immunoassay. Two sets of microspheres of different sizes (4.4 and 5.5 µM in diameter), each consisting of five bead populations internally dyed with different intensities of a fluorescent dye, were used (Figure 6.11). This allows for the simultaneous quantification of 10 cytokines. Fluorescently labelled beads are coated with primary antibodies, specific for each cytokine present in the sample. Biotin-conjugated secondary antibodies bind cytokines bound to the primary antibodies. Streptavidin-phycoerythrin binds the biotin conjugated secondary antibodies and emits fluorescent signals.

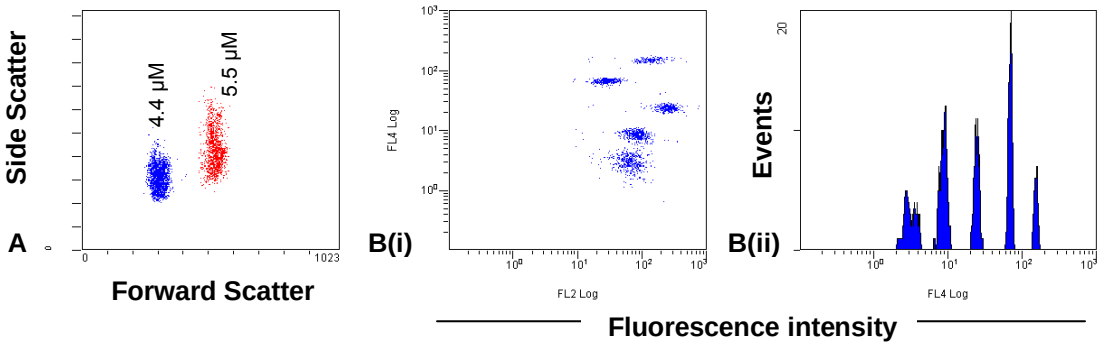

Figure 6.11: Identification of the 10 cytokines using the FlowCytomix Multiplex human Th1/Th2 10plex Kit I. Dot plot of two populations representing the two sizes of beads (A) and dot plots (Bi) and histograms (Bii) of the five different fluorescent intensities of the 4.4 µM diameter beads, each representing a cytokine (B).

Extracellular cytokines. Pro-inflammatory cytokines measured in the samples include IL-1α/β, possibly IL-6, IL-12, TNFα, and IFNγ. Anti-inflammatory cytokines measured in the samples include IL-4, possibly IL-6, and IL-10. Results showing significant differences are shown in Figure 6.12. The rest are shown in Appendix 6.

Only two donors (male and female) were used due to the difficulty to find healthy donors that are not on any medication – non steroidal anti-inflammatory drugs (NSAIDs), antihistamines and oestrogen – which may influence cytokine production. Male and female donors were chosen to see if differences exist between male and female. The experiment was only performed on two donors due to the high costs involved. (Phyto)sterols increased IL-1β and IL-6 production significantly in donor one (male) when compared to the CD/EtOH control. β-sitosterol and cholesterol also increased IL-1β production significantly in donor two (female). Campesterol increased IL-10 production ($p<0.01$) in PBMCs isolated from the male donor, while *H. hemerocallidea* increased IL-8 production ($p<0.01$) in PBMCs isolated from the female donor. Differences seen between male and female donors may be gender related, but this is only speculative and need further investigation.

Treatment of PBMCs with the other *Hypoxis* extracts and purified compounds did not have any significant effects on the production of the other cytokines. This may be explained by the absence of a stimulant (e.g. PMA, LPS and PHA), which needs to be present to induce cytokine production. PBMCs consist mainly of T cells, B cells and monocytes, which may be inappropriate cells to investigate pro- and anti-inflammatory cytokine production. To have a better view of the effects of *Hypoxis* extracts and its purified compounds on the cytokines involved in inflammation and phagocytosis, a macrophage cell line or differentiating monocytes to macrophages using an appropriate stimulant must be used. Samples were filter sterilized with the result that non-polar compounds (including phytosterols and other compounds found in the *Hypoxis* extracts) may have attached to the polar membranes of the Supor (polyethersulfone) syringe filters (Pall Life Sciences, MI, USA).

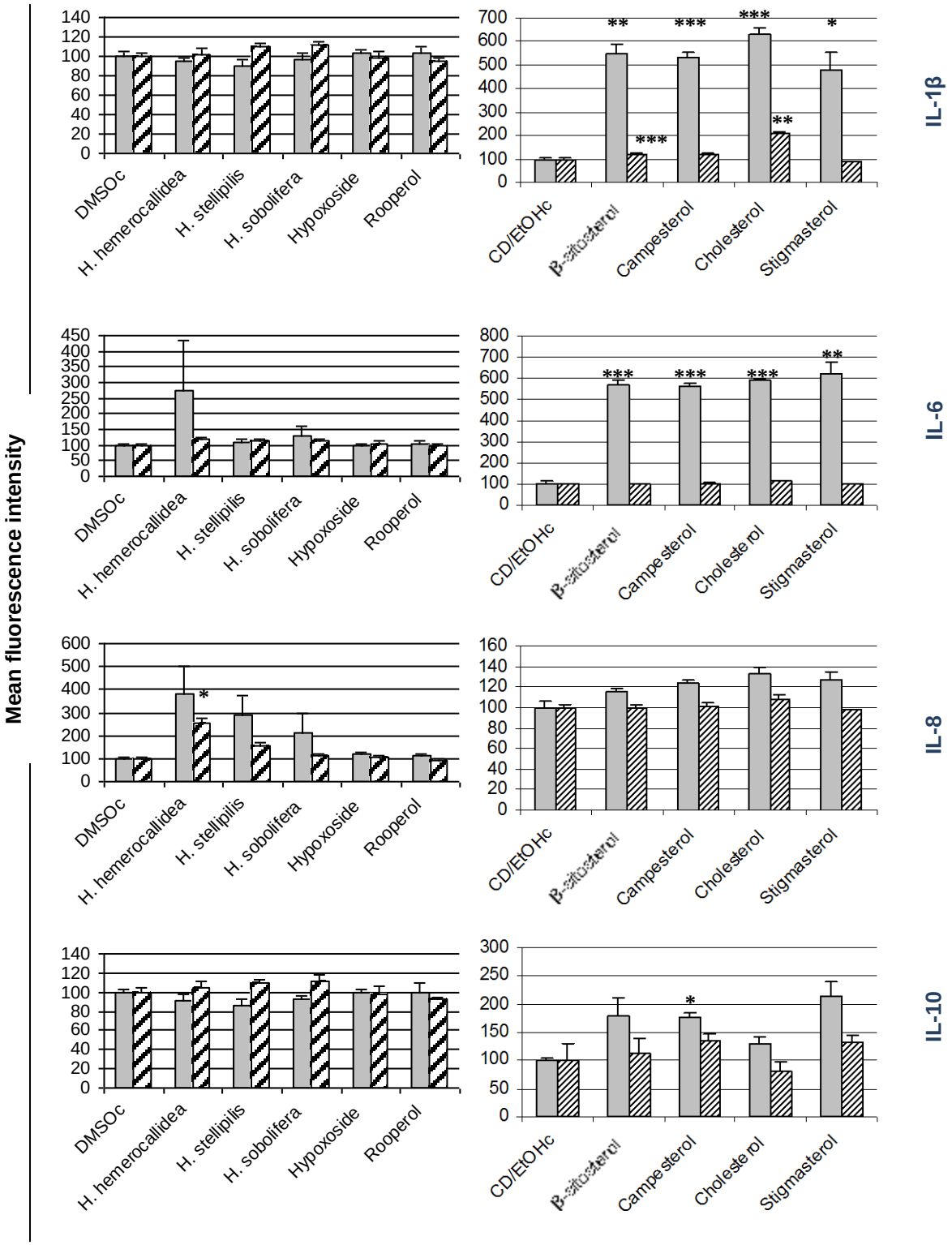

Figure 6.12: Extracellular cytokine production by PBMCs treated with *Hypoxis* extracts and its purified compounds for 48 hrs. Grey bars = donor 1/male; striped bars = donor 2/female. Error bars represent the SEM of triplicate values. Significance was determined using the two-tailed Student t-test: *p<0.01; **p<0.001; ***p<0.0001 compared to control.

Increased cytokine production was not due to endotoxin in the *Hypoxis* chloroform extracts, because endotoxin levels were less than the maximum level [<1 ng/mL of LPS (Pollock *et al*., 2003; Webb *et al*., 1998)] allowed in samples for immunological experiments. The PBMCs were exposed to very low levels of LPS in the present study (0.32 0.27, 0.25 ng/mL for *H. hemerocallidea*, *H. stellipilis* and *H. sobolifera*, respectively).

The predominantly pro-inflammatory results obtained in this study are in contradiction with results obtained in other studies. Nashed *et al*. (2005) have shown that a phytosterol-enriched (2%) diet over a 14 week period lowered pro-inflammatory cytokines (TNF-α and IL-6) and increased anti-inflammatory cytokines (IL-10) in apolipoprotein (apo) E-deficient mice when exposed to the inflammatory stimulus, LPS. Calpe-Berdiel *et al*. (2007) have shown an increase in IL-2 and IFN-γ release when ConA activated spleen lymphocytes, isolated from Apo E-deficient mice, were exposed to 2% phytosterols for 48 hrs and inflammation induced by turpentine. There was no change in IL-4 and IL-10 levels.

Macrophages are the main source of the pro-inflammatory cytokines, TNFα, IL-1β and IL-6. Overproduction of TNFα and IL-1 play an important role in the pathogenesis of septic shock, asthma, rheumatoid arthritis, and other diseases. Suppression of synthesis of these cytokines may be required for the treatment of above-mentioned diseases (Guzdek *et al*., 1996). Guzdek *et al*. (1996) have shown that rooperol and its derivatives suppress LPS-induced production of TNFα, IL-1 and IL-6 at protein level in human alveolar macrophages, blood monocytes and U937 cells, and rat alveolar macrophages. Diacetate and tetraacetate rooperol derivatives (IC_{50} values of 10-20 μM) were more potent inhibitors of cytokine synthesis than the sulfate derivative (IC_{50} values of 25-75 μM), possibly due to the enzymes available to release the esters from rooperol (Guzdek *et al*., 1996). Guzdek *et al*. (1998) have also shown that rooperol tetraacetate (10 μM) decreases TNFα, IL-1β and IL-6 mRNAs in the absence and presence of LPS in PMA differentiated U937 cells. Rooperol and its derivatives may inhibit inflammatory

cytokine synthesis by interfering with transcription factors (e.g. NF-κB and AP-1) required for cytokine gene transcription (Guzdek *et al*., 1998).

6.7. Conclusion

Differentiation of U937 cells to monocyte-macrophages was optimized using three time intervals (24, 48 and 72 hrs) and two differentiating agents [PMA and $1,25(OH)_2D_3$] at three concentrations (10, 50 and 100 nM). $1,25(OH)_2D_3$ was chosen as the differentiating agent, due to higher cell viability at high concentrations. A higher concentration (100 nM) and shorter differentiating period (24 hrs) were used. Monocyte-macrophages were confirmed by morphological characteristics (attachment of cells, clump- and pseudopodia formation) and CD11b/CD14 expression. Treatment of monocyte-macrophages with *H. hemerocallidea*, *H. stellipilis*, *H. sobolifera* and rooperol has shown for the first time (i) an increase in NO production and (ii) phagocytosis. *H. stellipilis* had a greater effect on NO production than *H. hemerocallidea* and *H. sobolifera*. The phytosterols had no effect on NO production. NO production was probably due to iNOS induction, which can be confirmed by inhibitors against cNOS, eNOS and iNOS. Small, but significant increases in phagocytosis were seen when monocyte-macrophages were pretreated with the *Hypoxis* chloroform extracts and rooperol. NO production and phagocytosis results confirmed that rooperol is the active compound and not hypoxoside. Although the treatments had no significant effects on COX-2 expression, experimental design may be changed to further investigate possible increases and decreases of COX-2 expression. *Hypoxis* chloroform extracts and its purified compounds may not effect the expression of COX-2, but may decrease or increase COX-2 activity. *Hypoxis* chloroform extracts, hypoxoside and rooperol had very little or no effect on anti- and pro-inflammatory cytokine production. The phytosterols tested increased pro-inflammatory cytokines (e.g. IL-1β and IL-6), which is in contradiction with decreased pro-inflammatory cytokines found in other studies.

Increased phagocytosis and NO production play important roles in removing apoptotic cells *in vivo* (Pepper *et al*., 1998) and promoting apoptosis in cancer (Brüne *et al*., 1998;

Choi *et al*., 2001), respectively. Phagocytosis and NO production are also important in eliminating microorganism, hence possible anti-bacterial properties. *Hypoxis* extracts and rooperol may play an important role in increasing phagocytosis and NO production for above mentioned biological effects.

CHAPTER 7

ANTIOXIDANT ACTIVITY

7.1. General Background

An antioxidant (syn. free radical scavengers) can be defined as a natural or synthetic substance, being enzymes or organic substances, which inhibit or prevent the damaging effects of oxidation in animal tissues (Huang *et al*., 2005; Krishnaiah *et al*., 2007). It decreases the adverse effects of reactive oxygen or nitrogen species on normal physiological function in humans (Huang *et al*., 2005).

Antioxidant compounds found in plants include carotenoids (e.g. lutein, β-carotene), flavonoids (e.g. quercetin, rutin, luteolin, kaempferol), cinnamic acids, benzoic acids, folic acid, ascorbic acid (syn. vitamin C), tocopherols (syn. vitamin E), tocotrienols, vitamin A, proanthocyanidin, and micronutrient elements or minerals (e.g. Cu, Mn, Zn, Fe, Se) (Ardestani and Yazdanparast, 2007; Brown *et al*., 1998; Krishnaiah *et al*., 2007; Lee *et al*., 2003; Matés *et al*., 1999; Papas, 1999). Synthetic antioxidants may have side effects when taken *in vivo*, while natural antioxidants have generally higher antioxidant activity compared to synthetic antioxidants (Krishnaiah *et al*., 2007). These dietary or exogenous antioxidants are important for normal functioning of the endogenous antioxidant system.

Characteristics of a potential antioxidant include:

- Absorption and bioavailability.
- Effective dose, safety and toxicity.
- Distribution in cells, tissue and extracellular fluids.
- Free radical scavenging ability.
- Metal chelating activity.
- Effects on gene expression.
- Interaction with cellular antioxidants or antioxidant enzymes.

- Detoxification of carcinogenic metabolites (Bagchi *et al*., 2000; Rice-Evans *et al*., 1997).

Nair *et al*. (2007b) have shown that a *H. hemerocallidea* aqueous extract and rooperol increase antioxidant activity [1,1-diphenyl-2-picryl hydrazine (DPPH) and ferric reducing ability of plasma (FRAP)], reduce quinolic acid induced lipid peroxidation and increase superoxide free radical scavenging activity. Laporta *et al*. (2007b) have shown that *H. hemerocallidea* and rooperol have high antioxidant capacity. Vivancos and Moreno (2005) investigated the effect of β-sitosterol on antioxidant enzymes and reduced glutathione (GSH)/glutathione disulfide (GSSG; oxidized). This chapter focuses on the effect of *Hypoxis* extracts and its purified compounds on ROS production in differentiated and undifferentiated U937 cells, and the FRAP antioxidant potential. The effects of *Hypoxis* extracts and its purified compounds on superoxide dismutase (SOD) activity in Chang liver cells were also investigated.

7.2. Reactive Oxygen Species (syn. respiratory burst, oxidative burst)

7.2.1. Background

Definition. Reactive oxygen species are ubiquitous, highly diffusible and reactive molecules (Barbieri *et al*., 2003) produced by molecular oxygen reduction during aerobic respiration and substrate oxidation in mammalian cells (Matés *et al*., 1999).

Biological properties. Small amounts of ROS (including O_2^- and H_2O_2) are continuously produced under normal conditions. ROS are produced for essential biological processes or as byproducts of metabolic processes (Krishnaiah *et al*., 2007). Low levels of ROS are important in biological processes, including the regulation of cellular functions (cell growth, differentiation, proliferation and apoptosis/necrosis), induction or suppression of gene expression (AP-1 and NF-κB transcription factors), activation of cell signalling pathways (MAPK, Erk, guanylyl cyclase, PLC/D and PLA_2), energy production, and phagocytosis (Ardestani and Yazdanparast, 2007; Barbieri *et al*., 2003; Hancock *et al*.,

2001; Kurz *et al*., 2004; Martin and Barrett, 2002; Matés *et al*., 1999; Salganik, 2001). Activation of gene expression and redox-sensitive signalling pathways are important in regulating cytokine production and inflammatory mediator expression (Barbieri *et al*., 2003; Forman and Torres, 2002; Martin and Barrett, 2002). ROS are ideal signalling compounds due to their small size, diffusion over short distances, several mechanisms for rapid and controllable production, and numerous mechanisms for rapid removal. To be considered a signalling molecule, ROS must (i) be produced by cells when stimulated to do so; (ii) have action on cells producing it or on nearby cells; (iii) be removed in order to turn off or reverse the signal. O_2^- and H_2O_2 fulfill these criteria (Hancock *et al*., 2001).

Sources. Endogenous sources of ROS include the (i) mitochondria: electrons released from the electron transport chain reduce O_2 to O_2^-, which may lead to the formation of H_2O_2 and OH^-; (ii) endoplasmic reticulum (ER): cytochrome P450 complexes generate O_2^- to metabolize and degrade hydrophobic toxic substances, steroids and drugs, by transforming it to hydrophilic compounds that can be removed from the body; (iii) phagocytes: produce O_2^-, H_2O_2 and OH^- to kill infectious microorganisms, bacteria- and virus-infected cells, and cancer cells; (iv) peroxisomes: degradation of fatty acids and other molecules is associated with H_2O_2 production (Barbieri *et al*., 2003; Krishnaiah *et al*., 2007; Salganik, 2001); (v) several enzymatic reactions: O_2^- is a by-product of oxygenases (including lipooxygenase and COX) and oxidases (NADPH- and xanthine oxidase), hepatic metabolism and oxyhemoglobin degradation (Barbieri *et al*., 2003; Martin and Barrett, 2002; Rodriguez *et al*., 2003). Exogenous sources of ROS include (i) radiation exposure to environment or manmade sources including gamma rays, UV irradiation and X-rays, which split water in the body to form OH^-; (ii) low percentage of O_2 breathed in is used to produce O_2^- (Krishnaiah *et al*., 2007; Martin and Barrett, 2002); (iii) ROS producers, including aldehydes, redox cycling quinones, heavy and transition metals, and thiol alkylating agents (Martin and Barrett, 2002).

Oxidative stress occurs due to the overproduction and/or incomplete removal of ROS by the body's defense mechanism (Ardestani and Yazdanparast, 2007; Núñez-Sellés, 2005), which may result in metabolic malfunction and damage to biological macromolecules

(Matés *et al*., 1999). ROS causing oxidative damage are divided into free oxygen radicals, which contain one or more unpaired electron(s) capable of independent existence, and nonradical ROS. Examples of free oxygen radicals and nonradicals are O_2^- and hydroxyl anion (OH^-), and H_2O_2, respectively. Free radicals can react with nonradicals to form a new radical (Krishnaiah *et al*., 2007; Shackelford *et al*., 2000). Endogenous factors contributing to oxidative stress include defects in mitochondrial respiration, nuclear polymorphism activation, enzyme system activation or inhibition, arachidonic acid metabolism, and Fe/Cu-related catalysis. Exogenous factors contributing to oxidative stress include environmental pollutants, solar radiation, urban air pollutants, exposure to toxic substances (e.g. fertilizers, pesticides, gasoline exhaust and chemical wastes), intoxication (e.g. alcohol, drugs and smoking), inadequate nutrition, drug metabolism and physical or psychical stress (Bagchi *et al*., 2000; Núñez-Sellés, 2005).

Protection against ROS. Antioxidant defense against ROS include preventive-, repairing- and scavenger mechanisms (Núñez-Sellés, 2005). It is divided into the enzymatic and non-enzymatic antioxidant defense systems.

Enzymatic antioxidant defense system (Figure 7.1) against ROS consists of SOD, catalase (CAT) and glutathione peroxidase (GPX). SOD catalyzes the dismutation of two molecules of the highly reactive O_2^- to O_2 and less reactive H_2O_2. Three forms of SOD, including cytosolic Cu/Zn-SOD, mitochondrial Mn-SOD and extracellular SOD, are found. Transition metals, especially Cu^{2+} and Mn^{2+}, at the active site allow for rapid electron exchange between the two O_2^- molecules. H_2O_2 is detoxified by CAT and GPX. CAT is mainly present in peroxisomes, contains ferric iron at the active site and reduces two H_2O_2 molecules into water and O_2. GPX is present in the mitochondria and cytosol, contain selenium at the active site and reduces H_2O_2 to water and O_2 in the presence of GSH. GSH acts as a substrate and transfers electrons to H_2O_2 (Matés *et al*., 1999; Rodriguez *et al*., 2003; Salganik, 2001). The GSH concentration is regulated by the reduction of GSSG via GSH reductase (Forman and Torres, 2002). Although GPX shares H_2O_2 as a substrate with CAT, it is the only enzyme to react with lipid and organic

hydroperoxides. Under oxidative stress conditions, H_2O_2 diffuses freely across the cellular membranes and undergo hemolytic cleavage when interacting with transition metal ions (Fe/Cu). Highly reactive and damaging OH^- radicals are formed, during the Fenton reaction. Lysosomes contain high concentrations of low molecular mass, labile and reactive iron, due to degradation of iron-containing proteins. Intralysosomal Fenton-type reactions may cause peroxidative-membrane destabilization, rupturing and release of hydrolytic enzymes (associated with cell apoptosis or necrosis depending on concentration) and iron into the cytosol. The Fenton reaction is site specific and can result in hydroxylation or other DNA modifications (Kurz *et al*., 2004; Matés *et al*., 1999; Rodriguez *et al*., 2003; Salganik, 2001). Small changes in physiological activity of antioxidant enzymes may have a huge effect on the resistance of cells to oxidant-induced damage to the genome and cell killing (Matés *et al*., 1999).

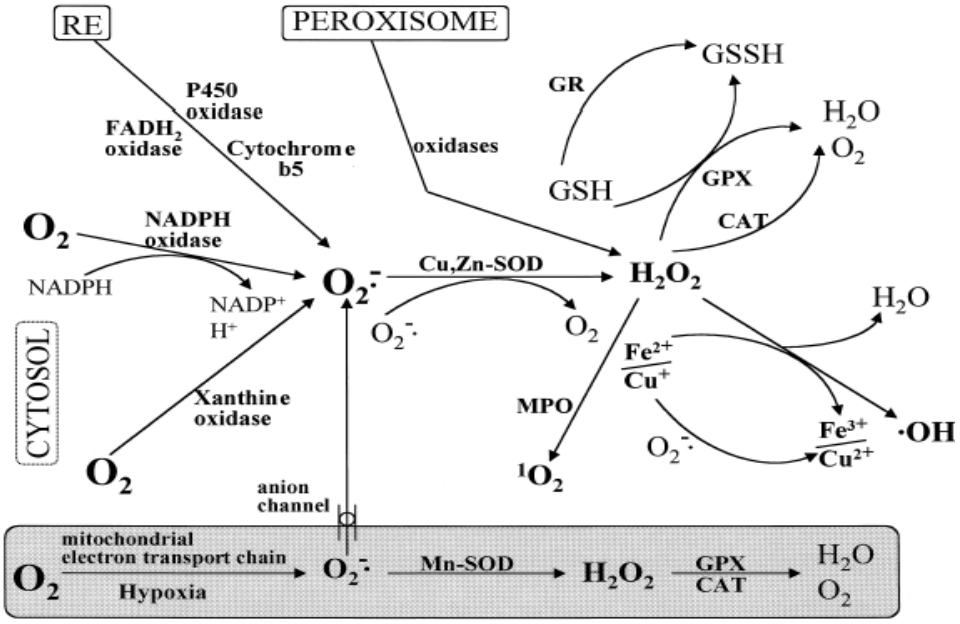

Figure 7.1: Summary of the enzymatic antioxidant defense system against ROS (Matés *et al*., 1999). See text for more detail.

The non-enzymatic antioxidant system consists of macromolecules and small molecules. Small molecular weight molecules directly scavenge free radicals (Rodriguez *et al*., 2003). Endogenously synthesized small molecules include ubiquinol, GSH, methionine,

uric acid, bilirubin and melatonin (Ardestani and Yazdanparast, 2007; Cao and Prior, 1998; Lee *et al*., 2003; Papas, 1999; Salganik, 2001). Exogenous or dietary small molecules were summarized under general background (section 7.1). Transition metal ions are eliminated by macromolecules including metallothioneins, ferritin, transferrin, cerulloplasmin, albumin and myoglobin, which protect against OH^- production (Núñez-Sellés, 2005; Salganik, 2001). Endogenous antioxidants provide insufficient protection against ROS due to continuous production of ROS needed for biological functions (Krishnaiah *et al*., 2007; Salganik, 2001).

Disadvantages. Excessive ROS production may damage lipids, proteins and DNA by causing lipid peroxidation, promoting oxidation and premutagenic modification of nucleotides, respectively (Ardestani and Yazdanparast, 2007; Bagchi *et al*., 2000; Salganik, 2001).

Excessive ROS may attack cells by:

- Modifying the DNA structure.
- Repressing gene expression by inhibiting or destructing transcriptional factors.
- Loss in cell membrane integrity by cell rupturing due to lipid oxidation, which may affect cell structure and function.
- Modifying cell function by accumulating oxidized low density lipoproteins.
- Activation or inactivation of enzymes.
- Sulfhydryl depletion.
- Altered calcium homeostasis (Ardestani and Yazdanparast, 2007; Bagchi *et al*., 2000; Núñez-Sellés, 2005; Salganik, 2001).

Pathological conditions alter the efficiency of the antioxidant defense system, resulting in ineffective scavenging and free radical overproduction (Ardestani and Yazdanparast, 2007). Imbalance of ROS production play a role in the pathogenesis of allergy, neurodegenerative diseases (e.g. Alzheimer's, Parkinson's, schizophrenia), cancer, atherosclerosis, diabetes, emphysema, heart diseases (e.g. cardiac and vessel injuries,

coronary heart disease), genetic and metabolic disorders, infectious diseases, ophthalmologic problems (cataracts), ageing, malaria, AIDS, autoimmune disorders (arthritis), gastrointestinal dysfunction, haemorrhagic shock, ischemia and reperfusion of many organs (Ardestani and Yazdanparast, 2007; Bagchi *et al*., 2000; Krishnaiah *et al*., 2007; Matés *et al*., 1999; Salganik, 2001; Shackelford *et al*., 2000).

ROS and cancer. Carcinoma cells are frequently under persistent oxidative stress. *In vitro*, tumour cell lines produce ROS at a greater rate than non-transformed cell lines (Brown and Bicknell, 2001). ROS are involved in the initiation and promotion of carcinogenesis (Röhrdanz and Kahl, 1997).

It is estimated that 2 x 10^4 DNA damaging events occur per cell per day in the human body. Oxidative damage is greater in the mitochondrial genome, due to ROS's close proximity compared to nuclear DNA (Shackelford *et al*., 2000). Increased oxidative stress in carcinoma may (i) increase DNA damage via single- or double-stranded DNA breaks, DNA-protein crosslinks, base (guanine and thymine) and sugar modifications, depurination and depyrimidination, and chromatid exchange, which result in increased mutation and tumour progression. ROS may inactivate tumour suppressor genes and increase proto-oncogene expression (Brown and Bicknell, 2001; Shackelford *et al*., 2000); (ii) activate growth promoting signalling pathways; (iii) increase angiogenesis via blood vessel growth and vasodilation; (iv) increase metastasis (Brown and Bicknell, 2001); (v) be associated with lower MnSOD, Cu/ZnSOD and CAT activities in tumour cells compared to normal cell counterparts (Röhrdanz and Kahl, 1997). Specific and non-specific repair processes remove most of the damaged DNA, but a small number of lesions escape repair and accumulate with age. Unrepairable damage to DNA leads to apoptosis and necrosis (severe and sudden injury by excessive ROS) (Martin and Barrett, 2002).

Large numbers of macrophages infiltrate tumours (e.g. breast cancer) and secrete TNFα, which play a role in oxygen radical production (Brown and Bicknell, 2001). Chemotherapy, including cisplatin, etoposide, doxorubicin and mitomycin C, may

increase oxidative stress in breast carcinomas by generating O_2^-. Radiotherapy and photodynamic therapy also generate oxygen radicals (Brown and Bicknell, 2001; Salganik, 2001).

Increased ROS levels induce apoptosis and necrosis in transformed cells, and oxidative carcinogenic damage in DNA; hence protecting against cancer. Cancer-preventative effect of antioxidants depends on the baseline level of ROS in cells, which is determined by ROS generation and antioxidant defense. Overproduction of ROS increases the risk in humans to develop cancer, cardiovascular diseases, cataracts, and other diseases. Antioxidants may decrease ROS levels by blocking cancer-protective apoptosis and phagocytosis in people with low ROS levels; hence promoting carcinogenesis. The biological effects of antioxidants in cancer are thus controversial (Martin and Barrett, 2002; Salganik, 2001). Antioxidants may interfere with the therapeutic activity of anticancer drugs that kill cancer cells by ROS-dependent apoptosis. For example, the antioxidant α-tocopherol (vitamin E) reduces ROS production and apoptosis in MCF-7 cells (Salganik, 2001).

Vegetables, fruits and seeds contain vitamin C and E, β-carotene and protease inhibitors, which may protect against cancer. Several plants contain bioflavonoids, proanthocyanidins, ellipiticine, taxol, indole derivatives, dithiolthiones, phytoestrogens and others, which have chemopreventative and/or anticancer properties with additional oxidative stress inhibitory properties (Bagchi *et al*., 2000).

ROS and phagocytosis. Phagocytes (including neutrophils, monocytes, macrophages, polymorphonuclear leukocytes and eosinophils) play an important role in the first line defense against bacteria, viruses and fungi (Salih *et al*., 2000). Bacterial engulfment by phagocytes is associated with enzyme activation, increased oxygen consumption and ROS production (Salganik, 2001). Respiratory burst does not only kill ingested microorganisms, but also cause endothelial damage, increased vascular permeability and cell death, which may result in sepsis, rheumatic diseases and adult respiratory distress syndrome (Guzik *et al*., 2003; Rothe and Valet, 1990). Electrons required to reduce O_2 to

O_2^- are supplied by NADPH (Forman and Torres, 2002; Salganik, 2001). Subunits of NADPH oxidase are found in the cytosol and assemble at the plasma membrane to form an active enzyme. Active NADPH oxidase produces the central free radical, O_2^-, involved in H_2O_2 production (Barbieri *et al*., 2003; Böhmer *et al*., 1992; Brown and Bicknell, 2001; Forman and Torres, 2002; Kampen *et al*., 2004). O_2^- dismutates spontaneously or by SOD activity to H_2O_2, which is converted to hypochlorous acid and chloramines via myeloperoxidase inside the phagosome (Forman and Torres, 2002; Rothe and Valet, 1990). In general, ROS production increase with increased bacterial concentration, but high bacterial concentrations may increase the risk of cell death and clumping (Kampen *et al*., 2004). Lack of NADPH oxidase, which is associated with chronic granulomatous disease, may result in a lack of ROS production and poor clearance of pathogenic bacteria and fungi (Forman and Torres, 2002). NADPH oxidase is also found in fibroblasts, mesangial cells, osteoclasts, endothelial cells and chondrocytes. Rate of ROS generation is very low in these cells compared to phagocytes; hence ROS's role in phagocytosis (Hancock *et al*., 2001).

ROS production is associated with phagocytosis, which has been investigated in Chapter 6 (section 6.5). This section focuses on the effect of *Hypoxis* extracts and its purified compounds on ROS production in undifferentiated and differentiated U937 cells.

7.2.2. Materials and Methods

Undifferentiated U937 cells. Human promonocytic leukemia U937 cells were counted, resuspended in RPMI1640: 10% fbs at cell densities of $1x10^6$ cells/mL. U937 cells were uniformly stained by adding 1 mM 2,7-dichlorofluorescein diacetate (DCFH-DA) stock solution to reach a final concentration of 1 μM. Cells were mixed and incubated in the dark for 30 min at 37 ºC. Excess DCFH-DA was removed and cells washed twice with complete medium by centrifuging at 250 x g for five min at room temperature. Fifty thousand cells were added to polypropylene tubes and treated with DMSO (2.5%, v/v), *H. hemerocallidea* (125 μg/mL), *H. stellipilis* (125 μg/mL), *H. sobolifera* (125 μg/mL), hypoxoside (50 μg/mL), rooperol (20 μg/mL), CD (4mM)/EtOH (5%, v/v), β-sitosterol

(30 μM), campesterol (30 μM), cholesterol (30 μM), stigmasterol (30 μM), PMA (10-100 nM) or LPS (100-500 ng/mL) for one hour at 37 °C. After treatment, cells were pelleted and washed with PBS as described above. Cells were resuspended in PBS (500 μL) and samples read on a Coulter FC500 flow cytometer. Mean fluorescence intensity (MFI) of treated cells was expressed as a percentage of the MFI of control cells. Statistical significance was determined using the two-tailed Student's t-test.

Differentiated U937 cells. U937 cells were counted, resuspended in RPMI1640: 10% fbs and differentiated for 24 hrs with 100 nM $1,25(OH)_2D_3$. Above procedure for undifferentiated U937 cells was followed.

7.2.3. Results and Discussion

Oxidative burst was measured by the reaction between DCFH-DA and ROS. Non-polar and non-fluorescent DCFH-DA was loaded into undifferentiated and differentiated U937 cells via passive membrane diffusion, where it remains trapped in the cells. Inside the cell, the dye is deacetylated by non-specific esterases to form the polar, non- or weakly fluorescent 2',7'-dichlorofluorescein (DCFH). ROS released after phagocytosis oxidize DCFH, via two electron oxidation, to highly green-fluorescent dichlorofluorescein (DCF) (Andoh *et al*., 2006; Böhmer *et al*., 1992; Zielonka and Kalyanaraman, 2008). Green fluorescence measured under conditions of intracellular oxidative stress is not a measure of intracellular H_2O_2 or other intracellular radicals, but a combination of several factors including GSH, altered iron uptake, increased peroxidase activity, cytochrome c release, and others (Zielonka and Kalyanaraman, 2008).

Undifferentiated U937 cells. U937 cells were treated with *Hypoxis* extracts and purified compounds for one hour, and ROS production measured (Figure 7.2).

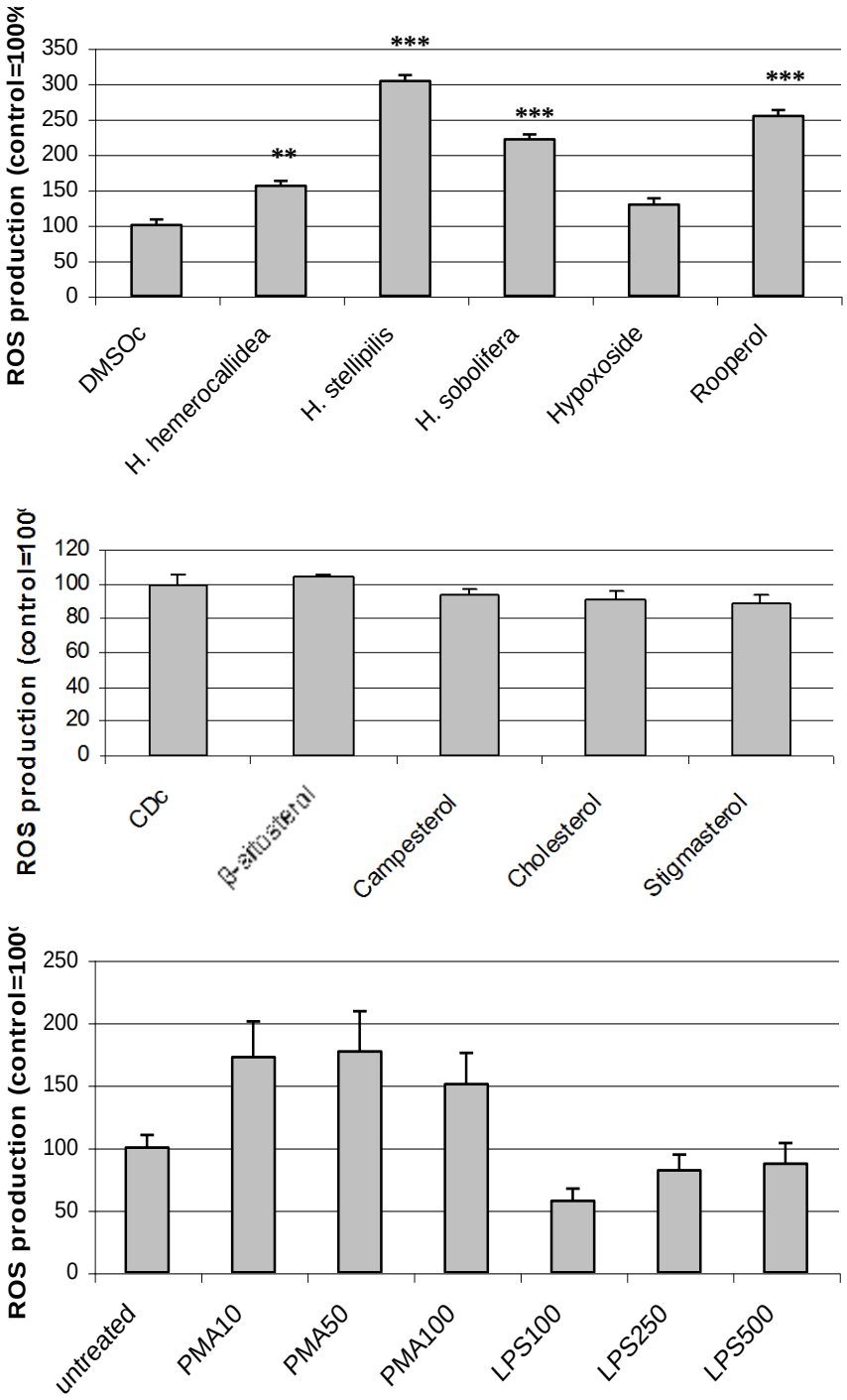

Figure 7.2: ROS production by undifferentiated U937 cells after one hour treatment with DMSOc, *Hypoxis* chloroform extracts, hypoxoside and rooperol (A), CD/EtOHc and (phyto)sterols (B), untreated, PMA and LPS (C). Bar graph percentages represent the increase in mean fluorescence intensity of cells staining positive for ROS production when treated samples were compared to control. Error bars represent the SD of triplicate values. One representative of three experiments performed. Significance was determined using the two-tailed Student t-test: *p<0.01; **p<0.001; ***p<0.0001 compared to control.

Significant amounts of ROS were produced when undifferentiated U937 cells were treated with the three *Hypoxis* extracts and rooperol. When compared to the controls, *H. hemerocallidea*, *H. stellipilis*, *H. sobolifera* and rooperol produced 1.6, 3.0, 2.2 and 2.5 times more ROS, respectively. ROS production by hypoxoside and PMA (50 nM) were not significantly different from the control, with only a 1.3 and 1.8 times increase for the former and latter, respectively. β-sitosterol, campesterol, cholesterol, stigmasterol and LPS had no effect on ROS production. Histogram overlays of the treatments showing significant differences are shown in Appendix 7.

Differentiated U937 cells. U937 cells were differentiated to monocyte-macrophages by $1,25(OH)_2D_3$, treated with *Hypoxis* extracts and purified compounds for one hour, and ROS production measured (Figure 7.3).

Significant amounts of ROS were produced when differentiated monocyte-macrophages were treated with the three *Hypoxis* extracts, rooperol and PMA. When compared to the controls, *H. hemerocallidea*, *H. stellipilis*, *H. sobolifera*, rooperol and PMA (50 nM) produced 1.8, 4.7, 2, 6.2 and 2.7 times more ROS, respectively. ROS production by hypoxoside, β-sitosterol, campesterol, cholesterol, stigmasterol and LPS (250 ng/mL) were not significantly different from the control, with only 1.1, 1.3, 1.4, 1.3, 1.2 and 1.3 times increase, respectively. Histogram overlays of the treatments showing significant differences are shown in Appendix 7. The optimal effect of the positive controls (PMA and LPS) may have occurred at lower concentrations; hence the absence of dose-related effects.

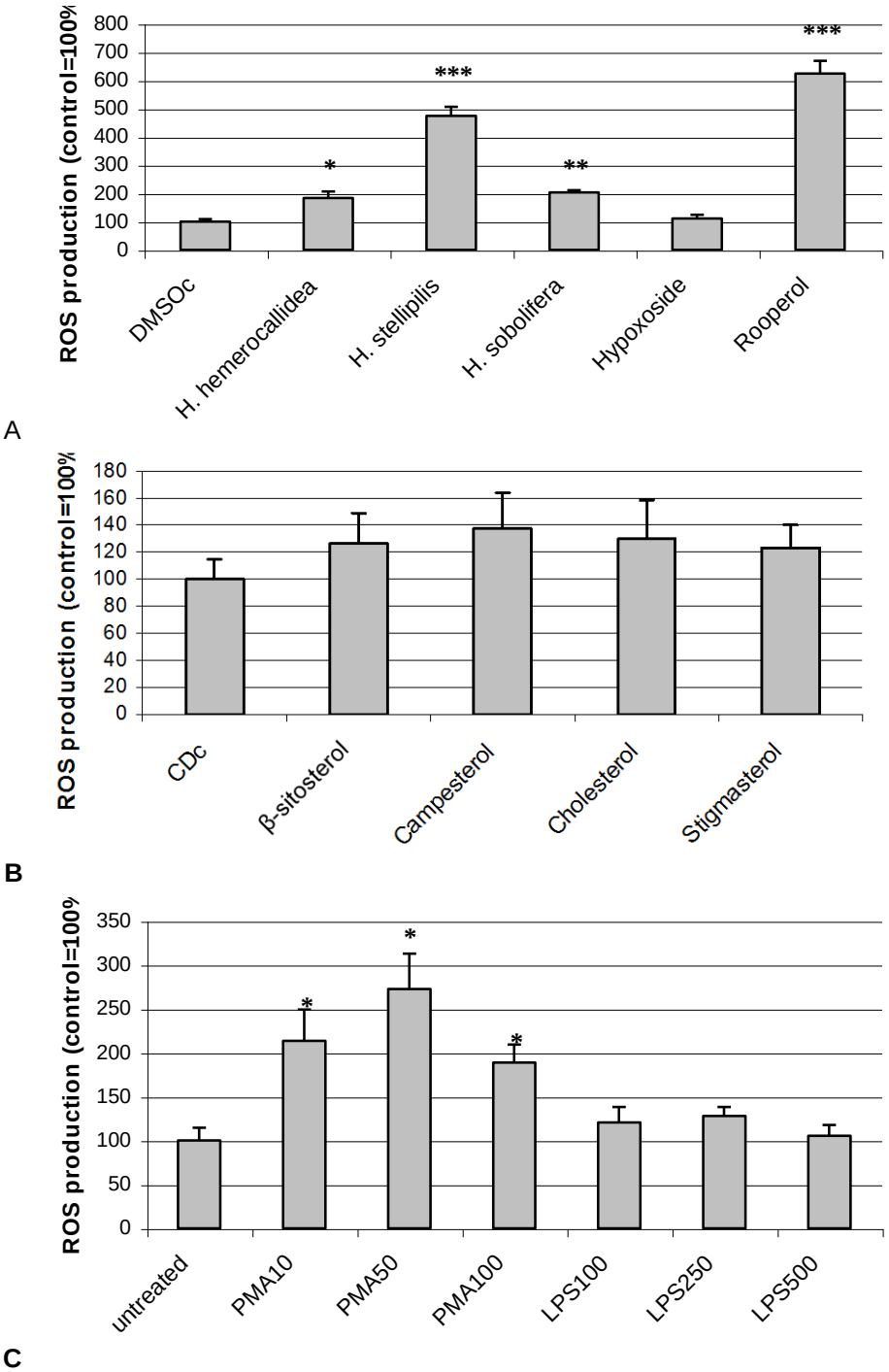

Figure 7.3: ROS production by differentiated U937 cells after one hour treatment with DMSOc, *Hypoxis* chloroform extracts, hypoxoside and rooperol (A), CD/EtOHc and (phyto)sterols (B), untreated, PMA and LPS (C). Bar graph percentages represent the increase in mean fluorescence intensity of cells staining positive for ROS production when treated samples were compared to control. Error bars represent the SD of triplicate values. One representative of three experiments performed. Significance was determined using the two-tailed Student t-test: *p<0.01; **p<0.001; ***p<0.0001 compared to control.

When comparing ROS production in undifferentiated (monocytes) and differentiated (monocyte-macrophages) U937 cells, a more pronounced increase in ROS production was seen in differentiated cells. This may be explained by the greater role played by macrophages during phagocytosis (Chapter 6; section 6.5). This was the first time that ROS production was investigated in differentiated and undifferentiated U937 cells when treated with *Hypoxis* extracts and its purified compounds.

Measurement of respiratory burst is an indication of defense against bacterial infections. Reduced respiratory burst is associated with impaired ability to kill bacteria and increased susceptibility to infectious diseases (Kampen *et al*., 2004). Guzdek *et al.* (1997) have shown that rooperol tetraacetate inhibits respiratory burst in human and rat macrophages. Mechanisms of respiratory burst inhibition by rooperol may include LPS priming, direct interaction with enzymatic pathway where oxygen radicals are formed by NADPH oxidase, and/or involvement of cell membrane constituents (e.g. PKC). Results of Guzdek *et al*. (1997) are in contradiction with the results found in this study. Barbieri *et al*. (2003) have shown that NADPH oxidase subunits are upregulated during monocytic differentiation with PMA. PMA stimulates NADPH oxidase assembly in phagocytes. PMA is a respiratory burst stimulant, which promotes ROS production via PKC activation. Stimulation of ROS production by bacteria is complex (Kampen *et al*., 2004). LPS, a component of the outer membrane of gram-negative bacteria, enhances oxidative burst (including the release of oxygen radicals and lysosomal enzymes) and phagocytosis in neutrophils *in vitro* (Böhmer *et al*., 1992). LPS had no effect on ROS production in this study. $1,25(OH)_2D_3$ was used to differentiate U937 cells to monocyte-macrophages, which may have upregulated NADPH oxidase subunits and stimulated NADPH oxidase assembly. The differences observed between differentiated and undifferentiated U937 cells may suggest an increase in ROS production by NADPH oxidase, which plays an important role in phagocytosis. Pretreatment of monocyte-macrophages with *Hypoxis* chloroform extracts, rooperol and β-sitosterol increased phagocytosis (Chapter 6, section 6.5) of pHrodo™ *E. coli* Bioparticles®. Increases were small, but significantly different. ROS production by the *Hypoxis* chloroform extracts, rooperol and β-sitosterol may have increased the phagocytotic ability of monocyte-macrophages.

This study has shown that β-sitosterol, campesterol, cholesterol and stigmasterol had no significant effect on ROS production in undifferentiated or differentiated U937 cells. DCFH-DA was preloaded into undifferentiated and differentiated U937 cells before treatments; hence only an increase in ROS production could be measured with treatments. Phytosterols may have decreased ROS production, but could not be measured. This is the major limitation of measuring ROS production using a dye. Moreno (2003) has shown that β-sitosterol (50-250 μM) decreases H_2O_2 and O_2^- production in PMA stimulated RAW264.7 macrophages. Inhibitory effects were seen after 3-6 hrs pretreatment with β-sitosterol before PMA stimulation. Rats fed an olive oil diet (β-sitosterol being the major phytosterol) released less O_2^-, decreased eicosanoid production and increased NO production. β-sitosterol may be involved in the AA cascade, associated with inflammation. AA is released from cellular phospholipids by $cPLA_2$ in response to physiological stimuli, prior to the COX and/or lipooxygenase pathways. β-sitosterol decreases ROS production and AA release simultaneously. ROS are involved in enhancing COX-2 expression and ROS-induced COX-2 expression. β-sitosterol alters membrane fluidity and activity of membrane bound enzymes like $cPLA_2$, which is involved in AA release and eicosanoid production (Moreno, 2003).

7.3. Antioxidant Capacity (syn. -efficiency, -power, -potential)

7.3.1. Background

The FRAP and DPPH assays are based on single electron transfer reactions, which measure the antioxidant reducing capacity. It measures the oxidant-scavenging capacity, instead of the preventive antioxidant capacity of the sample. These assays are based on chemical reactions *in vitro*, and cannot be compared to biological systems (Huang *et al*., 2005).

The FRAP assay measures the reduction of ferric (Fe^{3+})-tripyridyltriazine (TPTZ; oxidant) to blue coloured ferrous (Fe^{2+})-TPTZ at an acidic pH in the presence of an

antioxidant (Figure 7.4). The oxidant and antioxidant get reduced and oxidized, respectively (Benzie and Strain, 1996; Cao and Prior, 1998; Huang *et al*., 2005). The degree of colour change is proportional to the antioxidant concentration (Huang *et al*., 2005). The use of Fe^{2+} as a final indicator in the FRAP assay can cause problems when the antioxidant analyzed does not only reduce Fe^{3+} to Fe^{2+}, but also reacts with Fe^{2+} to form additional free radicals. The FRAP assay does not measure serum proteins (e.g. albumin) or low molecular weight SH-group-containing antioxidants (e.g. lipoic acid, some amino acids) (Cao and Prior, 1998). The FRAP assay is inexpensive, reagents are simple to prepare, results are highly reproducible, and the procedure is easy and fast (Benzie and Strain, 1996).

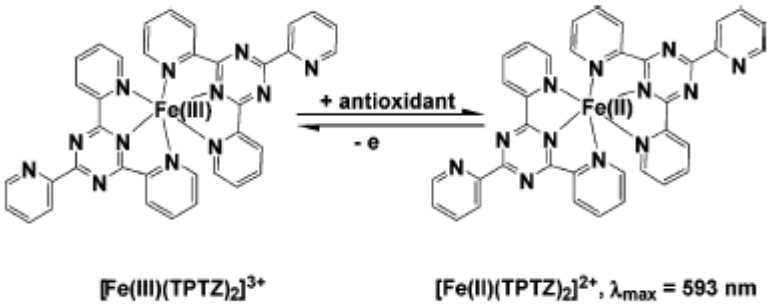

Figure 7.4: Reduction of Fe^{3+}-TPTZ to Fe^{2+}-TPTZ (Huang *et al*., 2006).

Nair *et al*. (2007b) investigated the antioxidant activities of *H. hemerocallidea*, hypoxoside and rooperol using the DPPH and FRAP assays. This section focuses on the antioxidant potential of *Hypoxis* extracts and its purified compounds.

7.3.2. Materials and Methods

Stock solutions of *H. hemerocallidea* (5 mg/mL), *H. stellipilis* (5 mg/mL), *H. sobolifera* (5 mg/mL), hypoxoside (1 mg/mL), rooperol (1 mg/mL), β-sitosterol (1 mM), campesterol (1 mM), cholesterol (1 mM) and stigmasterol (1 mM) were prepared in absolute EtOH. Ascorbic acid was dissolved in distilled water (1 mg/mL). A range of concentrations of *Hypoxis* extracts (62.5-5 000 μg/mL), hypoxoside and rooperol (1-200 μg/mL), phyto(sterols) (1-500 μM) and ascorbic acid (0.5-100 μg/mL) were tested for

ferric ion reducing power. A $FeSO_4$ standard curve, ranging between 50-1 000 μmol/L was prepared.

The FRAP reagent was prepared on the day of the assay by mixing 20 mL sodium acetate buffer (300 mM), 2 mL TPTZ solution (10 mM TPTZ and 40 mM HCl dissolved at 50 ºC in a water bath; freshly prepared), 2 mL $FeCl_3$ solution (20 mM ferric chloride in distilled water; freshly prepared) and 2.4 mL distilled water. The FRAP reagent should be straw coloured and kept at 37 ºC. Samples (10 μL) were transferred to a 96-well plate, FRAP reagent (240 μL) added, and incubated for five min at 37 °C. Absorbance was read at 593 nm using a BioTek® PowerWave XS spectrophotometer (Winooski, VT, USA). No background interference was present for the extracts or purified compounds at concentrations tested. Statistical significance was determined using the two-tailed Student's t-test.

7.3.3. Results and Discussion

The ferric reducing activity of *Hypoxis* extracts and its purified compounds (Figure 7.5A-D) were determined from a standard curve (Appendix 7) of $FeSO_4$ concentration (ranging between 50-1 000 μmol/L) as a function of absorbance at 593 nm (R^2 = 0.9916). Concentrations of *Hypoxis* extracts tested did not exceed 200 μg/mL, because a concentration of 125 μg/mL was used for the ROS (section 7.2) and NO (Chapter 6; section 6.3) production studies. Concentrations of rooperol and ascorbic acid were in a similar range for comparison sake and higher concentrations would not be physiologically relevant. Phytosterol concentrations in the serum ranges between 7 and 41 μM (von Holtz *et al*., 1998); hence the use of lower (phyto)sterol concentrations.

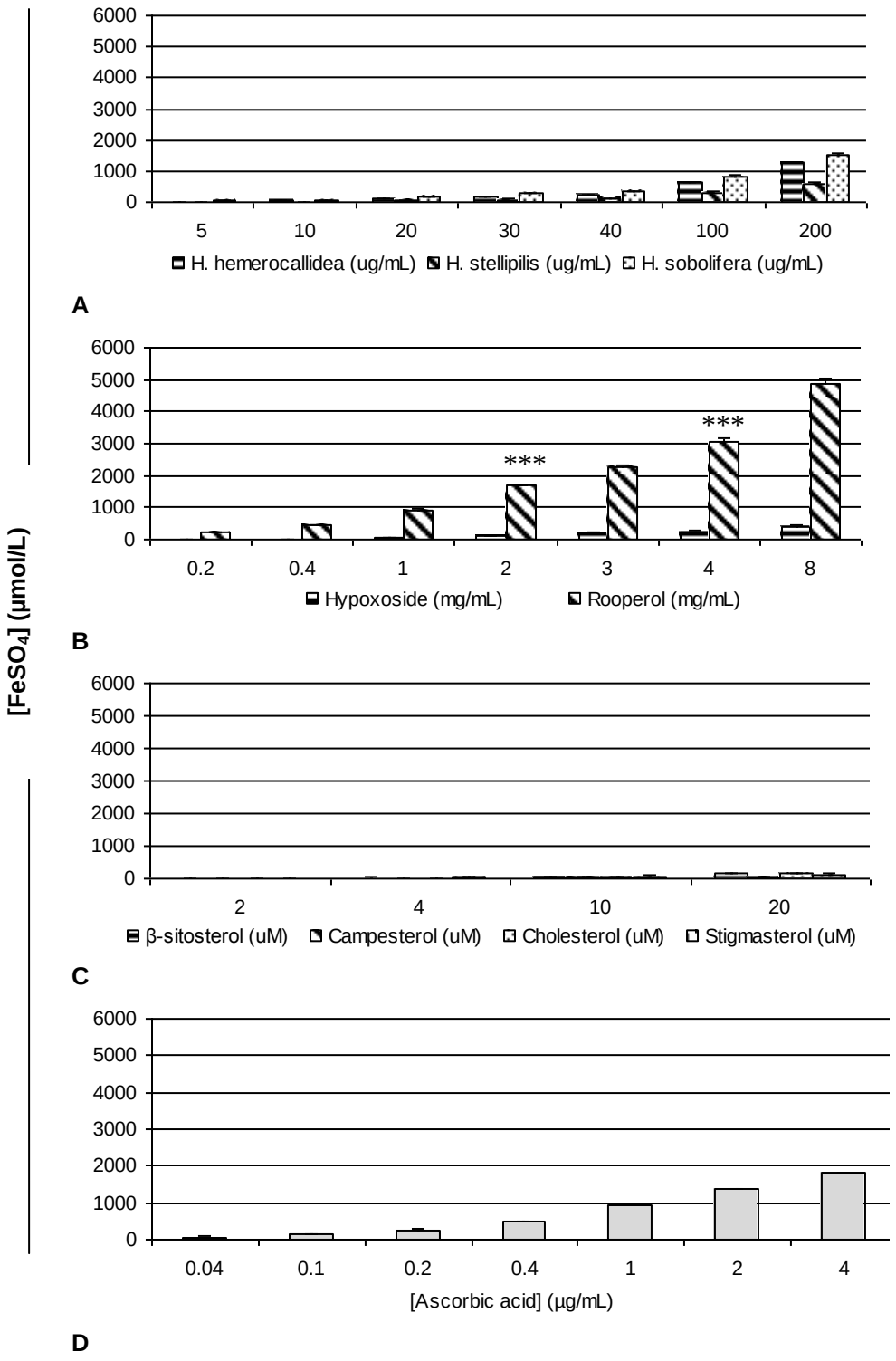

Figure 7.5: FRAP antioxidant potential of *Hypoxis* chloroform extracts (A), hypoxoside and rooperol (B), (phyto)sterols (C) and ascorbic acid (D). Error bars represent SD of quadruplicate values. Significance (comparing 1, 2 and 4 µg/mL of rooperol and ascorbic acid) was determined using the two-tailed Student t-test: *p<0.01; **p<0.001; ***p<0.0001.

The DPPH assay has shown no antioxidant capacity of *Hypoxis* chloroform extracts and its purified compounds (data not shown). Nair *et al*. (2007b) have shown that rooperol and quercetin had similar antioxidant capacity at the same concentrations (>8 μg/mL), while hypoxoside had no significant antioxidant capacity at high concentrations (32 μg/mL) when the DPPH assay was used. *H. sobolifera* had the greatest ferric reducing activity followed by *H. hemerocallidea* and *H. stellipilis*. The ferric reducing activity of rooperol (concentrations of 1, 2 and 4 μg/mL) was significantly greater ($p<0.0001$) than ascorbic acid at the same concentrations, which suggests that rooperol has greater antioxidant capacity than ascorbic acid. This is still the case if molar concentrations are compared: the corresponding molar concentrations for 1, 2 and 4 μg/ml are 5.7, 11.4 and 22.7 μM and 3.5, 7.1 and 14.2 μM for ascorbic acid and rooperol, respectively. Nair *et al*. (2007b) also showed that rooperol had significantly greater ferric reducing activity than ascorbic acid at the same concentrations (8, 16 and 32 μg/mL), while hypoxoside had no significant antioxidant capacity in the DPPH and FRAP assays. The present study confirmed that hypoxoside had very little ferric reducing activity when compared to the *Hypoxis* extracts and rooperol. Laporta *et al*. (2007b) have investigated the antioxidant capacity of hypoxoside, rooperol and *H. hemerocallidea* (containing 45% hypoxoside) using the thiobarbituric acid reactive substances (TBARS), oxygen radical absorbance capacity (ORAC) and Trolox equivalent antioxidant capacity (TEAC) assays. The TEAC assay has shown that rooperol had higher antioxidant activity than hypoxoside. The *H. hemerocallidea* extract had a higher antioxidant potency compared to green tea (70% catechins) and olive leaf (25% oleuropin) when using the ORAC assay.

Nair *et al*. (2007b) have shown high levels of antioxidant capacity with an aqueous extract of *H. hemerocallidea* (100, 500 and 1000 μg/mL), which increased with increasing concentration, when the DPPH and FRAP assays were used. A concentration dependent increase in ferric reducing activities was seen with *Hypoxis* extracts in this study.

Nair *et al*. (2007b) have shown that *H. hemerocallidea* extracts (2.5 and 5 mg/mL) and rooperol (7.5-30 μg/mL) significantly reduced quinolinic acid (QA) induced lipid peroxidation in rat liver. At 30 μg/mL rooperol completely abolished QA induced lipid peroxidation via scavenging free radicals or preventing QA-ferrous ion complex formation by interacting with ferrous ions. Hypoxoside (50 μg/mL) did not reduce lipid peroxidation (Nair *et al*., 2007). Laporta *et al*. (2007b) have shown that rooperol has a higher capacity to inhibit lipid peroxidation compared to hypoxoside, when measured by TBARS, which may be due to its strong affinity for phospholipid membranes. Rooperol's IC_{50} of total lipid peroxidation was lower than potent antioxidants isolated from green tea [(+)-catechin, (-)-epicatechin, (-)-epicatecin gallate, (-)-epigallocatechin gallate] and olive leaves (oleuropein and hydroxytyrosol), and was at similar concentrations as (-)-epicatechin gallate. A *H. hemerocallidea* extract had also a higher capacity to inhibit lipid peroxidation compared to green tea and olive leaf extracts.

In summary, this study showed for the first time that *H. hemerocallidea*, *H. stellipilis* and *H. sobolifera* chloroform extracts have *in vitro* antioxidant activities. Antioxidant activity of rooperol and very little or no antioxidant activity of hypoxoside were confirmed by previous reports by Nair *et al*. (2007b) and Laporta *et al*. (2007b).

7.4. Superoxide Dismutase

7.4.1. Background

SOD catalyzes the dismutation of two molecules of the highly reactive O_2^- to O_2 and less reactive, non-radical H_2O_2. See section 7.2 for more detail.

O_2^- is the central free radical, giving rise to H_2O_2 and OH^- formation; hence the investigation of SOD. This section focuses on the effect of *Hypoxis* extracts and its purified compounds on SOD activity.

7.4.2. Materials and Methods

Chang liver cells were seeded at densities of 40 000 cells/mL in 24-well plates and left to attach overnight at 37 ºC in a humidified incubator and 5% CO_2. Chang liver cells were chosen to investigate SOD activity, because hepatocytes contain high levels of detoxification enzymes. Cells were treated with DMSO (0.25%, v/v), *H. hemerocallidea* (125 µg/mL), *H. stellipilis* (125 µg/mL), *H. sobolifera* (125 µg/mL), hypoxoside (50 µg/mL), rooperol (20 µg/mL), CD (4 mM)/EtOH (5%, v/v), β-sitosterol (30 µM), campesterol (30 µM), cholesterol (30 µM), stigmasterol (30 µM), ciprofibrate (PPARα agonist; 1 mM) or rosiglitazone (PPARγ agonist; 1 mM) for 24 hrs. Supernatants were transferred to 1.5 mL Eppendorf tubes, cells pelleted by centrifuging at 2 500 x g for five min at room temperature and supernatant discarded. Adherent cells were washed with PBS and CytoBuster™ protein extraction reagent (100 µL; Novagen) was added and allowed to extract for five min at room temperature. Cells were scraped with a cell scraper and transferred to the appropriate Eppendorf tubes. Extracts were centrifuged at 15 000 x g for five min at 4 °C and the supernatants transferred to new Eppendorf tubes and kept on ice for analysis or frozen at -20 °C. SOD activity was determined using the SOD determination kit (Fluka/Sigma). In brief, samples and blanks were prepared as described in the protocol, incubated at 37 °C for 20 min and absorbance read at 450 nm using a BioTek® PowerWave XS spectrophotometer. SOD activity was determined using the following formula: [(S1-S3)-(SS-S2)]/(S1-S3) x 100, where S1 = slope of blank 1 without sample, S2 = slope of blank 2 without enzyme working solution, S3 = slope of blank 3 without sample and enzyme working solution, SS = slope of sample. Statistical significance was determined using the two-tailed Student's t-test.

7.4.3. Results and Discussion

The SOD determination kit is used to overcome the disadvantages (including poor water solubility, and interaction with or inhibition of xanthine oxidase) associated with NBT (Huang *et al*., 2005). The highly water-soluble 2-(4-iodophenyl)-3-(4-nitrophenyl)-5-

(2,4-disulfophenyl)-2H-tetrazolium monosodium salt is reduced to a water-soluble formazan dye by O_2^-. Figures 7.6A-C summarize the effect of *Hypoxis* extracts, hypoxoside, rooperol, (phyto)sterols and positive controls on SOD activity.

Hypoxis extracts, hypoxoside and rooperol had no significant effects on SOD activity (Fig. 7.6). β-sitosterol, campesterol and cholesterol significantly ($p<0.01$ to $p<0.001$) increased SOD activity, but the increases were lower than the two positive controls, ciprofibrate and rosiglitazone. *Hypoxis* extracts (crude extracts containing other compounds), hypoxoside and rooperol may act directly as antioxidants, as seen with increased FRAP antioxidant potential (Figure 7.5), rather than influencing the levels and activity of antioxidant enzymes, including SOD. The optimal effect of the positive control (rosiglitazone) may have occurred at lower concentrations, hence the absence of a dose-related effect.

Literature on the effect of *Hypoxis* extracts and its purified compounds on non-enzymatic and enzymatic antioxidant defense mechanisms are limited. Vivancos and Moreno (2005) have shown that β-sitosterol enhances the expression and activity of MnSOD (but not Cu/ZnSOD) and GPX activity, reduces O_2^- and H_2O_2 levels, impairs CAT activity, enhances the GSH/total glutathione ratio, and stimulates antioxidant enzymes via the estrogen/PI3K dependent pathways in RAW264.7 macrophages. These studies suggest that β-sitosterol protects against oxidative stress via antioxidant enzyme modulation (Vivancos and Moreno, 2005). The present study confirmed the effect of β-sitosterol on SOD activity and has shown for the first time that cholesterol and campesterol have similar effects to β-sitosterol, whereas stigmasterol had no effect.

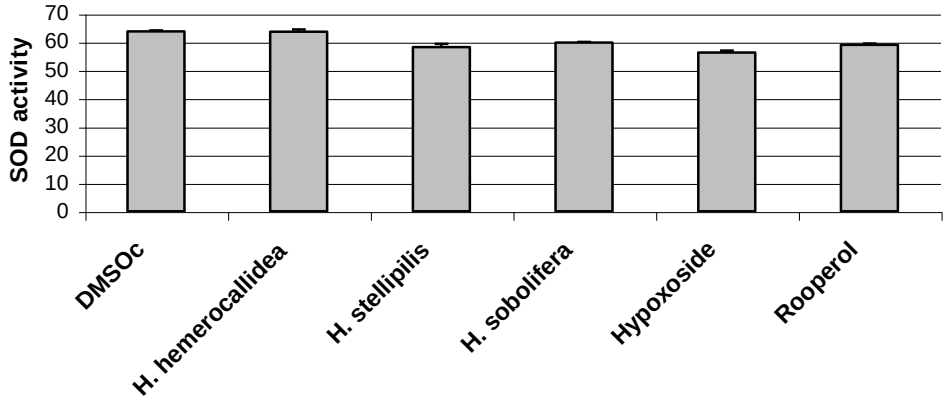

A

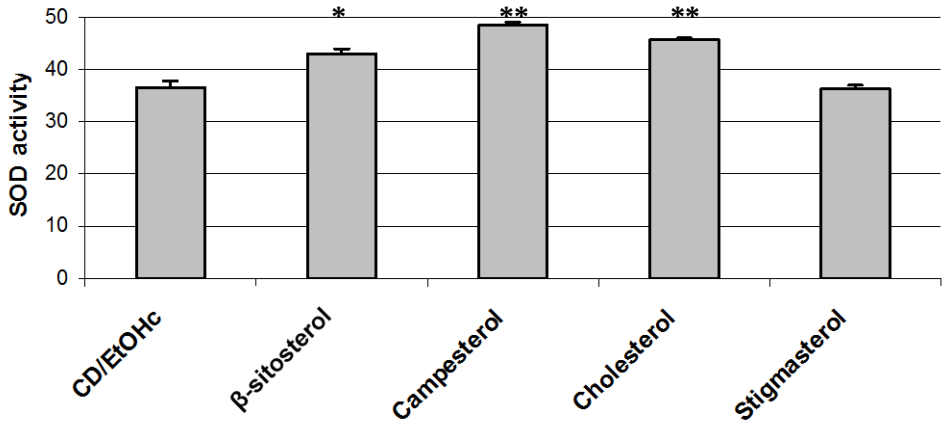

B

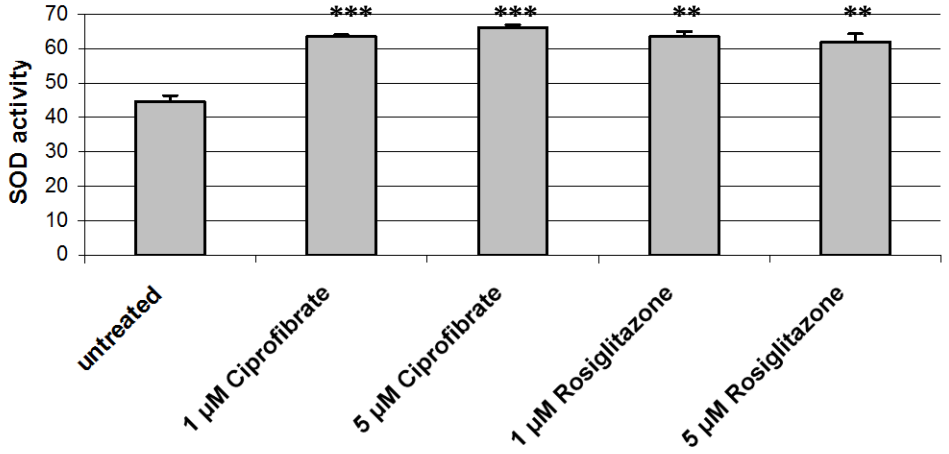

C

Figure 7.6: SOD activation of DMSOc, *Hypoxis* chloroform extracts, hypoxoside and rooperol (A), CD/EtOHc and (phyto)sterols (B), untreated, ciprofibrate and rosiglitazone (C) treated Chang liver cells. Error bars represent the SD of triplicate values. One representative of three experiments performed. Significance was determined using the two-tailed Student t-test: *p<0.01; **p<0.001; ***p<0.0001 compared to control.

7.5. Conclusion

The present study has shown, for the first time, that treatment of undifferentiated and differentiated U937 cells with *H. hemerocallidea*, *H. stellipilis*, *H. sobolifera* and rooperol increased ROS production. ROS production in monocyte-macrophages was probably due to the activation of NADPH oxidase, which plays an important role in phagocytes during phagocytosis. None of the (phyto)sterols tested had significant effects on ROS. Rooperol has greater ferric reducing activity than ascorbic acid at the same concentrations. Of the three plant extracts, *H. sobolifera* had the best ferric reducing activity while the phytosterols showed very low activity compared to the positive control. Increased SOD activity was absent in *Hypoxis* extract and rooperol treated Chang liver cells. β-sitosterol, campesterol and cholesterol all increased SOD activity but stigmasterol had no effect. Hypoxoside had no significant antioxidant effects, which further proves rooperol's role as the active compound. Pretreatment of monocytes or monocyte-macrophages with *Hypoxis* extracts and its purified compounds, followed by a ROS (e.g. PMA) producing stimulant, may explain possible preventative effects of the extracts or compounds tested. On the other hand pretreatment of a ROS stimulant, followed by *Hypoxis* extracts and its purified compounds, may explain possible 'treatable' effects of these extracts and compounds. Increased ROS production, antioxidant potential and SOD activation may contribute to the antimicrobial, anticancer, anti-inflammatory and immune stimulating properties of *Hypoxis* and its purified compounds. These activities may be dependent on the type of extract and purified compounds used.

CHAPTER 8
CONCLUDING REMARKS

The main aim of this study was to provide scientific data on the medicinal properties of one of the most controversial plants used in South Africa, and the most commonly sold medicinal plant in the Eastern Cape province of South Africa. This study compared the active compounds, and *in vitro* biological (including anticancer, anti-inflammatory and antioxidant) properties of three *Hypoxis* spp. chloroform extracts, namely *H. hemerocallidea*, *H. stellipilis* and *H. sobolifera*.

Identification and quantification of active compounds in *Hypoxis* extracts were important in explaining the biological activities of the crude extracts. Analytical analysis has for the first time shown the presence of hypoxoside in *H. hemerocallidea* and *H. stellipilis* chloroform extracts, and β-sitosterol as the main phytosterol in all three *Hypoxis* chloroform extracts. Trace amounts of campesterol, stigmasterol and stigmastenol were present in the three *Hypoxis* extracts. This confirms the presence of β-sitosterol, campesterol and stigmasterol as the three most commonly found phytosterols in plants. Phytosterols present in *Hypoxis* extracts were for the first time analyzed using a specifically developed GC method for their identification and quantification. HPLC analysis of the *Hypoxis* extracts has revealed the presence of unidentified compounds, which merits further investigation. The solvent choice for a *Hypoxis* extract plays an important role in the isolation of a specific compound. Polar and non-polar solvents were more effective in extracting more polar (e.g. hypoxoside and sterolins) and non-polar (e.g. sterols) compounds, respectively. Chloroform is a non-polar solvent and it can be concluded that the compounds isolated from the *Hypoxis* material were more non-polar compounds (phytosterols and other unknown compounds). All of the *in vitro* biological (anticancer, anti-inflammatory and antioxidant) effects seen in the *Hypoxis* chloroform extracts may be contributed to hypoxoside (*H. hemerocallidea* and *H. stellipilis*), phytosterols (three *Hypoxis* spp.) and/or unidentified compounds. An article on the analytical analysis of the hypoxoside and sterol(in)s content of the three *Hypoxis* spp. was published in the peer-reviewed journal, African Journal of Biotechnology.

β-glucosidase levels in the medium and lysates of HeLa, HT-29 and MCF-7 cancer cells were insufficient for the conversion of hypoxoside to rooperol, hence the addition of 100 μg/mL β-glucosidase to all *Hypoxis* extracts and hypoxoside treatments. IC_{50} values for hypoxoside and rooperol treated HeLa, HT-29 and MCF-7 cancer cells were determined. Cytotoxicity of *Hypoxis* extracts was low, with less than 20% of the cancer cells killed. In general, the *H. sobolifera* extract had the best overall cytotoxic effect against all three cancer cell lines investigated. Growth stimulation of HeLa and HT-29 cancer cells in the presence of a *H. stellipilis* extract is a concern, because *H. stellipilis* is often sold in the herbal shops of the Eastern Cape. Consumption of a *H. stellipilis* extract may have adverse effects on patients suffering from cancer and may have potential adverse health implications. Hypoxoside conversion to rooperol was investigated in the three cancer cell lines. DNA cell cycle arrest, caused by the *Hypoxis* extracts and rooperol, was investigated in the three cancer cell lines. DNA cell cycle arrest occurred in the late G1 and/or early S (confirmed by increased levels of $p21^{Waf1/Cip1}$), and G2/M phases after 15 and 48 hrs, respectively, of treatment. *H. sobolifera* (*Hypoxis* spp. with the best overall cytotoxic effect) and rooperol increased caspase-3 and -7 activation in HeLa and HT-29 cancer cells, and caspase-7 activation in MCF cancer cells. Only rooperol caused phosphatidylserine translocation in U937 leukemia cells after 15 hrs of treatment, which was associated with early apoptosis. *H. sobolifera* and rooperol increased DNA fragmentation in HeLa, HT-29 and MCF-7 cancer cells. Anticancer properties of the *Hypoxis* chloroform extracts may be attributed to the presence of β-sitosterol, which has been shown by other researchers to have anticancer properties. This was the first time that the anticancer mechanisms of action of rooperol and *Hypoxis* extract(s) were investigated. An article on rooperol's cytotoxicity and mechanism of action was accepted for publication in the peer-reviewed journal, Oncology Research.

Endoreduplication in *Hypoxis* extract and rooperol treated HeLa, HT-29 and MCF-7 cancer cells were first identified from histograms during DNA cell cycle analysis, as a peak of higher fluorescence intensity shifting past the G2/M phase. This is also the first time endoreduplication was seen in a *Hypoxis* extract and rooperol treated cancer cells.

Endoreduplication was confirmed by higher phospho-Akt, phospho-Bcl-2 and $p21^{Waf1/Cip1}$ levels in HeLa, HT-29 and MCF-7 cancer cells. No increase was seen in the total amount of unphosphorylated (inactive) Akt, suggesting enhanced signalling through Akt in the presence of these treatments rather than increased expression of signalling intermediates. Morphological features of cells undergoing endoreduplication include 'giant cells' and enlarged nuclei as shown by microscopy. Differences in cell size and complexity in dot plots confirmed endoreduplication. Endoreduplication may be a survival strategy of cancer cells prior to apoptosis, because cells with apoptotic morphological features (including cell membrane blebbing, apoptotic body formation and chromatin condensation) were seen among the 'giant' cells. Considering the possible involvement of endoreduplication in the development of drug resistance in chemotherapy, this observation also merits further investigation.

Monocyte to monocyte-macrophage differentiation of U937 leukemia cells was investigated using PMA and $1,25(OH)_2D_3$ at different concentrations and time intervals. Morphological features, including cell clumping, cell attachment (PMA only) and pseudopodia formation confirmed successful monocyte-macrophage differentiation. Furthermore, increased CD11b and CD14 cell surface marker expression confirmed monocyte-macrophage differentiation. $1,25(OH)_2D_3$ was used as the differentiation agent due to higher cell viability compared to PMA. It was the first time that NO production and phagocytosis were investigated in monocyte-macrophages using *Hypoxis* extracts and its purified compounds. *Hypoxis* extracts and rooperol significantly increased NO production in monocyte-macrophages. NO plays an important role in maintaining physiological/pathophysiological functions (low amounts) and inflammation (high amounts), and acts as an anti (low or physiological amounts)- or pro-apoptotic (high amounts) molecule in cancer. Although *Hypoxis* extracts and its purified compounds did not influence the expression of COX-2 in monocyte-macrophages, COX-2 activity may have been influenced as shown by previous studies. *Hypoxis* extracts and rooperol increased phagocytosis of pHrodo™ *E.coli* Bioparticles® by monocyte-macrophages. Increased phagocytosis may play an important role in the elimination of apoptotic cells expressing phosphatidylserine. Phagocytes (e.g. macrophages) activate NOS leading to

NO production for elimination of microorganisms. *Hypoxis* extracts and rooperol had very little effect on the levels of pro- and anti-inflammatory cytokines, compared to sterols. Increases in pro-inflammatory cytokines (e.g. IL-1β and IL-6) by sterols found in this study were in contradiction with other studies. Stimulation of PBMCs with an appropriate stimulant (e.g. LPS, PMA or PHA), prior to treatment, may provide information on the stimulatory and/or inhibitory effect of *Hypoxis* spp. extracts and its purified compounds on cytokine secretion.

It was the first time that ROS production was investigated in monocyte and monocyte-macrophages using *Hypoxis* extracts and its purified compounds. *Hypoxis* extracts and rooperol increased ROS production in undifferentiated (monocytes) and differentiated (monocyte-macrophages) U937 cells. ROS production was greater in differentiated than undifferentiated U937 cells, which may be explained by higher ROS production by macrophages. ROS play an important role in physiological functions, and may be involved in apoptosis and inflammation. Together with phagocytosis it plays an important role in microorganism elimination. Increased ROS and NO production may explain the antibacterial, antifungal, antiviral and anti-inflammatory properties seen with *Hypoxis* extracts. The FRAP assay confirmed the antioxidant potential of *Hypoxis* extracts and rooperol, with rooperol's antioxidant potential comparable to the strong antioxidant, ascorbic acid. *Hypoxis* extracts and rooperol had no effect on SOD activity in Chang liver cells, whereas small (but significant) differences were seen when treated with the phytosterols. This may suggest that *Hypoxis* extracts and rooperol may act directly as antioxidants (as seen from the antioxidant potential) rather than influencing antioxidant enzyme(s) levels and activities. This needs further investigation as other enzymes (CAT, GPX and GR) are also involved in the antioxidant defense system.

This study has shown and confirmed that non-toxic/inactive hypoxoside has very little or no *in vitro* biological properties and needs to be converted to cytotoxic/active rooperol. Hypoxoside was absent (*H. sobolifera*) or present at very low concentrations (*H. hemerocallidea* and *H. stellipilis*) in the chloroform extracts. This study has also shown that hypoxoside is not the only active compound in the *Hypoxis* chloroform extracts, in

contrast, hypoxoside was absent in the *H. sobolifera* chloroform extract which showed the best anticancer activity. Unknown/unidentified compounds may have contributed to the *in vitro* biological properties. Synergistic and/or additive effects between the known and unknown compounds in the chloroform *Hypoxis* extracts may have occurred. Differences between *Hypoxis* spp. were seen when the *in vitro* biological activities were investigated. *H. sobolifera* had the best anticancer and phagocytosis properties, whereas *H. stellipilis* had the highest NO and ROS production, and COX-2 lowering properties. *H. stellipilis* may thus be more effective in treating inflammatory diseases.

Chloroform extracts are not the traditional way of preparing *Hypoxis* extracts. Traditional ways of preparing *Hypoxis* extracts (water, ethanol or methanol) may extract different compounds (more polar compounds e.g. hypoxoside and phytosterolins), which may have different or the same *in vitro* biological activities. Care should be taken regarding the choice of *Hypoxis* spp. for a specific disease state. The correct identification and selling of medicinal plants (e.g. different *Hypoxis* spp. being used indiscriminately under the common name, African potato) for traditional medicine must be regulated and controlled.

From the results obtained it is clear that the *Hypoxis* chloroform extracts and its purified compounds have *in vitro* anticancer, anti-inflammatory and antioxidant, and possibly immune stimulating, properties. This study provides novel findings on the mechanisms of action of *in vitro* biological activities of *H. hemerocallidea*, as well as novel findings on the *in vitro* biological activities (and mechanisms of action) of *H. stellipilis* and *H. sobolifera*. Animal models have previously been used to demonstrate the *in vivo* antidiabetic and anti-inflammatory activities, but other biological activities still need to be confirmed in *in vivo* models.

References

Abegaz, B.M., Ngadjui, B.T., Bezabih, M., Mdee, L.K. 1999. Novel natural products from marketed plants of eastern and southern Africa. Pure Appl. Chem. 71 (6), 919-926.

Abidi, S.L. 2001. Chromatographic analysis of plant sterols in foods and vegetable oils. J. Chromatogr. A 935: 173-201.

Agapova, L.S., Ilyinskaya, G.V., Turovets, N.A., Ivanov, A.V., Chumakov, P.M., Kopnin, B.P. 1996. Chromosome changes caused by alterations of p53 expression. Mutation Res. 354: 129-138.

Agapova, L.S., Ivanov, A.V., Sablina, A.A., Kopnin, P.B., Sokova, O.I., Chumakov, P.M., Kopnin, B.P. 1999. p53-dependent effects of RAS oncogene on chromosome stability and cell cycle checkpoints. Oncogene 18: 3135-3142.

Albrecht, C.F., Theron, E.J., Kruger, P.B. 1995a. Morphological characterization of the cell-growth inhibitory activity of rooperol and pharmacokinetic aspects of hypoxoside as an oral prodrug for cancer therapy. S. Afr. Med. J. 85 (9): 853-860.

Albrecht, C.F., Kruger, P.B., Smit, B.J., Freestone, M., Gouws, L., Miller, R., van Jaarsveld, P.P. 1995b. The pharmacokinetic behaviour of hypoxoside taken orally by patients with lung cancer in a phase I trial. S. Afr. Med. J. 9: 861-865.

Andersson, S.W., Skinner, J., Ellegard, L., Welch, A.A., Bingham, S., Mulligan, A., Andersson, H., Khaw, K-T. 2004. Intake of dietary plant sterols is inversely related to serum cholesterol concentration in men and women in the EPIC Norfolk population: a cross-sectional study. Eur. J. Clin. Nutr. 58: 1378-1385.

Andoh, Y., Mizutani, A., Ohashi, T., Kojo, S., Ishii, T., Adachi, Y., Ikehara, S., Taketani, S. 2006. The antioxidant role of a reagent, 2’,7’-dichlorodihydrofluorescin diacetate, detecting reactive oxygen species and blocking the induction of heme oxygenase-1 and preventing cytotoxicity. J. Biochem. 140: 483-489.

Ardestani, A., Yazdanparast, R. 2007. Antioxidant and free radical scavenging potential of *Achillea santolina* extracts. Food Chem. 104: 21-29.

Aubry, J-P., Blaecke, A., Lecoanet-Henchoz, S., Jeannin, P., Herbault, N., Caron, G., Moine, V., Bonnefoy, J-Y. 1999. Annexin V used for measuring apoptosis in the early events of cellular cytotoxicity. Cytometry 37: 197-204.

Avni, D., Yang, H., Martelli, F., Hofmann, F., ElShamy, W., Ganesan, S., Scully, R., Livingston, D.M. 2003. Active localization of the retinoblastoma protein in chromatin and its response to S phase DNA damage. Mol. Cell 12 (3): 735-746.

Awad, A.B., Chen, Y-C., Fink, C.S., Hennessey, T. 1996. β-sitosterol inhibits HT-29 human colon cancer cell growth and alters membrane lipids. Anticancer Res. 16. 2797-2804.

Awad, A.B., von Holtz, R.L., Cone, J.P., Fink, C.S., Chen, Y-C. 1998. β-sitosterol inhibits the growth of HT-29 human colon cancer cells by activating the sphingomyelin cycle 18. Anticancer Res. 18: 471-479.

Awad, A.B., Fink, C.S. 2000. Phytosterols as anticancer dietary components: evidence and mechanism of action. J. Nutr. 130: 2127-2130.

Awad, A.B., Williams, H., Fink, C.S. 2001a. Phytosterols reduce *in vitro* metastatic ability of MBA-MB-231 human breast cancer cells. Nutr. Cancer 40 (2): 157-164.

Awad, A.B., Smith, A.J., Fink, C.S. 2001b. Plant sterols regulate rat vascular smooth muscle cell growth and prostacyclin release in culture. Prostaglandins Leukot. Essent. Fatty Acids 64 (6): 323-330.

Awad, A.B., Roy, R., Fink, C.S. 2003a. β-sitosterol, a plant sterol, induces apoptosis and activates key caspases in MDA-MB-231 human breast cancer cells. Oncol. Rep. 10: 497-500.

Awad, A.B., Williams, H., Fink, C.S. 2003b. Effect of phytosterols on cholesterol metabolism and MAP kinase in MDA-MB-231 human breast cancer cells. J. Nutr. Biochem. 14: 111-119.

Awad, A.B., Toczek, J., Fink, C.S. 2004. Phytosterols decrease prostaglandin release in cultured P388D1/MAB macrophages. Prostaglandins Leukot. Essent. Fatty Acids 70: 511-520.

Awad, A.B., Fink, C.S., Trautwein, E.A., Ntanios, F.Y. 2005a. β-sitosterol stimulates ceramide metabolism in differentiated $Caco_2$ cells. J. Nutr. Biochem. 16: 650-655.

Awad, A.B., Burr, A.T., Fink, C.S. 2005b. Effect of resveratrol and β-sitosterol in combination on reactive oxygen species and prostaglandin release by PC-3 cells. Prostaglandins Leukot. Essent. Fatty Acids 72: 219-226.

Awad, A.B., Chinnam, M., Fink, C.S., Bradford, P.G. 2007. β-sitosterol activates Fas signaling in human breast cancer cells. Phytomedicine 14: 747-754.

Bagchi, D., Bagchi, M., Stohs, S.J., Das, D.K., Ray, S.D., Kuszynski, C.A., Joshi, S.S., Pruess, H.G. 2000. Free radicals and grape seed proanthocyanidin extract: importance in human health and disease prevention. Toxicol. 148: 187-197.

Baker, C.S.R., Hall, R.J.C., Evans, T.J., Pomerance, A., Maclouf, J., Creminon, C., Yacoub, M.H., Polak, J.M. 1999. Cyclooxygenase-2 is widely expressed in atherosclerotic lesions affecting native and transplanted human coronary arteries and colocalizes with inducible nitric oxide synthase and nitrotyrosine particularly in macrophages. Arterioscler. Thromb. Vasc. Biol. 19: 646-655.

Balunas, M.J., Kinghorn, A.D. 2005. Drug discovery from medicinal plants. Life Sci. 78: 431-441.

Barbieri, S.S., Eligini, S., Brambilla, M., Tremoli, E., Colli, S. 2003. Reactive oxygen species mediate cyclooxygenase-2 induction during monocyte to macrophage differentiation: critical role of NADPH oxidase. Cardiovasc. Res. 60: 187-187.

Bates, S., Ryan, K.M., Philips, A.C., Vousden, K.H. 1998. Cell cycle arrest and DNA endoreduplication following $p21^{Waf1/Cip1}$ expression. Oncogene 17: 1691-1703.

Barnes, P.J. 1998. Anti-inflammatory actions of glucocorticoids: molecular mechanisms. Clin. Sci. 94: 557-572.

Barrios-Rodiles, M., Chadee, K. 1998. Novel regulation of cyclooxygenase-2 expression and prostaglandin E2 production by IFN-gamma in human macrophages. J. Immunol. 161: 2441-2448.

Beck, K-F., Eberhardt, W., Frank, S., Huwiler, A., Meßmer, U.K., Mühl, H., Pfeilschifter, J. 1999. Inducible NO synthase: role in cellular signaling. J. Exp. Biol. 202: 645-653.

Benzie, I.F.F., Strain, J.J. 1996. The ferric reducing ability of plasma (FRAP) as a measure of "antioxidant power": the FRAP assay. Anal. Biochem. 239: 70-76.

Berger, A., Jones, P.J.H., Abumweis, S.S. 2004. Plant sterols: factors affecting their efficacy and safety as functional food ingredients. Lipids Health Dis. 3: doi. 10.1186/1476-511X-3-5.

Bertholet, S., Tzeng, E., Felley-Bosco, E., Mauël, J. 1999. Expression of the inducible NO synthase in human monocytic U937 cells allows high output nitric oxide production. J. Leukoc. Biol. 65: 50-58.

Blanc, C., Deveraux, Q.L., Krajewski, S., Jänicke, R.U., Porter, A.G., Reed, J.C., Jaggi, R., Marti, A. 2000. Caspase-3 is essential for procaspase-9 processing and cisplatin-induced apoptosis of MCF-7 breast cancer cells. Cancer Res. 60: 4386-4390.

Böhmer, R.H., Trinkle, L.S., Staneck, J.L. 1992. Dose effect of LPS on neutrophils in a whole blood flow cytometric assay of phagocytosis and oxidative burst. Cytometry 13: 525-531.

Bottura, C., Ferrari, I. 1963. Endoreduplication in acute leukemia. Blood 21: 207-212.

Bouic, P.J.D., Etsebeth, S., Liebenberg, R.W., Albrecht, C.F., Pegel, K., van Jaarsveld, P.P. 1996. Beta-sitosterol and beta-sitosterol glucoside stimulate human peripheral blood lymphocyte proliferation: implications for their use as an immunomodulatory vitamin combination. Int. J. Immunopharmacol. 18 (12): 693-700.

Bouic, P.J.D., Lamprecht, J.H. 1999. Plant sterols and sterolins: a review of their immune-modulating properties. Altern. Med. Rev. 4 (3): 170-177.

Boukes, G.J., van de Venter, M., Oosthuizen, V. 1998. Quantitative and qualitative analysis of sterols/sterolins and hypoxoside contents of three *Hypoxis* (African potato) spp. Afr. J. Biotechnol. 7 (11): 1624-1629.

Bratton, S.B., Cohen, G.M. 2001. Apoptotic death sensor: an organelle's alter ego? TRENDS Pharmacol. Sci. 22 (6): 306-315.

Breytenbach, M., Clark, A., Lamprecht, J., Bouic, P., 2001. Flow cytometric analysis of the Th1-Th2 balance in healthy individuals and patients infected with the human immunodeficiency virus (HIV) receiving a plant sterol/sterolin mixture. Cell Biol. Int. 25 (1): 43-49.

Briskin, D.P. 2000. Medicinal plants and phytomedicines. Linking plant biochemistry and physiology to human health. Plant Physiol. 124: 507-514.

Brown, J.E., Khodr, H., Hider, R.C., Rice-Evans, C.A. 1998. Structural dependence of flavanoid interactions with Cu^{2+} ions: implications for their antioxidant properties. Biochem. J. 330: 1173-1178

Brown, N.S., Bicknell, R. 2001. Hypoxia and oxidative stress in breast cancer. Oxidative stress: its effects on the growth, metastatic potential and response to therapy of breast cancer. Breast Cancer Res. 3: 323-327.

Brown, G., Hughes, P.J., Michell, R.H. 2003. Cell differentiation and proliferation – simultaneous but independent. Exp. Cell Res. 291: 282-288.

Brüne, B., von Knethen, A., Sandau, K.B. 1998. Nitric oxide and its role in apoptosis. Eur. J. Pharmacol. 351: 261-272.

Brunet, A., Bonni, A., Zigmond, M.J., Lin, M.Z., Juo, P., Hu, L.S., Anderson, M.J., Arden, K.C., Blenis, J., Greenberg, M.E. 1999. Akt promotes cell survival by phosphorylating and inhibiting a Forkhead transcription factor. Cell 96: 857-868.

Buwa, L.V., van Staden, J. 2006. Antibacterial and antifungal activity of traditional medicinal plants used against venereal diseases in South Africa. J. Ethnopharmacol. 103: 139-142.

Calpe-Berdiel, L., Escolà-Gil, J.C., Benítez, S., Bancells, C., González-Sastre, F., Palomer, X., Blanco-Vaca, F. 2007. Dietary phytosterols modulate T-helper immune response but do not induce apparent anti-inflammatory effects in a mouse model of acute, aseptic inflammation. Life Sci. 80: 1951-1956.

Cao, G., Prior, R.L. 1998. Comparison of the different analytical methods for assessing total antioxidant capacity of human serum. Clin. Chem. 44 (6): 1309-1315.

Caughey, G.E., Cleland, L.G., Penglis, P.S., Gamble, J.R., James, M.J. 2001. Roles of cyclooxygenase (COX)-1 and COX-2 in prostanoid production by human endothelial cells: selective up-regulation of prostacyclin synthesis by COX-2. J. Immunol. 167: 2831-2838.

Chan, T.A., Morin, P.J., Vogelstein, B., Kinzler, K.W. 1998. Mechanisms underlying nonsteroidal anti-inflammatory drug-mediated apoptosis. Proc. Natl. Acad. Sci. 95: 681-686.

Chang, B-D., Broude, E.V., Fang, J., Kalinichenko, T.V., Abdryashitov, R., Poole, J.C., Roninson, I.B. 2000. $p21^{Waf1/Cip1/Sdi1}$-induced growth arrest is associated with depletion of mitosis-control proteins and leads to abnormal mitosis and endoreduplication in recovering cells. Oncogene 19: 2165-2170.

Chibazakura, T., McGew, S.G., Cooper, J.A., Yoshikawa, H., Roberts, J.M. 2004. Regulation of cyclin-dependent kinase activity during mitotic exit and maintenance of genome stability by p21, p27, and p107. PNAS 101 (13): 4465-4470.

Choi, B-M., Pae, H-O., Jang, S.I., Kim, Y-M., Chung, H-T. 2001. Nitric oxide as a pro-apoptotic and anti-apoptotic modulator. J. Biochem. Mol. Biol. 35 (1): 116-126.

Choi, Y.H., Kong, K.R., Kim, Y-A., Jung, K-O., Kil, J-H., Rhee, S-H., Park, K-Y. 2003. Induction of Bax and activation of caspases during β-sitosterol-mediated apoptosis in human colon cancer cells. Int. J. Oncol. 23: 1657-1662.

Chun, K-S., Surh, Y-J. 2004. Signal transduction pathways regulating cyclooxygenase-2 expression: potential molecular targets for chemoprevention. Biochem. Pharmacol. 68: 1089-1100.

Chung, H-T., Pae, H-O., Choi, B-M., Billiar, T.R., Kim, Y-M. 2001. Nitric oxide as a bioregulator of apoptosis. Biochem. Biophys. Res. Commun. 282: 1075-1079.

Clancy, R.M., Amin, A.R., Abramson, S.B. 1998. The role of nitric oxide in inflammatory and immunity. Arthritis Rheum. 41 (7): 1141-1151.

Clancy, R., Varenika, B., Huang, W., Ballou, L., Attur, M., Amin, A.R., Abramson, S.B. 2000. Nitric oxide synthetase/COX-cross talk: nitric oxide activates COX-1 but inhibits COX-2-derived prostaglandin production. J. Immunol. 165: 1582-1587.

Cohen, G.M., Sun, X-M., Snowden, R.T., Dinsdale, D., Skilleter, D.N. 1992. Key morphological features of apoptosis may occur in the absence of internucleosomal DNA fragmentation. Biochem. J. 286: 331-334.

Collins, K., Jacks, T., Pavletich, N.P. 1997a. The cell cycle and cancer. Proc. Natl. Acad. Sci. 94: 2776-2778.

Collins, J.A., Schandl, C.A., Young, K.K., Vesely, J., Willingham, M.C. 1997b. Major DNA fragmentation is a late event in apoptosis. J. Histochem. Cytochem. 45 (7): 923-934.

Contarini, G., Povolo, M., Bofitto, E., Berardi, S. 2002. Quantitative analysis of sterols in dairy products: experiences and remarks. Int. Dairy J. 12: 573-578.

Coqueret, O. 2003. New roles for p21 and p27 cell-cycle inhibitors: a function for each cell compartment? TRENDS Cell Biol. 13 (2): 65-70.

Cortés, F., Pastor, N. 2003. Induction of endoreduplication by topoisomerase II catalytic inhibitors. Mutagenesis 18 (2): 105-112.

Cortés, F., Mateos, S., Pastor, N., Domínguez, I. 2004. Towards a comprehensive model for induced endoreduplication. Life Sci. 76: 121-135.

Cragg, G.M., Newmann, D.J. 2005. Plants as a source of anti-cancer agents. J. Ethhnopharmacol. 100: 72-79.

Cruz, G.V.B., Pereira, P.V.S., Patrício, F.J., Costa, G.C., Sousa, S.M., Frazão, J.B., Aragão-Filho, W.C., Maciel, M.C.G., Silva, L.A., Amaral, F.M.M., Barroqueiro, E.S.B., Guerra, R.N.M., Nascimento, F.R.F. 2007. Increase of cellular recruitment, phagocytosis ability and nitric oxide production induced by hydroalcoholic extract from *Chenopodium ambrosioides* leaves. J. Ethnopharmacol. 111: 148-154.

Cryns, V., Yuan, J. 1999. Proteases to die for. Genes & Dev. 12: 1551-1570.

Cunha, S.S., Fernandes, J.O., Oliveira, M.B.P.P. 2006. Quantification of free and esterified sterols in Portuguese olive oils by solid-phase extraction and gas chromatography-mass spectrometry. J. Chromatogr. A 1128: 220-227.

Dale, D.C., Boxer, L., Liles, W.C. 2008. The phagocytes: neutrophils and macrophages. Blood 112: 935-945.

Datto, M.B., Yu, Y., Wang, X-F. 1995. Functional analysis of the transforming growth factor β responsive elements in WAF1/Cip1/p21 promoter. J. Biol. Chem. 270 (48): 28623-28628.

De Brabander, H.F., Verheyden, K., Mortier, V., Le Bizec B., Verbeke, W., Courtheyn, D., Noppe, H. 2007. Phytosterols and anabolic agents versus designer drugs. Anal. Chim. Acta 586: 49-56.

De Jong, A., Plat, J., Mensink, R.P. 2003. Metabolic effects of plant sterols and stanols. J. Nutr. Biochem. 14: 362-369.

Del Bello, B., Valentini, M.A., Mangiavacchi, P., Comporti, M., Maellaro, E. 2004. Role of caspase-3 and -7 in Apaf-1 proteolytic cleavage and degradation events during cisplatin-induced apoptosis in melanoma cells. Exp. Cancer Res. 293: 302-310.

De Graaf, M., Boven, E., Scheeren, H.W., Haisma, H.J., Pinedo, H.M. 2002. Beta-glucuronidase-mediated drug release. Curr. Pharmaceut. Des. 8: 1391-1403.

Dinarello, C.A. 2000. Pro-inflammatory cytokines. CHEST 118: 503-508.

Dold, A.P., Cocks, M.L. 2002. The trade in medicinal plants in the Eastern Cape Province, South Africa. S. Afr. J. Sci. 98: 589-597.

Drewes, S.E., Hall, A.J., Learmonth, R.A., Upfold, U.J. 1984. Isolation of hypoxoside from *Hypoxis rooperi* and synthesis of (E)-1,5-bis(dimethoxyphenyl)pent-4-en-1-yne. Phytochemistry 23 (6): 1313-1316.

Drewes, S., Liebenberg, R.W. 1987. Rooperol and its derivatives. US Patent 4644085.

Drewes, S.E., Scogings, U.J., Wenteler, G.L. 1989. Structure determination of a phenolic pent-1-en-4-yne derivative from *Hypoxis rooperi*. Phytochemistry 28 (1): 153-156.

Drewes S. E., Khan, F. 2004. The African potato (*Hypoxis hemerocallidea*): a chemical-historical perspective. S. Afr. J. Sci. 100: 425-430.

Drewes, S.E., Elliot, E., Khan, E., Dhlamini, J.T.B., Gcumisa, M.S.S. 2008. *Hypoxis hemerocallidea* – not merely a cure for benign prostate hyperthrophy. J. Ethnopharmacol. 119: 593-598.

DuBois, R.N., Abramson, S.B., Crofford, L., Gupta, R.A., Simon, L.S., van de Putte, L.B.A., Lipsky, P.E. 1998. Cyclooxygenase in biology and disease. FASEB J. 12: 1063-1073.

Elmore, S. 2007. Apoptosis: a review of programmed cell death. Toxicol. Pathol. 35 (4): 495-5161.

Erasto, P., Adebola, P.O., Grierson, D.S., Afolayan, A.J. 2005. An ethnobotanical study of plants used for the treatment of diabetes in the Eastern Cape Province, South Africa. Afr. J. Biotechnol. 4 (12): 1458-1460.

Erenpreisa, J., Cragg, M.S. 2001. Mitotic death: a mechanism of survival? A review. Canc. Cell Int. 1: 1-7.

Fadeel, B., Gleiss, B., Högstrand, K., Chandra, J., Wiedmer, T., Sims, P.J., Henter, J-I., Orrenius, S., Samali, A. 1999. Phosphatidylserine exposure during apoptosis is a cell-type-specific event and does not correlate with plasma membrane phospholipid scramblase expression. Biochem. Biophys. Res. Comm. 266: 504-511.

Fadeel, B., Orrenius, S. 2005. Apoptosis: a basic biological phenomenon with wide-ranging implications in human disease. J. Int. Medicine. 258: 479-517.

Fennell, C.W., Light, M.E., Sparg, S.G., Stafford, G.I., van Staden, J. 2004. Assessing African plants for efficacy and safety: agricultural and storage practices. J. Ethnopharmacol. 95: 113-121.

Fleet, J.C. 2004. Genomic and proteomic approaches for probing the role of vitamin D in health. Am. J. Clin. Nutr. 80: 1730-1734.

Flores-Rozas, H., Kelman, Z., Dean, F.B., Pan, Z-Q., Harper, J.W., Elledge, S.J., O'Donnell, M., Hurwitz, J. 1994. Cdk-interacting protein 1 directly binds with proliferating cell nuclear antigen and inhibits DNA replication catalyzed by the DNA polymerase δ holoenzyme. Proc. Natl. Acad. Sci. 91: 8655-8659.

Forman, H.J., Torres, M. 2002. Reactive oxygen species and cell signaling. Am. J. Respir. Crit. Care Med. 166: 4-8.

Fotakis, G., Timbrell, J.A. 2006. *In vitro* cytotoxicity assays: comparison of LDH, neutral red, MTT and protein assay in hepatoma cell lines following exposure to cadmium chloride. Toxicol. Lett. 160: 171-177.

Frank, T.F., Yang, S-I., Chan, T.O., Datta, K., Kazlauskas, A., Morrison, D.K., Kaplan, D.R., Tsichlis, P.N. 1995. The protein kinase encoded by the Akt proto-oncogene is a target of the PDGF-activated phosphatidylinositol 3-kinase. Cell. 81: 727-736.

Frank, T.F., Kaplan, D.R., Cantley, L.C. 1997. PI3K: downstream AKTion blocks apoptosis. Cell 88: 435-437.

Frommel, T.O., Zarling, E.J. 1999. Chronic inflammation and cancer: potential role of Bcl-2 gene family members as regulators of cellular antioxidant status. Med. Hypotheses 52 (1): 27-30.

Galeffi, C., Multari, G., Msonthi, J.D., Nicoletti, M., Marini-Bettolo, G.B. 1987. Nyasicoside, a new glucoside of *Hypoxis nyasica* Bak. Tetrahedron 43 (15): 3519-3522.

García, A., Serrano, A., Abril, E., Jimenez, P., Real, L.M., Cantón, J., Garrido, F., Ruiz-Cabello, F. 1999. Differential effect on U937 cell differentiation by targeting transcriptional factors implicated in tissue- or stage-specific induced integrin expression. Exp. Hermatol. 27: 353-364.

Gasparini, G., Longo, R., Sarmiento, R., Morabito, A. 2003. Inhibitors of cyclo-oxygenase 2: a new class of anticancer agents? Lancet Oncol. 4: 605-616.

Gogos, C.A., Drosou, E., Bassaris, H.P., Skoutelis, A. 2000. Pro- versus anti-inflammatory cytokine profile in patients with severe sepsis: a marker for prognosis and future therapeutic options. J. Infect. Dis. 181: 176-180.

Gopinath, V.K., Musa, M., Samsudin, A.R., Lalitha, P., Sosroseno, W. 2006. Role of nitric oxide in hydroapatite-induced phagocytosis by murine macrophage cell line (RAW264.7). Arch. Oral Biol. 51: 339-344.

Gorczyca, W. 1999. Cytometric analyses to distinguish death processes. Endocrine-Rel. Cancer 6: 17-19.

Goudjil, H., Torrado, S., Fontecha, J., Martínez-Castro, I., Fraga, M.J., Juárez, M. 2003. Composition of cholesterol and its precursors in ovine milk. Lait 83: 153-160.

Grafi, G. 1998. Cell cycle regulation of DNA replication: the endoreduplication perspective. Exp. Cell Res. 244: 372-378.

Greenberg-Ofrath, N.O.A., Terespolosky, Y., Kahane, I., Bar, R. 1993. Cyclodextrins as carriers of cholesterol and fatty acids in cultivation of mycoplasmas. Appl. Environ. Microbiol. 59 (2): 547-551.

Greenwald, P., Clifford, C.K., Milner, J.A. 2001. Diet and cancer prevention. Eur. J. Cancer 37: 948- 965.

Grkovich, A., Johnson, C.A., Buczynski, M.W., Dennis, E.A. 2006. Lipopolysaccharide-induced cyclooxygenase-2 expression in human U937 macrophages is phosphatidic acid phosphohydrolase-1-dependent. J. Biol. Chem. 281 (44): 32978-32987.

Gross, A., McDonnell, J.M., Korsmeyer, S.J. 1999. Bcl-2 family members and the mitochondria in apoptosis. Genes & Dev. 13: 1899-1911.

Gulmann, C., Espina, V., Petricoin, E., Longo, D.L., Santi, M., Knutsen, T., Raffeld, M., Jaffe, E.S., Liotta, L.A., Feldman, A.L. 2005. Proteomic analysis of apoptotic pathways reveals prognostic factors in follicular lymphoma. Clin. Cancer Res. 11 (16): 5847-5855.

Gurib-Fakum, A. 2006. Medicinal plants: traditions of yesterday and drugs of tomorrow. Mol. Aspects Med. 27: 1-93.

Guzdek, A., Nizankowska, E., Allison, A.C., Kruger, P.B., Koj, A. 1996. Cytokine production in human and rat macrophages and dicatechol rooperol and esters. Biochem. Pharmacol. 52: 991-998.

Guzdek, A., Turyna, B., Allison, A.C., Stadek, K., Koj, A. 1997. Rooperol, an inhibitor of cytokine synthesis, decreases the respiratory burst in human and rat leukocytes and macrophages. Mediators Inflamm. 6: 53-57

Guzdek, A., Rokita, H., Cichy, J., Allison, A.C., Koj, A. 1998. Rooperol tetraacetate decreases cytokine mRNA levels and binding capacity of transcription factors in U937 cells. Mediators Inflamm. 7: 13-18.

Guzik, T.J., Korbut, R., Adamek-Guzik, T. 2003. Nitric oxide and superoxide in inflammation and immune regulation. J. Physiol. Pharmacol. 54 (4): 469-487.

Half, E., Tang, X.M., Gwyn, K., Sahin, A., Wathen, K., Sinicrope, F.A. 2002. Cyclooxygenase-2 expression in human breast cancers and adjacent ductal carcinoma *in situ*. Cancer Res. 62: 1676-1681.

Hanahan, D., Weinberg, R.A. 2000. The hallmarks of cancer. Cell. 100: 57-70.

Hancock, J.T., Desikan, R., Neill, S.J. 2001. Role of reactive oxygen species in cell signaling pathways. Biochem. Soc. Transact. 29 (2): 345-350.

Hase, Y., Fujioka, S., Yoshida, S., Sun, G., Umeda, M., Tanaka, A. 2005. Ectopic endoreduplication caused by sterol alteration results in serrated petals in *Arabidopsis*. J. Exp. Bot. 56 (414): 1263-1268.

Hodgetts, J., Hoy, T.G., Jacobs, A. 1988. Assessment of DNA content and cell cycle distribution of erythroid and myeloid cells from the bone marrow. J. Clin. Pathol. 41: 1120-1124.

Holst-Hansen, C., Brünnner, N. 1998. MTT-cell proliferation assay. In: Celis, J. E. Cell biology: a laboratory handbook, 2nd ed. San Diego, California: Academic Press: 16-18.

Horký, M., Wurzer, G., Kotala, V., Anton, M., Vojtěšek, B., Vácha, J., Wesierska-Gadek, J. 2000. Segregation of nucleolar components coincides with caspase-3 activation in cisplatin-treated HeLa cells. J. Cell Sci. 114: 663-670.

Hostettmann, K., Marston, A., Ndjoko, K., Wolfender, J-L. 2000. The potential of African plants as source of drugs. Curr. Org. Chem. 4: 973-1010.

Houghton, P., Fang, R., Techatanawat, I., Steventon, G., Hylands, P.J., Lee, C.C. 2007. The sulphorhodamine (SRB) assay and other approaches to testing plant extracts and derived compounds for activities related to reputed anticancer activity. Methods 42: 377-387.

Huang, Y., Chang, C-C., Trosko, J.E. 1985. Aphidicolin-induced endoreduplication in Chinese hamster cells. Cancer Res. 43: 1361-1364.

Huang, Z-F., Massey, J.B., Via, D.P. 2000. Differential regulation of cyclooxygenase-2 (COX-2) mRNA stability by interleukin 1β (IL-1β) and tumor necrosis factor-α (TNF-α) in human *in vitro* differentiated macrophages. Biochem. Pharmacol. 59: 187-194.

Huang, D., Ou, B., Prior, R.L 2005. The chemistry behind antioxidant capacity assays. J. Agric. Food Chem. 53: 1841-1856.

Huh, H.Y., Pearce, S.F., Yesner, L.M., Schindler, J.L., Silverstein, R.L. 1996. Regulated expression of CD36 during monocyte-to-macrophage differentiation: potential role of CD36 in foam cell formation. Blood 87 (5): 2020-2028.

Igel, M., Giesa, U., Lütjohann, D., von Bergmann, K. 2003. Comparison of the intestinal uptake cholesterol, plant sterols, and stanols in mice. J. Lipid Res. 44: 533-538.

Illidge, T.M., Cragg, M.S., Fringes, B., Olive, P., Erenpreisa, J.A. 2000. Polyploid giant cells provide a survival mechanism for p53 mutant cells after DNA damage. Cell Biol. Int. 24 (9): 621-633.

Jäger, A.K., Hutchings, A., van Staden, J. 1996. Screening of Zulu medicinal plants for prostaglandin-synthesis inhibitors. J. Ethnopharmacol. 52: 95-100.

Jakulj, L., Trip, M.D., Sudhop, T., von Bergmann, K., Kastelein, J.J.P., Vissers, M.N. 2005. Inhibition of cholesterol absorption by the combination of dietary plant sterols and ezetimibe: effects on plasma lipid levels. J. Lipid Res. 46: 2692-2698.

Jänicke, R.U., Sprengart, M.L., Wati, M.R., Porter, A.G. 1998. Caspase-3 is required for DNA fragmentation and morphological changes associated with apoptosis. J. Biol. Chem. 279 (16): 9357-9360.

Jiménez, W., Ros, J., Morales-Ruiz, M., Navasa, M., Solé, M., Colmenero, J., Sort, P., Rivera, F., Arroyo, V., Rodés, J. 1999. Nitric oxide production and inducible nitric oxide synthase expression in peritoneal macrophages of cirrhotic patients. Hepatology 30 (3): 670-676.

John, P.C.L., Qi, R. 2008. Cell division and endoreduplication: doubtful engines of vegetative growth. Trends Plant Sci. 13 (3): 121-127.

Jokobsen, A. 1983. The use of trout erythrocytes and human lymphocytes for standardization in flow cytometry. Cytometry 4: 161-165.

Kagawa, S., Gu, J., Honda, T., McDonnell, T.J., Swisher, S.G., Roth, J.A., Fang, B. 2001. Deficiency of caspase-3 in MCF7 cells blocks Bax-mediated nuclear fragmentation but not cell death. Clin. Cancer Res. 7: 1474-1480.

Kampen, A.H., Tollersrud, T., Lund, A. 2004. Flow cytometric measurement of neutrophil respiratory burst in whole bovine blood using live *Staphylococcus aureus*. J. Immunol. Methods 289: 47-55.

Kastan, M.B., Bartek, J. 2004. Cell-cycle checkpoints and cancer. Nature 432: 316-323.

Katerere, D.R., Eloff, J.N. 2008. Anti-bacterial and anti-oxidant activity of *Hypoxis hemerocallidea* (Hypoxidaceae): can leaves be substituted for corms as a conservation strategy? S. Afr. J. Bot. 74: 613-616.

Kennedy, S.G., Wagner, A.J., Conzen, S.D., Jordán, J., Bellacosa, A., Tsichlis, P.N., Hay, N. 1997. The PI 3-kinase/Akt signaling pathway delivers an anti-apoptotic signal. Genes & Dev. 11: 701-713.

Kim, S-J., Bang, O-K., Lee, Y-S., Kang, S.S. 1998. Production of inducible nitric oxide is required for monocytic differentiation of U937 cells induced by vitamin E-succinate. J. Cell Sci. 111: 435-441.

Koduru, S., Grierson, D.S., Afolayan, A.J. 2007. Ethnobotanical information of medicinal plants used for the treatment of cancer in the Eastern Cape Province, South Africa. Curr. Sci. 92 (7): 906-908.

Kojima, M., Morisaki, T., Uchiyama, A., Doi, F., Mibu, R., Katano, M., Tanaka, M. 2001. Association of enhanced cyclooxygenase-2 expression with possible local immunosuppression in human colorectal carcinomas. Ann. Surg. Oncol. 8 (5): 458-465.

Koopman, G., Reutekingsperger, C.P.M., Kuijten, G.A.M., Keehnen, R.M.J., Pals, S.T., van Oers, M.H.J. 1994, Annexin V for flow cytometric detection of phosphatidylserine expression on B cells undergoing apoptosis. Blood 84 (5): 1415-1420.

Korhonen, R., Lahti, A., Kankaanranta, H., Moilanen, E. 2005. Nitric oxide production and signaling in inflammation. Curr. Drug Targets 4: 471-479.

Krahling, S., Callahan, M.K., Williamson, P., Schlegel, R.A. 1999. Exposure of phosphatidylserine is a general feature in the phagocytosis of apoptotic lymphocytes by macrophages. Cell Death Diff. 6: 183-189.

Krishnaiah, D., Sarbatly, R., Bono, A. 2007. Phytochemical antioxidants for health and medicine – a move towards nature. Biotechnol. Mol. Biol. Rev. 1 (4): 97-104.

Kritchevsky, D., Chen, S.C. 2005. Phytosterols-health benefits and potential concerns: a review. Nutr. Res. 25: 413-428.

Kroemer, G., Galluzzi, L., Vandenabeele, P., Abrams, J., Alnemri, E.S., Baehrecke, E.H., Blagosklonny, M.V., El-Deiry, W.S., Golstein, P., Green, D.R., Hengartner, M., Knight, R.A., Kumar, S., Lipton, S.A., Malorni, W., Nunez, G., Peter, M.E., Tschopp, J., Yuan, J., Piacentini, M., Zhivotovsky, B., Melino, G. 2009. Classification of cell death: recommendations of the nomenclature committee on cell death. Cell Death Diff. 16: 3-11.

Kruger, P.B., Albrecht, C.F., Liebenberg, R.W., van Jaarsveld, P.P. 1994. Studies on hypoxoside and rooperol analogues from *Hypoxis rooperi* and *Hypoxis latifolia* and their biotransformation in man by using high-performance liquid chromatography with in-line sorption enrichment and diode-array detection. J.Chromatogr. B 662: 71-78.

Kulseth, M.A., Mustorp, S.L., Uhlin-Hansen, L., Öberg, F., Kolset, S.O. 1998. Serglycin expression during monocyte differentiation of U937-1 cells. Glycobiol. 8 (8): 747-753.

Kurosaka, K., Watanabe, N., Kobayashi, Y. 1998. Production of pro-inflammatory cytokines by phorbol myristate acetate-treated THP-1 cells and monocyte-derived macrophages after phagocytosis of apoptotic CTLL-2 cells. J. Immunol. 161: 6245-6249.

Kurz, T., Leake, A., von Zglinicki, T., Brunk, U.T. 2004. Relocalized redox-active lysosomal iron is an important mediator of oxidative-stress-induced DNA damage. Biochem J. 378: 1039-1045.

Lagarda, M.J., García-Llatas, G. Farré, R. 2006. Analysis of phytosterols in foods. J. Pharm. Biomed. Anal. 41: 1486-1496.

Laporta, O., Funes, L., Garzón, M.T., Villalaín, J., Micol, V. 2007a. Role of membranes on the antibacterial and anti-inflammatory activities of the bioactive compounds from *Hypoxis rooperi* corm extract. Arch. Biochem. Biophys. 467 (1): 119-131.

Laporta, O., Pérez-Fons, L., Mallavia, R., Caturla, N., Micol, V. 2007b. Isolation, characterization and antioxidant capacity assessment of the bioactive compounds derived from *Hypoxis rooperi* corm extract (African potato). Food Chem. 101: 1425-1437.

Lee, S.E., Hwang, H.J., Ha, J-S., Jeong, H-S., Kim, J.H. 2003. Screening of medicinal plant extracts for antioxidant activity. Life Sci. 73: 167-179.

Ling, W.H., Jones, P.J.H. 1995. Dietary phytosterols: a review of metabolism, benefits and side effects. Life Sci. 57 (3): 195-206.

Louw, C.A.M., Regnier, T.J.C., Korsten, L. 2002. Medicinal bulbous plants of South Africa and their traditional relevance in the control of infectious diseases. J. Ethnopharmacol. 82: 147-154.

Lu, R., Pitha, P.M. 2001. Monocyte differentiation to macrophage requires interferon regulation factor 7. J. Biol. Chem. 276 (48): 45491-45496.

MacAuley, A., Cross, J.C., Werb, Z. 1998. Reprogramming the cell cycle for endoreduplication in rodent trophoblast cells. Mol. Biol. Cell 9: 795-807.

Makunga, N.P., Philander, L.E., Smith, M. 2008. Current perspectives on an emerging formal natural products sector in South Africa. J. Ethnopharmacol. 119: 365-375.

Malíková, J., Swaczynová, J., Kolář, Z., Strnad, M. 2008. Anticancer and antiproliferative activity of natural brassinosteroids. Phytochemistry 69: 418-426.

Marini, M., Musiani, D., Sestili, P., Cantoni, O. 1996. Apoptosis of human lymphocytes in the absence or presence of internucleosomal DNA cleavage. Biochem. Biophys. Res. Commun. 229: 910-915.

Marini-Bettolo, G.B., Patamia, M., Nicoletti, M., Galeffi, C., Messana, I. 1982. Hypoxoside, a new glycoside of uncommon structure from *Hypoxis obtuse* Busch. Tetrahedron 38 (11): 1683-1687.

Marini-Bettolo, G.B., Nicoletti, M., Messana, I., Galeffi, C., Msonthi, J.D., Chapya, W.A. 1985. Glucosides of *Hypoxis nyasica* Bak. the structure of nyasoside, a new glucoside biologically related to hypoxoside. Tetrahedron 41 (4): 665-670.

Marini-Bettolo, G.B., Galeffi, C., Multari, G., Pallazzino, G., Messana, I. 1991. Interjectin, a derivative from *Hypoxis interjecta* and *Hypoxis multiceps*. Tetrahedron 47 (33): 6717-6724.

Martin, S.J., Reutelinsperger, C.P.M., McGahon, A.J., Rader, J.A., van Schie, R.C.A.A., LaFace, D.M., Green, D.R. 1995. Early redistribution of plasma membrane phosphatidylserine is a general feature of apoptosis regardless of the initiating stimulus: inhibition by overexpression of Bcl-2 and Abl. J. Exp. Med. 182: 1545-1556.

Martin, K.R., Barrett, J.C. 2002. Reactive oxygen species as double-edged swords in cellular processes: low-dose cell signaling versus high-dose toxicity. Human Exp. Toxicol. 21: 71-75.

Martin Del Valle, E.M. 2004. Cyclodextrins and their uses: review. Process Biochem. 39: 1033-1046.

Martinez, F.O., Gordon, S., Locati, M., Mantovani, A. 2006. Transcription profiling of the human monocyte-to-macrophage differentiation and polarization: new molecules and patterns of gene expression. J. Immunol. 177: 7303-7311.

Másson, M., Loftsson, T., Másson, G., Stefánsson, E. 1999. Cyclodextrins as permeation enhancers: some theoretical evaluations and *in vitro* testing. J. Control. Release 59: 107-118.

Matés, J.M., Péres-Gómez, C., NúÑez de Castro, I. 1999. Antioxidant mechanisms and human diseases. Clin. Biochem. 32: 595-603.

McCullough, M.L., Giovannucci, E.L. 2004. Diet and cancer prevention. Oncogene 23: 6349-6364.

McGaw, L.J., Eloff, J.N. 2008. Ethnoveterinary use of southern African plants and scientific evaluation of their medicinal properties. J. Ethnopharmacol. 119: 559-574.

McGee, M.M., Hyland, E., Campiani, G., Ramunno, A., Nacci, V., Zisterer, D.M. 2002. Caspase-3 is not essential for DNA fragmentation in MCF-7 cells during apoptosis induced by the pyrrolo-1,5-benzoxazepine, PBOX-6. FEBS Lett. 515: 66-70.

McNamee, J.P., Bellier, P.V., Kutzner, B.C., Wilkins, R.C. 2005. Effect of pro-inflammatory cytokines on spontaneous apoptosis in leukocyte sub-sets within a whole blood culture. Cytokine 31: 161-167.

Messana, I., Msonthi, J.D., Di Vicente, Y., Multari, G., Galeffi, C. 1989. Mononyasine A and mononyasine B: two glucosides from *Hypoxis nyasica*. Phytochemistry 28 (10): 2807-2809.

Miller, M.J.S., Grisham, M.B. 1995. Nitric oxide as a mediator of inflammation? – You had better believe it. Mediators Inflamm. 4: 387-396.

Mills, E., Cooper, C., Seely, D., Kanfer, I. 2005. African herbal medicines in the treatment of HIV: *Hypoxis* and *Sutherlandia*. An overview of evidence and pharmacology. Nutr. J. 4 (19): doi.10.1186/1475-2891-4-19.

Mingo-Sion, A.M., Marietta, P.M., Koller, E., Wolf, D.M., Van Den Berg, C.L. 2004. Inhibition of JNK reduces G2/M transit independent of p53, leading to endoreduplication, decreased proliferation, and apoptosis in breast cancer cells. Oncogene 23: 596-604.

Moghadasian, M.H. 2000. Pharmacological properties of plant sterols *in vivo* and *in vitro* observations. Life Sci. 67: 605-615.

Moilanen, E., Moilanen, T., Knowles, R., Charles, I., Kadoya, Y., Al-Saffar, N., Revell, R.A., Moncada, S. 1997. Nitric oxide synthase is expressed in human macrophages during foreign body inflammation. Am. J. Pathol. 150: 881-887.

Moon, D-O., Kim, M-O., Choi, Y. H., Kim, G-Y. 2008a. β-sitosterol induces G2/M arrest, endoreduplication, and apoptosis through the Bcl-2 and PI-3K/Akt signaling pathways. Cancer Lett. 264: 181-191.

Moon, D-O., Kim, M-O., Choi, H.Y., Kim, N.D., Chang, J-H., Kim, G-Y. 2008b. Bcl-2 overexpression attenuates SP600125-induced apoptosis in human leukemia U937 cells. Cancer Lett. 264: 316-325.

Mooney, L.M., Al-Sakkaf, K.A., Brown, B.L., Dobson, P.R.M. 2002. Apoptotic mechanisms in T47D and MCF-7 human breast cancer cells. Br. J. Cancer 87: 909-917.

Moreau, R.A., Whitaker, B.D., Hicks, K.B. 2002. Phytosterols, phytostanols, and their conjugates in foods: structural diversity, quantitative analysis, and health-promoting uses. Prog. Lipid Res. 41: 457-500.

Moreno, J.J. 2003. Effect of olive oil minor components on oxidative stress and arachidonic acid mobilization and metabolism by macrophages RAW264.7. Free Radic. Biol. Med. 35 (9): 1073-1081.

Morita, I. 2002. Distinct functions of COX-1 and COX-2. Prostag. Other Lipid Mediat. 68-69: 165-175.

Murphy, K.M., Ranganathan, V., Farnsworth, M.L., Kavallaris, M., Lock, R.B. 2000. Bcl-2 inhibits Bax translocation from cytosol to mitochondria during drug-induced apoptosis of human tumour cells. Cell Death Diff. 7: 102-111.

Nagata, S. 2000. Apoptotic DNA fragmentation. Exp. Cell Res. 256: 12-18.

Nair, P.K.R., Rodriguez, S., Ramachandran, R., Alamo, A., Melnick, S.J., Escalon, E., Garcia Jr., P.I., Wnuk, S.F., Ramachandran, C. 2004. Immune stimulation properties of a novel polysaccharide from the medicinal plant *Tinospora cordifolia*. Int. Immunopharmacol. 4: 1645-1659.

Nair, V.D.P., Kanfer, I. 2006. High-performance liquid chromatography method for the quantitative determination of hypoxoside in African potato (*Hypoxis hemerocallidea*) and commercial products containing the plant material and/or its extracts, J. Agric. Food Chem. 54: 2816-2821.

Nair, V.D.P., Kanfer, I., Hoogmartens, J. 2006. Determination of stigmasterol, β-sitosterol and stigmastenol in oral dosage forms using high performance liquid chromatography with evaporative light scattering detection. J. Pharm. Biomed. Anal. 41: 731-737.

Nair, V.D.O., Foster, B.C., Arnason, J.T., Mills, E.J., Kanfer, I. 2007a. *In vitro* evaluation of human cytochrome P450 and P-glycoprotein-mediated metabolism of some phytochemicals in extracts and formulations of African potato. Phytomedicine 14: 498-507.

Nair, V.D.P., Dairam, A., Agbonon, A., Arnason, J.T., Foster, B.C., Kanfer, I. 2007b. Investigation of the antioxidant activity of African potato (*Hypoxis hemerocallidea*). J. Agric. Food Chem. 55: 1707-1711.

Nashed, B., Yeganeh, B., HayGlass, K.T., Moghadasian, M.H. 2005. Antiatherogenic effects of dietary plant sterols are associated with inhibition of pro-inflammatory cytokine production in Apo E-KO mice. J. Nutr. 135: 2438-2444.

Nelson, D.L., Cox, M.M.. 2000. Lehninger: Principles of Biochemistry 3rd Ed. Worth Publishers. New York, USA: 1152pp.

Neukam, K., Pastor, N., Cortés. 2008. Tea flavanols inhibit cell growth and DNA topoisomerase II activity and induce endoreduplication in cultured Chinese hamster cells. Mutation Res. 654: 8-12.

Nicoletti, M., Galeffi, C., Messana, I., Marini-Bettolo, G.B. 1992. *Hypoxidaceae*: Medicinal uses and the norlignan constituents. J. Ethnopharmacol. 36: 95-101.

Niculescu III, A.B., Chen, X., Smeets, M., Hengst, L., Prives, C., Reed, S.I. 1998. Effects of $p21^{Waf1/Cip1}$ at both the G1/S and the G2/M cell cycle transitions: pRb is a critical determinant in blocking DNA replication and in preventing endoreduplication. Mol. Cell. Biol. 18 (1): 629-643.

Nojima, H. 2004. G1 and S-phase checkpoints, chromosome instability, and cancer. Methods Mol. Biol. 280: 3-49.

Núñez-Sellés, A.J. 2005. Antioxidant therapy: myth or reality? J. Braz. Chem. Soc. 16 (4): 699-710.

Nussler, A.K., Billiar, T.R. 1993. Inflammation, immunoregulation, and inducible nitric oxide synthase. J. Leukoc. Biol. 54: 171-178.

Oberhammer, F., Wilson, J.W., Dive, C., Morris, I.D., Hickman, J.A., Wakeling, A.E., Walker, P.R., Sikorska, M. 1993. Apoptotic death in epithelial cells: cleavage of DNA to 300 and/or 50 kb fragments prior to or in the absence of internucleosomal fragmentation. EMBO J. 12 (9): 3679-3684.

Ojewole, J.A.O. 2006. Antinociceptive, anti-inflammatory and antidiabetic properties of *Hypoxis hemerocallidea* Fisch. & C.A. Mey. (Hypoxidaceae) corm [‘African Potato’] aqueous extract in mice and rats. J. Ethnopharmacol. 103: 126-134.

Ojewole, J.A.O. 2008. Anticonvulsant activity of *Hypoxis hemeorcallidea* Fisch. & C. A. Mey. (Hypoxidaceae) corm (African potato) aqueous extract in mice. Phytother. Res. 22: 91-96.

Opal, S.M., DePalo, V.A. 2000. Anti-inflammatory cytokines. CHEST 117: 1162-1172.

Ostlund, R.E. 2002. Phytosterols in human nutrition. Annu. Rev. Nutr. 22: 533-549.

Papas, A.M. 1999. Diet and antioxidant status. Food Chem. Toxicol. 37: 999-1007.

Pegel, K.H. 1976. Extraction of sterolins from plant material. US Patent 3933789.

Pegel, K.H. 1979. Active plant extracts of Hypoxidaceae and their use. US Patent 4160860/4198401.

Pegel, K.H. 1980. Sterolins and their use. US Patent 4188379.

Pegel, K.H. 1997. The importance of sitosterol and sitosterolin in human and animal nutrition. S. Afr. J. Sci. 93: 263-268.

Pepper, C., Thomas, A., Tucker, H., Hoy, T., Bentley, P. 1998. Flow cytometric assessment of three different methods for the measurement of *in vitro* apoptosis. Leukemia Res. 22: 439-444.

Pérez, C., Vilaboa, N.E., Aller, P. 1994. Etoposide-induced differentiation of U937 promonocytic cells: AP-1-dependent gene expression and protein kinase C activation. Cell Growth Diff. 5: 949-955.

Persky, V., van Horn, L. 1995. Epidemiology of soy and cancer: perspectives and directions. J. Nutr. 125: 709S-7012S.

Pestell, R.G., Albanese, C., Reutens, A.T., Segall, J.E., Lee, R.J., Arnold, A. 1999. The cyclins and cyclin-dependent kinase inhibitors in hormonal regulation of proliferation and differentiation. Endocrine Rev. 20 (4): 501-534.

Peters-Golden, M., Canetti, C., Mancuso, P., Coffey, M.J. 2004. Leukotrienes: underappreciated mediators of innate immune responses. J. Immunol. 173: 589-594.

Piironen, V., Lindsay, D.G., Miettinen, T.A., Toivo, J., Lampi, A-M. 2000. Plant sterols: biosynthesis, biological function and their importance to human nutrition. J. Sci. Food Agric. 80: 939-966.

Planchais, S., Glab, N., Inzé, D., Bergounioux, C. 2000. Chemical inhibitors: a tool for plant cell cycle studies. FEBS Lett. 476: 78-83.

Pollock, K.G.J., McNeil, K.S., Mottram, J.C., Lyons, R.E., Brewer, J.M., Scott, P., Coombs, G.H., Alexander, J. 2003. The *Leishmania mexicana* cysteine protease, CPB2.8, induces potent Th2 responses. J. Immunol. 170: 1749-1753.

Potgieter, M., Wenteler, G.L., Drewes, S.G. 1988. Synthesis of rooperol [1,5-bis(3',4'-dihydroxyphenyl)pent-1-en-4-yne]. Phytochemistry 27 (4): 1101-1104

Proskuryakov, S.Y., Konoplyannikov, A.G., Gabai, V.L. 2003. Necrosis: a specific form of programmed cell death? Exp. Cell Res. 283: 1-16.

Puig, P-E., Guilly, M-N., Bouchot, A., Droin, N., Cathelin, D., Bouyer, F., Favier, L., Ghiringhelli, F., Kroemer, G., Solary, E., Martin, F., Chauffert, B. 2008. Tumor cells can escape DNA-damaging cisplatin through DNA endoreduplication and reversible polyploidy. Cell Biol. Int. 32: 1031-1043.

Quílez, J., García-Lorda, P., Salas-Salvadó, J. 2003. Potential uses and benefits of phytosterols in diet: present situation and future directions. Clin. Nutr. 22 (4): 343-351.

Reddy, L., Odhav, B., Bhoola, K.D. 2003. Natural products for cancer prevention: a global perspective. Pharmacol. Therapeut. 99: 1-13.

Reed, J.C. 1998. Bcl-2 family proteins. Oncogene 17: 3225-3236.

Riboli, E., Norat, T. 2003. Epidemiologic evidence of the protective effect of fruit and vegetables on cancer risk. Am. J. Clin. Nutr. 78: 559-569.

Rice-Evans, C.A., Miller, N.J., Paganga, G. 1997. Antioxidant properties of phenolic compounds. Trends Plant Sci. 2 (4): 152-159.

Richelle, M., Enslen, M., Hager, C., Groux, M., Tavazzi, I., Godin, J-P., Berger, A., Métairon, S., Quaile, S., Piguet-Welsch, C., Sagaloxics, L., Green, H., Fay, L.B. 2004. Both free and esterified plant sterols reduce cholesterol absorption and the bioavailability of β-carotene and α-tocopherol in normocholesterolemic humans. Am. J. Clin. Nutr. 80: 171-177.

Risa, J., Risa, A., Adsersen, A., Gauguin, B., Stafford, G.I., van Staden, J., Jäger, A.K. 2004. Screening of plants used in southern Africa for epilepsy and convulsions in the $GABA_A$-benzodiazepine receptor assay. J. Ethnopharmacol. 93: 177-182.

Rocca, B., FitzGerald, G.A. 2002. Cyclooxygenase and prostaglandins: shaping up the immune response. Int. Immunopharmacol. 2: 603-630.

Rodriguez, C., Mayo, J.C., Sainz, R.M., Antolín, I., Herrera, F., Martín, V., Reiter, R.J. 2003. Regulation of antioxidant enzymes: a significant role for melatonin. J. Pineal. Res. 36: 1-9.

Röhrdanz, E., Kahl, R. 1997. Alterations of antioxidant enzyme expression in response to hydrogen peroxide. Free Radic. Biol. Med. 24 (1): 27-38.

Roninson, I.B. 2002. Oncogenic functions of tumour suppressor $p21^{Waf1/Cip1/Sdi1}$: association with cell senescence and tumour-promoting activities of stromal fibroblasts. Cancer Lett. 179: 1-14.

Rothe, G., Valet, G. 1990. Flow cytometric analysis of respiratory burst activity in phagocytes with hydroethidine and 2',7'-dichlorofluorescin. J. Leukoc. Biol. 47: 440-448.

Rots, N.Y., Iavarone, A., Bromleigh, V., Freedman, L.P. 1999. Induced differentiation of U937 cells by 1,25-dihydroxyvitamin D3 involves cell cycle arrest in G1 that is preceded by a transient proliferative burst and an increase in cyclin expression. Blood 93 (8): 2721-2729.

Salganik, R.I. 2001. The benefits and hazards of antioxidants: controlling apoptosis and other protective mechanisms in cancer patients and the human population. J. Am. Coll. Nutr. 20 (5): 464-472.

Salih, H.R., Husfeld, L., Adam, D. 2000. Simultaneous cytofluorometric measurement of phagocytosis, burst production and killing of human phagocytes using *Candida albicans* and *Staphylococcus aureus* as target organisms. Clin. Microbiol. Infect. 6: 251-258.

Salvemini, D., Misko, T.P., Masferrer, J.L., Seibert, K., Currie, M.G., Needleman, P. 1993. Nitric oxide activates cyclooxygenase enzymes. Proc. Natl. Acad. Sci. 90: 7240-7244.

Schuette, R., LaPointe, M.C. 2000. Phorbol ester stimulates cyclooxygenase-2 expression and prostanoid production in cardiac myocytes. Am. J. Heart Circ. Physiol. 279: 719-725.

Scott, G., Springfield, E.P. 2004. Pharmaceutical monographs of 60 indigenous plant species used as traditional medicines in South Africa. South African National Biodiversity Institute (SANBI) plant information website at www.plantzafrica.com.

Semenov, D.V., Aronov, P.A., Kuligina, E.V., Potapenko, M.O., Richter, V.A. 2004. Oligonucleosome DNA fragmentation of caspase-3 deficient MCF-7 cells in palminate-induced apoptosis. Nucleos. Nucleot. Nucleic Acids. 23 (6&7): 831-836.

Shackelford, R.E., Kaufmann, W.K., Paules, R.S. 2000. Oxidative stress and cell cycle checkpoint function. Free Radic. Biol. Med. 28 (9): 1387-1404.

Shale, T.L., Stirk, W.A., van Staden, J. 1999. Screening of medicinal plants used in Lesotho for anti-bacterial and anti-inflammatory activity. J. Ethnopharmacol. 67: 347-354.

Shayo, C.S., Mladovan, A.G., Baldi, A. 1997. Differentiating agents modulate topoisomerase I activity in U-937 promonocytic cells. Eur. J. Pharmacol. 324: 129-133.

Sheng, H., Shao, J., Washington, M.K., DuBois, R.N. 2001. Prostaglandin E2 increases growth and motility of colorectal carcinoma cells. J. Biol. Chem. 276 (21): 18075-18081.

Shigemassa, K., Tian, X., Gu, L., Shiroyama, Y., Nagai, N., Ohama, K. 2003. Expression of cyclooxygenase-2 and its relationship to p53 accumulation in ovarian adenocarcinomas. Int. J. Oncol. 22: 99-105.

Sibanda, S., Ntabeni, O., Nicoletti, M., Galeffi, C. 1990. Nyasol and 1,3)5)-diphenyl-1-pentene related glycosides from *Hypoxis angustifolia*. Biochem. Syst. Ecol. 18 (7/8): 481-483.

Simstein, R., Burow, M., Parker, A., Weldon, C., Beckman, B. 2003. Apoptosis, chemoresistance, and breast cancer: insights from the MCF-7 cell model system. Exp. Biol. Med. 228: 995-1003.

Singh, Y. 1999. *Hypoxis*: yellow stars of horticulture, folk remedies and conventional medicine. Veld & Flora (September): 123-125.

Singh, Y. 2007. *Hypoxis* (Hypoxidaceae) in southern Africa: Taxonomic notes. S. Afr. J. Bot. 73: 360-365.

Sivaprasad, U., Machida, Y.J., Dutta, A. 2007. APC/C – the master controller of origin licensing? Cell Div. 2 (8): doi. 10.1186/1747-1028-2-8.

Smit, B.J., Albrecht, C.F., Liebenberg, R.W., Kruger, P.B., Freestone, M., Gouws, L., Theron, E., Bouic, P.J.D., Etsebeth, S., van Jaarsveld, P.P. 1995. A phase I trial of hypoxoside as an oral prodrug for cancer therapy – absence of toxicity. S. Afr. Med. J. 9: 865-870.

Spizzo, G., Gastl, G., Wolf, D., Gunsilius, E., Steurer, M., Fong, D., Amberger, A., Margreiter, R., Obrist, P. 2003. Correlation of COX-2 and Ep-CAM overexpression in human invasive breast cancer and its impact on survival. Br. J. Canc. 88: 574-578.

Springfield, E.P., Eagles, P.K.F., Scott, G. 2005. Quality assessment of South African herbal medicines by means of HPLC fingerprinting. J. Ethnopharmacol. 101: 75-83.

Srivastava, V., Negi, A.S., Kumar, J.K., Gupta, M.M., Khanuja, S.P.S. 2005. Plant-based anticancer molecules: a chemical and biological profile of some important leads. Bioorg. Med. Chem. 13: 5892-5908.

Steenkamp, V. 2003a. Traditional herbal remedies used by South African women for gynaecological complaints. J. Ethnophamacol. 86: 97-108.

Steenkamp, V. 2003b. Phytomedicine for the prosate. Fitoterapia 74: 545-552.

Steenkamp, V., Gouws, M.C. 2006. Cytotoxicity of six South African medicinal plant extracts used in the treatment of cancer. S. Afr. J. Bot. 72: 630-633.

Steenkamp, V., Gouws, M.C., Gulumian, M., Elgorashi, E.E., van Staden, J. 2006. Studies on antibacterial, anti-inflammatory and antioxidant activity of herbal remedies used in the treatment of benign prostatic hyperplasia and prostatitis. J. Ethnopharmacol. 103: 71-75.

Stefanini, M. 1985. Enzymes, isoenzymes, and enzyme variants in the diagnosis of cancer. Cancer 55: 1931-1936.

Stewart, Z.A., Leach, S.D., Pietenpol, J.A. 1999. $p21^{Waf1/Cip1}$ inhibition of cyclin E/Cdk2 activity prevents endoreduplication after mitotic spindle disruption. Mol. Cell. Biol. 19 (1): 205-215.

Sudo, T., Ueno, N.T., Saya, H. 2004. Functional analysis of APC-Cdh1. Methods Mol. Biol. 281: 189-198.

Sugimoto-Shirasu, K., Roberts, K. 2003. “Big it up”: endoreduplication and cell-size control in plants. Curr. Opin. Plant Biol. 6: 544-553.

Sun, X-M., MacFarlane, M., Zhuang, J., Wolf, B.B., Green, D.R., Cohen, G.M. 1999. Distinct caspase cascades are initiated in receptor-mediated and chemical-induced apoptosis. J. Biol. Chem. 274 (8): 5053-5060.

Sutou, S., Tokuyama, F. 1974. Induction of endoreduplication in cultured mammalian cells by some chemical mutagens. Cancer Res. 34: 2615-2613.

Tapiero, H., Townsend, D.M., Tew, K.D. 2003. Phytosterols in the prevention of human pathologies. Biomed. Pharmacother. 57: 321-325.

Theron, E.J., Albrecht, C.F., Kruger, P.B., Jenkins, K., van der Merwe, M.J. 1994. β-glucosidase activity in fetal bovine serum renders the plant glucoside, hypoxoside, cytotoxic toward B16-F10-BL-6 mouse melanoma cells. In Vitro Cell. Div. Biol. 30A: 115-119.

Tiscornia, A., Cairoli, E., Marquez, M., Denicola, A., Pritsch, O., Cayota, A. 2009. Use of diaminofluoresceins to detect and measure nitric oxide in low level generating human immune cells. J. Immunol. Methods 342: 49-57.

Toivo, J., Lampi, A-M., Aalto, S., Piironen, V. 2000. Factors affecting sample preparation in the gas chromatographic determination of plant sterols in whole wheat flour. Food Chem. 68: 239-245.

Trichopoulou, A., Lagiou, P., Kuper, H., Trichopoulos, D. 2000. Cancer and Mediterranean dietary traditions. Cancer Epidemiol., Biomarkers Prev. 9: 869-873.

Tsiftsoglou, A., Pappas, I.S., Vizirianakis, I.S. 2003. Mechanisms involved in the induced differentiation of leukemia cells. Pharmacol. Therapeut. 100: 257-290.

Tsuji, M., Kawano, S., DuBois, R.N. 1997. Cyclooxygenase-2 expression in human colon cancer cells increases metastatic potential. Proc. Natl. Acad. Sci. 94: 3336-3340.

Van der Merwe, M.J., Jenkins, K., Theron, E., van der Walt, B.J. 1993. Interaction of the di-catechols rooperol and nordihydroguaiaretic acid with oxidative systems in the human blood. Biochem. Pharmacol. 45 (2): 303-311.

Vanderplank, H.J. 1998. Wildflowers of the Port Elizabeth area: Swartkops to Sundays rivers. Bluecliff Publishing 1st Ed. Hunters Retreat. South Africa: p46

Van Engeland, M., Ramaekers, F.C.S., Schutte, B., Reutelingsperger, C.P.M. 1996. A novel assay to measure loss of plasma membrane asymmetry during apoptosis of adherent cells in culture. Cytometry 24: 131-139.

Van Engeland, M., Nieland, L.J.W., Ramaekers, F.C.S., Schutte, B., Reutelingsperger, C.P.M. 1998. Annexin V-affinity assay: a review on an apoptosis detection system based on phosphatidylserine exposure. Cytometry 31: 1-9.

Van Wyk, B-E., van Oudtshoorn, B., Gericke, N. 1997. Medicinal plants of South Africa. Briza Publications. Pretoria, South Africa: 156-157.

Van Wyk, B-E., Gericke, N. 2000. People's plants: a guide to useful plants of southern Africa. Briza Publications. Pretoria, South Africa: 146-147.

Van Wyk, B-E. 2008. A broad review of commercially important southern African medicinal plants. J. Etnopharmacol. 119 (3): 342-355.

Verhoven, B., Schlegel, R.A., Williamson, P. 1995. Mechanisms of phosphatidylserine exposure, a phagocyte recognition signal, on apoptotic T lymphocytes. J. Exp. Med. 182: 1597-1601.

Vermes, I., Haanen, C., Steffens-Nakken, H., Reutelingsperger, C. 1995. A novel assay for apoptosis: flow cytometric detection of phosphatidylserine expression on early apoptotic cells using fluorescein labelled Annexin V. J. Immunol. Methods 184: 39-51.

Vivancos, M., Moreno, J.J. 2005. β-sitosterol modulates antioxidant enzyme response in RAW264.7 macrophages. Free Radic. Biol. Med. 39: 91-97.

Von Holtz, R.L., Fink, C.S., Awad, A.B. 1998. β-sitosterol activates the sphingomyelin cycle and induces apoptosis in LNCaP human prostatic cancer cells. Nutr. Cancer 32 (1): 8-12.

Vorster, H.H., Raal, F.J., Ubbink, J.B., Marais, A.D., Rajput, M.C., Ntanios, F.Y. 2003. Functional foods with added plant sterols for treatment of hypercholesterolaemia and prevention of ischaemic heart disease. SAJCN 16 (2): 49-58

Wallerath, T., Deckert, G., Ternes, T., Anderson, H., Li, H., Witte, K., Förstermann, U. 2002. Resveratrol, a polyphenolic phytoalexin present in red wine, enhances expression and activity of endothelial nitric oxide synthase. Circulation 106: 1652-1658.

Webb, J.R., Campos-Neto, A., Ovendale, P.J., Martin, T.I., Stromberg, E.J., Badoro, R., Reed, S.G. 1998. Human and murine immune responses to a novel *Leishmania major* recombinant protein encoded by members of a multicopy gene family. Infect. Immun. 66: 3279-3289.

Wenteler, G.L., Pegel, K.H., Drewes, S., Kundig, H. 1991. Process for the preparation of rooperol. US Patent 5008471.

Willett, W.C. 2000. Diet and cancer. The Oncologist 5: 393-404.

Willett, W.C. 2001. Diet and cancer: one view at the start of the millennium. Cancer Epidemiol. Biomarkers Prev. 10: 3-8.

Wolf, B.B., Schuler, M., Echeverri, F., Green, D.R. 1999. Caspase-3 is the primary activator of apoptotic DNA fragmentation via DNA fragmentation factor-45/inhibitor of caspase-activated DNase inactivation. J. Biol. Chem. 274(43): 30651-30656.

Yuste, V.J., Bayascas, J.R., Llecha, N., Sánchez-López, I., Boix, J., Comella, J.X. 2001. The absence of oligonucleosomal DNA fragmentation during apoptosis of IMR-5 neuroblastoma cells. J. Biol. Chem. 276(25): 22323-22331.

Zha, S., Yegnasubramanian, V., Nelson, W.G., Isaacs, W.B., De Marzo, A.M. 2004. Cyclooxygenases in cancer: progress and perspective. Cancer Lett. 215: 1-20.

Zhang, X., Geoffroy, P., Miesch, M., Julien-David, D., Raul, F., Aoudé-Werner, D., Marchioni, E. 2005. Gram-scale chromatographic purification of β-sitosterol synthesis and characterization of β-sitosterol oxides. Steroids 70: 886-895.

Zielonka, J., Kalyanaraman, B. 2008. "ROS-generating mitochondrial DNA mutations can regulate tumor cell metastasis" – a critical commentary. Free Radic. Biol. Med. 45: 1217-1219.

www.cansa.org.za

www.biochem.roche.com

www.promega.com

www.who.int.

African Journal of Biotechnology Vol. 7 (11), pp. 1624-1629, 3 June, 2008
Available online at http://www.academicjournals.org/AJB
ISSN 1684–5315 © 2008 Academic Journals

Full Length Research Paper

Quantitative and qualitative analysis of sterols/sterolins and hypoxoside contents of three *Hypoxis* (African potato) spp.

Gerhardt J. Boukes, Maryna van de Venter* and Vaughan Oosthuizen

Department of Biochemistry and Microbiology, Faculty of Science, PO Box 77000, Nelson Mandela Metropolitan University, Port Elizabeth 6031, South Africa.

Accepted 25 April, 2008

The glycoside, hypoxoside, identified and isolated from the corms of the African potato (*Hypoxis hemerocallidea*) has shown promising anticancer activities. The African potato is used as an African traditional medicine for its nutritional and medicinal properties. Most research has been carried out on *H. hemerocallidea* (formerly known as *H. rooperi*), with very little or nothing on other *Hypoxis* spp. Thin layer chromatography (TLC) was used to confirm the presence of sterols/sterolins, whereas a GC method was developed to identify and quantify sterols (especially β-sitosterol) in chloroform extracts of *H. hemerocallidea, H. stellipilis* and *H. sobolifera* var. *sobolifera*. High performance liquid chromatography (HPLC) was used to identify and quantify hypoxoside content in these *Hypoxis* spp. TLC results showed that *H. sobolifera* var. *sobolifera* contained the most sterols and sterolins compared to the other two *Hypoxis* spp. Gas chromatography (GC) results show that β-sitosterol and campesterol were the two main phytosterols present in the *Hypoxis* extracts. *H. sobolifera* var. *sobolifera* and *H. hemerocallidea* contained the most β-sitosterol and hypoxoside, respectively. *H. sobolifera* and *H. hemerocallidea* contained 74.69 µg of β-sitosterol and 12.27 µg of hypoxoside per 5 mg of chloroform extracts, respectively. These results show a significant difference in the sterol/sterolin and hypoxoside contents between species of the genus *Hypoxis*, which may influence their degree of biological activities.

Key words: *Hypoxis*, TLC, GC, HPLC, sterol(in)s, hypoxoside.

INTRODUCTION

Hypoxis hemerocallidea Fisch., C.A. Mey. and Avé-Lall., syn. *H. rooperi,* (commonly known as the African potato; belonging to the family *Hypoxidaceae*) topped the list of the 60 most frequently traded plant species in the Eastern Cape, South Africa, when studies were conducted among street traders, traditional healers, store-owners and clinic patients (Dold and Cocks, 2002).

Glycosides, isolated from *Hypoxis* species, have a common pent-1-en-4-yne backbone or a slight modification of it (Sibanda et al., 1990; Messana et al., 1989; Marini-Bettolo et al., 1985; Nicoletti et al., 1992 and Marini-Bettolo et al., 1991). The glycoside, hypoxoside ((E)-1, 5-bis (4'-β-D-glucopyranosyloxy-3'-hydroxyphenyl) pent-4-en-1-yne) (Marini-Bettolo et al., 1982 and Drewes et al., 1984) has shown promising anticancer activities. *In vitro* conversion, catalyzed by β-glucosidase, of non-toxic hypoxoside to cytotoxic rooperol (Drewes and Liebenberg, 1987) has shown growth inhibition of 60 human cancer cell lines tested including breast, colon, uterus, melanoma and non-small cell lung cancer cell lines (Albrecht et al., 1995 and Smit et al., 1995).

Sterols are amphiphilic molecules consisting of hydroxyl groups forming the hydrophilic heads and sterane skeletons with side chains forming the hydrophobic tails (Heldt, 2005). Cholesterol ($C_{27}H_{45}OH$) is the main sterol found in mammals where it plays an important role in the structure and function of cell membranes, production of bile, as precursor of hormones and a role in the immune

*Corresponding author. E-mail: maryna.vandeventer@nmmu.ac.za. Tel: +27415042813. Fax: +27415042814.

system (De Brabander et al., 2007). Sterols found in plants are known as phytosterols and over 250 phytosterols and their related compounds have been identified (De Brabander et al., 2007) in foods like plant oils, nuts, seeds, cereals, fruits and vegetables (Piironen et al., 2000; Ostlund, 2002). Phytosterols differ from cholesterol in being alkylated at C-24 with C_1 or C_2 substituents (Buchanan et al., 2000). In nature, plants contain sterols with their associated sterolins (glucosides), which are easily destroyed by glycosidic enzymes (Pegel, 1976).

Phytosterols cannot be synthesized by humans and are thus consumed from the diet. The most commonly found phytosterols are sitosterol (C_{29}), campesterol (C_{28}) and stigmasterol (C_{29}) (Pegel, 1980; Ostlund, 2002). Phytosterols are incorporated in a variety of food products (functional foods (Vorster et al., 2003)) due to their cholesterol-lowering effect, hence providing protection against cardiovascular disease (Tapiero et al., 2003). Studies with phytosterols, especially β-sitosterol, have shown inhibition of several cancer cell lines including colon (Raicht et al., 1980; Choi et al., 2003 and Awad et al., 1998), prostate (von Holtz et al., 1998) and breast (Steenkamp and Gouws, 2006; Ju et al., 2004; Awad et al., 2003 and Awad et al., 2001). The role of plant sterols as immune modulators (Bouic et al., 2001; Bouic and Lamprecht, 1999; Bouic 2002 and Breytenbach et al., 2001) and anti-inflammatory agents (Quilez et al., 2003; Pegel, 1979) has also been described.

Some of the compounds (hypoxoside, β-sitosterol and other sterols/sterolins) that may be responsible for the medicinal properties of *Hypoxis* have been identified in *H. hemerocallidea* but the quantity of these in different *Hypoxis* spp. is unknown. Various species of *Hypoxis* are sold and used indiscriminately without any evidence that they contain equal quantities of sterols/sterolins and hypoxoside. The main aims of this study were to identify and quantify the sterol/sterolin and hypoxoside contents of *H. hemerocallidea*, *H. stellipilis* Ker Gawl. and *H. sobolifera* var *sobolifera* (Jacq.) Nel.

MATERIALS AND METHODS

Reagents and chemicals

Sterol standards (β-sitosterols [purity > 90%], campesterol [purity > 65%], cholesterol [purity > 99%], desmosterol [purity ≥ 85%], ergosterol [purity ≥ 95%], fucosterol [purity ~ 95%], stigmasterol [purity ~ 95%] and stigmastenol [purity > 95%]) were purchased from Sigma Chemical Co. (MO, USA). HPLC grade acetonitrile and methanol were purchased from Romil Ltd. (Cambridge, UK). Water was obtained from a Milli-Q Compact System (Millipore, Bedford, MA).

Plant material

Corms of *H. hemerocallidea* (PEU 14798) and *H. stellipilis* (PEU 14841) were purchased in Port St Johns and Port Elizabeth (Xhosa traditional medicine shop), respectively, in the Eastern Cape, South Africa. Corms of *H. sobolifera* var *sobolifera* (PEU 14840) were collected near Plettenberg Bay in the Southern Cape, South Africa. Corms of the three *Hypoxis* spp. were planted in the same soil type and exposed to equal amounts of sunlight, humidity and water for at least six months before they were harvested and used fresh. The plants were identified by Y. Singh from the South African National Biodiversity Institute (SANBI) and voucher specimens were deposited in the Nelson Mandela Metropolitan University herbarium.

Isolation of hypoxoside and sterols/sterolins

Corms of *H. hemerocallidea*, *H. stellipilis* and *H. sabolifera* were washed, peeled, grated and crushed using a mortar and pestle. Chloroform was added to the plant material in a 1:1 (v:w) ratio, vortexed (5 min), extracted (15 min) and centrifuged (3645 x g for 5 min) at room temperature. The supernatant was removed and the extracting method repeated with the same plant material. The chloroform was evaporated *in vacuo* and mass of extracts determined. After mass determination the extracts were redissolved in chloroform until further use.

TLC

β-Sitosterol (2 µg) and stigmasterol (2 µg) standards (Supelco, USA) and *Hypoxis* extracts (500 µg) dissolved in chloroform were spotted onto 20 x 20 cm silica coated aluminum plates (Merck, Germany) and air dried. Chromatogram tanks were equilibrated for one hour using toluene – diethyl ether (40:40, v/v) and chloroform – ethyl acetate – formic acid (5:4:1, v/v/v) as mobile phases for sterol and sterolin identification, respectively. TLC plates were developed for ±20 min or until the solvent front was ±1 cm from the top of the plate. Detection of sterols/sterolins was performed as described by Scott and Springfield (2004). In brief, TLC plates were dried at room temperature and developed by firstly dipping into a solution containing 5% sulfuric acid in 96% ethanol for 15 s followed by a solution containing 1% vanillin in 96% ethanol for 15 s and dried at room temperature. Once dried, plates were heated at 80 – 100°C for five min. Photos of the developed TLC plates were taken with the AlphaImager™ 3400 (Alpha Innotech.).

GC

GC analysis of sterols was performed using a Thermo Finnigan Focus gas chromatograph equipped with a FID and an Autoinjector AI3000, with Delta Chromatography 5.0 software. The column used for GC separation was a SAC™-5 capillary column (Supelco, 30 m × 0.25 mm i.d. × 0.25 µm film thickness). The thermal conditions were: 80°C for 2 min; 10°C.min^{-1} to 300°C; 300°C for 14 min. The carrier gas was He (1 ml.min^{-1} constant flow) and the injection volume was 2 µl (splitless). A sterol mixture (containing 100 µg/ml of each sterol standard) was spiked individually to identify the peaks. An increase in peak area was used as criteria to identify each peak.

HPLC

High performance liquid chromatography (HPLC) analysis of hypoxoside was performed using a Beckman System Gold high performance liquid chromatograph equipped with Solvent Module 128, Diode Array Detector Module 169. The column used for HPLC separation was a Nucleosil C_{18} column (Supelco, 5 µm, 150 × 4.6 mm i.d.). Detection of hypoxoside was performed as described by Nair and Kanfer (2006). In brief, acetonitrile – water (20:80, v/v) was used as mobile phase in isocratic mode at a flow rate of 1 ml/min and the injection volume was 10 µl. Detection was achieved in the

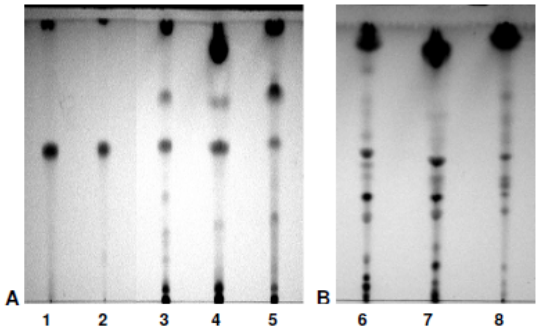

Figure 1. TLC plate of the (A) sterols and (B) sterolins found in chloroform *Hypoxis* spp. extracts (1) β-sitosterol, (2) stigmasterol, (3/6) *H. hemerocallidea*, (4/7) *H. sobolifera* and (5/8) *H. stellipilis*.

range of 200 - 400 nm and hypoxoside was detected at a wavelength of 260 nm. Stock solutions of hypoxoside (1 mg/ml), *H. hemerocallidea* (5 mg/ml), *H. stellipilis* (10 mg/ml) and *H. sobolifera* (10 mg/ml) were prepared in methanol and filtered through 0.2 µm syringe filters (Corning Incorporated, New York, USA).

RESULTS AND DISCUSSION

Chloroform has been shown to be very effective in dissolving sterols (Toivo et al., 2000) due to its non-polar nature. The presence of sterols and sterolins in the chloroform extracts of *H. hemerocallidea*, *H. stellipilis* and *H. sobolifera* var *sobolifera* was confirmed via TLC. Modification of the mobile phase, toluene – diethyl ether – 1.75 M acetic acid (1:1:1, v/v/v) used by Scott and Springfield (2004), to toluene – diethyl ether (40:40, v/v) resulted in better sterol separation (Figure 1A). The spots of the sterol standards (stigmasterol and β-sitosterol) had the same Rf value of 0.53. Cholesterol, campesterol, desmosterol, ergosterol, fucosterol and stigmastenol migrated the same distance on the TLC plates (data not shown), with the spots differing only in colour ranging from pink to blue. This made it impossible to identify and quantify individual sterols in the *Hypoxis* extracts, using TLC.

The mobile phase used for sterolin identification consisted of chloroform – ethyl acetate – formic acid (5:4:1, v/v/v). The sterolins in the *Hypoxis* extracts could not be identified or quantified due to the unavailability of sterolin standards (Figure 1B). From the results obtained, different sterolins (based on Rf values) were detected and differences in sterolin composition could clearly be seen between the three *Hypoxis* species (Figure 1).

GC is the technique of choice to analyze the presence of sterols in food (Cunha et al., 2006; Contarini et al., 2002; Toivo et al., 2000; Lagarda et al., 2006 and Goudjil et al., 2003) due to shorter analysis times, less peak interference, improved resolution, greater detection sensitivity (low nanogram range) and thermal stability of the capillary columns (Abidi, 2001). The SAC-5™ capillary column, consisting of 95% dimethylpolysiloxane and 5% phenyl, is specially packed for the analysis of plant and animal sterols. The sterol/stanol standard mixture (100 µg of each sterol/mL), consisting of β-sitosterol (30.6 min), campesterol (29.3 min), cholesterol (27.8 min), desmosterol/ergosterol (28.9 min), fucosterol (28.3 min), stigmasterol (29.7 min) and stigmastenol (30.9 min) was well separated, except for desmosterol and ergosterol, which eluted at the same retention time, with good resolution on the SAC-5™ column within a period of 32 min (Figure 2).

From GC analysis, it was clear that β-sitosterol was the main phytosterol found in the chloroform extracts of *H. hemerocallidea*, *H. stellipilis* and *H. sobolifera*. Trace amounts (<10 µg per 5 mg of *Hypoxis* extract) of campesterol were also found in all three *Hypoxis* spp. extracts, whereas trace amounts of desmosterol/ergosterol, stigmasterol, stigmastenol were found only in certain *Hypoxis* spp. A standard curve of β-sitosterol concentration (ranging between 10 - 100 µg/mL) as a function of peak height (R^2 = 0.9531, R_T = 30.6 min) was used to quantify β-sitosterol content. *H. sobolifera* contained the most β-sitosterol with ±2.5 and 7.5 times more β-sitosterol compared to *H. hemerocallidea* and *H. stellipilis*, respectively (Table 1).

The presence of β-sitosterol and campesterol as the two major phytosterols in *Hypoxis* correspond to published data (Moghadasian, 2000; Pegel, 1976). According to a minireview by Moghadasian (2000), 95% of dietary phytosterols consist of sitosterol and campesterol (approximately 65 and 30%, respectively), whereas the other phytosterols (mainly stigmasterol) and stanols make up the other 5%.

This is the first time that GC was used to identify and quantify the presence of sterols in *Hypoxis* extracts. Nair et al. (2006) have used high performance liquid chromatography to determine the presence of β-sitosterol, stigmasterol and stigmastenol in commercially available oral dosage forms reported to contain material or extracts of *Hypoxis*. Using the SAC-5™ capillary column eliminated time-consuming preparation steps, for example extraction of lipid fraction from sample material, saponification (alkaline hydrolysis), extraction of non-saponifiables and derivatization of the sterol standards and *Hypoxis* extracts (Toivo et al., 2000).

The presence of hypoxoside has been identified in several South African species of *Hypoxis* (Nicoletti et al., 1992) including *H. hemerocallidea* (Nair and Kanfer, 2006), but not in *H. stellipilis* or *H. sobolifera*. The HPLC method described by Nair and Kanfer (2006) was used to quantify hypoxoside content in the three *Hypoxis spp* (Figure 3). Hypoxoside was detected after 12.5 minutes and quantified from a standard curve of hypoxoside concentration (ranging between 5 - 100 µg/mL) as a function of peak area (R^2 = 0.9971, R_T = 30.6).

Of the three *Hypoxis* species tested for hypoxoside

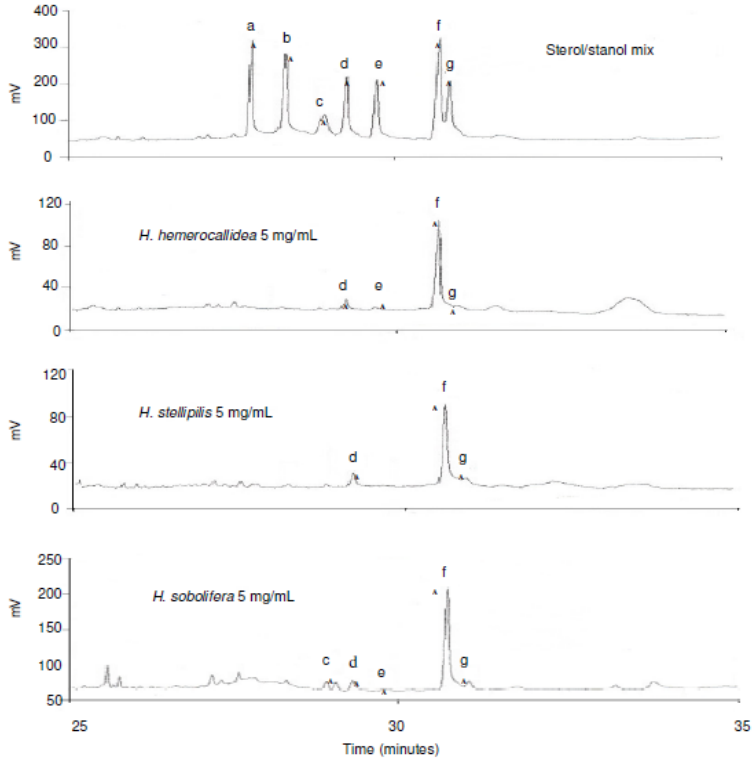

Figure 2. GC chromatograms of standards and chloroform *Hypoxis* extracts: (a) cholesterol, (b) fucosterol, (c) desmosterol/ergosterol, (d) campsterol, (e) stigmasterol, (f) β-sitosterol and (g) stigmastenol.

Table 1. Content and total percentage of β-sitosterol per 5 mg of chloroform *Hypoxis* extracts.

***Hypoxis* spp.**	**Content (µg)**	**Yield (%)***
H. hemerocallidea	29.38	0.59
H. stellipilis	10.05	0.2
H. sobolifera	74.69	1.49

*w/w

Table 2. Content and total percentage of hypoxoside per 5 mg of chloroform *Hypoxis* extracts

Hypoxis spp.	**Content (µg)**	**Yield (%)***
H. hemerocallidea	12.27	0.12
H.stellipilis	7.93	0.08
H. sobolifera	Undetectable	-

* w/w

content, only *H. hemerocallidea* and *H. stellipilis* contained hypoxoside. *H. sobolifera*, which showed the highest anticancer activity (unpublished data), had undetectable levels of hypoxoside (Table 2).

Since chloroform, the solvent used in this study, is not the best solvent for hypoxoside extraction, the presence of this glycoside in *H. sobolifera* was investigated using more polar solvents. A water extract of *H. sobolifera* has shown no hypoxoside content, whereas ethanol, methanol and acetone extracts of *H. sobolifera* yielded 60.66, 49.13 and 60.35 µg per 5 mg of extract, respectively. Hypoxoside is therefore present in *H. sobolifera* but in much smaller amounts than in *H. hemerocallidea* and *H. stellipilis*. Previous studies have used 30 - 75% ethanol (Pegel, 1979) and methanol (Nair and Kanfer, 2006) to extract hypoxoside from *H. hemerocallidea*. Traditional healers/herbalists use water and boiling to make *Hypoxis* extracts, which may yield hypoxoside and sterolins

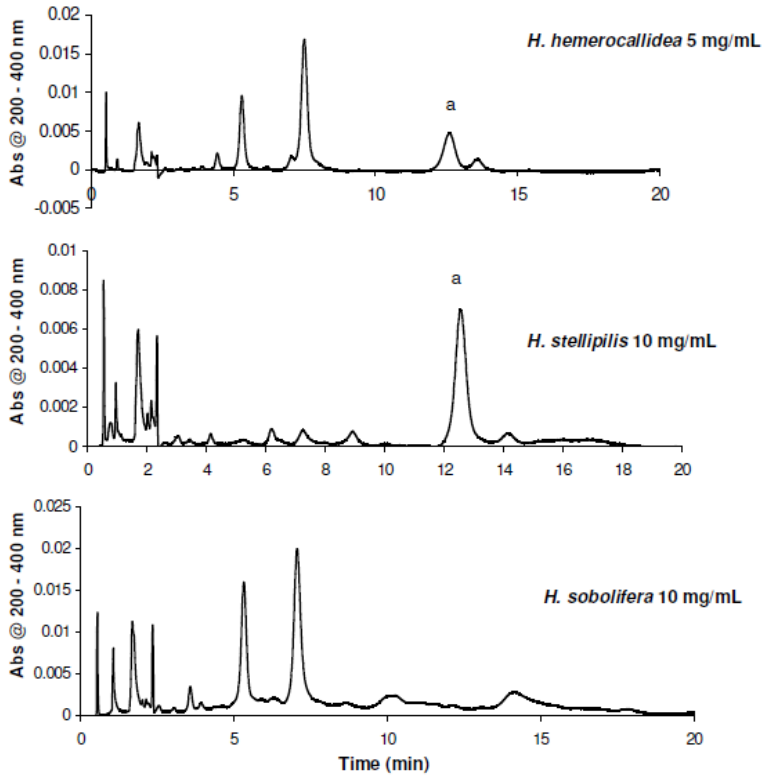

Figure 3. HPLC chromatograms of the hypoxoside content of chloroform *Hypoxis* extracts: (a) hypoxoside detected at 260 nm.

(Pegel, 1976). Due to the polar nature of hypoxoside it would be better to use more polar solvents for extractions in the future, if more emphasis is placed on the effect of hypoxoside in the *Hypoxis* extracts.

This is the first time that hypoxoside and sterol contents were quantified in *H. stellipilis* and *H. sobolifera*, and as far as we know in *H. hemerocallidea*. Both the sterol and hypoxoside contents were shown to vary between the three species. Differences in the hypoxoside and sterol/sterolin contents of the three *Hypoxis* spp. investigated may explain the differences in anticancer activity (unpublished data) obtained against certain cancer cell lines. *Hypoxis* species are used indiscriminately in traditional medicine and are sold under the common name 'African potato' in herbal shops. Further investigation is required to determine the implications of these findings in the uses of *Hypoxis* as a traditional remedy. Consumption of the three different *Hypoxis* species, which have different sterols/sterolins and hypoxoside content, may have adverse or favorable effects depending on the concentration of extract consumed. Sterols/sterolins and hypoxoside may have synergistic effects, which need to be investigated.

ACKNOWLEDGMENTS

The authors want to thank the NRF (GUN 2069228) and the MRC for funding this study, and Dr. C. Albrecht for donating purified hypoxoside.

REFERENCES

Abidi SL (2001). Chromatographic analysis of plant sterols in foods and vegetable oils. J. Chromatogr. A 935: 173-201.

Albrecht CF, Theron EJ, Kruger PB (1995). Morphological characterization of the cell-growth inhibitory activity of rooperol and pharmacokinetic aspects of hypoxoside as an oral prodrug for cancer therapy. S. Afr. Med. J. 85: 853-860.

Awad AB, Fink CS (2000). Phytosterols as anticancer dietary components: evidence and mechanism of action. J. Nutr. 130: 2127-2130.

Awad AB, von Holtz RL, Cone JP, Fink CS, Chen YC (1998). β-sitosterol inhibits the growth of HT-29 human colon cancer cells by activating the sphingomyelin cycle. Anticancer Res. 18: 471-479.
Awad AB, Williams H, Fink CS (2001). Phytosterols reduce in vitro metastatic ability of MDA-MB-231 human breast cancer cells. Nutr. Cancer 40: 157-164.
Awad AB, Williams H, Fink CS (2003). Effect of phytosterols on cholesterol metabolism and MAP kinase in MDA-MB-231 human breast cancer cells. J. Nutr. Biochem. 14: 111-119.
Bouic PJD (2002). Sterols and sterolins: new drug for the immune system? DDT 7: 775-778.
Bouic PJD, Etsebeth S, Liebenberg RW, Albrecht CF, Pegel K, van Jaarsveld PP (1996). Beta-sitosterol and beta-sitosterol glucoside stimulate human peripheral blood lymphocyte proliferation: implications for their use as an immunomodulatory vitamin combination. Int. J. Immunopharmacol. 18: 693-700.
Bouic PJD, Lamprecht JH (1999). Plant sterols and sterolins: a review of their immune-modulating properties. Altern. Med. Rev. 4: 170-177.
Breytenbach U, Clark A, Lamprecht J, Bouic PJD (2001). Flow cytometry analysis of the Th1-Th2 balance in healthy individuals and patients infected with the human immunodeficiency virus (HIV) receiving a plant sterol/sterolin mixture. Cell Biol. Int. 25: 43-49.
Buchanan BB, Gruissem W, Jones RL (2000). Biochemistry and molecular biology of plants. American Society of Plant Physiologists, Rochville (Maryland), pp 901-911.
Choi YH, Kong KR, Kim YA, Jung KO, Kil JH, Rhee SH, Park KY (2003). Induction of Bax and activation of caspases during β-sitosterol-mediated apoptosis in human colon cancer cells. Int. J. Oncol. 23: 1657-1662.
Contarini G, Povolo M, Bofitto E, Berardi S (2002). Quantitative analysis of sterols in dairy products: experiences and remarks. Int. Dairy J. 12: 573-578.
Cunha SS, Fernandes JO, Oliveira MBPP (2006). Quantification of free and esterified sterols in Portuguese olive oils by solid-phase extraction and gas chromatography-mass spectrometry. J. Chromatogr. A 1128: 220-227.
De Brabander HF, Verheyden K, Mortier V, Le Bizec B, Verbeke V, Courtheyn D, Noppe H (2007). Phytosterols and anabolic agents versus designer drugs. Anal. Chim. Acta 586: 49-56.
Dold AP, Cocks ML (2002). The trade in medicinal plants in the Eastern Cape Province, South Africa. S. Afr. J. Sci. 98: 589-597.
Drewes SE, Hall AJ, Learmonth RA, Upfold UJ (1984). Isolation of hypoxoside from *Hypoxis rooperi* and synthesis of (E)-1,5-bis(3',4'-dimethoxyphenyl)pent-4-en-1-yne. Phytochemistry 23: 1313-1316.
Drewes S, Liebenberg RW (1987). Rooperol and its derivates. U.S. Patent 4644085.
Goudjil H, Torrado S, Fontecha J, Martínez-Castro I, Fraga MJ, Juárez M (2003). Composition of cholesterol and its precursors in ovine milk. Lait 83: 153-160.
Heldt HW (2005). Plant Biochemistry 3rd Ed., Elsevier Academic Press, London, pp 364-367.
Ju YH, Clausen LM, Allred KF, Almada AL, Helferich WG (2004). β-sitosterol, β-sitosterol glucoside, and a mixture of β-sitosterol and β-sitosterol glucoside modulate the growth of estrogen-responsive breast cancer cells in vitro and in ovariectomized athymic mice. J. Nutr. 134: 1145-1151.
Lagarda MJ, García-Llata G, Farré R (2006). Analysis of phytosterols in food. J. Pharm. Biomed. Anal. 40: 1486-1496.
Marini-Bettolo GB, Galeffi C, Multari G, Palazzino G, Messana I (1991). Interjectin, a derivative of nyasicoside from *Hypoxis interjecta* and *Hypoxis multiceps*. Tetrahedron 37: 6717-6724.
Marini-Bettolo GB, Nicoletti M, Messana I, Galeffi C, Msonthi JD, Chapya WA (1985). Glucosides of *Hypoxis nyasica* Bak. The structure of nyasoside, a new glucoside biologically related to hypoxoside. Tetrahedron 41: 665-670.
Marini-Bettolo GB, Patamia M, Nicoletti M, Galeffi C, Messana I (1982). Hypoxoside, a new glycoside of uncommon structure from *Hypoxis obtusa* Busch. Tetrahedron 38: 1683-1687.
Messana I, Msonthi JD, De Vicente Y, Multari G, Galeffi C (1989). Mononyasine A and mononyasine B: two glucosides from *Hypoxis nyasica*. Phytochemistry 29: 2807-2809.
Moghadasian MH (2000). Pharmacological properties of plant sterols *in vivo* and *in vitro* observations. Life Sci. 67: 605-615.
Nair VDP, Kanfer I (2006). High-performance liquid chromatography method for the quantitative determination of hypoxoside in African potato (*Hypoxis hemerocallidea*) and commrcial products containing the plant material and/or its extracts, J. Agric. Food Chem. 54: 2816-2821.
Nair VDP, Kanfer I, Hoogmartens J (2006). Determination of stigmasterol, β-sitosterol and stigmastenol in oral dosage forms using high performance liquid chromatography with evaporative light scattering detection. J. Pharm. Biomed. Anal. 41: 731-737.
Nicoletti M, Galeffi C, Messana I, Marini-Bettolo GB (1992). *Hypoxidaceae*. Medicinal uses and the norlignan constituents. J. Ethnopharmacol. 36: 95-101.
Ostlund RE (2002). Phytosterols in human nutrition. Annu. Rev. Nutr. 22: 533-549.
Pegel KH (1976). Extraction of sterolins from plant material. U.S. Patent 3933789.
Pegel KH (1979). Active plant extracts of Hypoxidaceae and their use. U.S. Patent 4160860.
Pegel KH (1980). Sterolins and their use. U.S. Patent 4188379.
Piironen V, Lindsay DG, Miettinen TA, Toivo J, Lampi AM (2000). Plant sterols: biosynthesis, biological function and their importance to human nutrition. J. Sci. Food Agric. 80: 939-966.
Quilez J, Garcia-Lorda P, Salas-Salvado J (2003). Potential uses and benefits of phytosterols in diet: present situation and future directions. Clin. Nutr. 22: 343-351.
Raicht RFD, Cohen BI, Fazzini EP, Sarwal AN, Takahashi M (1980). Protective effect of plant sterols against chemically induced colon tumors in rats. Cancer Res. 40: 403-405.
Scott G, Springfield EP (2004). Pharmaceutical monographs of 60 indigenous plant species used as traditional medicines in South Africa. South African National Biodiversity Institute (SANBI) plant information website at www.plantzafrica.com.
Sibanda S, Ntabeni O, Nicoletti M, Galeffi C (1990). Nyasol and 1,3(5)-diphenyl-1-pentene related glycosides from *Hypoxis angustifolia*. Biochem. Syst. Ecol. 18: 481-483.
Smit BJ, Albrecht CF, Liebenberg RW, Kruger PB, Freestone M, Gouws L, Theron E, Bouic PJD, Etsebeth S, van Jaarsveld PP (1995). A phase I trial of hypoxoside as an oral prodrug for cancer therapy – absence of toxicity. S. Afr. Med. J. 85: 865-870.
Steenkamp V, Gouws MC (2006). Cytotoxicity of six South African medicinal plant extracts used in the treatment of cancer. SAJB 72: 630-633.
Tapiero H, Townsend DM, Tew KD (2003). Phytosterols in the prevention of human pathologies. Biomed. Pharmacother. 57: 321-325.
Toivo J, Lampi A-M, Aalto S, Piironen V (2000). Factors affecting sample preparation in the gas chromatographic determination of plant sterols in whole wheat flour. Food Chem. 68: 239-245.
Vorster HH, Raal FJ, Ubbink JB, Marais AD, Rajput MC, Ntanois FY (2003). Functional foods with added plant sterols for treatment of hypercholesterolaemia and prevention of ischaemic heart disease. SAJCN 16: 49-58.
von Holtz RL, Fink CS, Awad AB (1998). β-sitosterol activates the sphingomyelin cycle and induces apoptosis in LNCaP human prostate cancer cells. Nutr. Cancer 32: 8-12.

APPENDICES

APPENDIX 1: LITERATURE REVIEW

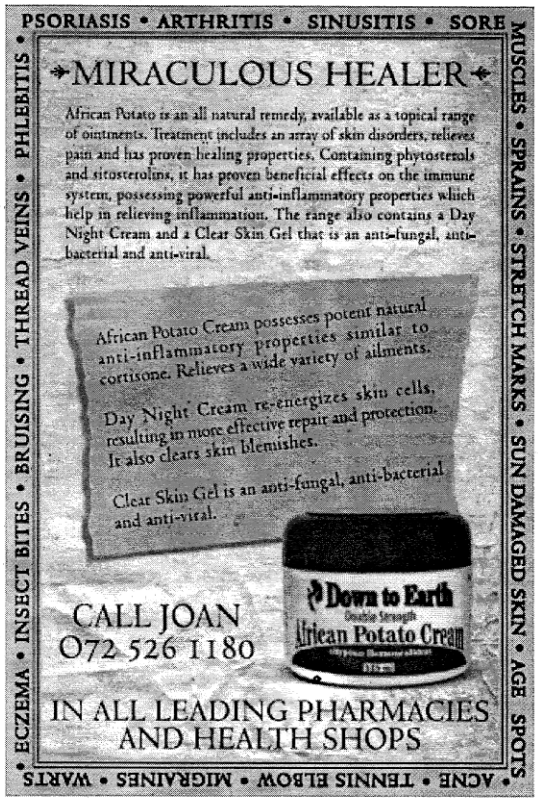

African Potato Cream

Testimonials obtained from the general public by Dr Otto Sap

1. A 53 year-old man had eczema spots on the back of his neck and for three years none of the treatment he had tried worked, so eventually he used AFRICAN POTATO CREAM and within two days it cleared up and it has not returned!

2. An 80 year-old lady had problems with both arms and legs. The skin was extremely thin and you could see lots of brown spots, some open and also big red spots under the skin because as soon as she bumped into something big blood spots came up. Her right leg was so bad that part of the skin was open (a varicose ulcer) because of weak blood vessels. She complained of pain, itching, bleeding now and then and she used bandages. The day after applying AFRICAN POTATO CREAM the pain and itching disappeared and after two weeks you could see that new skin was forming on the borders of the open wound. I saw her after a year and there was only a little spot of +- 4cm visible and this healed three months later. The skin of both arms was much better and thicker.

3. A 76 year-old man had had a bad skin for a long while. He went to the dermatologist every couple of months to have precancerous spots removed either by burning or by surgery. Just after one of these session the patient started with African potato cream and Clear Skin Gel. The skin reacted very well and the cancer spots have not returned

4. A 43 year-old woman and a 33 year-old man were both diagnosed with acne rosacea and no therapies were successful. After using Clear Skin Gel in the morning and AFRICAN POTATO CREAM in the evening, in both cases cleared up and the spots never returned.

5. About 10 young ladies, between 12 and 19 years of age, all with acne on their face and upper back found the acne clearing up very well by using Clear Skin Gel. I also asked them to use Revive Day/Night cream, which they still do as their skin feels very smooth and looks good.

Wild News Issue # 146 – 10 December 2008 page 9

PRODUCT INFORMATION

DOWN TO EARTH

AFRICAN POTATO CREAM DOUBLE STRENGTH (125ml & 250ml)

The African Potato (Hypoxis hemerocallidea) has remained unmodified for over 300 000 years and contains up to 50 000 times as many sterols as modern vegetables. Plant sterols/sterolins (which possess potent anti-inflammatory properties similar to cortisone, but without the side effects) decrease the blood levels of cortisol as well as the factors which induce inflammation like, for example, tissue damage, muscular aches and stiffness. The active ingredient of *sterols* and *sterolins* gives effective relief for the treatment of ACHING JOINTS, ARTHRITIS, CRACKED HEELS, COLD SORES, FIBROSITIS, GOUT, INSECT BITES, SUNBURN, RHEUMATOID ARTHRITIS, PSORIASIS, MUSCLE INJURIES, SPRAINS, SUN DAMAGED SKIN, MUSCULAR PAINS, SKIN RASH, SINUSITIS, TENNIS ELBOW, INSECT BITES, MIGRAINES, ECZEMA, WARTS. It is also an excellent daily moisturiser.

CLEAR SKIN GEL (125ml)

Clear Skin Gel is an Anti-Fungal, Anti-Bacterial and Anti-Viral product. Aloe Vera forms the base for this product. It contains Tea Tree Oil, which is a strong antiseptic and disinfectant, Echinacea which is an effective healing aid, Calendula which relieves pain and reduces swelling and Comfrey which acts as an astringent and speeds up the healing process.Clear Skin Gel may be used for the treatment of DANDRUFF, ECZEMA, HEMORRHOIDS/PILES, HERPES SIMPLEX/COLD SORES, INSECT BITES, PIMPLES/ACNE, PSORIASIS, RINGWORM, ATHLETE'S FOOT, SCARRING, SHINGLES, VARICOSE ULCERS, WARTS, SUNBURN, MOLES and BURNS.

REVIVE DAY/NIGHT CREAM (50ml)

The Revive Day/Night Cream is manufactured exclusively for the use as a moisturiser and night cream. It re-energises the skin cells, resulting in the stimulation of tired, dehydrated skin, regenerates and strengthens the skin's moisture barrier and reduces the appearance of fine lines and signs of ageing, resulting in a smoother and healthier skin. Also clears skin blemishes. It contains Avocado Oil, Aloe Vera, Evening Primrose, Wheat Germ, Comfrey and the Hypoxis Extract.

PLEASE NOTE: WE DO NOT USE ANY PETROLEUM JELLY OR AQUEOUS CREAM IN THE MANUFACTURE OF THE ABOVE PRODUCTS.

TESTIMONIALS

- I live in Zimbabwe. When visiting RSA in May I bought a jar of your Down to Earth Double Strength African Potato Cream in the hopes that it would alleviate/cure the *psoriasis* that I had had on my feet for many years. To my delight, it has almost cleared up and only shows signs of returning if I forget the daily application. Over the years I have tried many things but with little success. I also bought a jar of your Revive Day/Night Cream – that too, is having a very beneficial effect. Thank you. Carol Nethersole.
- My wife has severe *eczema*. I had been to Hayfields Pharmacy to purchase some cream when I was introduced the African Potato Cream. I was given a sample to try and I was amazed at the result. Thank you. MB Sahibdeen.
- When we last visited the South Coast we purchased a tub of your Down to Earth Double Strength African Potato Cream. We were interested for it's *pain reducing* and *muscle relaxing* qualities as I suffer from the painful condition *fibromyalgia*. We have found it quite effective and it works as a really excellent massage cream. Regards. Natasha Oehme.
- I bought a jar of your Double Strength African Potato Cream at the market in Plettenberg Bay in June and have found it a great help for *arthritic ankles*! And *brown, sun damaged skin*! I was wondering if there was somewhere in the Southern Suburbs of Cape Town where I could get another jar? Kind regards. Dee Charton (Mrs).
- I am using the African Potato Cream Double Strength for *lesions* which I have had spreading all over my body for 13 years. There were on my back , red and raw. Started using on Sunday nearly clear by Thursday. Mary Jarvis.
- Am using it for *pressure sores* and *tender skin*. My husband is 84 and is in nappies every day. Now after 2 days, I can't believe the result. Thank you, at last something that helps. Helen Smith.
- I was sceptical to use this product but after using a sample given to me I was able to see for myself the change in my skin and even use it for my dog who has *warts.* Truly a miracle product. Helga Viggers.
- I have been using the African Potato Cream for 5 months and can't do without it. I have tried all the anti-inflammatory products available at chemists but the African Potato Cream has been the best. My husband is 84 years old, a *diabetic* and blind. Suffers from a *pinched nerve* and *worn out disc* in back. All treatments have been done but he is in *constant pain*. This product relieves him of pain all the time. I cannot do without it. Thanking all involved in producing this product. Mrs Hwelen Benadie, Edenvale.

APPENDIX 3: PLANT SELECTION, EXTRACTION AND ANALYTICAL ANALYSIS OF COMPOUNDS IN *HYPOXIS* SPP

1. TLC plates

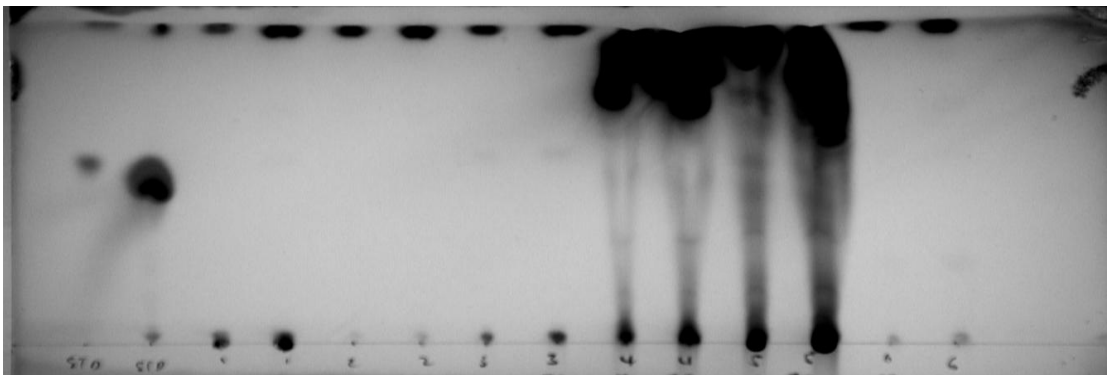

1 2 3 4 5 6 7 8 9 10 11 12 13 14

Figure 1.1: Extraction of sterols from *H. sobolifera* using water (3, 4), methanol (5, 6), ethanol (7, 8), acetone (9, 10), chloroform (11, 12) and dichloromethane (13, 14) over a 24 hrs period. Lanes 1 and 2 represent MODUCARE®

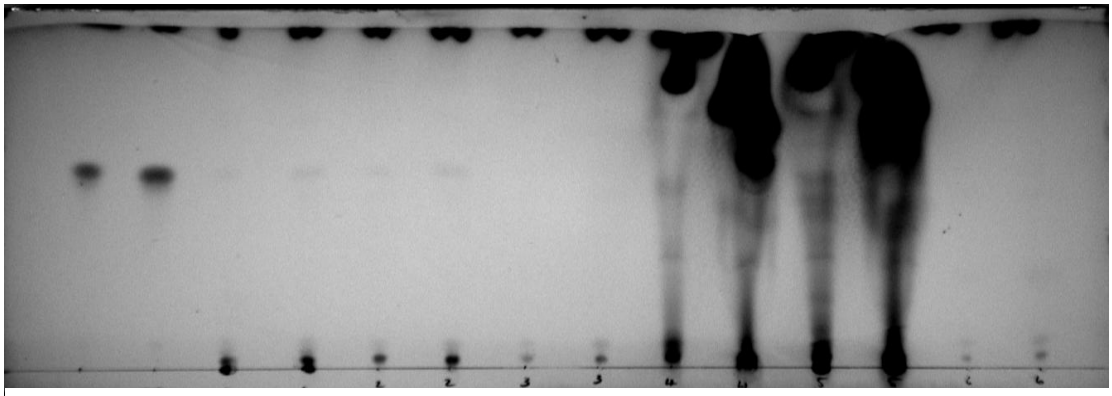

1 2 3 4 5 6 7 8 9 10 11 12 13 14

Figure 1.2: Extraction of sterols from *H. sobolifera* using water (3, 4), methanol (5, 6), ethanol (7, 8), acetone (9, 10), chloroform (11, 12) and dichloromethane (13, 14) over a 48 hrs period. Lanes 1 and 2 represent MODUCARE®

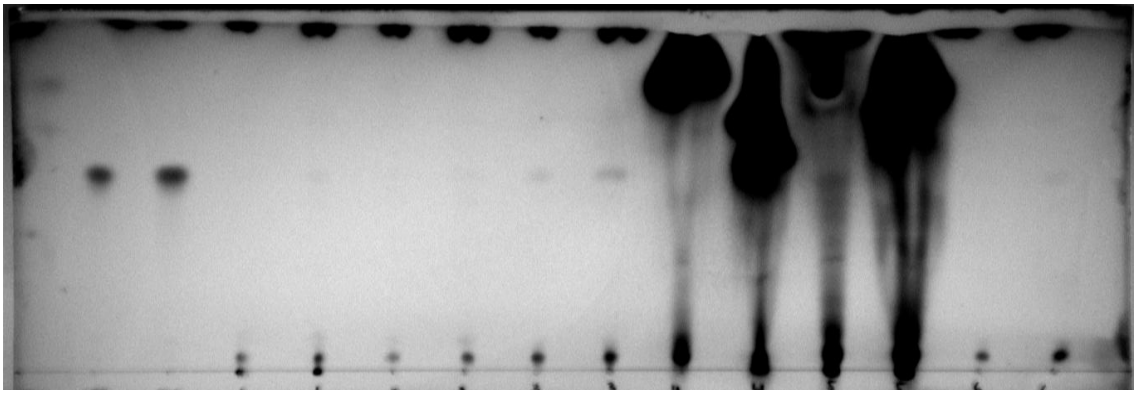

Figure 1.3: Extraction of sterols from *H. sobolifera* using water (3, 4), methanol (5, 6), ethanol (7, 8), acetone (9,10), chloroform (11, 12) and dichloromethane (13, 14) over a 72 hrs period. Lanes 1 and 2 represent MODUCARE®

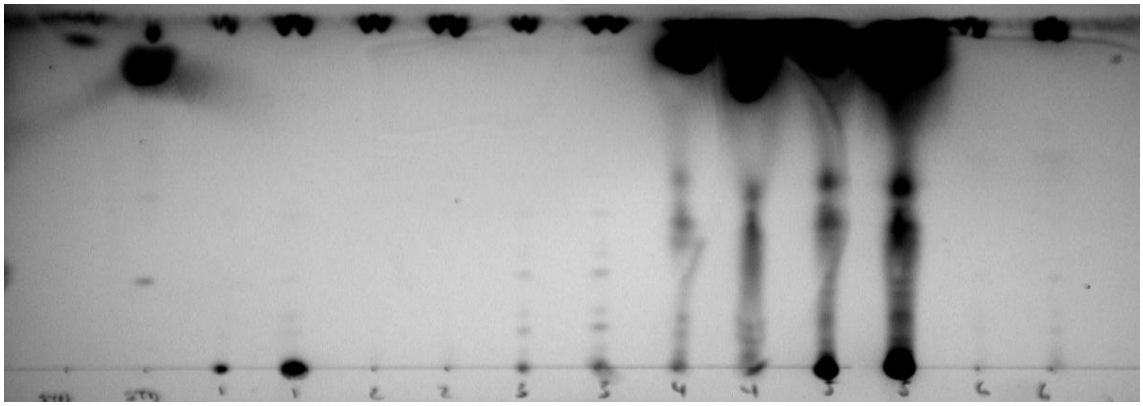

Figure: Extraction of sterolins from *H. sobolifera* using water (3, 4), methanol (5, 6), ethanol (7, 8), acetone (9, 10), chloroform (11, 12) and dichloromethane (13, 14) over a 24 hrs period. Lanes 1 and 2 represent MODUCARE®

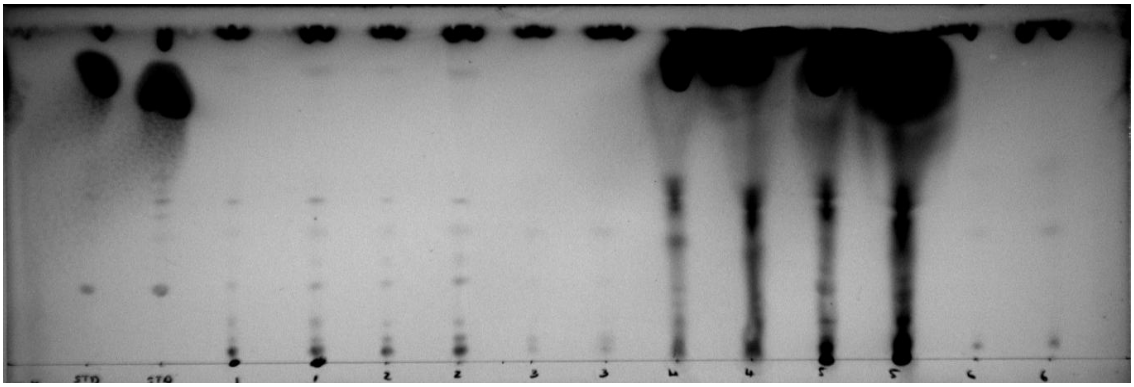

Figure 1.5: Extraction of sterolins from *H. sobolifera* using water (3, 4), methanol (5, 6), ethanol (7, 8), acetone (9, 10), chloroform (11, 12) and dichloromethane (13, 14) over a 48 hrs period. Lanes 1 and 2 represent MODUCARE®

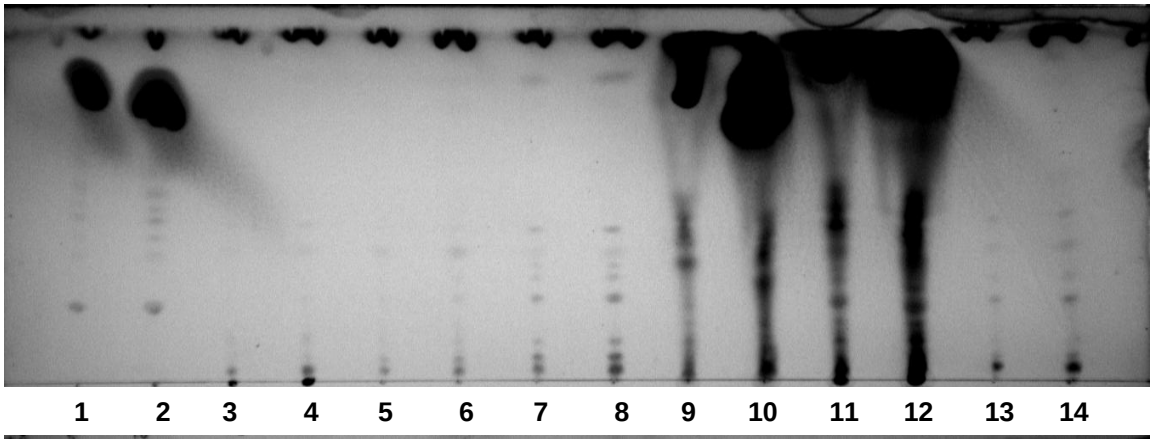

Figure 1.6: Extraction of sterolins from *H. sobolifera* using water (3, 4), methanol (5, 6), ethanol (7, 8), acetone (9, 10), chloroform (11, 12) and dichloromethane (13, 14) over a 72 hrs period. Lanes 1 and 2 represent MODUCARE®

2. Standard curves

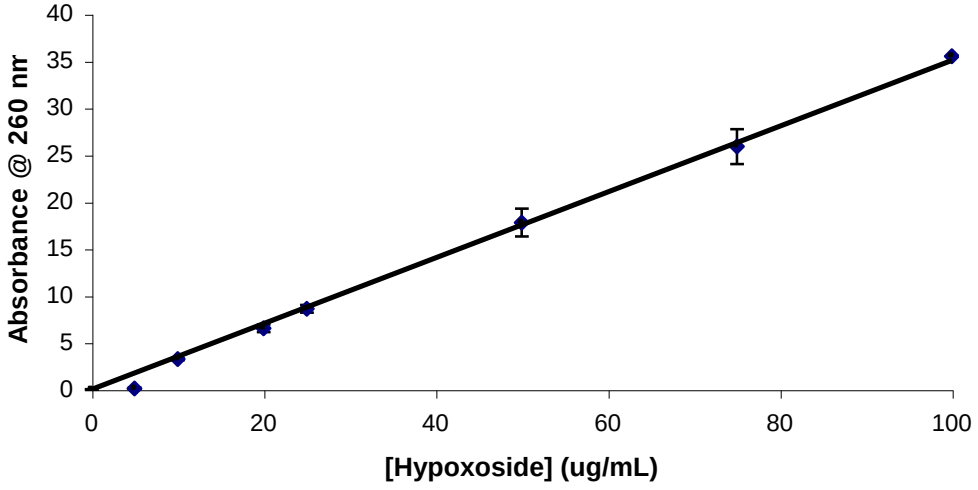

Figure 2.1: Standard curve of hypoxoside concentration as a function of absorbance @ 260 nm for the quantification of hypoxoside. Error bars represent SD of triplicate values. R^2 = 0.9971

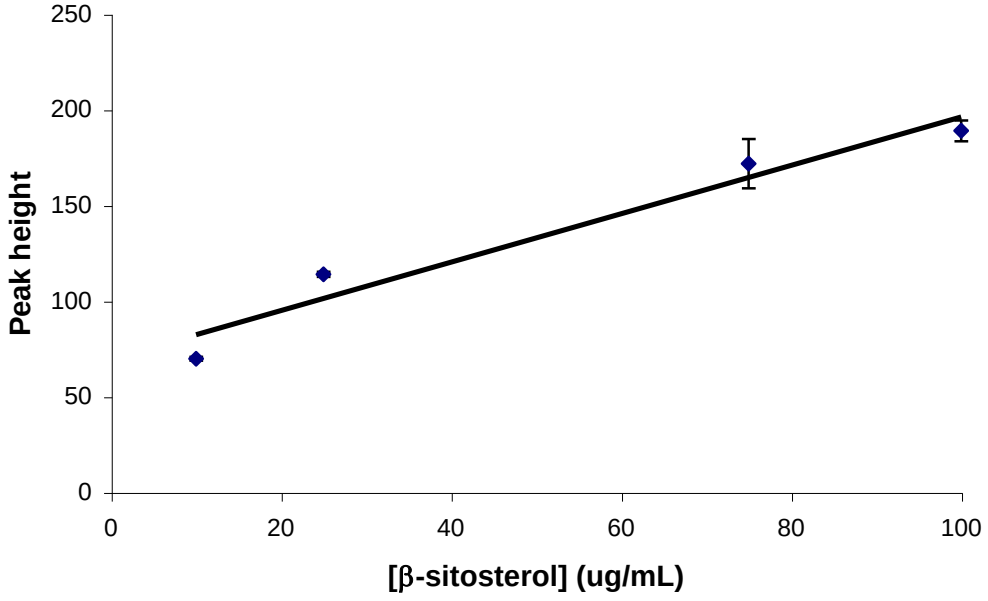

Figure 2.2: Standard curve of β-sitosterol concentration as a function of peak height for the quantification of β-sitosterol. Error bars represent SD of triplicate values. R^2 = 0.9531

3. HPLC chromatograms

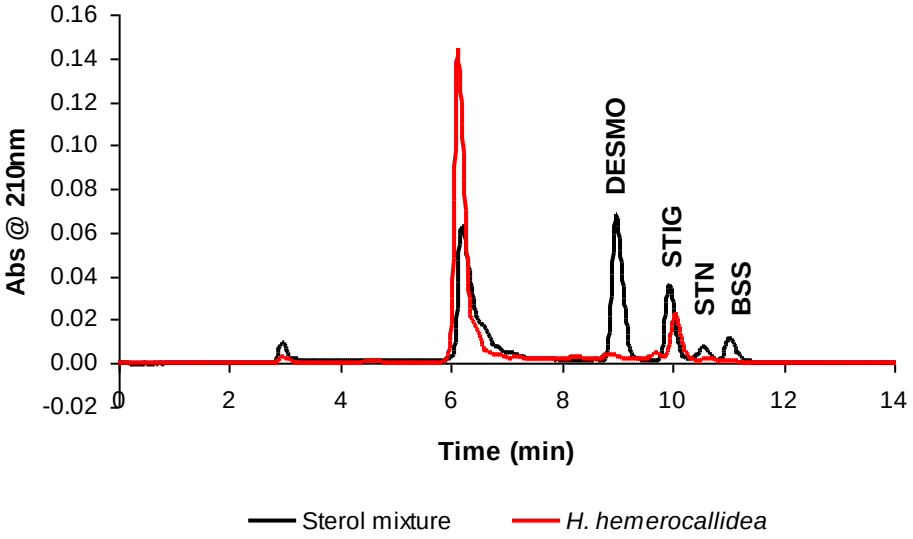

Figure 3.1: HPLC chromatogram overlays of the separation of a sterol mixture and *H. hemerocallidea*. The Nucleosil C18 column, a mobile phase of CH_3CN: MeOH (90:10; v/v) and a flow rate of 0.5 mL/min were used for sterol separation. Stock solution of *H. hemerocallidea* was 5 mg/mL. Abbreviations: DESMO = desmosterol, STIG = stigmasterol, STN = stigmastenol, BSS = β-sitosterol

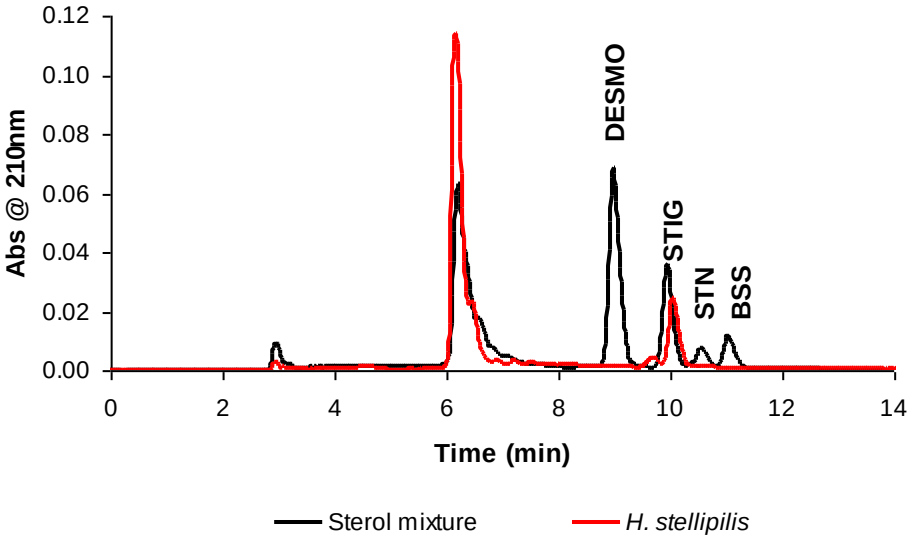

Figure 3.2: HPLC chromatogram overlays of the separation of a sterol mixture and *H. stellipilis*. The Nucleosil C18 column, a mobile phase of CH_3CN: MeOH (90:10; v/v) and a flow rate of 0.5 mL/min were used for sterol separation. Stock solution of *H. stellipilis* was 10 mg/mL. Abbreviations: DESMO = desmosterol, STIG = stigmasterol, STN = stigmastenol, BSS = β-sitosterol

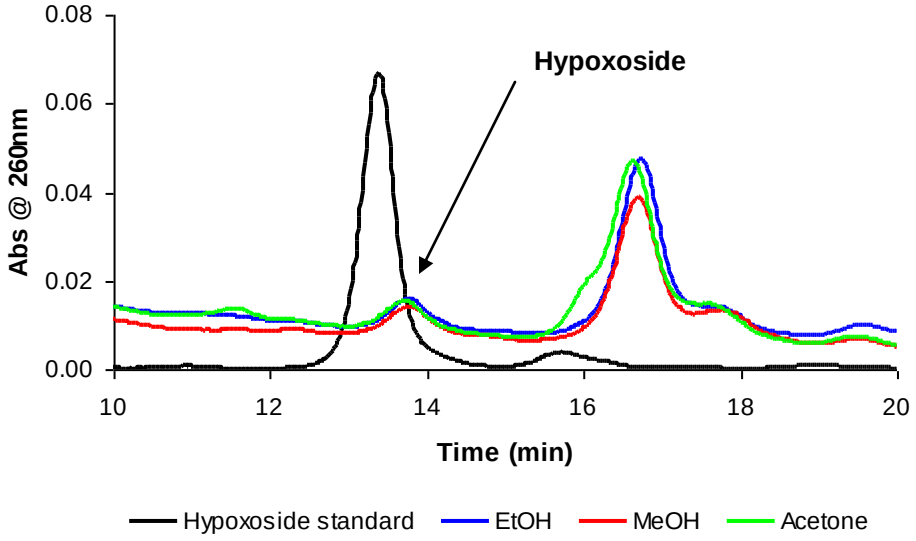

Figure 3.3: HPLC chromatogram overlays of the hypoxoside content of *H. sobolifera* EtOH, MeOH and acetone extracts. The Nucleosil C18 column, a mobile phase of CH_3CN: H_2O (20:80; v/v) and a flow rate of 1 mL/min were used for hypoxoside separation. One representative of three experiments performed. Stock solutions of *H. sobolifera* was 10 mg/mL.

APPENDIX 4: ANTICANCER ACTIVITY AND MECHANISM(S) OF ACTION

1. β-glucosidase Activation

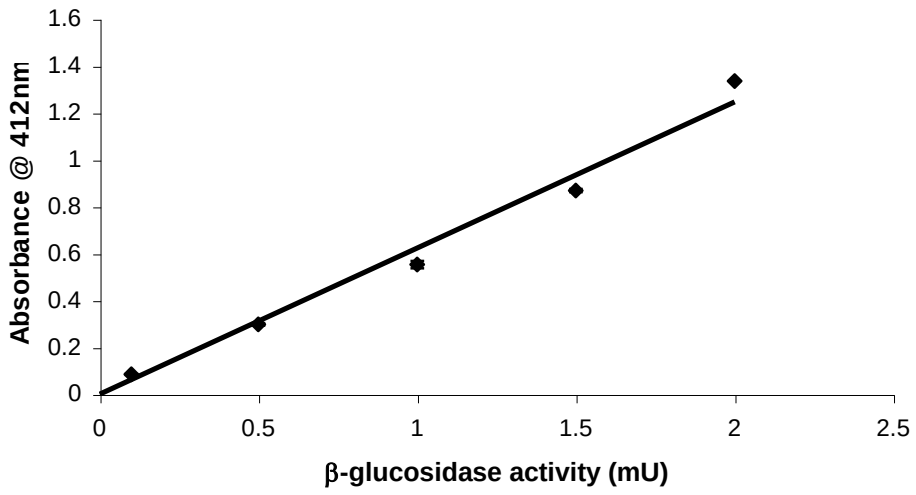

Figure 1.1: Standard curve of β-glucosidase activity as a function of absorbance @ 412 nm. Error bars represent SD of triplicate values. R^2 = 0.9971

2. Sterol Cytotoxicity

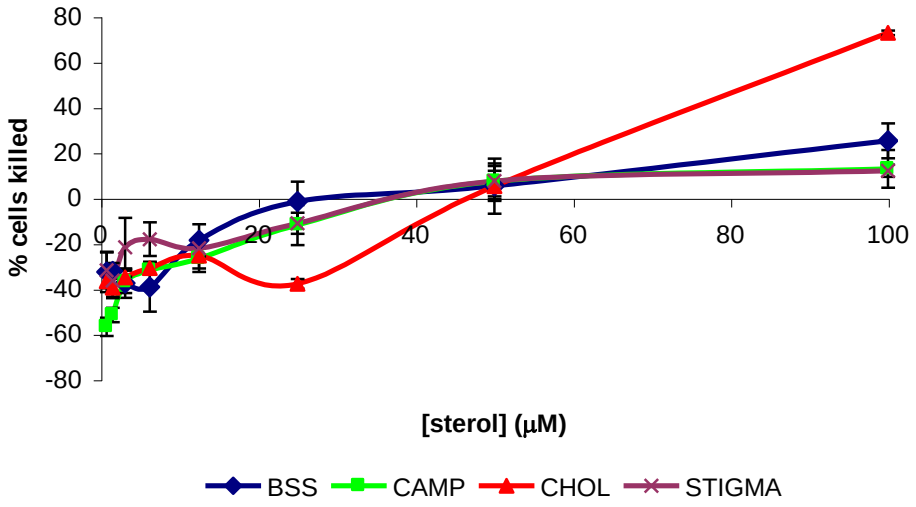

Figure 2.1: Percentage of HeLa cancer cells killed when treated with β-sitosterol, campesterol, cholesterol and stigmasterol at concentrations of between 0.78-100 µM after 48 hrs exposure. MTT assay was performed. Error bars represent SEM of quadruplicate values. CD (4 mM) and 5% EtOH (5%, v/v) were used to dissolve the sterols. Abbreviations: BSS = B-sitosterol; CAMP = campesterol; CHOL = cholesterol; STIG = stigmasterol

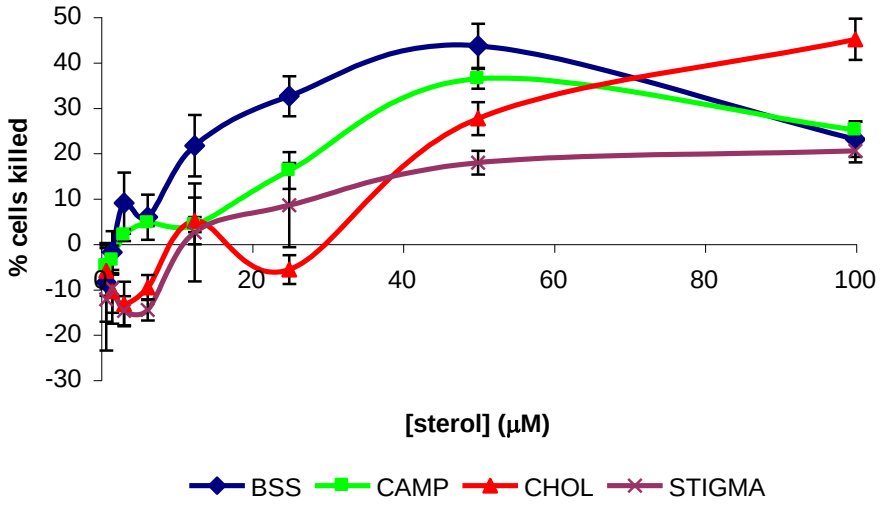

Figure 2.2: Percentage of HT29 cancer cells killed when treated with β-sitosterol, campesterol, cholesterol and stigmasterol at concentrations of between 0.78-100 µM after 48 hrs exposure. MTT assay was performed. Error bars represent SEM of quadruplicate values. CD (4 mM) and 5% EtOH (5%, v/v) were used to dissolve the sterols. Abbreviations: BSS = B-sitosterol; CAMP = campesterol; CHOL = cholesterol; STIG = stigmasterols.

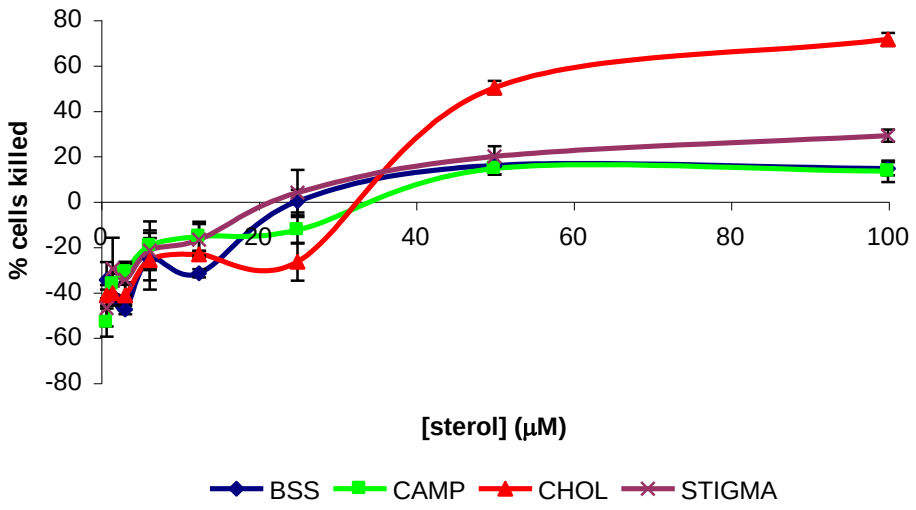

Figure 2.3: Percentage of MCF-7 cancer cells killed when treated with β-sitosterol, campesterol, cholesterol and stigmasterol at concentrations of between 0.78-100 µM after 48 hrs exposure. MTT assay was performed. Error bars represent SEM of quadruplicate values. CD (4 mM) and 5% EtOH (5%, v/v) were used to dissolve the sterols. Abbreviations: BSS = B-sitosterol; CAMP = campesterol; CHOL = cholesterol; STIG = stigmasterol.

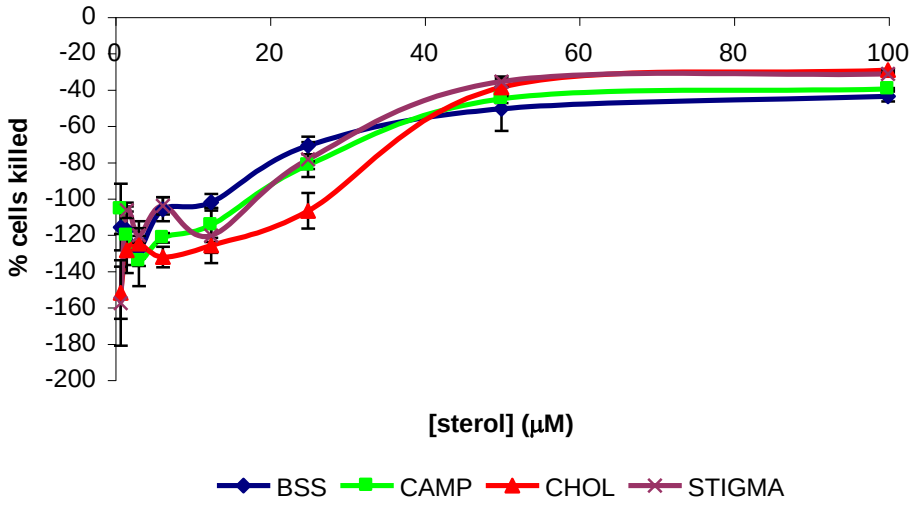

Figure 2.4: Percentage of PBMCs cancer cells killed when treated with β-sitosterol, campesterol, cholesterol and stigmasterol at concentrations of between 0.78-100 µM after 48 hrs exposure. MTT assay was performed. Error bars represent SEM of quadruplicate values. CD (4 mM) and 5% EtOH (5%, v/v) were used to dissolve the sterols. Abbreviations: BSS = B-sitosterol; CAMP = campesterol; CHOL = cholesterol; STIG = stigmasterol

3. Cyclodextrin Cytotoxicity

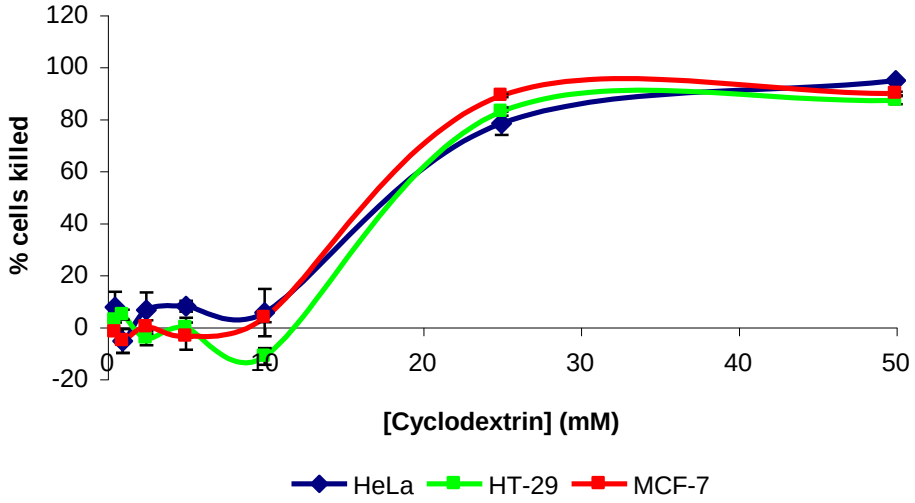

Figure 3.1: Cytotoxic effects of 2-hydroxypropyl-β-cyclodextrin (0.5-50 mM) on HeLa, HT-29 and MCF-7 cancer cell lines after 48 hrs exposure. Error bars represent SEM values of quadruplicates.

4. Time Study: Conversion of hypoxoside to rooperol

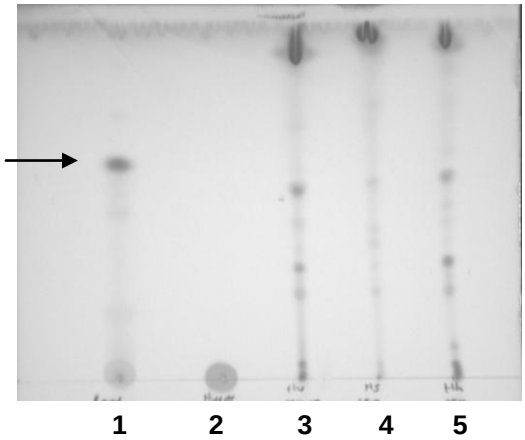

Figure 4.1: TLC separation of rooperol using chloroform: ethylacetate: formic acide (5:4:1) as mobile phase. Lanes 1-5 represent rooperol (5 µg; arrow), hypoxoside (5 µg), *H. sobolifera* (250 µg), *H. stellipilis* (250 µg) and *H. hemerocallidea* (250 µg), respectively.

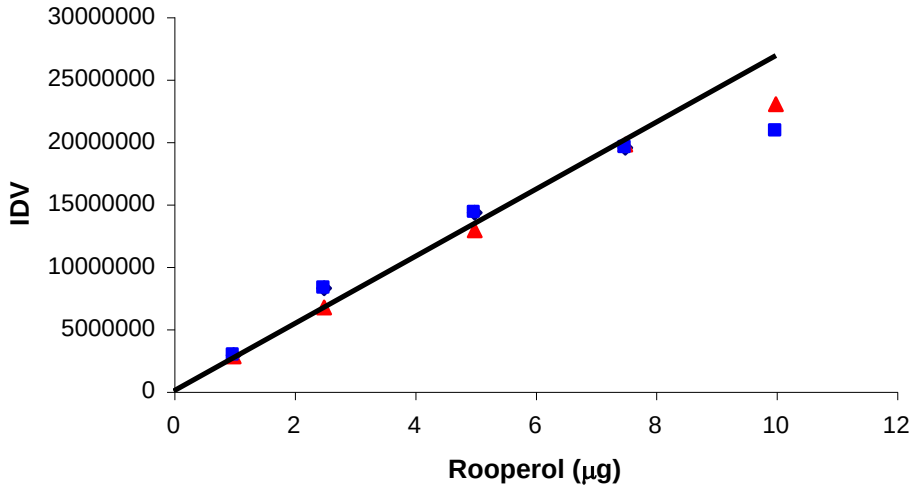

Figure 4.2: Standard curve of rooperol as a function of IDV. Red triangles and blue squares represent duplicate experiment (R^2 = 0.9905).

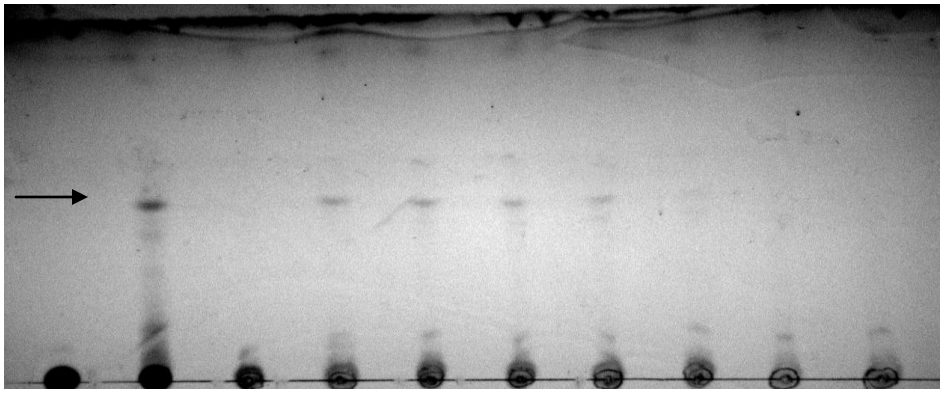

Hypoxo Roop 0 3 6 9 12 24 36 48

Figure 4.3: Conversion of hypoxoside to rooperol (arrow) in the presence of β-glucosidase in HeLa cancer cells over time.

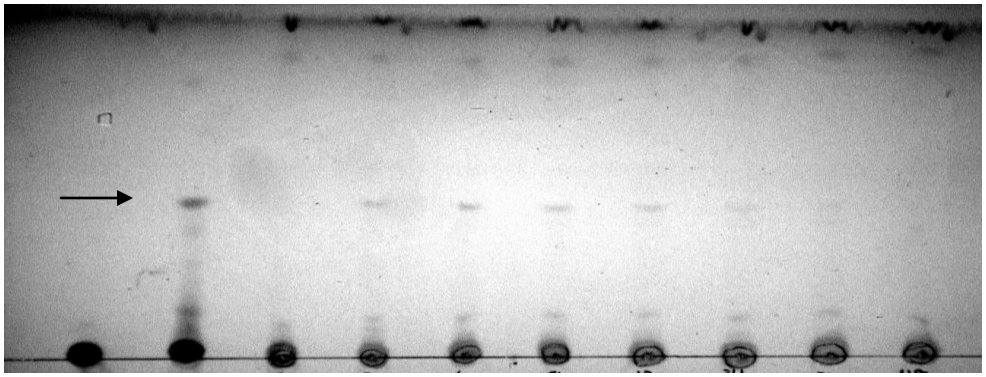

Hypoxo Roop 0 3 6 9 12 24 36 48

Figure 4.4: Conversion of hypoxoside to rooperol (arrow) in the presence of β-glucosidase in HT29 cancer cells over time.

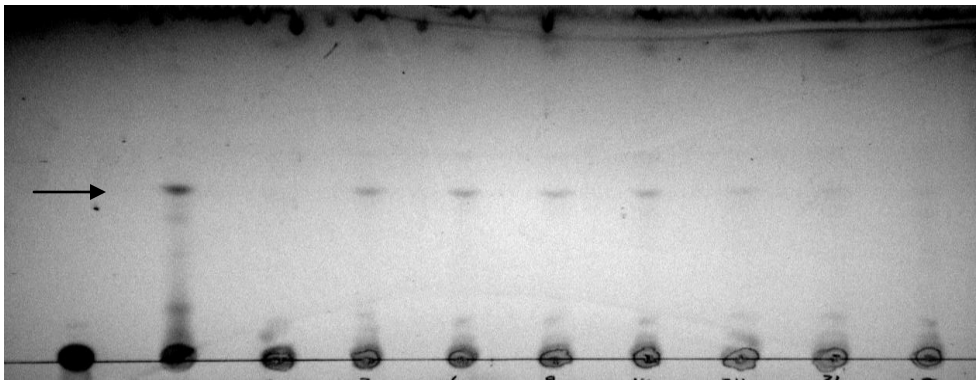

Hypoxo Roop 0 3 6 9 12 24 36 48

Figure 4.5: Conversion of hypoxoside to rooperol (arrow) in the presence of β-glucosidase in MCF7 cancer cells over time.

5. Annexin V-FITC

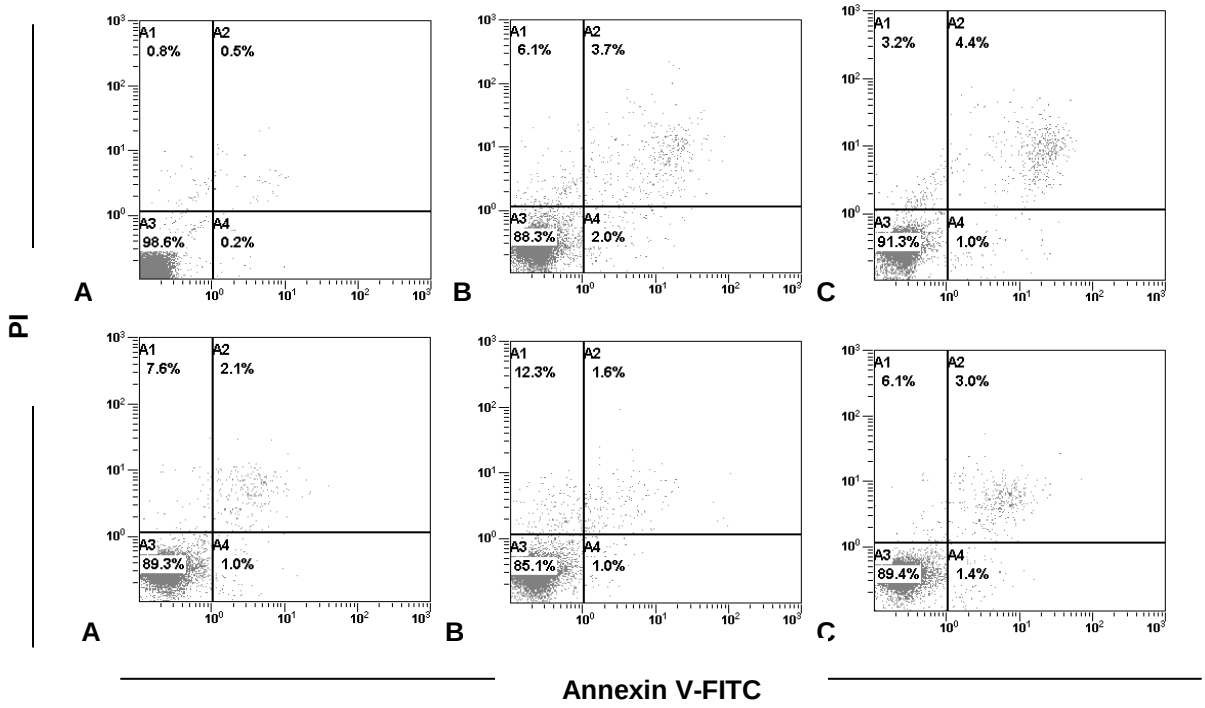

Figure 5.1: Dot plots of Annexin V-FITC and PI stained U937 cells after 15 and 48 hrs exposure to *H. hemerocallidea* (A), *H. stellipilis* (B) and *H. sobolifera* (C). One representative of three experiments performed.

6. DNA Fragmentation

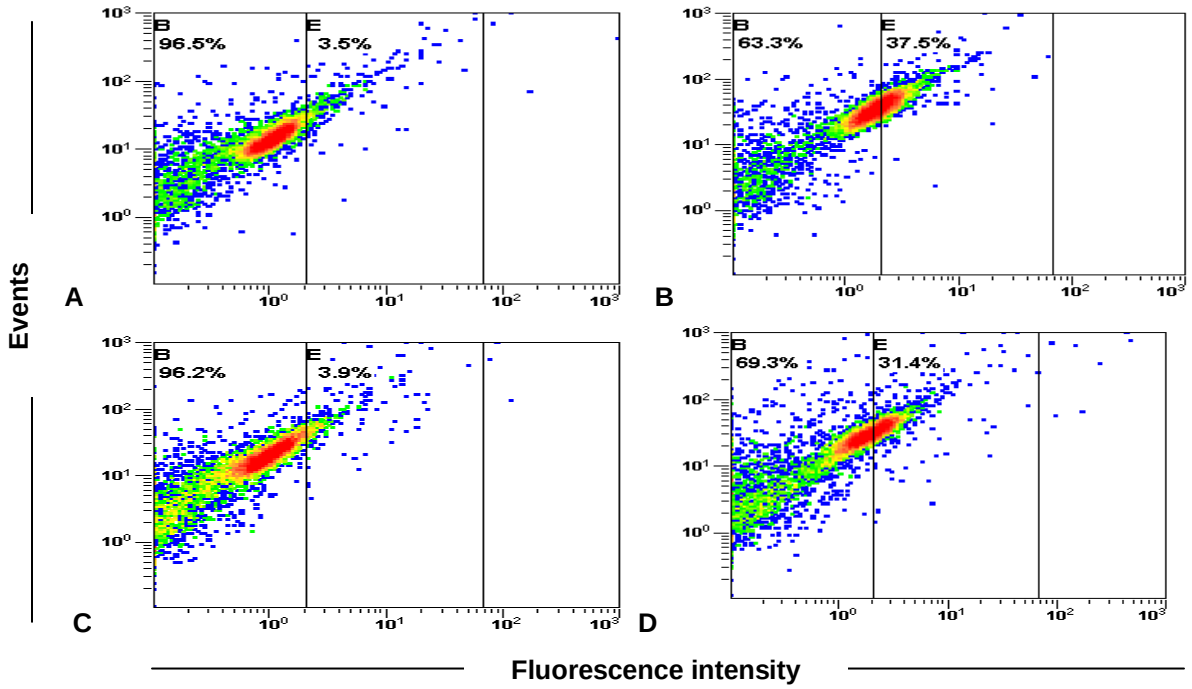

Figure 6.1: Density plots of DMSO (A; 0.25%, v/v), *H. sobolifera* (B; 125 µg/mL), rooperol (C; IC_{50} value) and cisplatin (D; 50 µM) treated HeLa cancer cells. 10 000 events were recorded. One representative of three experiments performed.

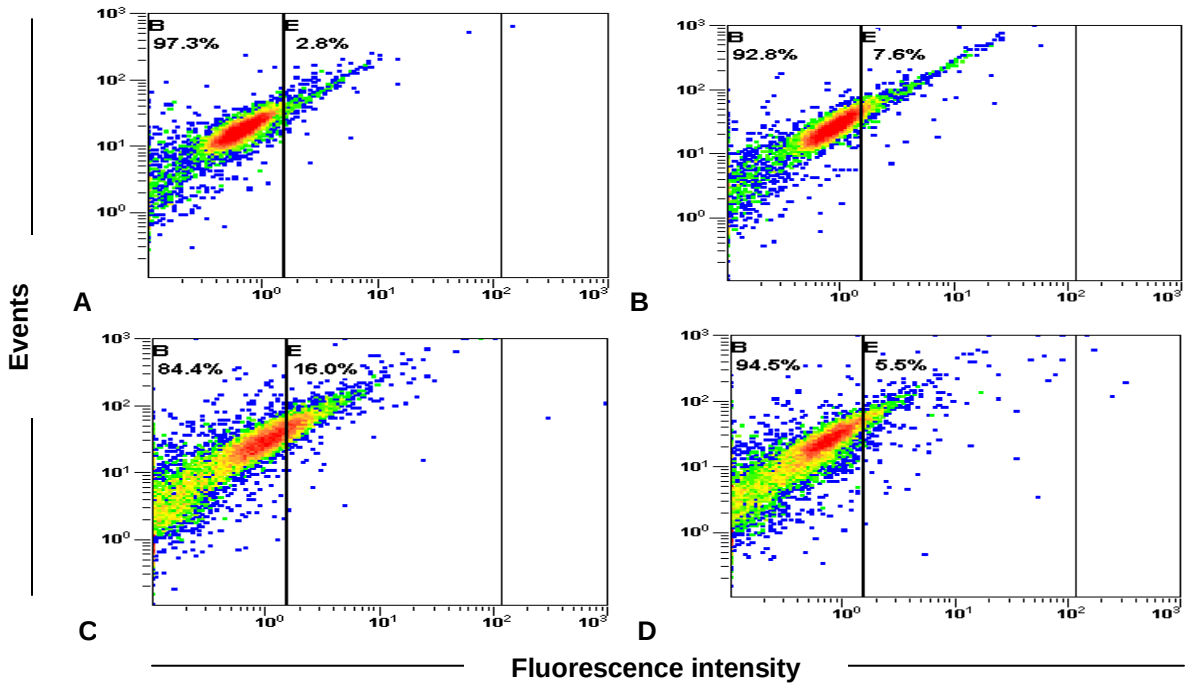

Figure 6.2: Density plots of DMSO (A; 0.25%, v/v), *H. sobolifera* (B; 125 µg/mL), rooperol (C; IC_{50} value) and cisplatin (D; 50 µM) treated MCF-7 cancer cells. 10 000 events were recorded. One representative of three experiments performed.

ANNEXIN 6: ANTI-INFLAMMATORY ACTIVITY

1. NO production

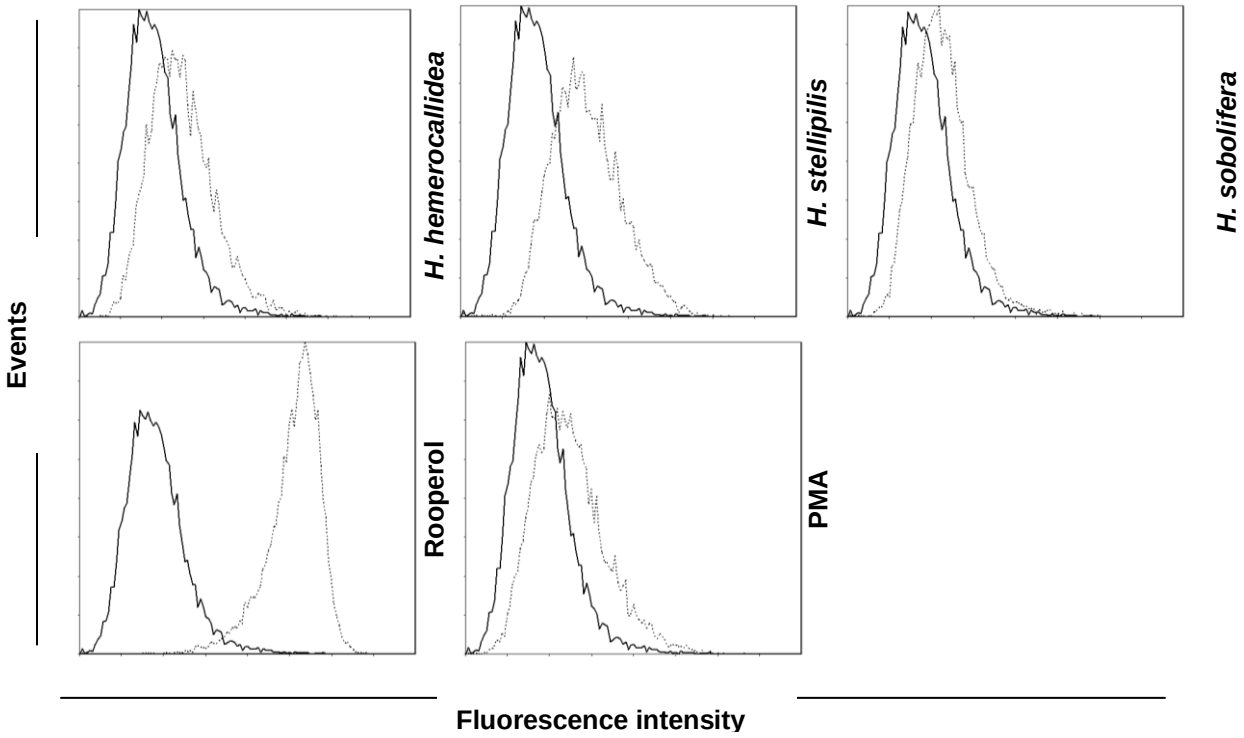

Figure 1.1. Histograms of NO production in monocyte-macrophages after six hrs of treatment with *H. hemerocallidea, H. stellipilis, H. sobolifera,* rooperol and PMA (20 mM). One representative of three experiments performed in triplicate. 10 000 events recorded. Solid lines = DMSO control; dotted lines = treatment

2. Cyclooxygenase-2

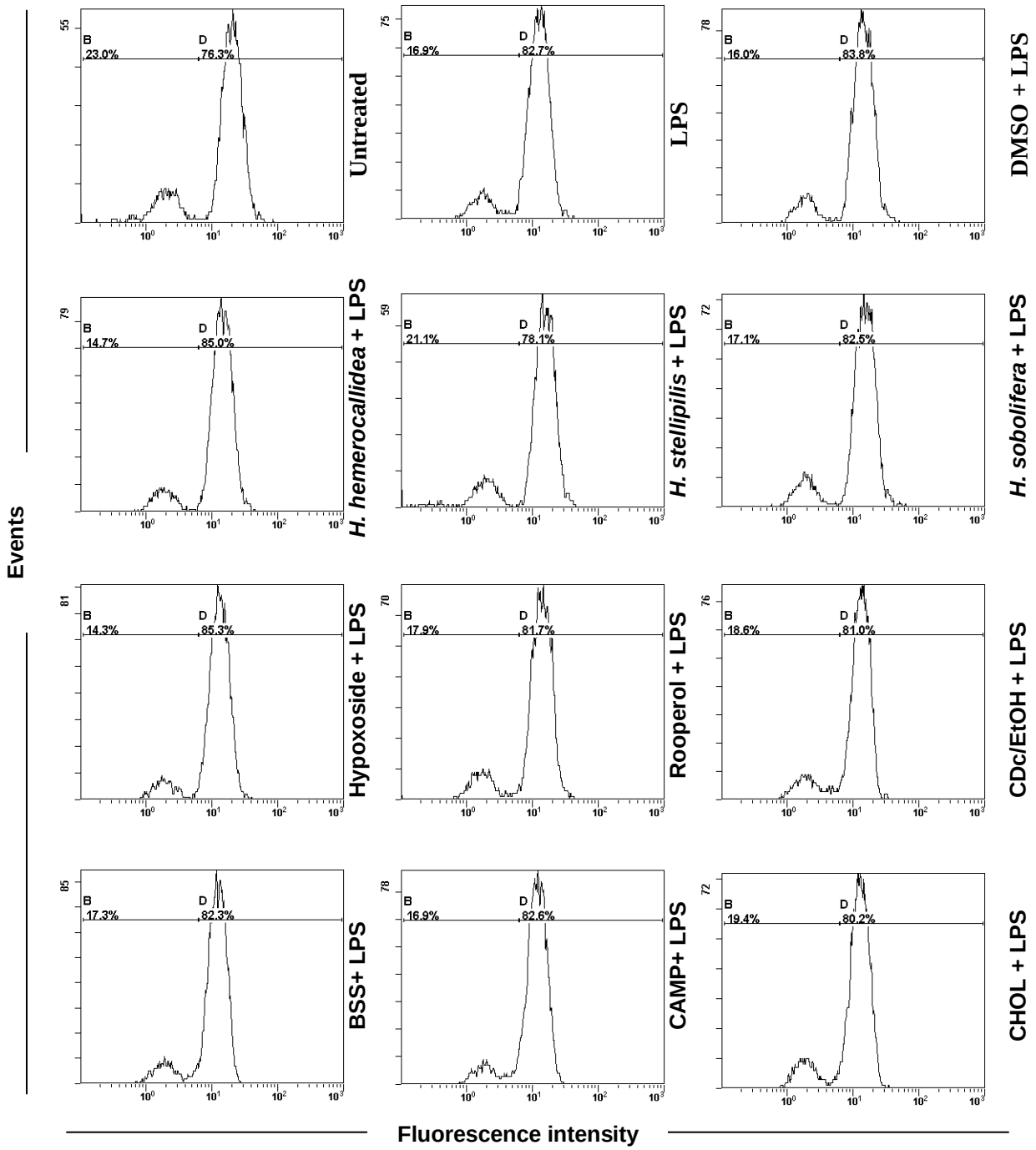

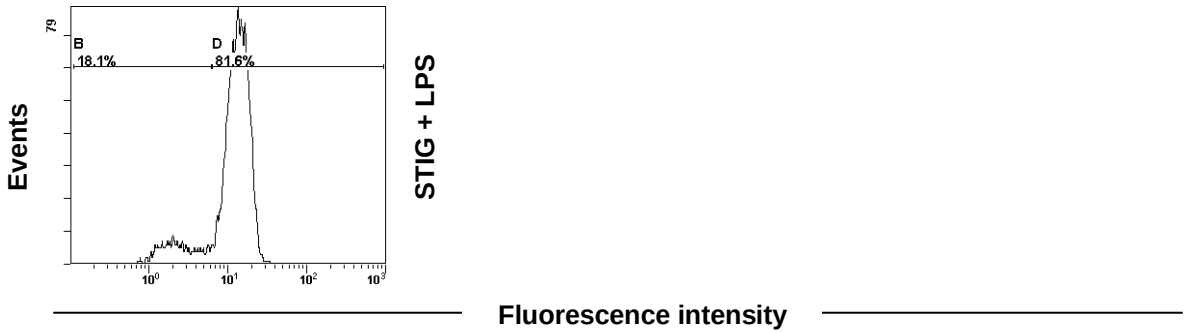

Figure 2.1: Histograms of COX-2 expression in monocyte-macrophages after six hrs treatment with *Hypoxis* extracts and purified compounds in the presence of 250 ng/mL LPS. 10 000 events were recorded. Percentages on histograms represent the change in COX-2 levels.

3. Phagocytosis

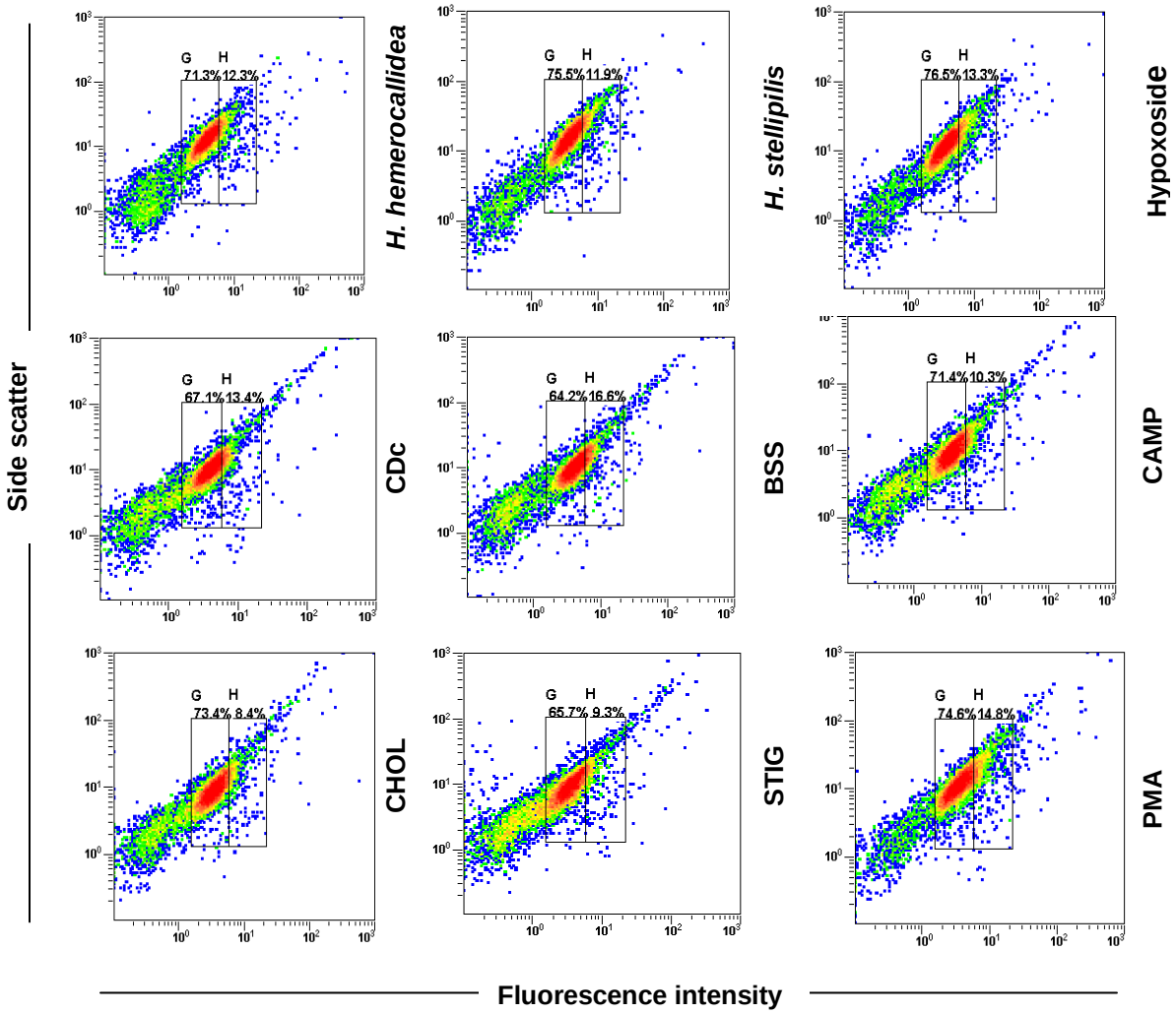

Figure 3.1: Density plots of phagocytosis of pHrodo™ *E. coli* bioparticles® by monocyte-macrophages, pretreated with *H. hemerocallidea*, *H. stellipilis*, hypoxoside, CDc, BSS, CAMP, CHOL, STIG and PMA (20 nM).

4. Pro- and anti-inflammatory cytokines

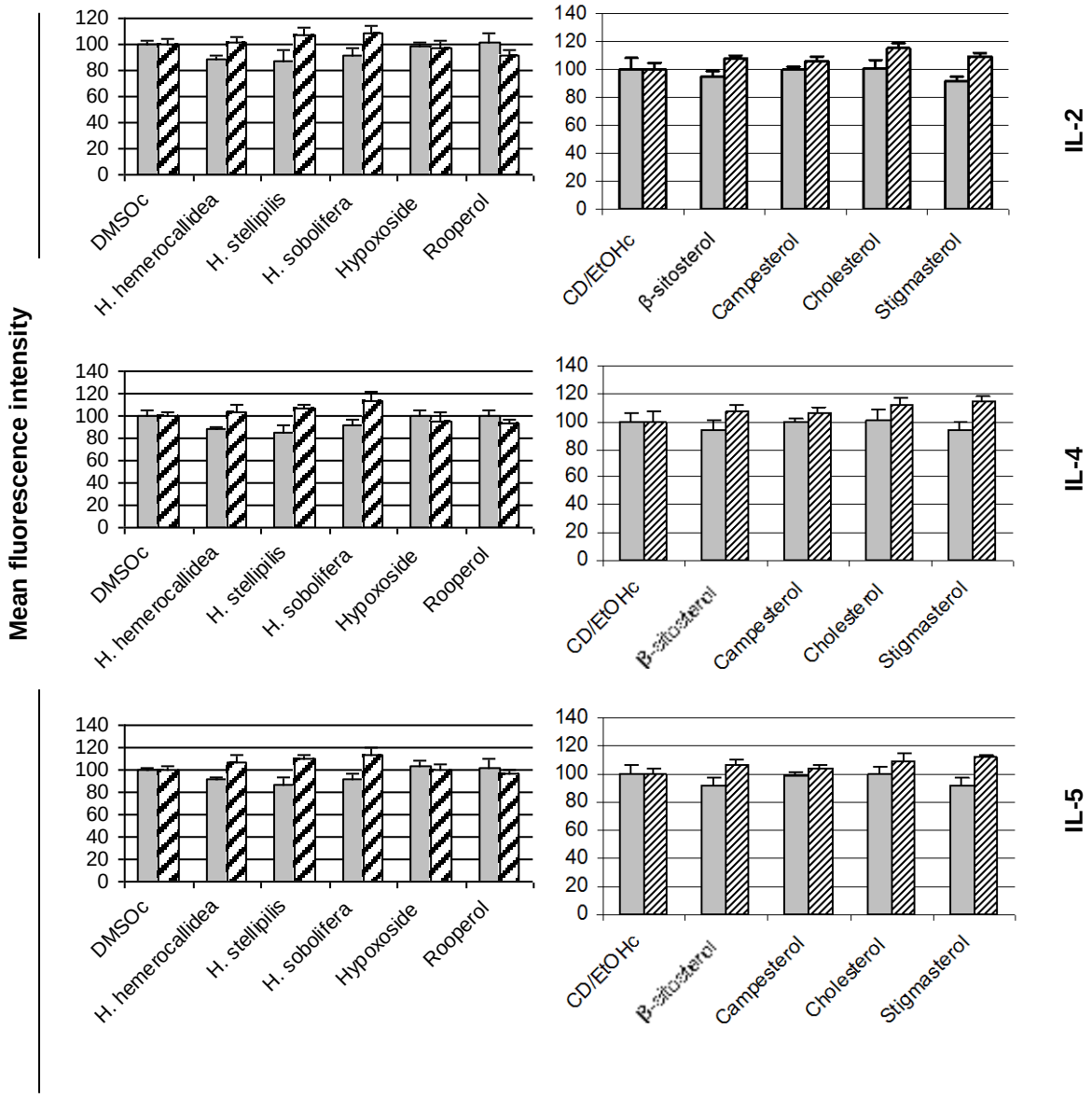

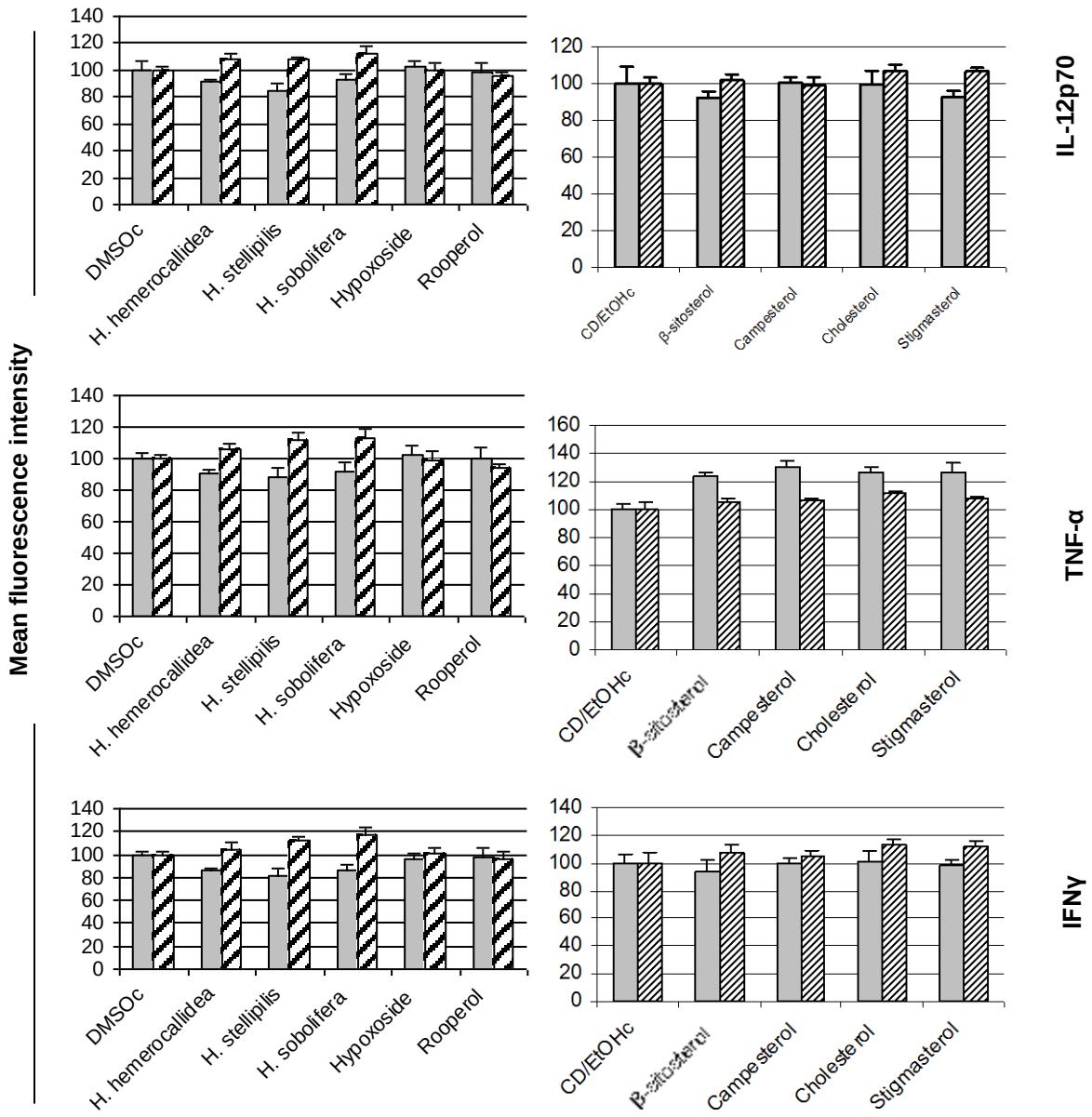

Figure 4.1: Extracellular cytokine production by PBMCs treated with *Hypoxis* extracts and its purified compounds for 48 hrs. Grey bars = donor 1/male; striped bars = donor 2/female. Error bars represent the SEM of triplicate values.

APPENDIX 7: ANTIOXIDANT ACTIVITY

1. ROS production

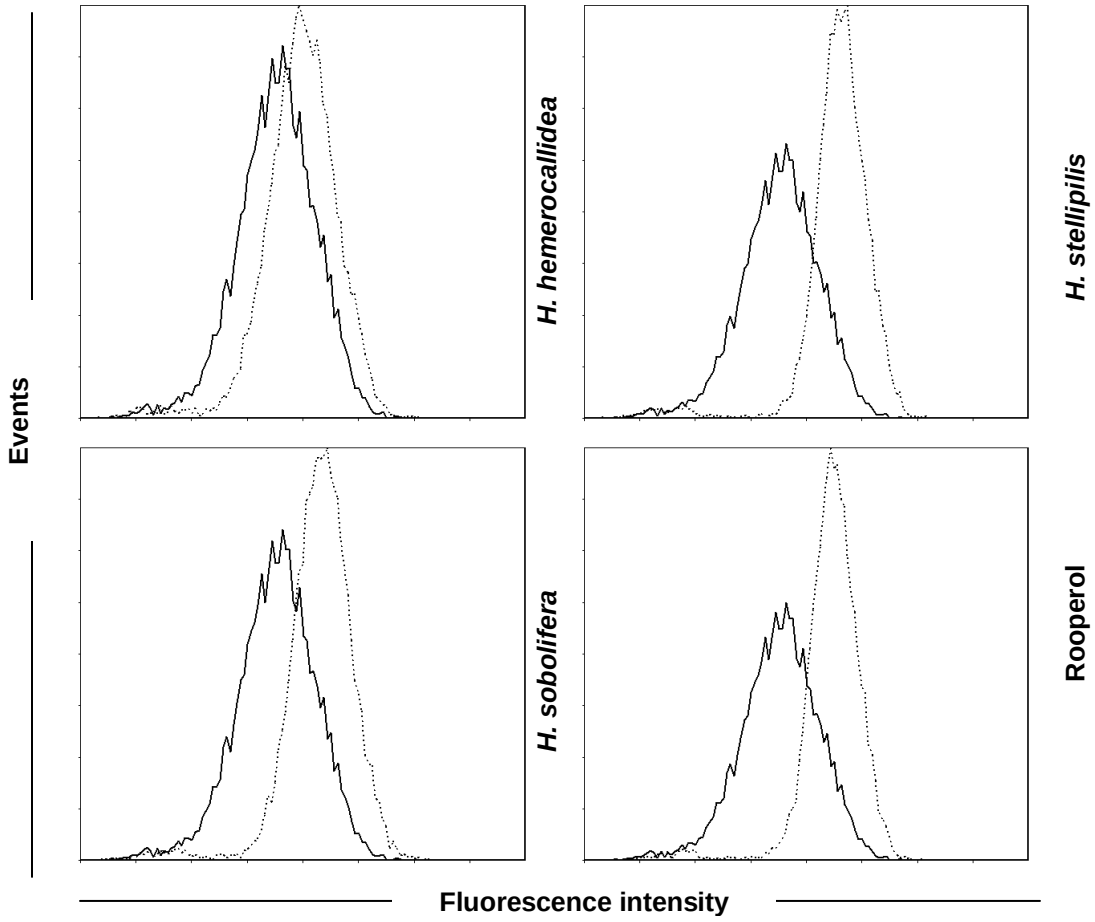

Figure 1.1: Histograms of ROS production in undifferentiated U937 cells after one hour of treatment with *H. hemerocallidea, H. stellipilis, H. sobolifera,* and rooperol. One representative of three experiments performed in triplicate. 10 000 events recorded. Solid lines = DMSO control; dotted lines = treated

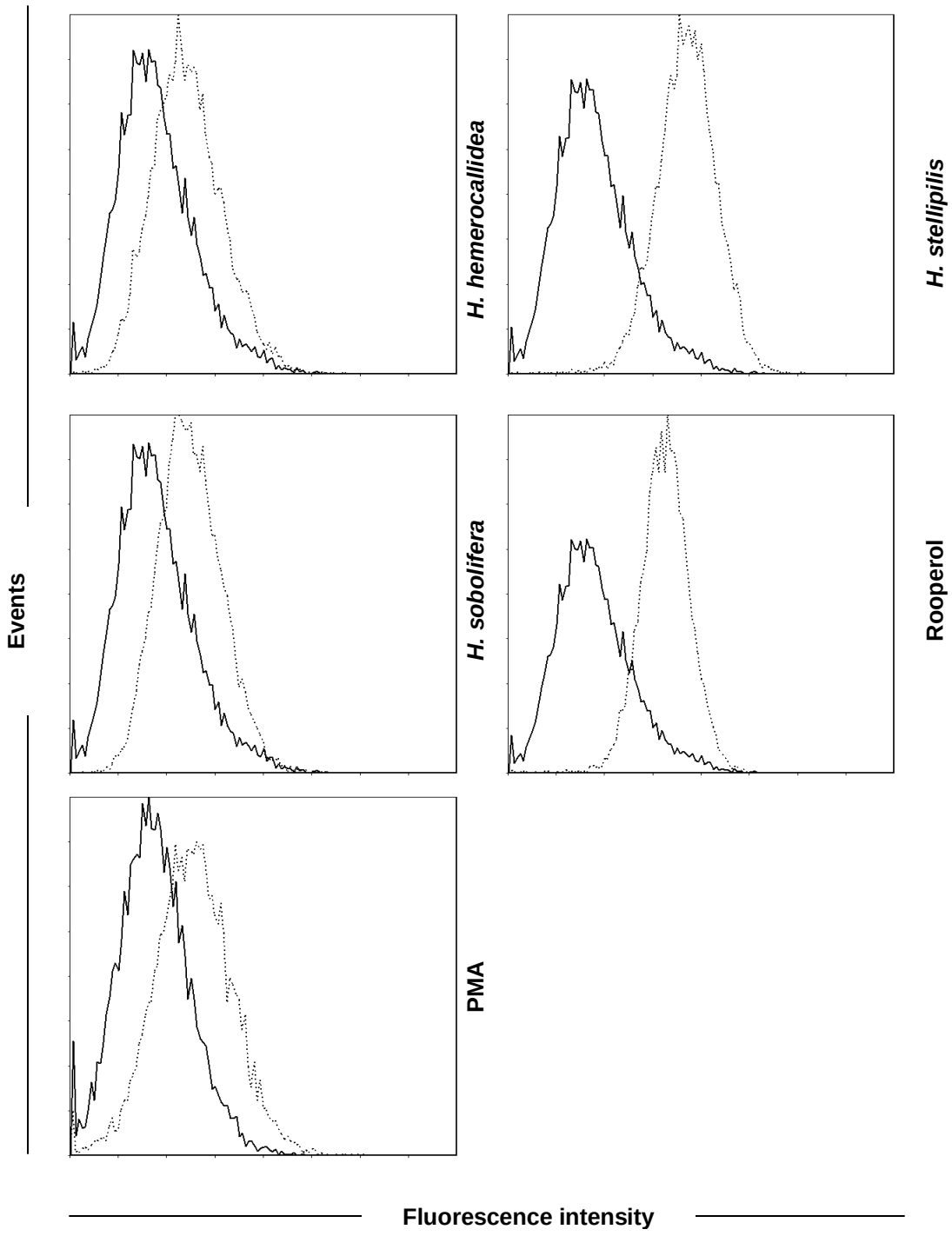

Figure 1.2: Figure 1.1: Histograms of ROS production in differentiated U937 cells after one hour of treatment with *H. hemerocallidea, H. stellipilis, H. sobolifera,* rooperol and PMA (50 nM). One representative of three experiments performed in triplicate. 10 000 events recorded. Solid lines = DMSO control; dotted lines = treated

2. Standard curve for FRAP determination

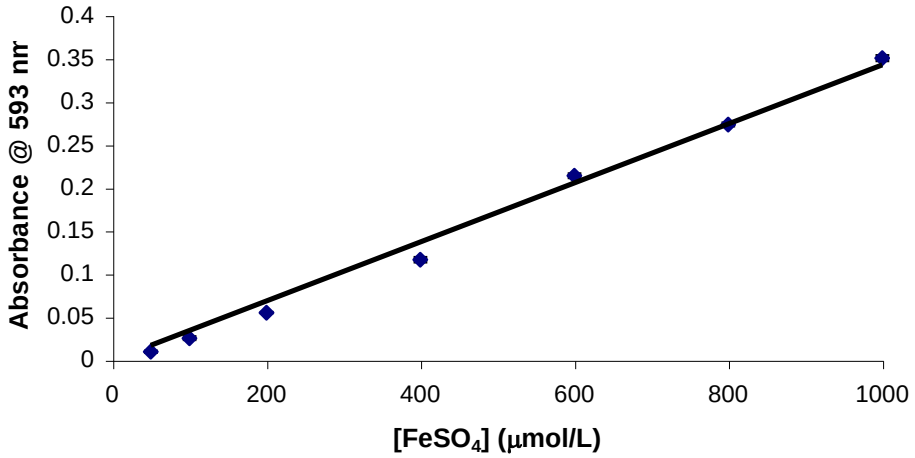

Figure 2.1: Standard curve of $FeSO_4$ as a function of absorbance @ 593 nm to determine FRAP. Error bars represent SD of triplicate values. R^2 = 0.9916